University of Strathclyde

Department of Naval Architecture, Ocean and Marine Engineering

Improving The Hydrodynamic Performance of Stepped Hulls Through Enhanced Analysis Techniques

Angus Gray-Stephens

A thesis presented in fulfilment of the requirements for the degree of Doctor of Philosophy

2022

This thesis is the result of the author's original research. It has been composed by the author and has not been previously submitted for examination which has led to the award of a degree.

Signed: Date: 15/05/22

Acknowledgments

I have spent three and a half very enjoyable years in Glasgow working on my PhD. I am very grateful for this time and the opportunity to pursue my own research. I will always remember this time fondly and the experience will be with me for the rest of my life. I would like to thank everyone who has contributed and helped me towards completing my PhD research by providing advice, support and friendship.

First and foremost, I would like to offer my special thanks to my primary supervisor, Dr Tahsin Tezdogan, who truly went above and beyond to support me throughout my studies. His belief in me and encouragement inspired me to pursue a PhD, and I am incredibly grateful to have had this opportunity. I have benefited immensely from his extensive experience and invaluable advice in both my academic and personal life. I could not have asked for a more supportive, enthusiastic or caring supervisor, who has consistently been there for me throughout my studies. For this I am forever indebted, and I cannot express my thanks enough. I am also very grateful to my second supervisor, Professor Sandy Day, whom I would like to thank for his detailed insights. His outlook always gave a fresh perspective to my work.

I would like to thank the University of Strathclyde Faculty of Engineering for the use of the ARCHIE-WeSt High Performance Computing facilities, with which all CFD results were generated. I would also like to thank the NAOME department for the use of the Kelvinside Hydrodynamics Laboratory, the towing tank at which the experimental study was conducted. Many thanks are given to Grant Dunning, Steven Black and Saishuai Dai for their assistance and expertise. I am very grateful to all of our department's staff who provided help and support throughout my eight years at the university, their efforts are very much appreciated.

I would also like to extend my gratitude to Kostas Karantonis and Siemens Industry Software Ltd. for providing me with a six month license for HEEDS MDO, without which the research presented in the final study of this thesis would not have been possible. Gabriel Amine-Eddine and Richard Martin provided expensive assistance with the software and the Archie WeST HPC.

I would like to thank my colleagues and friends with whom I have many amazing experiences and memories with. A special mention goes to Peter Cameron and Ewan Rycroft who began their studies at the same time as me, encouraging me to undertake a PhD. Also to Moritz Troll, who commenced his research the following year. Thank you for your friendship, support and motivation, both personally and academically. I wish you all every success and hope that you complete your studies in the near future!

I cannot begin to express my thanks to Maxime Renfrew, who has been extremely understanding and supportive. She has provided drive and motivation, particularly during the final write up of my thesis when she was always there for me adding fun and excitement to my life. Her support has been incredibly uplifting and has helped keep me sane during this busy period. For this I am incredibly grateful.

Finally, I would like to extend my deepest thanks to my family. They have always supported me and believed in me. My hard-working mum and dad have provided unconditional love and care, giving me and my brother every opportunity that they could. I can turn to them when times are rough, and count on them to support me no matter what. I honestly could not ask for anything more - I am truly thankful for everything that they have done for me.

Contents

List of Figures

List of Tables

Nomenclature

Symbol	Units	Meaning
Δt	s	Timestep
L	m	Length overall
U	ms^{-1}	Vessel speed
y^+		Non-dimensional wall distance
u_*	ms^{-1}	Friction velocity
y	m	Wall distance
ν	m^2/s	Kinematic viscosity
δ	m	Boundary later thickness
x	m	Length of flat plate
R_n		Reynolds number
δ_S		Simulation error
T		Truth (Experimental data)
S		Simulation result
δ_{SM}		Modelling error
δ_{SN}		Numerical error
$\delta^*_{RE_{i,1}}$		Error (Generalized Richardson Extrapolation)
R_i		Convergence ratio
r_i		Refinement ratio
P_i		Order of accuracy
$\varepsilon_{i,32}$		Difference between course and fine data
$\varepsilon_{i,21}$		Difference between fine and medium data
δ^*_i		Numerical error
C_i		Correction factor
U_i		Solution uncertainty
H	$Beams$	Height of freesurface elevation
A		Constant
L_k	$Beams$	Length of wetted keel
τ	$Degrees$	Trim
C_V		Speed coefficient
X	$Beams$	Distance aft of the transom
L_1	m	Spray root length
L_k	m	Wetted keel length
L_c	m	Wetted chine length
b	m	Beam
L_2	m	Calm water intersection length
β	$Degrees$	Deadrise
$L_{1_{Aft}}$	m	Spray root length (aft hull)
$L_{k_{Aft}}$	m	Wetted keel length

$L_{c_{Aft}}$	m	Wetted chine length
b_L	m	Local beam
β_L	$Degrees$	Local deadrise
τ_L	$Degrees$	Local trim
N	N	Component of resistance force normal to bottom
T	N	Thrust
ϵ	$Degrees$	Shaft angle
m	kg	Mass
g	ms^{-2}	Acceleration due to gravity
D_f	N	Frictional drag
c	m	Distance from center of lift to CG
a	m	Distance from center of D_f to CG
f	m	Distance from thrust line to CG
Cl_β		Lift coefficient of a deadrise surface
Cl_0		Lift coefficient zero deadrise
λ		Mean wetted length to beam ratio
ρ	kg/m^3	Density
$\mathrm{V_m}$	m/s^{-1}	Mean velocity over bottom surface
ΔC_f		Roughness allowance
D_p	N	Pressure drag
C_p	m	Distance of center of pressure from transom
l_p	m	Distance of center of pressure from point of intersection with water
Ω		Percentage of weight carried by forebody
γ	N	Error in vertical equilibrium
F_L	N	Force of lift
x_{CL}	m	Intersection of flow aft of a step on the CL
Ls	m	Step length
L_w	m	Wetted length when afterbody is in chines dry condition
b_{wave_rise}	m	Wetted beam at first step when forebody is in chines dry condition
x_{int}	m	Intersection of undisturbed freesurface with afterbody
Vs	m	Step height
$L_{1_{ad}}$	m	Spray root length (side wetting)
b_{ad}	m	Beam of additional side wetting
$Lift_{ad}$	N	Lift from additional side wetting
A_{WS}	m^2	Area of wetted surface

Abstract

The inclusion of steps presents an attractive solution to improving the efficiency of high-speed planing vessels, yet analysis tools and the available knowledge for improving stepped hulls are considerably under-developed. The research presented in this thesis addresses these issues, seeking answers to the question: *"How can we enhance and accelerate analysis techniques for stepped hulls through knowledge developed from numerical simulations and can hydrodynamic performance be improved through the application of these tools."*

The studies in this thesis apply state-of-the-art Fluid Dynamics (CFD) to examine the impact that the addition of steps has to a planning hull, investigating the mechanisms through which efficiency is improved. The fluid flow is analysed as it separates at each step and interacts with the remainder of the hull, with existing methods of modelling this behaviour being evaluated and novel modelling strategies being proposed.

The knowledge established through these investigations is applied to develop mathematical models for the performance prediction of single and double-stepped planing hulls, aiming to address the limitations and enhance the accuracy of those currently available. The proposed models displayed high degrees of accuracy, calculated the resistance with an average error of 2.50% and 1.29% respectively for single and double stepped hulls.

The enhanced analysis techniques are applied to investigate how the hydrodynamic performance of single and double stepped hulls may be improved. This was successfully achieved, identifying design trends and establishing relationships between design parameters that may be universally applied by designers to lower the resistance of stepped hulls.

Chapter 1 – Introduction

This chapter presents the general perspectives of the issues covered in this thesis. The research question that the work addresses is detailed, and the motivations behind this are outlined. The aims and objectives of each chapter are summarised, and the novelties are highlighted. Finally, an overview of the structure and layout of the thesis is provided.

1.1 General Perspectives

It has always been a fundamental aim of the naval architect to design hull vessels with efficient hull forms. While it is not always integral to a vessels operation that the resistance is minimised, it is beneficial in almost all cases. In recent years the global community has seen a shift toward becoming more environmentally responsible, notably with the adoption of the Paris Agreement (United Nations, 2015). Within the marine sector measures such as the compulsory Energy Efficiency Design Index (EEDI) and voluntary Energy Efficiency Operational Indicator (EEOI)) shows commitment toward this goal. The combination of new regulations and the societal shift toward becoming environmentally responsible results in an even greater need to design efficient hull forms across the entire marine industry.

While the emissions of small, planing vessels are considerably less significant than those produced by coastal and deep-sea shipping, there has still been notable progress by sector in recent years, and it is a topic of ongoing interest. Recent developments have seen some manufacturers turning to novel green technologies, such as batteries and hydrogen fuel cells. When less energy dense power sources such as these are employed the need for efficient hulls is amplified significantly to prevent a loss in performance.

Developing efficient planing hulls with reduced resistance characteristics is desirable for several reasons in addition to the reduction in emissions. More efficient hull forms will achieve a decrease in their operational costs, an attractive prospect for all operators. They may also allow vessels to meet strict speed and range requirements, as is often imposed by military, coast guard and law enforcement clients, as well as the private sector.

One of the most effective solutions to reduce the resistance of a planing hull is through the incorporation of steps to the hull. Steps take the form of transverse discontinuities behind each of which there are air inlets, and the hull is elevated. A triple-stepped hull is detailed in Figure 1.1, however several Stepped Hull configurations exist. These steps should be located aft of both the vessels centre of gravity and centre of pressure.

When a stepped vessel is operating in the planing regime, the high-speed flow aft of each step results in a low-pressure area that draws air in through the inlets at the side of the hull. This causes the flow on the underside of the hull to separate at each step, reducing the wetted area of the vessel. It has been shown that the inclusion of steps is capable of producing a decrease of 10-15% in the hydrodynamic resistance (Loni *et al.*, 2013). The incorporation of steps to a planing hull typically leads to an increase of 6 – 10 knots in speed for a given engine power (Sorensen, 2011).

Figure 1.1 - Triple-stepped hull (Navtek LLC)

The underlying theory explaining why stepped hulls experience a reduction in resistance is like that of any lifting surface. The highest-pressure is found at the leading edge, resulting in the largest portion of lift being generated in this region. The remainder of the surface produces comparatively little lift, contributing mostly to drag. By splitting the bottom of a hull into separate planing surfaces, the same amount of dynamic lift may be generated whilst reducing the amount of hull in contact with the water, therefore reducing the frictional drag component (Ghassemi, Kamarlouei and Veysi, 2015). This phenomenon is found in wing theory, where it is seen that that high aspect ratio foils to have better lift to drag ratios that low aspect ratio foils. The introduction of steps essentially turns a planning hull from one low-aspect ratio lifting surface, into multiple connected high-aspect ratio lifting surfaces (Sorensen, 2011).

While the reduction in resistance is generally the primary advantage of stepped hulls, they also experience increased longitudinal stability (Veysi *et al.*, 2015) due to the fact that lift is generated by multiple surfaces (Danielsson and Strømquist, 2012). As the pivot point of an unstepped hull is located at the transom, there is little to resist pitching when an outside excitation force, such as a wave, acts upon the vessel. The introduction of steps moves this pivot point forward to the step, with the entire aft portion of the hull acting to dampen pitch motions (Peters, 2010). As a result, stepped hulls are more stable in rough water (Dashtimanesh, Tavakoli and Sahoo, 2017), providing a better work platform from which to carry out operations. Slamming is prevented and fatigue on the crew is reduced. Stepped hulls are less sensitive to changes in the longitudinal centre of gravity (Danielsson and Strømquist, 2012), reducing restrictions on the weight distribution of their outfit (Svahn, 2009) and resulting in a more versatile vessel. A final advantage to the increased longitudinal stability is that stepped hulls are less prone to the self-exited, oscillatory longitudinal instability known as porpoising (Savitsky and Morabito, 2010).

Stepped hulls do, however, face a number of drawbacks and can be dangerous if they are poorly designed. Accidents occur when there is a sudden loss of directional stability, or 'spin-out' (Morabito *et al.*, 2014). One cause of this the submerging of an air-inlet during a tight turn or in wavy conditions, resulting in 'back-flow' and a sudden increase in resistance one side of the vessel. A second cause of spin outs is the change in the longitudinal centre of lateral resistance due to the reduced wetted area at the aft portion of the hull. In an aggressive turn the aft section may ‘lose grip’ of the water and overtake the rest of the vessel (Sorensen, 2011). While solutions exist to both these causes, they require careful consideration during the design process.

The dangers associated with poorly designed stepped hulls resulted in a lack of demand for stepped hulls in the consumer market until more recent years, with their application limited to racing powerboats where the reward outweighed the risks. Well-designed step configurations ensure the vessel does not experience any of these drawbacks, as was pointed out by (Morabito *et al.*, 2014). Despite this, the lack of demand, coupled with the considerable increase in design complexity, construction difficulty and cost, and general lack of knowledge and experience on the topic has resulted in a lack of research being conducted upon stepped hulls until recently. In 2005 it was concluded by (Clement, 2005) that “calculation methods [for stepped hulls] are non-existent”. This conclusion was drawn again in 2009 by (Svahn, 2009), in 2013 by (Loni *et al.*, 2013). Even as recently as 2015 (Ghassemi, Kamarlouei and Veysi, 2015) stated ‘there is no adequate method for performance prediction of stepped hulls yet’.

Whilst high-speed hulls have always been of interest to naval architects, substantially less time and resources have been invested into their research and development than larger, more commercially exploitable topics. In recent years however, there has begun a steady progression in the available work researching high-speed hulls. Notably, as is the case across the board with all topics relating to naval architecture, this has been facilitated through the numerical studies using CFD to model the complex flow.

The use of CFD as a tool for the hydrodynamic assessment of ships has grown considerably in the past 20 years. This is accountable to advancements in the power and availability of computational resources, leading to the development of more accurate CFD codes. Users have become more confident employing CFD as it has become more reliable and established as a design tool, and the accuracy of marine CFD has improved considerably, with an error of less 4% being typical for conventional vessels (Larson, Stern and Visonneau, 2014). With such high confidence levels in the results and the flexibility offered by a numerical workflow it is undeniable that CFD is becoming an ever more important tool in the design process of conventional ships.

With the clear potential offered by CFD and the lack of available research regarding stepped hulls despite their notable benefits, especially in the context of improving hull efficiency to facilitate the use of more environmentally friendly power solutions, this thesis sets out to answer the following research question:

"How can we enhance and accelerate analysis techniques for stepped hulls through knowledge developed from numerical simulations and can hydrodynamic performance be improved through the application of these tools."

This research in this thesis applies state-of-the-art numerical methods, and the capabilities of High-Performance Computing to the analysis of stepped hulls. It looks to develop the understanding of stepped hulls by conducting CFD studies, determining the effects that the addition of steps has upon the performance of a planing hull, investigating the mechanisms through which stepped hulls achieve a reduction in resistance and establishing the conditions in which it is beneficial to include steps. Comprehensive analysis of the fluid flow under a stepped hull will be carried out, developing understanding of the free surface elevation as the flow separates aft of a step. The composition of the wetted area is investigating for different step configurations, with the components of flow that are responsible for each wetted section being identified. The knowledge and understanding that is developed over the course of this numerical analysis is then applied to develop mathematical models for the performance prediction of single and double-stepped planing hulls, aiming to address the limitations and enhance the accuracy of those currently available in the literature. Finally, the enhanced analysis techniques that are developed over the course of this research are applied to investigate how the hydrodynamic performance of single and double stepped hulls may be improved. The design trends that lead to a reduction in resistance are established and the relationships between design parameters are detailed, allowing the knowledge to be employed by designers of stepped hulls.

Throughout this thesis, the commercial CFD software Star-CCM+, version 13.04.011, developed by Siemens Digital Industries Software, is employed as the unsteady RANS solver. The ARCHIE-WeST High-Performance Computing (HPC) facilities at the University of Strathclyde leveraged to reduce the time it takes to run the complex simulations. This cluster comprises of 64 Lenovo SD530 nodes with 192GB of RAM per node (4.8GB per core). Each node has 40 cores, powered by Intel Xeon Gold 6138 (Skylake) processors @2.0GHz.

1.2 Motivations behind this Work

Before detailing the overall aims and specific objectives of this thesis, an overview of the general motivations behind the research conducted in each chapter is presented. In addition, a brief demonstration of the how each of these studies addresses a gap in the literature is provided.

- To properly take advantage of stepped hulls the mechanisms through which they achieve a reduction in resistance must be properly understood. It is necessary to determine how the introduction of steps effects the performance of a planing hull across the full speed range to evaluate when steps may be considered beneficial to the hulls operational profile. Single and double stepped configurations must be considered to determine the differences and understand the impact that these decisions has on the pressure and shear components of resistance, as well as how it impacts the equilibrium position of the hull. (Chapter 3)

- Without reliable CFD simulations it is not possible to take advantage of this rapidly developing technology to conduct meaningful analysis. While it has been shown that CFD for conventional hulls is robust and accurate, CFD for high-speed hulls is significantly less reliable (ITTC Specialist Committee on CFD in Marine Hydrodynamics, 2014). Developing numerical set-ups that improve accuracy allows more confidence to be placed in the results and broadens the scope of research that may be conducted using these tools. Exploring the use of more computationally expensive wall treatments to resolve the entire near wall turbulent boundary layer offers a promising means by which this may be achieved. Another means by which greater confidence may be placed in CFD of planing hulls is by developing understanding sources of error such as Numerical Ventilation (De Luca *et al.*, 2016; De Marco *et al.*, 2017a) and quantifying their effects on accuracy. (Chapter 3)

- Researchers attempting to develop an analytical performance prediction method for stepped hulls have reported significant inaccuracies introduced to their models through an inability to accurately model the freesurface elevation aft of each of the steps (Dashtimanesh, Tavakoli and Sahoo, 2017). Modelling this flow is integral to accurately determine the wetted area of the afterbody. Two methods have been proposed for this purpose, the Savitsky Wake Equations (Savitsky and Morabito, 2010) and the Linear Wake Assumption (Danielsson and Strømquist, 2012), however, there has been no evaluation of their accuracy in comparison to experimental or numerical data of the flow as it separates aft of a step. (Chapter 4)

- It is highlighted by (Dashtimanesh, Tavakoli and Sahoo, 2017) that there exists an urgent need to conduct extensive experiments to extract the flow pattern under a stepped hull. There is a distinct lack of experimental data or analysis for the flow in this region due to difficulties in measuring it. CFD offers an attractive solution to this, allowing the extraction and analyses the flow pattern from under single and double stepped hulls. (Chapter 4)

- While CFD is becoming an increasingly relied upon too, mathematical models for performance prediction that are accurate, simple and rapid remain valuable design tools, allowing prospective designs to be evaluated quickly and easily without the need for specialist training or facilities. At several points over the past 20 years, authors have concluded that no adequate method for performance prediction of stepped hulls yet exists (Clement, 2005; Svahn, 2009; Loni *et al.*, 2013; Ghassemi, Kamarlouei and Veysi, 2015). Existing models are incapable of fully accounting for the physical wetted area or flow patterns of stepped hulls in a satisfactory manner, further decreasing their accuracy and applicability. (Chapter 5)

- Improving the hydrodynamic performance of stepped hulls allows naval architects to fully take advantage of these highly efficient hull forms. Cases in which stepped hull are considered generally have speed or range design requirements which are achieved through the reduced resistance of the hull form. The ability to improve the performance of these hulls helps them meet, and even exceed the increasingly stringent requirements of the incorporation of green power sources. Developing design trends and relationships between the key design variables offers a promising source of information that may be applied by designers in the preliminary design phases to quickly improve the performance of a prospective hull. (Chapter 6)

1.3 Research Aims and Objectives

The main aim of this thesis is to develop enhanced analysis techniques for stepped hulls and apply these tools to determine how the hydrodynamic performance may be improved. The specific objectives of this thesis have been formulated to address the issues highlighted in the motivations and are stated as follows:

- To **conduct** a review of the available literature on analysis and performance prediction of unstepped and stepped planing hulls
- To **enhance** the accuracy with which stepped and unstepped hulls may be modelled by unsteady RANS simulations, employing this tool to **develop** understanding of the flow characteristics of stepped hulls
- To **quantify** the effects of Numerical Ventilation and **develop** understanding of how the phenomena influences the results of a simulation
- To **evaluate** the effects that the introduction of steps has upon the performance of a planing hull and **investigate** the mechanisms through which a reduction in resistance is achieved
- To **extract** and **analyse** the fluid flow as it separates aft of a step, investigating the accuracy of various means of modelling this
- To **enhance** the knowledge of the composition of the wetted area of a single and double stepped hulls, **proposing** procedures to calculate each wetted component
- To **propose** and **evaluate** novel semi-empirical performance prediction methods through the application of the developed understanding of the flow characteristics of stepped hulls
- To **improve** the hydrodynamic performance of stepped hulls through the application of the tools developed by this research
- To **determine** design trends and relationships that may be applied universally to improve the performance of stepped hulls

1.4 Structure of Thesis

The structure of the thesis is summarised briefly in the present section.

- Chapter 2 (CRITICAL REVIEW) presents a detailed literature survey on the modelling of hydrodynamic performance of stepped and unstepped planing hulls. It first outlines historical developments before focusing upon modern techniques and the application of CFD. The chapter goes on to present a literature survey on topics specific to each of the main chapters of this thesis.

- Chapter 3 (NUMERICAL MODELING OF UNSTEPPED, SINGLE-STEPPED AND DOUBLE-STEPPED HULL VARIANTS) presents a CFD-based unsteady RANS study evaluating the performance of unstepped, single stepped and double stepped hulls. Approaches that improve the level of confidence that may be placed in CFD of high-speed hulls are investigated, though increasing the accuracy and quantifying the effects of one of the largest sources of error. The effects of the addition of steps to a planing hull is investigated and discussed in detail, revealing the mechanisms through which a reduction in resistance is achieved. The results are validated against available experimental data and are shown to be in better agreement than state-of-the art studies reported in the literature.

- Chapter 4 (EXPERIMENTAL AND NUMERICAL ANALYSIS OF FLUID FLOW AS IT SEPERATES AFT OF A STEP) presents an investigation into the freesurface elevation of the fluid as it separates aft of a step, and the interaction of forebody flow with the mid and afterbodies. Experimental data is developed to validate the accuracy of CFD in this application, after which the CFD tool developed in the previous chapter is employed to evaluate the flow of single and double stepped hulls. Analytical methods of calculating the freesurface elevation are quantitively analysed in relation to the CFD data, with conclusions on their applicability being drawn.

- Chapter 5 (DEVELOPMENT OF AN ANALYTICAL MATHEMATICAL MODEL FOR THE PERFORMANCE PREDICTION OF STEPPED HULLS) novel semi-empirical models are proposed for the performance prediction of single and double stepped hulls and evaluated in comparison to experimental and numerical data. These models build upon performance prediction models that have been previously published, seeking to enhance their accuracy and range of applicability. The proposed models draw upon the knowledge of interaction of forebody flow with the mid and afterbodies developed in the previous chapter, implementing novel procedures for the calculation of wetted surfaces and the fluid forces acting upon these. Significant improvements in accuracy are shown in comparison to existing models.

- Chapter 6 (A STUDY INTO IMPROVING THE HYDRODYNAMIC PERFORMANCE OF STEPPED HULLS) presents an investigation into how the hydrodynamic performance of single and double stepped in calm water may be improved. The CFD and novel semi-empirical model developed in the previous chapters are coupled with an automated optimisation workflow to determine how much the performance may be improved, as well as to develop large data sets, evaluating thousands of prospective designs. Analysis of these data sets reveals trends and relationships that reduce the resistance of stepped hulls, and which may be universally applied by designers of stepped hulls to improve performance.

- Chapter 7 (CONCLUSIONS AND FURTHER RESEARCH) presents a discussion of how the work conducted over the course of this thesis has contributed to the existing knowledge, highlighting key findings and providing an assessment on the degree to which the aims and objectives set out in the present chapter have been addressed. Additionally, it goes on to suggest interesting topics for future work that have become apparent.

Chapter 2 – Critical Review

Research into the hydrodynamic analysis and performance prediction of stepped and unstepped is discussed and reviewed in this chapter. The historical development of research into these topics is presented to give context to the work conducted in this thesis, after which a literature survey into the specific topics researched by this thesis is presented.

2.1 Introduction

Several studies have been published that set out to investigate the hydrodynamic performance of high-speed planing hulls. The modelling of such vessels is a complex task, however the ability to do this is vital in the design process. In general, these analysis tools can be classified into four categories: experimental tank tests, empirical methods, analytical methods and state-of-the-art fully nonlinear unsteady RANS computations.

The application of these tools to stepped and unstepped hulls is detailed. Specific attention is given to the development of Computational Fluid Dynamics techniques for these hulls, and the of accuracy of that these achieve. The available knowledge on the interaction of the fluid as it separates at the step and interacts with the after bodies is detailed, and the development of mathematical performance prediction models is reviewed. Finally, advancements that have been made with the goal of improving performance are detailed.

This critical review sets out to assess the available literature, detailing the research that has been conducted to date while highlighting areas which are lacking and worthy of further investigation. Additionally, it tries to frame the studies undertaken in this thesis in the broad context of the available literature so that the need for each of them is apparent, and their contribution and value to the research community is understood.

2.2 A Historic Overview of the Hydrodynamic Analysis of High-Speed Vessels Through Experiments

This section gives an overview of the experimental studies and research progression for stepped and unstepped hulls. It provides a background into the research conducted of these hulls, aiming to provide the reader with a baseline understanding and timeline of the research interest in these hull forms. This section is intended to give context to the topics that are reviewed in the following sections.

2.2.1 Experiments on Planing Surfaces

Fundamental research into the hydrodynamics of planing surfaces began in the early 1900's, motivated by developing the hydrodynamic understanding of seaplane floats. One of the earliest experimental studies into the properties of prismatic planing surfaces was conducted by (Baker, 1912). Famously, the work of (Von Karman, 1929) may be considered the first steps toward the mathematical modelling of planing surfaces, as he proposed a method of calculating the force on a vertically impacting wedge. This was built upon and improved by (Wagner, 1931, 1932) in which a relation based upon potential flow theory for the pressure distribution of the wedge water entry problem was developed. Experimental work continued with (Sottorf, 1934) conducting a systematic exploration of flat planing surfaces, while (Shoemaker, 1934; Sambraus, 1938; Sedov, 1947; Locke, 1948), accumulating a large set of experimental data for the hydrodynamic characteristics constant deadrise prismatic surfaces.

2.2.2 Experiments on Planing Hulls

The early experimental studies of flat plates and simple prismatic deadrise surfaces developed into more comprehensive investigations of planing hulls. Several systematic series were published, studying the effect of the design variables upon performance. Notably there was the Series 50 study of (Davidson and Suarez, 1949) and the TMB Series 62 of (Clement and Blount, 1963), which was extended by (Keuning and Gerritsma, 1982) and (Keuning and Terwisga, 1993) to further investigate the effects of deadrise. (G. Fridsma, 1969) made significant contributions to the seakeeping performance of planing hulls, publishing the first systematic series of model tests for regular waves. The Naples Systematic Series (NSS) by (De Luca and Pensa, 2017) is the most recent systematic series, developed to fulfil the ITTC Resistance Committee request that new benchmark data for validation of numerical simulations. The series was extended by (De Luca and Pensa, 2019) to consider the seakeeping performance in irregular head seas.

Of particular interest to the work presented in this thesis is the work of (Taunton, Hudson and Shenoi, 2010) who publish calm water performance data for a new series of high-speed hard chine planing hulls. This series is representative of modern high speed hull forms and is one of the only publicly available datasets the examines single and double stepped hull variants of the parent hull. The study extended by (Taunton, Hudson and Shenoi, 2011) to address the lack of availability of seakeeping data for systematic series of high-speed planing vessels.

In addition to these studies of systematic series of planing hulls, researchers have investigated many other aspects and factors affecting the performance and hydrodynamic characteristics of planing hulls over the years. Experimental investigations into the proposing phenomena were undertaken by (Day and Haag, 1952; Celano, 1998), developing empirical relations for its prediction. Work was carried out to investigate the effect of a heeled planing hull by (Savitsky, Prowse and Lueders, 1958), generating limited equations from the experimental data. This was one of the early studies focusing upon the instability of planing hulls, however, in the 1990's interest in this increased. (Brown and Klosinski, 1994b, 1994a) performed direct stability tests on three prismatic planing hulls. (Ikeda, Katayama and Okumara, 2000) experimentally measured the hydrodynamic derivatives of a planing hull through Planar Motion Mechanism (PMM) tests, concluding that yaw and roll angles influence the hydrodynamic forces of the hull. (Katayama, Iida and Ikeda, 2006) went on to investigate the loss of stability a planing hull is subject to during turning motion.

(Morabito, 2015) measured the sway force acting upon the bottom of a planing hull experimentally in order to validate a semi-analytical approach. Numerous other experimental studies are available investigating aspects of planing hulls, such as the pressure resistance component of a planing hull (Latorre and Tamiya, 1975), the effects of operating in shallow water (Reyling, 1976), the flow around a planing hull and its the wave pattern (Latorre, 1982), the spray pattern and the frictional component of resistance (Latorre, 1983), and the nearfield longitudinal wake profile (Savitsky and Morabito, 2010; Gray-Stephens, Tezdogan and Day, 2020a). Some authors have gone as far as conducting full-scale seakeeping experiments and comparing these to model-scale experiments (Judge and VanDerwerken, 2019).

It can be concluded that over the years considerable time and effort has been invested in the experimental analysis of unstepped hulls. Despite this, they remain a very active area of research, with several novel studies being published in recent years.

2.2.3 Experiments on Stepped Hulls

The first documented proposal for a stepped hull was that of Reverend C. M. Ramus in 1872, for a vessel 370 ft in length with a 2500 ton displacement and zero deadrise. The proposal was experimentally tested by (Froude, 1872) at the Torquay Towing Tank, however the investigation was not successful, finding the hull resulted in higher resistance than the conventional hull forms.

As petrol powered engines were developed in the early 1900's, so too were planning and stepped hulls. Notably these vessels were built for the Gold Cup and Harmsworth powerboat races in which speed was the only goal, resulting in the development of the first hydroplane hulls. From 1915 – 1940 there was a global uptake in the motor torpedo boats and fast patrol boats, many of which featured stepped hulls. The performance of these early vessels however, varied considerably with several being very inefficient.

Research on the application of steps to planing surfaces was continued by the National Advisory Committee for Aeronautics investigating the hydrodynamic properties of seaplane floats, looking to determine how take off may be made easier through the resistance reduction resulting from the steps. Systematic studies resulting from these investigations were published by (Parkinson, Olson and House, 1939) and (Kapryan and Clement, 1949).

Theoretical discussion with respect to the use of cambered surfaces for stepped hulls and the potential impact upon performance was published by (Clement, 1969) and (Clement, 1979). Model test data that was relevant to stepped hulls remained very limited in 1991, with the majority of data stemming from research into seaplane float performance, as highlighted by (Clement and Koelbel, 1991). (Filing, 1993) conducted one of the first experimental studies of a single stepped planing hull. Both free and fixed model experiments were conducted, investigating the hulls equilibrium position as well as the contribution of the fore and aft hulls to the forces and moment. (Gassman and Kartinen, 1994) went on to continue this study, investigating the effect of step location and the longitudinal centre of gravity location. (Becker, Loreto and Shell, 2008) conducted tests focusing upon stepped hulls in the pre-planing regime, finding that under these conditions the step type had little impact upon the speed at which separation occurs. They concluded that stepped hulls are not beneficial until higher speeds.

(Taunton, Hudson and Shenoi, 2010) published the first systematic series of planing hulls that included a single and double stepped variant. Notably, the complete data set and model geometry was made publicly available, making the results suitable for validation of numerical and mathematical models. This was one of the first instances of an experimental study testing a double stepped planing hull. The results showed stepped hulls significantly reduced the resistance of directly comparable planing hulls. (Taunton, Hudson and Shenoi, 2011) went on to extent this study, testing all the models in regular waves.

In more recent years (Garland, 2011) tested an unstepped and an adjustable stepped model, setting out to gain insight into the advantages and disadvantages of operating stepped hulls across the range of speeds. (Miranda and Vitiello, 2014) undertook model experiments and full-scale sea trial tests upon a two stepped hull to analyse the propulsive performance characteristics of a stepped planing vessel powered by an outboard engine. (Lee, Pavkov and Mccue-weil, 2014) set out to develop the understanding of how step configuration and displacement effect the performance of a double stepped hull, investigating seven different step configurations in calm water. (De Marco *et al.*, 2017a) conducted towing tank tests in calm water for the model of a single-step hull model which was intended to be the first model of a new systematic series consisting of 8 hulls, however at this time the series remains unpublished.

It is apparent that stepped hulls have received significantly less attention than unstepped hulls, with limited experimental studies being published to date. (De Marco *et al.*, 2017a) point out the lack systematic series of model tests of stepped hulls and (Dashtimanesh, Tavakoli and Sahoo, 2017) highlight the fact that there '*exists an urgent need for conducting more experimental tests on stepped hull*s.' This is specifically in relation to the flow associated with a stepped hull and wake pattern aft of each step. In addition to this assertion, (Najafi *et al.*, 2019) noted that there was an evident lack of study on wetted surfaces of the stepped planing hulls. The author set out to address this through an experimental study in which the forebody and afterbody wetted areas are qualitatively analysed through use of underwater photographs.

It is clear that research into stepped hulls is considerably less mature than research into planing hulls, however there is seen to be a growing interest in recent years with an increase in the number of experimental studies.

2.3 Hydrodynamic Analysis of Planing Hulls through CFD

As computer technology progressed methods were developed of resolving 3D nonlinear problems and taking into account the fully viscous flow around a body using Computational Fluid Dynamics. By utilising CFD methods the full Navier-Stokes Equations are solved for the fluid in the domain. A number of techniques have been developed to deal with the turbulent aspect of such flows, of which Reynolds Averaged Navier Stokes (RANS) is the most computationally efficient and is viewed as the most applicable method for most marine CFD applications. This approach relies upon Reynold's decomposition, in which an instantaneous quantity is decomposed into time-averaged and fluctuating quantities. When RANS is employed the phase-averaged conservation of mass and momentum equations are coupled with statistical models to determine the unresolved turbulence. The present section reviews the use of RANS based CFD to study high speed hulls.

2.3.1 Early CFD Analysis of Planing Hulls

In 1994 a CFD workshop was organised to discuss the implementation of steady RANS methods to solve free-surface flows around ships. Following this workshop RANS methods have been applied to several marine hydrodynamics problems. As the technology developed and computational resources become more widely available, the use of CFD has been seen to increase significantly.

One of the first applications of CFD to study the hydrodynamics of a planing hull was undertaken by (Caponneto, 2001). Three trim angles and three sinkage's were simulated for each speed, with quadratic interpolation of the results being used to determine the final running trim of the hull. This was a rather rudimentary study by today's standards, with a mesh of only 230,000 cells and a single iteration per timestep, however the study demonstrated the potential of CFD in this application. (Azcueta, 2003) went on to present the results of quasi-steady and unsteady simulations of a prismatic hull in calm water and regular waves, modelled using the commercial solver COMET. The software was coupled with a 6 DOF body motion module to calculate the positioning of the hull in relation to the hydrodynamic forces acting upon it. The coupling of the CFD solver to the motion solver was a significant progression, further developing and showcasing the potential of this technology.

Further work was published by (Brizzolara and Serra, 2007) showing CFD was capable of calculating the resistance of a wedge shaped prismatic hull with an average error of 10% when compared to experimental data. In this study the hull was fixed in trim and sinkage. Whilst further demonstrating that CFD could be applied to planing hulls with reasonable accuracy, the technology was still not at a level where it was practical to study the performance of planing hulls. Instead, the research focused upon the application of CFD to planing hulls.

It was pointed out by (Brizzolara and Villa, 2010) that despite the fact that naval architecture community has started to intensively apply CFD methods in the steady and unsteady analysis of ships, there was still only a few available examples in which planing hulls were studied. This was due to the physical hydrodynamic complexity of the planing problem and the lack of confidence that may be expected of the numerical results. In the years that followed there was considerably more interest in the use of CFD to model planing hulls, and the accuracy and reliability of such simulations improved considerably, as will be summarised in the following section.

2.3.2 Accuracy of CFD as Applied to Planing Hulls

This section sets out to review the levels of accuracy with which previous numerical studies were able to model planing hulls. A summary of the available literature over the past ten years is presented by Table 2.1.The errors detailed are the average error between the CFD results and the validation data reported in the studies.

Table 2.1 - Summary of numerical studies investigating unstepped planing hulls

Publication	Year	Resistance Error	Sinkage Error	Trim Error
Numerical simulation of a planing vessel at high speed (Su *et al.*, 2012)	2012	15%	n/a	15%
Toward numerical modelling of the stepped and non-stepped planing hull (Veysi *et al.*, 2015)	2015	~ 10%	n/a	n/a
An Extended Verification and Validation Study of CFD Simulations for Planing Hulls (De Luca *et al.*, 2016)	2016	7.50%	3%	11%
Towards CFD guidelines for planing hull simulations based on the Naples Systematic Series (Mancini, de Luca and Ramolini, 2017)	2017	7%	n/a	16%
Effects of Loading Conditions on Hydrodynamics of a Hard-Chine Planing Vessel Using CFD and a Dynamic Model (Kazemi and Salari, 2017)	2017	> 5%	n/a	19.36%
Numerical Calculations of Resistance and Running Attitude of a Planing Hull (Kahramanoglu, Yildiz and Yilmaz, 2018)	2018	7%	9%	25%
On hydrodynamic analysis of stepped planing crafts (Najafi and Nowruzi, 2019)	2019	7%	n/a	n/a
Hydrodynamic evaluation of a planing hull in calm water using RANS and Savitsky's method (Khazaee, Rahmansetayesh and Hajizadeh, 2019a)	2019	2.77%	9.17%	12.01%
Numerical Modelling of a Planing Craft with a V-Shaped Spray Interceptor Arrangement in Calm Water (Lakatoš *et al.*, 2020)	2020	7%	10%	16%
Inhibition and Hydrodynamic Analysis of Twin Side-Hulls on the Porpoising Instability of Planing Boats (Wang *et al.*, 2021)	2021	10.26%	8.73%	4.06%

Table 2.1 shows the average reported resistance error has been decreasing gradually in recent years as researchers gain experience, and software developers enhance the capabilities of commercial CFD packages. Average resistance errors of 15% were reported in 2012 (Su *et al.*, 2012), decreasing to approximately 10% in 2015 (Veysi *et al.*, 2015). The ITTC stated that mean prediction error of less than 10% could be achieved compared to the model-scale and full-scale test results in 2014 (ITTC Specialist Committee on CFD in Marine Hydrodynamics, 2014). (De Luca *et al.*, 2016) decrease this further, concluding that '*simulations of the planing crafts were critical with respect to the displacement hulls. Nevertheless, the comparison error for CT was reduced, reaching values lower than 7.5% (instead of the 10.0% declared in ITTC [2014])*'. While the average error for this study was 7.5%, the authors reported a range of resistance errors from 3.7% - 9.3%, showing that despite the improvements there are still significant challenges in developing simulations of planing hulls. Following the study by De Luca, a number of other authers presented results with a similar level of accuracy, indicating that a mean resistance error of around 7% was attainable (De Marco *et al.*, 2017b; Mancini, de Luca and Ramolini, 2017; Kahramanoglu, Yildiz and Yilmaz, 2018; Lakatoš *et al.*, 2020). Despite this apparent increase in the expected accuracy, it should be noted that this is still a developing topic and the confidence in achieving this level of accuracy is not as high as for conventional vessels, with authors still reporting average errors as high as 10.26% (Wang *et al.*, 2021).

(Khazaee, Rahmansetayesh and Hajizadeh, 2019a) reported the lowest prediction error for resistance, with a mean value of 2.77% for their numerical simulation of Hull C as experimentally tested by (Taunton, Hudson and Shenoi, 2010). This is a considerable improvement upon previously reported errors for the resistance prediction of planing hulls. Unfortunately, further analysis of the study has raised some concerns as to the validity of this result. The simulation was run on a mesh of 950,000 elements, considerably smaller than the majority of the work presented in the literature, where a mesh of several million elements is the norm for such problems. The study was run on a system with a 3.1 GHz Intel ® Core™ i5 processor with 4 GB of RAM, so lack of computational resources was likely a limiting factor. Of significantly more concern is the selection of timestep of 0.01s, which is larger than the ITTC's recommendation of 0.005s as a maximum (ITTC - Recommended Procedures and Guidelines, 2011). There is no timestep study to justify this choice of timestep, or to assess the resultant numerical errors due to the temporal discretisation. A final concern that was raised whilst reviewing this study is that there appears to be signs of Numerical Ventilation in the presented VOF plot of the hull. There is not only centre line streaking, but also secondary side hull patches. As will be discussed, Numerical Ventilation is one of the largest sources of error in CFD simulations of planing hulls and has the effect of artificially decreasing the calculated resistance by altering the fluid properties in the near wall cells. It is apparent from studying the literature that the resistance calculated by CFD is typically high for planing hulls, and the presence of Numerical Ventilation would artificially lower this error. While none of these concerns invalidate the study, they do mean that the results should be treated with caution and the expectation of resistance errors below 3% for planing hulls should not made until this level of accuracy is confirmed by further studies.

(Kazemi and Salari, 2017) reported the second lowest prediction error for resistance, stating that the resistance error was below 5% for all validation cases. For this study there were only three validation cases with a speed range of $8.05ms^{-1} - 11.50ms^{-1}$, where each of the cases featured a different loading condition. While this study shows the potential accuracy of CFD it only presents errors for a small snapshot of the speed range that is applicable. Several of the other studies presented in Table 2.1 acheived very high levels of accuracy for certain speeds, but the accuracy is brought down by increased errors or different speeds across the full range studied. (Wang *et al.*, 2021) is a good example of this, presenting a comparison of numerical results against experimental data for 12 speeds in the range of Froude numbers 0.42 – 2.52. For one case the resistance error was 0.20%, however, as the speed increased so too did the error until a maximum of 18.15%. Due to the limitation of validation cases to three conditions it is not possible to conclude from (Kazemi and Salari, 2017) that marine CFD of planing hulls has reached a level where mean errors of below 5% can consistently be achieved.

There is considerably less focus and discussion on the accuracy of the sinkage and trim results in the literature, with the key metric of most studies being the resistance. It is apparent that these parameters are far more sensitive and more difficult to model numerically for planing hulls. In Table 2.1 is seen that trim is often the least reliably calculated parameter, at times resulting in an average error of over 20%, while sinkage errors of 10% are not uncommon. Due to the small nature of these parameters in absolute terms, where a typical running trim is 2° and the sinkage in model scale is in the order of mm, it is perhaps not surprising that these values are subject to larger percentage errors than the larger resistance values. (De Luca *et al.*, 2016) points out that errors in the evaluation of resistance may be closely linked to the errors in the evaluation of running trim, reasoning that it is well known and observed that simulations of planing hulls are often less capable of accurately computing trim, and there is a strong correlation between dynamic trim and resistance at high speed. This relationship was reported by (Sottorf, 1934), and states that the total resistance contains a component of induced resistance attributable to both the lift force and the viscous resistance of the hull, where this induced component of resistance varies closely with the trim of the hull. Additionally, for small angles the viscous component is influenced by trim as a result of variations in the wetted surface. As a result, the incorrect calculation of a vessels trim introduces errors into both components of resistance. De Luca also points out that the difficulties in the calculation of trim arises as a result of difficulties in determining the canter of pressure, or more generally the pressure distribution over the entire hull bottom, which is affected significantly by edge effects and the hydrodynamic lift.

The current state of affairs is summarised well by (De Luca *et al.*, 2016), stating that it is possible to reduce the average resistance comparison error to values below 7.5%.

This level of accuracy is confirmed by a number of papers modelling planing hulls over a broad speed range. There are indications from a number of studies that a higher degree of accuracy is attainable for specific speed cases, however, developing a simulation that is capable of maintaining this accuracy over a broad range of speeds is problematic. Most studies are able to attain a sinkage error of >10%, while by far the most significant level of error lies in the calculation of trim, where errors of up to 20% are not uncommon. (Mancini, de Luca and Ramolini, 2017) concludes that results with this level of error may be considered to show good agreement with experimental data, pointing out that while there is room for improvement with comparison errors in the range of 0-20%, they may be considered satisfactory given the complex nature of the problem and the history of CFD simulations of planing hulls.

2.3.2.1 Numerical ventilation in CFD Analysis of Planing Hulls

With the increase in the use of numerical simulation of planing hulls, one of the issues of employing CFD for this application was uncovered. This was the phenomena of Numerical Ventilation, which occurs when the when the free surface interface is not properly captured properly. This results in air being transported under the hull in the near wall cells, changing the properties of the fluid and introducing error into the results of the simulation. The presence of this air is a result of a modelling error and is not physically representative of the real-world situation. (Viola, Flay and Ponzini, 2012) was one of the first publications to discuss Numerical Ventilation, noting that although the phenomena was well known to CFD users and vendors it has rarely been mentioned or discussed in scientific publications. (Böhm and Graf, 2014) reason that the lack of discussion on this topic is attributable to the fact numerical ventilation only occurs with specific bodies for which there is a scarcity of ongoing research. Böhm presented a a review of the Volume-of-Fluid method may lead to interface smearing, proposing modifications to the interface capturing model to reduce the effects of Numerical Ventilation. (Olin, 2015) encountered Numerical Ventilation in his study of the numerical modelling of spray formation on planing hulls, finding that mesh refinement played a role in the level of Numerical Ventilation. Both (De

Luca *et al.*, 2016) and (De Marco *et al.*, 2017a) agree that Numerical Ventilation may considered one of the main sources of error in numerical simulations of planing hulls. It is apparent that this is not a factor that is considered by several authors as the literature revealed several publications in which numerical ventilation was clearly visible in the presented VOF plots.

2.4 Hydrodynamic Analysis of Stepped Hulls through CFD

Much like the experimental research of stepped hulls it was found that the numerical studies of stepped hulls were not yet at the same level as those of unstepped planing hulls. The use of CFD in this regard is reviewed in the following section.

2.4.1 CFD Analysis of Stepped Hulls

The first example of a RANS solver being applied to the problem of a stepped hull was the study conducted by (Garland, 2012). Despite the fact that realistic planing hulls were being simulated with free sink and trim by 2012, this initial study into CFD for stepped hulls simplified the problem to a 2D static one. This simplification reduce the large number of challenging flow features that must be modelled to simulate a stepped hull, while demonstrating the potential of the technology.

A three-dimensional stepped hull was numerically modelled by (Veysi *et al.*, 2015), who set out to determine the effect of a step upon the hydrodynamic characteristics of a planing hull. The experimental data of (Taunton, Hudson and Shenoi, 2010) was employed as validation data of the set-up, showing the average resistance error was approximately 10%. This was once again a rather rudimentary CFD set up in comparison to the those employed for unstepped hulls at this time. The simulation was fixed in sinkage and trim (set to the experimental values) and was run as steady state. (Lotfi, Ashrafizaadeh and Esfahan, 2015) also employ a steady state simulation that is fixed in trim and sinkage, employing a procedure to calculate the final position of the hull by using three fixed-position simulations.

(De Marco *et al.*, 2017a) undertook what may be considered one of the most comprehensive numerical studies of stepped hulls to date, initially presenting the results of towing tank tests of a single stepped hull in calm water. The same geometry was then analysed using RANS and LES to solve the full unsteady flow equations, marching the numerical simulations in time with a pseudo-compressibility approach. The geometry was free to sink and trim, with Dynamic Free Body Interaction (DFBI) module of Star CCM+ being used to determine the forces acting upon the body, before solving the governing equations of body motion and relocate the body. This was the first hulls motion was modelled and the transient effects were considered, finally bringing the complexity of the CFD set up being used to the same level as was standard for unstepped hulls.

From this point in time onwards there was an increase in the research of stepped hulls that was conducted by CFD. (Du *et al.*, 2019) points out that the uptake of CFD methods for the study of stepped hulls occurred later than for conventional planing hulls due to the more complex nature of such hulls, especially in the capture of the water-air interface as the flow separates and reattaches aft of the step. (Dashtimanesh, Esfandiari and Mancini, 2018) undertook a three-dimensional numerical study into the performance of a double stepped hull using the implicit unsteady solver of Star CCM+. A morphing mesh approach was to deal with hull motion, coupled with the DFBI method. The study undertook a numerical evaluation of the effect of step upon the hydrodynamic characteristics of a hull. Key metrics such as lift, trim angle, resistance and wetted surface were compared to experimental data. The largest error of 15.52% was for the wetted surface, which was attributed to the fact that some fluid flow phenomena such as flow separation from steps, multiphase flow, and water spray behind the steps were not accurately modelled. (Kazemi *et al.*, 2019) investigated how hull configuration effects the hydrodynamic behaviour of stepped vessels, specifically looking at a single stepped hull operating under different displacements and LCG positions over a range of speeds. (Esfandiari, Tavakoli and Dashtimanesh, 2019) looked to investigate the performance of stepped hulls in rough water. A non-stepped and double stepped hull were numerically modelled for two different wave lengths to determine their dynamic responses.

(Du *et al.*, 2019) investigates the scale effect of a stepped planing hull, modelling at model scale and at full scale. (Vitiello *et al.*, 2020) continues investigating the use of full-scale CFD making comparisons with sea trial data of a double stepped hull, reporting a 17.3% average comparison error. Additionally, model test data of the vessel is extrapolated to full scale using the ITTC standard procedure, for which there is a 27.5% comparison error. CFD was shown to be the more reliable full scale analysis tool, however, the authors note that this application is far from mature and further studies are required. This is restricted by the availability and reliability of sea trial data for planing vessels.

Recently (Sajedi and Ghadimi, 2020) used CFD to investigate the longitudinal stability of planing vessels and how the addition of steps effects this. (Dashtimanesh, Tavakoli, *et al.*, 2020) developed the understanding of a single stepped hull in non-zero heel condition. Numerical simulations of the viscous flow around a heeled single stepped hull were undertake using Star CCM+ in order to evaluate the impact of asymmetric planing on the vessel's performance.

There has been a rapid development in the complexity of numerical simulations of stepped hulls since (De Marco *et al.*, 2017a) showed the technology to be accurate and robust in 2017. CFD is for stepped hulls is now at a level where it may be used to develop knowledge and improve performance, with reasonable levels of confidence being placed in the results.

2.4.2 Accuracy of CFD as Applied to Stepped Planing Hulls

This section sets out to establish the levels of accuracy with which previous numerical studies were able to model stepped hulls. A summary of the available literature over the past ten years is presented in Table 2.2.

Table 2.2 - Summary of numerical studies investigating stepped planing hulls

Publication	Year	Resistance Error	Sinkage Error	Trim Error
Toward numerical modelling of the stepped and non-stepped planing hull (Veysi *et al.*, 2015)	2015	~10%	n/a	n/a
Numerical investigation of a stepped planing hull in calm water (Lotfi, Ashrafizaadeh and Esfahan, 2015)	2015	5.25%	12.86%	30.62%
Experimental and numerical hydrodynamic analysis of a stepped planing hull (De Marco *et al.*, 2017c)	2017	9.60%	42.90%	12.80%
Performance prediction of two-stepped planing hulls using morphing mesh approach (Dashtimanesh, Esfandiari and Mancini, 2018)	2018	4.86%	n/a	8.85%
Hydrodynamics analysis of stepped planing hull under different physical and geometrical conditions (Kazemi *et al.*, 2019)	2019	> 5%	n/a	7.52%
Numerical Investigation on the Scale Effect of a Stepped Planing Hull (Du *et al.*, 2019)	2019	13.70%	7.90%	12.40%
A Study on the Air Cavity under a Stepped Planing Hull (Yang *et al.*, 2019)	2019	5.91%	11.68%	11.28%
Experimental and Numerical Investigation of Stepped Planing Hulls in Finding an Optimized Step Location and Analysis of Its Porpoising Phenomenon (Sajedi and Ghadimi, 2020)	2020	3.50%	6.50%	9.50%
Numerical study on a heeled one-stepped boat moving forward in planing regime (Dashtimanesh, Tavakoli, *et al.*, 2020)	2020	7.80%	11.13%	3.22%

All studies in the Table 2.2 are for single stepped hulls, with the exemption of (Dashtimanesh, Esfandiari and Mancini, 2018). Largely similar numerical set ups are employed by all studies from 2017 onwards. (De Marco *et al.*, 2017c; Du *et al.*, 2019; Yang *et al.*, 2019) use the $k - \omega\ SST$ turbulence model, while the rest of the studies employ the $k - \varepsilon$ model. The mesh sizes range from 0.9 million to 7 million, with an average cell count of 3.4 million.

When Table 2.2 is examined, it is seen that there is considerable scatter in the level of accuracy for numerical modelling stepped hulls. There is no apparent trend in the error of the resistance results. It is noted that all of these studies took place over a short time frame, so CFD techniques and the collective experience of the research community saw limited developments over this time. The previous analysis of planing hulls saw the development over a 20 year time period in which CFD solvers progressed significantly.

While the accuracy of CFD in predicting resistance initially looks promising when looking at these studies, upon further investigation a number of concerns are raised. The first of these concerns is that Numerical Ventilation is not mentioned once in any of these studies. This is known to be a significant issue in simulations of planing hulls, and as such it should be addressed in simulations of stepped hulls. When the most accurate study is examined (Sajedi and Ghadimi, 2020), significant Numerical Ventilation is seen in Figure 17 as presented in the paper. Two large streaks are present on the forebody while the entire afterbody is subject to a mixture of fluids. This is the case too for the second most accurate study, as presented by (Dashtimanesh, Esfandiari and Mancini, 2018). When Fig 14. and 15. as published in their paper are consulted it is seen that significant numerical ventilation is present. In some cases, the streaking is so prevalent that free-surface tunnels are formed under the hull as the volume fraction is lower than 0.5. The presence of Numerical Ventilation is known to significantly lower the computed resistance of a hull.

As highlighted by (Stern, Wilson and Shao, 2006) verification is an important part of any CFD analysis. The point of this is to conduct a quantitative assessment of the numerical uncertainty (U_{SN}) that arises from modelling errors due to the spatial and temporal discretisation of a continuum. Of the studies in Table 2.2 (Dashtimanesh, Tavakoli, *et al.*, 2020) conduct no form of verification, (Lotfi, Ashrafizaadeh and Esfahan, 2015; Veysi *et al.*, 2015; Du *et al.*, 2019) present rudimentary mesh studies with no quantitative analysis, and the remaining publications put forward only grid convergence studies. None of the studies attempt to quantify the uncertainty due to temporal discretisation through a timestep study. The numerical uncertainty returned by some of the grid studies is concerningly high. (Kazemi *et al.*, 2019) reported numerical uncertainty of 7.81% in resistance, 6.99% in trim and 7.79% in sinkage. (Yang *et al.*, 2019) reported maximum numerical uncertainty of 17.76% in resistance, 8.30% in trim and 3.34% in sinkage. (Sajedi and Ghadimi, 2020) reported numerical uncertainty of 5.85% in resistance. With numerical errors of this magnitude little confidence can be held in the results despite the perceived high levels of accuracy.

All the studies presented in Table 2.2 with a resistance error of less than 5% have been shown to suffer either from Numerical Ventilation or unreasonably high levels of numerical uncertainty. With that in mind, it is reasonable to assume the level of accuracy with which stepped hulls are currently able to be modelled reliably to have a resistance error of between 5% - 10%. Indeed, the average error of all examined numerical stepped hull studies was 7.29%. While a number of authors have employed CFD as an analysis tool for stepped hulls, the practice is far from mature and there is still some way to go in developing reliable and accurate simulations.

2.5 The Interaction of Forebody Flow with the Afterbody

As was noted by (Dashtimanesh, Esfandiari and Mancini, 2018) a likely source of error in simulations of stepped hulls arises from the modelling of flow phenomena such as flow separation from steps, multiphase flow, and water spray behind the steps. For a simulation, or indeed any method of performance prediction of stepped hulls to be accurate, it must be able to model the fluid flow as it separates at the step and interacts with the after body. If this is not modelled accurately then the wetted areas of the afterbodies will be incorrect, and subsequently the forces and moments that are calculated will not be representative of the physical condition.

2.5.1 Modelling the Complex Flow Under a Stepped Hull with Mathematical Models

The available research into this topic is severely limited, with (Savitsky and Morabito, 2010) conducted the only investigation into the nearfield freesurface elevation of a planing hull to date. The aim was to develop empirical equations that quantitatively defined the longitudinal freesurface elevation profiles aft of a prismatic planing hull. These equations allow designers of stepped planing hulls to determine how the flow of the forward hull would intersect with the aft hull. Initially the authors planned to extract data from existing publications, but after a broad literature review, concluded that none was applicable. This further highlights the lack of available research on this topic. Due to the lack of data the authors conducted an extensive experimental test program to provide results. Photographs of the plate then allowed the longitudinal freesurface elevation profile to be extracted, using the grid as a reference. Whilst this presents a simple and fast method of gathering data it is relatively crude and there is no discussion on if and how the presence of the plate affects the wake itself, as the wake comprises of complex 3D flow. The authors use the experimental data to evaluate the developed empirical equations, finding a good agreement between the results. There is a noticeable scatter in the results, and it is clear that while an empirical equation may be capable of providing a good representation of the freesurface elevation profiles they will not be entirely accurate for all cases. It is also important to note that while the authors intended the equations to be used in the design of stepped hulls there was no validation conducted in this application, and the equations themselves were developed from the flow aft of an unstepped hull. While the phenomena that is occurring are very similar, there is no guarantee that the presence of the after body does not affect the freesurface elevation below a stepped hull without further investigation. The lack of data relating to this flow is due to the complexity arising from measuring the free surface elevation below a stepped hull.

The closest a publication comes to addressing this is that of (Najafi *et al.*, 2019), who noted that there was an evident lack of study on wetted surfaces of the stepped planing hulls. The author set out to address this through an experimental study to evaluate the hydrodynamic characteristics and the bottom wetted surfaces of a single stepped planing hull. Their study is limited to the forebody operating in the chines dry condition and does not consider the additional side wetting where the stagnation line crosses the step. While the study does not extract the freesurface elevation from below the stepped hull, photos are taken of the wetted areas. These are then used to determine the ventilation lengths, which are compared to those as calculated by the Stavisky Wake Equations. It is seen that in the majority of cases the centreline equation is accurate, however there is a maximum error of 10.54%. No errors are presented for the quarterbeam profiles. When the intersection points as calculated by the Savitsky's Wake Equations are used to calculate the wetted area of the aft hull there was an average error of 9.30%, with a maximum error of 24.88%. There is no analysis of the conditions under which the equations are less accurate. Further analysis of the applicability and accuracy of the savitstky wake equation is an area in which further study is required.

The lack of data regarding the interaction of forebody flow with the afterbody is something that is again highlighted by (Dashtimanesh, Tavakoli and Sahoo, 2017), who found that significant inaccuracies introduced to their performance prediction model through an inability to accurately model the freesurface elevation aft of each of the steps. They went on to state *'there exists an urgent need to conduct extensive set of experiments for various stepped hulls and extract the flow pattern behind each step.'*

2.5.1.1 Linear Wake Assumption

The linear wake assumption is a means of calculating the nearfield longitudinal freesurface elevation profile aft of a planing hull, originally proposed by Lorne Campbell, a naval architect with 36 years' experience specialising in high speed craft (Danielsson and Strømquist, 2012). It was conceived as a means of determining how the forebody wake would intersect with the after body of a stepped hull and is only valid for the region close to the transom of the hull.

It makes the assumption that at high speeds, the high density of water results in the fluid having too much inertia to 'move out the way' of an incoming hull. Instead, it is proposed that the surface layer is 'scraped off' by the hull and thrown aside as spray, leaving the underlying streamlines undeflected. These undeflected streamlines remain running parallel to the original free surface.

Danielsson and Strømquist (2012) were the first researchers to develop a semi-empirical analytical model for stepped hulls using the linear wake assumption, stating it was reasonable at high speeds and for short ventilation lengths. The assumption was found to produce an analytical tool that was capable of modelling resistance relatively well, however, this over-predicted trim by 80% when compared to experiments. Similarly, Dashtimanesh et al. (2017) applied the linear wake assumption in their semi-empirical analytical model for stepped hulls. They found the assumption led to a reasonable agreement between their mathematical results and experimental data, however the model was unreliable at predicting trim. They reasoned that this may be due to the linear wake assumption being incapable of appropriately modelling the fluid flow separation from the step.

A number of researchers have applied the linear freesurface elevation profile as a means of calculating the afterbodies wetted area in 2D+t models of stepped hulls (Bilandi *et al.*, 2018, 2019, 2020; Niazmand Bilandi, Dashtimanesh and Tavakoli, 2019; Bilandi, Dashtimanesh and Tavakoli, 2020). In these studies the average error in calculating resistance is ranges from 11.43% - 14%, with (Niazmand Bilandi, Dashtimanesh and Tavakoli, 2019) concluding that '*the reason for the difference between the accuracy of the results of the wetted surface and resistance can be due to variation in fluid flow separation from aft step which cannot be appropriately modelled by linear wake theory and the shape of the wetted surface, which here is assumed to be triangular.*'.

Despite the fact that numerous studies employ the linear wake assumption there has been no research to verify its accuracy in comparison to any numerical or experimental results. The only justification for its use in the literature is that the models give reasonable results when it is employed, however it has been twce highlighted as a potential source of error. Its continual use stems from an initial publication in the Master's Thesis of Danielsson and Strømquist (2012), who employ the method following an email conversation with Lorne Campbell. No data is provided to show the model to be accurate. All subsequent studies that employ the Linear Wake Assumption reference this initial appearance and then the subsequent papers that employ it in justification of its use, however at no point has it been shown to be appropriate for this application. This is a significant failing and is a point that is highlighted for further investigation.

2.5.2 Modelling the Complex Flow Under a Stepped Hull With CFD

While there has been a rapid increase of numerical studies investigating stepped hulls in recent years, there is little information available to evaluate the accuracy CFD in modelling freesurface elevation of the flow as it separates aft of a step. Following a study of the available literature no examples of experimental data being used to validate or evaluate the performance of CFD this application were found. A number of studies do, however, make comparisons between Savitsky's Wake Equations and their CFD results as validation cases.

(Faison, 2014)compared the freesurface profile aft of a transverse steps caulculated with the Savitskty Wake Equtaions with CFD generated profiles of swept back and cambered steps. The study found there to be significant differences between the numerical and empirical profiles, however, the authors were unable to determine if the differences were accountable to the change in design, or inaccuracies in one of the methods employed. (Ghadimi *et al.*, 2015) used the Savitsky Wake Equations to validate CFD in modelling the CL freesurface profile, before investigate how altering the transom stern may reduce the wakes rooster tail height. Reasonably good correlation was found, but once again the authors are not able to comment on the reasons behind the differences. Similarly, (Lotfi, Ashrafizaadeh and Esfahan, 2015) compared a CFD generated CL freesurface elevation profile to the equivalent one calculated using the Savitsky Wake Equations. The two methods are shown to have poor correlation, with an average error of 20%. Most recently, (Bakhtiari and Ghassemi, 2017) investigated the effect of a forward swept step angle on the performance of a planing hull with CFD. They employed the results of the Savitsky Wake Equations as part of their validation procedure, showing that there is a reasonable level of agreement between the two methods, but that they do not exactly agree.

No examples were found in the literature of the nearfield freesurface elevation calculated by CFD being verified against any source of data other than the Savitsky Wake Equations. Those using the Savitsky Wake Equations to validate their CFD model often found discrepancies between the two methods, however, they were not able to identify which of the methods were closer to the physical solution. The lack of investigation into this topic is in part due to the lack of experimental nearfield wake data available in the public domain. While validating CFD against the Savitsky Wake Equations gives some confidence in the solutions, it is a rudimentary validation. The scatter that was present between the experimental data used to generate the equations and the profiles they calculate shows they are not entirely accurate and as such a level of uncertainty exists. This level of uncertainty makes it impossible to undertake an in-depth investigation into the modelling of nearfield longitudinal freesurface elevation profiles using the Savitsky Wake Equations alone, as the exact solution is not known.

Researchers have made comparisons of experimental mid and far-field wake cuts with CFD results for conventional displacement ships. Analysis of the work submitted to the Gothenburg 2010 Workshop revealed that wave cuts closest to the hull tend to be well predicted, however, as distance from the hull increases the results varied considerably (Larson, Stern and Visonneau, 2014). This workshop was for a KCS vessel, and it is well known that CFD is significantly more accurate when evaluating conventional displacement ships compared to planing hulls. An example of this comparison being made for planing hulls was undertaken by (Mancini, 2015). The study compared the numerical results for the wake field to the experimental mid and far field wave cuts of the Naples Systematic Series. It was found that CFD was able to model the trends in a satisfactory manner, however, it was noted that there were differences in both the amplitudes and phase of the results.

From this review of the literature it is not possible to conclusively say that CFD is able to model the nearfield freesurface elevation aft of a planing hull, or step, with a high level of confidence. There is a clear lack of experimental data available to validate against. This is an area which urgently requires investigation so that means of modelling the interaction of the forebody flow of stepped hulls with the afterbodies may be developed and evaluated.

2.6 Analytical Models for the Performance Prediction of Planing Surfaces

In order for experimental data to be of practical use to designers it is desirable to establish empirical equations and analytical performance prediction models. These relate the physical geometry of the hull to the hydrodynamic properties when in the planing condition, such as the hydrodynamic lift, drag, pitching moment and wetted area.

2.6.1 Mathematical Models for Planing Hulls

A significant effort was invested in the theoretical study and empirical-data analysis of the phenomena of planing in 1947 by the Davidson Laboratory of the Stevens Institute of Technology, produced 16 technical reports investigating all aspects of planing surfaces. The findings of the reports investigating lift, drag and wetted area were summarised by (Korvin-Kroukovsky, Savitsky and Lehman, 1949) resulting in an empirical equation for determining the lift force of a planing surface. The wetted area and the centre of pressure were shown to be important factors in this regard. These empirical equations were further developed by (Savitsky and Neidinger, 1954) to extend their range of applicability.

(Savitsky, 1964) presented the first computational procedure capable of calculating the resistance and trim of a planing hull, capable of calculating all unknown parameters through the utilisation of empirical equations. This is considered the first accurate and complete performance prediction tool to be developed for the designers of planing hulls. Over the subsequent years attempts have been made to enhance this model, with (Savitsky and Brown, 1976) making an effort to allow for the consideration of warped hull shapes and trim tabs in their calculations. (Savitsky, DeLorme and Datla, 2007) developed a procedure for the inclusion of whisker spray through the use of empirical relationships, while (Syamsundar and Datla, 2008) proposed modifications to allow the model to consider the effects of interceptors upon hull performance. More recently (Savitsky, 2012) developed an empirical model to further modify his 1964 work and allow it to account for warped planing hull forms.

The Savitsky method of calculating the resistance of a planing hull is a valuable design tool. It has been in use for almost 60 years, and is still employed by numerous researchers (Sukas *et al.*, 2017; Khazaee, Rahmansetayesh and Hajizadeh, 2019a; Javaherian and Gilbert, 2021; SANCAK and ÇAKICI, 2021). The method has been shown to be robust and has an acceptable level of accuracy, with a typical error in resistance of ~10%. It is a valuable early design tool that facilitates the rapid evaluation of prospective hull forms. Additionally, it is a powerful research tool that allows the differences between hulls to be determines. In this application accuracy is not a critical issue, as it is often the case that relative differences between hulls is enough to draw conclusions. The method is considerably less complex than CFD, and its rapid nature is a significant advantage.

2.6.2 Mathematical Models for the Stepped Hulls

The semi-empirical model as developed by (Savitsky, 1964) for unstepped planing hulls has been shown to be very successful. The developed equations were not applicable to stepped hulls as there was no practical way to determine how the flow from the forebody intersected with the afterbody. To this end, (Savitsky and Morabito, 2010) conducted a series of model tests to derive empirical equations that could quantitatively define the centreline and quarterbeam freesurface elevation profile aft of a planing hull. The purpose of this study was to develop equations that were of a form that may be easily applied by designers of stepped planing hulls to determine how the flow aft of the step intersects with the afterbody. The study went on to briefly propose how the new equations may be applied to the design of a stepped hull in conjunction with the model was developed by (Savitsky, 1964), however there is no method developed to calculate the forces acting on the afterbody as it intersects with the wake of the forebody rather than the calm water surface. It was suggested that the established planing lift equations be used with the added condition that the vertical velocity of local free surface wake profile be included when defining the effective trim angle of the afterbody. There is, however, no analysis or application of the proposed method and as such no comment can be made on its applicability or accuracy.

(Svahn, 2009) then went on to develop a new mathematical model for the performance prediction of a single stepped hull. This was based upon the empirical resistance equations of (Savitsky, 1964), employing the work of (Savitsky and

Morabito, 2010) to determine the wetted area of the afterbody. The novelty that Svahn introduced to his method was the addition of local deadrise and trim values to calculate the forces on the afterbody. These values attempted to orient the afterbody with the wake in a way that allowed the standard Savitsky equations to be used to calculate the forces as for calm water. This approach proved more successful in determining the lift of the afterbody than the rudimentary method of including a vertical velocity of local free surface wake profile. The study by Svahn attempted to validate the method by benchmarking it against three production hulls. There was no resistance data available, however, the top speeds and engine powers were known. The comparison between the developed method and the full-scale data showed a promising correlation, however, this was a very crude validation. It was noted that Shahn's method was incompatible with a chines dry planing condition, with this being highlighted as an area for future work.

(Mancini *et al.*, 2018) point out that the Svahn method contains numerous limitations and ambiguities, with the lack of proper validation with experimental data being one of the key issues. (Loni *et al.*, 2013) developed a MATLAB program that implemented the mathematical model proposed by (Svahn, 2009). While no further validation study was put forward, the program was used to rapidly analyse a large number of stepped hull configurations to investigate the effects of various parameters on stepped planing hull performance. These parametric studies act as a good guide for designers in the initial design stage of a stepped hull, and this study shows the benefits of having a mathematical model that can rapidly evaluate prospective designs and establish design trends. (Lotfi, Ashrafizaadeh and Esfahan, 2015) performed CFD analysis of a single stepped hull, comparing the results with those calculated by Svahn's semi-empirical method. It was reported that there was a good corelation between the experimental and numerical results, while Svahn's method was considerably less accurate. It was remarked that at some volumetric Froude numbers Svahn's method was unable to follow the trends of the experimental data. Additionally, Svahn's method was not applicable for cases in which the hull was operating in a forebody chines dry condition, meaning it could not be used to generate results above a certain speed.

(Danielsson and Strømquist, 2012) went on to attempt to extend the method developed by (Svahn, 2009) for application with a double stepped planing hull. The authors were initially unsuccessful in this, finding that the resulting model was overly complex. The use of Savitsky's wake equations (Savitsky and Morabito, 2010) was found to result in 'unreasonably long ventilation lengths', and the model failed in finding an equilibrium condition. They state that the reason for this is "*believed to be because the project boat is outside the range of validity of the wake profile equations, and perhaps also because the equations are intended for single stepped hulls*." Instead, the authors replaced the wake equations with the linear wake assumption, where the freesurface elevation profile is considered horizontal, and parallel to the horizon from the separation at the step, as suggested by Lorne Campbell. No further study has been undertaken to validate the use of the linear wake assumption against the physical flow of a stepped hull, however several studies have employed it while giving reference to (Danielsson and Strømquist, 2012) as justification for its application. In addition to the implementation of the linear wake assumption, the authors assumed a local deadrise of 2 degrees as it was no longer possible to calculate this value. Once again there was no validation of the model against experimental data, with the benchmarking of the model being done against the installed power of a production vessel in a manner similar to (Svahn, 2009).

(Dashtimanesh, Tavakoli and Sahoo, 2017) built upon the work of (Danielsson and Strømquist, 2012), presenting the same mathematical model with more detailed verification and analysis. The paper states that the local deadrise is calculated, which would represent an improvement over the previous model, however, no equation or explanation is offered as to how this is achieved. The authors found average comparison errors of 9% in resistance and 17% in trim when modelling Hull C2. The mathematical model showed good corelation for speeds over $7\ ms^{-1}$, however, it lacked accuracy for the lower speed range. This lack of accuracy was attributed to the Linear Wake Assumption being invalid at lower velocities. It was also noted that the accuracy of the Linear Wake Assumption was limited by the vessel's displacement and step height, with no experimental data available to quantify its applicability.

While mathematical performance prediction models for unstepped hulls can be said to be accurate and robust the same cannot be said for those developed for unstepped hulls. The development of these has been limited by the lack of experimental data in relation to stepped hulls, and they generally try to adapt methods for unstepped hulls. Questions are raised about the uncertainty of how the forebody flow interacts with the afterbody, and this is a potential source of errors. These models generally achieve errors of between 10 -15% when compared to experimental data. Additionally, these models are often subject to limitations, and do not consider physical full wetted area of a stepped hull, instead applying a simplified approach. This is an area of ongoing research with the development of accurate and robust models being a valuable objective, as demonstrated by the quantity of research that employs the Stavisky method when evaluating unstepped hulls.

2.7 Improving the performance of Stepped Hulls

With the growing interest in stepped hulls and advances in the techniques through which their performance may be evaluated came further work to determine the most effective step configurations and improve their performance.

(Loni *et al.*, 2013) developed a computer programme based upon Svahns method (Svahn, 2009). The limitations of this method were not addressed in the development of this program; however, it was employed to conduct a study of the effects of various parameters on stepped planing hull performance. The authors investigated four parameters which were systematically varied while all other parameters were constant to establish their individual influence. Large variations in the computed resistance were found, while the step height was found to be the most influential parameter.

(Lee, Pavkov and Mccue-weil, 2014) undertook an experimental study to systematically investigate the variation of step configuration and displacement upon the performance of a double stepped planing hull. Seven step configurations were studied at three displacements and four speeds. Displacement was found to have the same effect upon performance regardless of the step layout. The performance was found to be influenced greatly by the configuration of steps.

(Di Caterino *et al.*, 2018) undertook a study into the design of a double stepped hull using an analytical 2D+T method. The authors varied three parameters concurrently, developing eight candidate hulls. It was found that the variation of these parameters caused a range in resistance of 9%. This study showed the potential gains that were possible through the correct design of a stepped hull.

(Najafi and Nowruzi, 2019) studied the effects of five configurations of transverse steps on hydrodynamic characteristics of the Fridsma planing craft using a CFD method. The authors found the configuration of the transverse steps to significantly affect the flow pattern on the fore and afterbody of the stepped hull, recommending further evaluation into the step design.

(Dashtimanesh, Roshan, *et al.*, 2020) employed a numerical-based method to develop understanding of the effect of step height and its location on hydrodynamic characteristics of stepped planing 2D plates. The authors studied eight double stepped configurations, and six single stepped configurations in which the hight and location of the steps were systematically varied. They found the step height to be the most influential factor on hull resistance. In the case of two stepped hulls it was also found that the location of the second step had a large effect of the behaviour of the planing plate.

(Sajedi and Ghadimi, 2020) undertook a three-dimensional numerical study of a single stepped planing hull, which they validated through an experimental investigation. Their numerical study set out to investigate the effects of the step location on the performance of a hull, and also its longitudinal stability. They studied 10 different cases in which the location of the step was systematically varied, finding that there was significant influence on both the trim and resistance. Following this they extracted the optimum location of the step from their data set.

All of the available work in the literature follows a Design of Experiments (DOE) methodology. This is a systematic method in which the relationship between factors effecting a process and the output of that process is determined in a systematic way. The DOE methodology is used to determine cause-and-effect relationships, for instance how the location of a step influences the resistance. While this methodology is good for finding simplistic relationships, which may be used to improve designs, it does not determine the optimum design of a stepped hull.

2.8 Concluding Remarks

In this chapter a literature review has presented looking into hydrodynamic analysis, performance prediction and optimisation of stepped and unstepped hulls, with a specific focus upon the work to be undertaken in each of the subsequent chapters of this thesis. During this review the following gaps in the available literature have been identified:

1. While NV has been identified as a prevalent issue in numerical simulations of planing hulls, no study quantify the effect that its presence may have
2. The accuracy of CFD simulations of planing hulls is seen to be lower than that of conventional marine CFD. Simulations of stepped hulls are effected by numerical ventilation and large numerical uncertainties. No studies attempt to address this, or investigate methods of enhancing the accuracy, such as wall treatment.

3. There is a lack of experimental data of the nearfield wake region of a planing hull, and there is no analysis of the accuracy of methods developed to model this flow
4. No attempt has been made to extract or analyse the flow pattern behind each step of a stepped hull
5. Current mathematical performance prediction models of stepped hulls do not perform with high degrees of accuracy, and are subject to a number of limitations
6. Research into how the performance of stepped hulls may be improved has been simplistic and is limited in scope. No true optimisation studies have been conducted of stepped hulls.

The studies as presented in the main chapters of this thesis set out to address each of these gaps, expanding upon the knowledge of stepped planing hulls.

Chapter 3 – Numerical Modelling of Unstepped, Single-Stepped and Double-Stepped Hull Variants

This chapter sets out to develop knowledge of stepped hulls through numerical modelling. A detailed analysis of the hydrodynamic characteristics of an unstepped hull, a single stepped-hull and a double-stepped hull is undertaken. Resistance is broken down into its pressure and shear components, and the equilibrium position of the vessel is examined over a range of speeds. Differences between the step configurations are examined to form a thorough understanding of the effects that the addition of steps has upon the performance of a planing hull. The developed numerical set up is shown to be accurate, allowing it to be employed in Chapter 4 to develop knowledge of the flow characteristics as the fluid separates aft of a step.

3.1 Introduction

When designing any hull form it is generally a key requirement of the naval architect to design a hull that is efficient in order to minimise fuel consumption and maximise speed. In the case of planing hulls, where speed is typically a high priority design objective this especially holds true. The inclusion of steps in the design of a planing hull offers a valuable means through which significant resistance reductions can be made, increasing the hull efficiency at higher speeds. When considering the addition of steps, it is important that the effects upon the performance of the vessel are fully understood, a topic that this chapter sets out to address. While steps reduce resistance at high speeds, they reduce efficiency at lower speeds, so it is important that the operational profile of the vessel is considered to ensure that the appropriate decisions are made.

While experimental testing is an effective design tool for evaluating prospective designs, it is time consuming and costly. Additionally, there are limitations in what is feasible to measure experimentally, such as the composition of resistance, pressure distributions and free surface elevation as the flow separated aft of a step. CFD offers a valuable alternative design tool, facilitating a thorough analysis of the hydrodynamic characteristics of stepped hulls and allowing the mechanisms through which resistance reduction is achieved to be studied in far greater detail. A comprehensive study into the effects of the addition of steps upon the performance of a planing hull can therefore be undertaken.

In order to model planing and stepped hulls and obtain meaningful results it is important that numerical CFD models are accurate and reliable. Table 2.1 revealed the application of CFD to planing hulls has improved in accuracy over the years as techniques and knowledge are developed. There does, however, remain a variation in the accuracy of different studies and there is still a way to go before CFD may be employed for planing bodies with the level of confidence that it is applied to conventional marine problems. This is similar to the state of play for the modelling of stepped hulls using CFD, as summarised by Table 2.2. It is obvious this is an even less mature topic, with most studies being conducted in the last 5 years. It is clearly of benefit to designers and the research community to establish methods that are seen to improve the accuracy and reliability of CFD for planing hulls.

Wall treatment is an important factor to consider when developing CFD tools to analyse planing hulls, however it is on that has received little attention to date, as seen in the literature where the overwhelming majority of studies investigating planing hulls employ wall functions. It is recommended that a low y^+ approach is followed for cases in which an accurate prediction of the boundary layer velocity is important, such as drag calculations (CD Adapco, 2018), however simulation time and cell count are often a critical issue leading to the adoption of the high y^+ approach. In the context of conventional marine CFD the ITTC states that the wall function approach performs remarkably well at predicting the resistance and does not seem to compromise the quality of the solution (ITTC Specialist Committee on CFD in Marine Hydrodynamics, 2014). Despite this, there are early indications that the choice of wall treatment has considerably more influence in the accuracy of simulations of planing hulls, as reported by (Gray-Stephens, Tezdogan and Day, 2020b). The utilisation of the more computationally expensive low y^+ approach offers a potential means through which the accuracy of planing hull CFD may be improved further.

Numerical Ventilation is one of the largest sources of error in CFD modelling of planing hulls and remains an issue that goes unaddressed by several studies. While the previous studies have established strategies through which the effects of Numerical Ventilation may be minimised, there is still no quantitative data on its effects upon the results of a simulation. Quantifying the impact of Numerical Ventilation allows users to understand and account for its effects in the same manner as quantifying the numerical uncertainty of a simulation allows it to be used with confidence.

This chapter presents a CFD-based unsteady RANS study evaluating the performance of unstepped, single stepped and double stepped hulls. Approaches that improve the level of confidence that may be placed in CFD of high-speed hulls are investigated, though increasing the accuracy and quantifying the effects of one of the largest sources of error. The effects of the addition of steps to a planing hull is investigated and discussed in detail, revealing the mechanisms through which a reduction in resistance is achieved. The results are validated against available experimental data and are shown to be in better agreement than state-of-the art studies reported in the literature.

3.1.1 Aims and Objectives

This chapter aims to develop knowledge of stepped hulls through numerical modelling, determining the effects that the addition of steps has upon the performance of a planing hull. It sets out to conduct a detailed hydrodynamic analysis to reveal the mechanisms through which stepped hulls achieve a reduction in resistance, determining the conditions in which it is beneficial to include steps.

Without reliable CFD simulations it is not possible to conduct any meaningful analysis through the use of this numerical tool. A secondary aim of this chapter is to improve the level of confidence that may be placed in CFD simulations of planing hulls. This is achieved quantifying the effects of numerical ventilation so that its impact upon the resistance is better understood, and establishing the influence that wall treatment has on the accuracy.

In order to achieve these aims, a key objective of this chapter is to develop and validate a robust and accurate CFD set up for the analysis of unstepped, single-stepped and double stepped hulls. This tool will then be employed in the following chapter to develop knowledge of the flow as it separates aft of a step. Additionally, a number of further objectives have been identified:

1. **Develop** a CFD simulation that may be considered accurate and robust in modelling planing hulls
2. **Verify** the numerical set up so that the numerical uncertainty is quantified and understood
3. **Analyse** the accuracy of the CFD simulation for application with unstepped, single and double stepped hulls, investigating the effect of wall treatmeant
4. **Quantify** the effects of Numerical Ventilation to develop understanding of how the phenomena influences the results of a simulation
5. **Conduct** hydrodynamic analysis of each hull variant to develop the understanding of stepped hulls

3.1.2 Methodology

In this chapter the experimental results of (Taunton, Hudson and Shenoi, 2010) were used as validation data to verify the degree of accuracy of the CFD model. These experimental results publish data of an unstepped hull, as well as single and double-stepped variants of this hull operating in calm water. It is the only example of a stepped hull systematic series being experimental tested with available in the public domain (De Marco *et al.*, 2017b). In addition to the complete data set being published, 3D CAD models are freely available.

Initially, a CFD simulation was developed for an unstepped planing hull. The set up was investigated and a number of parameters varied in sensitivity studies to ensure the most accurate set up was established. The recommendations outlined in (Gray-Stephens, Tezdogan and Day, 2020b, 2021) were implemented to ensure that Numerical Ventilation was minimised and that the simulation was capable of accurately modelling the flow associated with the near field freesurface elevation profiles. The final set up is reported in Section 3.3 of this chapter, which was suitable with both a high and low y^+ approach to wall treatment.

A comprehensive verification study was undertaken to establish the reliability of the simulations and quantify the levels of uncertainty. As this was a research study as opposed to a design exercise, there was no design speed, or speed of significantly more importance as the whole experimental range was under consideration. The initial set up and verification study were for the $9.21ms^1$ (Froude number of 3.12) condition. This speed was selected as it is around the midpoint of the speed range tested, and as such a simulation developed for this speed should be capable of modelling both the higher and lower speed cases.

The set up was then adapted for the single and double stepped hull geometries (as detailed in Figure 3.1) through the introduction of further meshing controls. These modifications were required to ensure that the simulation was capable of modelling the flow as it separates from the step and intersects with the aft hull. It is assumed that similar levels of numerical uncertainty for all step configurations, and as such the uncertainty as calculated in the verification study of unstepped hulls is used for both the single and double stepped variants. This assumption is valid as the physics for all cases was identical, and the only minor differences in the mesh was the prism layer thickness and additional refinement zones to capture the separating flow.

Following the development of an accurate CFD simulation, this tool will be employed to investigate the differences that result from the different step configurations through detailed analysis of the hydrodynamic characteristics. Resistance is broken down into its pressure and shear components, and the equilibrium position of the vessel is examined over a range of speeds. The phase replacement strategy in which all cells containing a mixture of fluids in a designated zone are replaced with 100% water is employed to quantify the effects of Numerical Ventilation. This strategy allows the results with the effects of NV to be directly compared to those without. It also allows use of this approach for the more complex, mixed flow regimes of stepped hulls to be assessed.

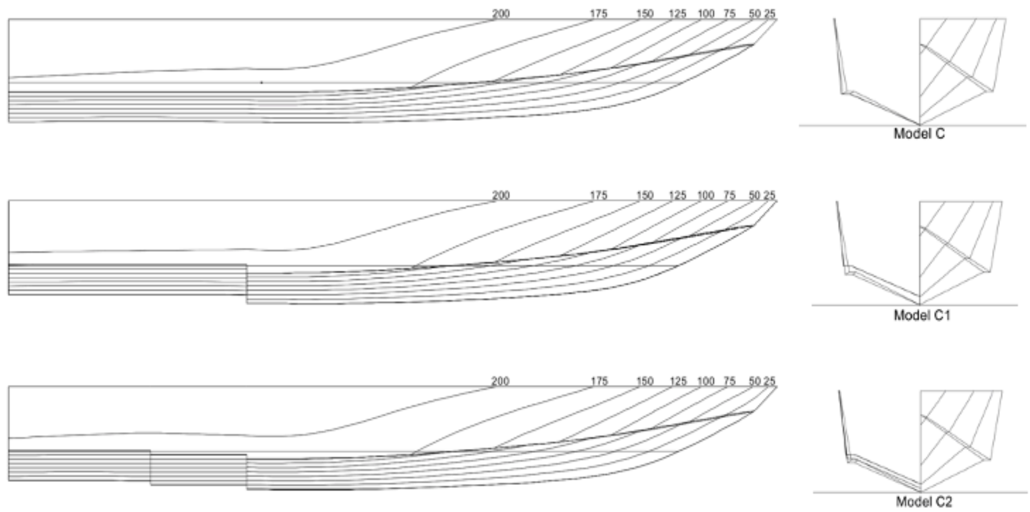

Figure 3.1 - Lines Plans of Hull C, Hull C1 & Hull C2

3.2 Experimental Data

The numerical results will be validated against experimental data developed by (Taunton, Hudson and Shenoi, 2010) for a series of high-speed hard chine planing hulls in both calm water. The study aimed to extend the speed range for which data is available for planing hulls. It was undertaken at the GKN Westland Aerospace No.3 Test Tank, at a test facility in Cowes on the Isle of Wight. The tank had a length of 198m, a breadth of 4.57m, a depth of 1.68m and a maximum carriage speed of $15ms^{-2}$.

The models were tested in calm water at speeds of $4ms^{-2}$ to $13ms^{-2}$ in accordance with ITTC Procedures to measure the resistance, dynamic trim and dynamic sinkage. Additionally, the dynamic wetted area (aft of the spray root line) was determined from photographs taken of each run. There is no universal or recommended method or experimentally determining this parameter (ITTC, 2008), and there is a high degree of difficulty in accurately measuring it, resulting in the largest experimental uncertainty of around 10%.

The parent hull (Hull C) for the study conducted by Taunton is typical of high-speed interceptor craft and race boats, with a L/B ratio of 4.3 and a transom deadrise angle of 22.5°. The series of four models was developed from this parent hull through a variation in L/B ratio. The variations to this ratio were selected to extend the speed range for which data are available, determined through an investigation into previous experimental investigations of planing craft performance. Additionally, variants of Hull C having a single (Hull C1) and double (Hull C2) stepped configuration were tested. The lines plan of these three models can be seen in Figure 3.1, while their parameters are detailed in Table 3.1.

Table 3.1 - Hull Parameters

	Hull C	**Hull C1**	**Hull C2**
Length (m)	2.00	2.00	2.00
Beam (m)	0.399	0.399	0.399
Displacement (kg)	24.8	24.8	24.8
Deadrise (°)	22.5	22.5	22.5
LCG (m)	0.66	0.66	0.66
VCG (m)	0.1051	0.1051	0.1051
Gyy (m)	0.32	0.32	0.32
First Step Length (m)	-	0.62	0.25
Second Step Length (m)	-	0.02	0.37
First Step Height (m)	-	-	0.1
Second Step Height (m)	-	-	0.1

The models were towed by a single free-to-heave post, attached at the longitudinal centre of gravity and were free to pitch, however were restrained in yaw. It was assumed that the thrust line passed through the centre of gravity as the models were not representative of a real vessel, and as such no corrective moment was applied to account for the thrust lever. For full details of the experimental tests please refer to (Taunton, Hudson and Shenoi, 2010). The results of the model tests are published in full, while the CAD geometries of each of the models is available online.

3.3 Numerical Modelling

This section provides details of the numerical simulation employed by this study. Investigations into the sensitivity of the simulation were undertaken, with the best performing set-up being selected and described. As the objective of this study was not to develop new code, detailed information into the numerical workings of CFD code are not presented. Further information regarding the inner workings of CFD can be found in (Ferziger and Perić, 2002).

3.3.1 Physics Modelling

Computational Fluid Dynamics allows the quantitative prediction of fluid flow phenomena based upon the fundamental laws that govern fluid motion; the conservation of mass, linear momentum, angular momentum, and energy. These conservation laws for the continuum are expressed using an Eulerian approach, in which a given volume represents a portion of space through which fluid can flow, as opposed to tracking individual fluid particles in space and time.

The solver uses the finite volume method, dividing the computational domain into a finite number of small control volumes. Discrete versions of the integral form of the conservation equations are then applied to each of these cells. A second order convection scheme was used for the momentum equations and a first-order temporal scheme was applied to discretise the unsteady term in the governing equations. A segregated flow solver was employed, solving the integral conservation equations of mass and momentum in a sequential manner. The continuity and momentum equations were linked with a predictor-corrector approach, using the SIMPLE pressure-velocity coupling algorithm to ensure the mass conservation constraint on the velocity field is fulfilled

The 'Volume of Fluid' (VOF) method tracked and located the position of the fluid-fluid interface, or free surface. The VOF multiphase model is an interface-capturing method, capable of predicting the distribution and movement of the interface of immiscible phases. It is known for its numerical efficiency, making the assumption that the same governing equations that apply to single phase problems can be solved for the cells containing a mixture of fluids, and only introducing a single new variable, the volume fraction. A single set of momentum and energy equations is shared by all the phases and solved implicitly, with the properties of the 'equivalent fluid' in cells containing a mixture being determined by the material properties of the constituent fluids and the phase volume fraction. The volume fraction defines the spatial distribution of each phase at a given time is driven by the phase mass conservation equation and is calculated by solving a transport equation for the phase volume fraction.

The VOF wave model in Star CCM+ allows the simulation of surface gravity waves at the interface of the phases. A flat wave is utilised to model an undisturbed plane of fluid, which is representative of the calm water condition.

The Dynamic Fluid Body Interaction (DFBI) module simulates the motion of a rigid body in response to the forces excreted by the fluid flow. The interaction of the body with the physics continuum determines the forces that act upon it, allowing the resultant force and moment to be calculated. The governing equations of motion are solved to determine the new position of the body (CD Adapco, 2018). This model allows up to six degrees of motion, however, to simplify the simulation the vessel was only free to move in two – pitch and heave.

3.3.1.1 Choice of Timestep

To account for the transient effects, the governing equations must be discretized in time as well an in space. Temporal discretization is somewhat simpler to deal with than spatial effects, as the governing equations are parabolic in time. The solution at a given time is influence only by its history and not by its future. A time marching procedure is implemented in which the time dimension is divided into a set of discrete timesteps, with the solver calculating a new solution for each step forward.

An implicit unsteady approach was employed in all numerical simulations presented in this thesis. Using this approach, the physical timestep size is often governed by the transient phenomena being modelled as opposed to the Courant number. It is vital to ensure that the chosen timestep is suitable to resolve the flow features of interest. The ITTC make the following recommendation for pseudo-transient resistance simulations, defining the timestep as function of the vessels speed and the length (26th ITTC Specialist Committee on CFD in Marine Hydrodynamics, 2014).

$$\Delta t = 0.005 \sim 0.01 \frac{L}{U} \tag{3.1}$$

The ITTC define L as the length between perpendiculars of the vessel, however in the case of planning hulls it is more appropriate to take L as the wetted length of the keel of the vessel.

For the present study, Equation (3.2) was used to calculate the timestep. This has been shown to produced accurate results when applied to planning hulls in the authors previous work (Gray-Stephens, Tezdogan and Day, 2021). A verification study was conducted to justify this choice by formally assessing the numerical uncertainty accountable to the temporal discretisation. The results of the V&V study are presented in Section 3.4.

$$\Delta t = 0.02 \frac{L}{U} \tag{3.2}$$

It should be noted that in almost all cases the timestep calculated using Equation (3.2) falls within the range defined by the ITTC by Equation (3.1). For cases where the calculated value did not fall within this range, the maximum recommended limit of 0.005s was applied. Table 3.2 details the timestep for each of the runs.

Six inner iterations were completed for each timestep to ensure that the solution was fully converged before being marched forwards in time. Due to the large gradients that were present during the calculation of the initial flow field, it was sometimes necessary to increase the number of inner iterations at initialisation to improve the stability of the simulation and prevent divergence.

3.3.1.2 Turbulence Modelling

Two equation turbulence models such as $k-\varepsilon$ and the $k-\omega$ have become industry standard models and are applicable to most engineering problems. These models add two transport equations to represent the turbulent properties of the flow, such as the convection and diffusion of turbulent energy. In these models the first transported variable, k, is the turbulent kinetic energy while the second transported variable is either ε, the turbulent dissipation or ω, the specific turbulence dissipation rate.

Two-equation turbulence models are known to give accurate predictions when applied to ship hydrodynamics (ITTC - Recommended Procedures and Guidelines, 2011). Analysis of the entries to Gothenburg 2010 Workshop showed no visible improvement in accuracy for resistance prediction when turbulence models that are more advanced than the two-equation models were used (Larson, Stern and Visonneau, 2014). It found that $k-\omega$ was by far the most applied turbulence model with 80% of the submissions for the workshop using some form of variation of it.

A review of the literature revealed that in the majority of cases in which CFD is used to investigate planing hulls either the $k-\varepsilon$ (Brizzolara and Villa, 2010; Lotfi, Ashrafizaadeh and Esfahan, 2015; Bakhtiari, Veysi and Ghassemi, 2016; De Luca *et* *al.*, 2016; Dashtimanesh, Esfandiari and Mancini, 2017; Sukas *et al.*, 2017) or $k - \omega\ SST$ (Castiglione *et al.*, 2011; Wang *et al.*, 2012; Frisk and Tegehall, 2015; Ghassemi, Kamarlouei and Veysi, 2015; De Marco *et al.*, 2017a; Mancini, de Luca and Ramolini, 2017) models are applied. Whilst both models have been shown to be comparable in terms of resistance prediction the $k - \omega\ SST$ is known to be superior at predicting separating flows and wake patterns (ITTC Specialist Committee on CFD in Marine Hydrodynamics, 2014; Larson, Stern and Visonneau, 2014). As such, this model was selected despite the fact that it is more computationally expensive.

3.3.1.3 Wall Treatment

In most flow problems walls are a source of vorticity, resulting in the gradients of the flow variables. Accurately predicting the flow and turbulence parameters in the wall boundary layer is essential to determine the fluid forces. The behaviour of the flow in this region near is a complex phenomenon that is made up the viscous sublayer (where the flow is dominated by viscous effects), the buffer layer (where viscous and turbulent stresses are of the same order) and the log-law layer (where turbulence stress dominates the flow). The concept of wall y+, the dimensionless wall distance as defined by Equation (3.3) is used to distinguish between these components, with its value being used to determine the characteristics of the flow.

$$y^{+} = \frac{u_{*}y}{\nu} \tag{3.3}$$

Wall treatment models are a set of configurations and assumptions that are used by a CFD solver to model the near wall turbulence quantities such as the turbulence dissipation, turbulence production and the wall shear stress. These are categorised as high or low y^{+} wall treatment, with each following a different approach to resolve the flow in the boundary layer.

The low y^{+}approach resolves the entire near wall turbulent boundary layer. No modelling used to predict the flow, with the transport equations being solved all the way to the wall cell and the wall shear stress being computed as in laminar flows. In order to resolve the viscous sublayer the mesh has to be suitably fine, with a y^{+} value of one or less, ensuring that the centre of the wall cell located in the viscous sublayer. This approach can be very computationally expensive as a large number of prism layer cells may be required to ensure the wall cell is placed within the viscous sublayer (CD Adapco, 2018).

The high y^+approach models the viscous sub layer and the buffer layer using wall functions for the turbulence production, the turbulence dissipation and the wall shear stress. These are values are derived from equilibrium turbulent boundary layer theory. Using wall functions to model these means that the mesh is not required to resolve the viscous sublayer and the buffer layer and can therefore be far courser. For a high y^+approach to be valid there should be y^+ that is larger than 30 to ensure that the wall cell is in the log-law region of the flow. There have been successful applications of a high y^+approach using a y^+value of up to 500 in marine and civil engineering applications, however best practice guides recommend an upper limit of 100 unless a thorough validation is carried out. Following a high y^+approach results in a significant saving in computational time as far fewer prism layer cells are required (CD Adapco, 2018).

The decision on whether to adopt a high or low y^+approach is generally based upon the computational resources that are available. For conventional marine CFD the wall function approach performs remarkably well at predicting the resistance and does not seem to compromise the quality of the solution (ITTC Specialist Committee on CFD in Marine Hydrodynamics, 2014). Only a single study was found in the review of the literature in which a low y^+approach was applied to planing hulls, showing there to be notable differences accountable to the choice of wall treatment (Gray-Stephens, Tezdogan and Day, 2020b).

In the present study both a high y^+approach with a target y^+ of 40 and a low y^+approach with a target y^+ of 1 is applied to all cases so that the impact of wall treatment may be assessed. As y^+ varies with the fluid velocity, as demonstrated by

Equation (3.3), the height of the near wall cell must be varied with speed to maintain a constant y^+ value. The height of the near wall cell for each case is shown in Table 3.2. In all cases a growth rate of 1.2 was used to populate the prism layer mesh with cells, leading to between 6 and 26 prism layers depending upon the speed case and the wall treatment.

Table 3.2 – First Cell Height & Timestep for all Cases

		$y^+ = 40$			$y^+ = 1$		
Model	**Speed (ms^{-1})**	**First Cell Height (m)**	**No of Layers**	**Timestep (s)**	**First Cell Height (m)**	**No of Layers**	**Timestep (s)**
Hull C	5.09	4.65E-04	9	0.00500	1.16E-05	19	0.00500
Hull C	7.11	3.33E-04	11	0.00357	8.32E-06	20	0.00357
Hull C	9.21	2.57E-04	11	0.00304	6.42E-06	21	0.00304
Hull C	11.13	2.13E-04	12	0.00243	5.31E-06	21	0.00243
Hull C	13.09	1.81E-04	13	0.00206	4.52E-06	22	0.00206
Hull C1	4.08	6.38E-04	8	0.00500	1.59E-05	22	0.00500
Hull C1	6.25	4.16E-04	10	0.00448	1.04E-05	23	0.00448
Hull C1	8.13	3.20E-04	11	0.00322	8.00E-06	24	0.00322
Hull C1	10.13	2.57E-04	15	0.00251	6.42E-06	25	0.00251
Hull C1	12.05	2.16E-04	12	0.00207	5.40E-06	26	0.00207
Hull C2	4.05	5.82E-04	6	0.00500	1.36E-05	20	0.00500
Hull C2	6.25	3.77E-04	7	0.00419	8.83E-06	21	0.00419
Hull C2	8.13	2.90E-04	8	0.00317	6.79E-06	22	0.00317
Hull C2	9.18	2.57E-04	9	0.00277	6.01E-06	23	0.00277
Hull C2	11.13	2.12E-04	9	0.00228	4.96E-06	24	0.00228
Hull C2	12.05	1.96E-04	10	0.00211	4.58E-06	24	0.00211

3.3.2 Computational Domain and Boundary Conditions

The computational domain was sized appropriately to ensure that the presence of the boundaries did not influence the solution, in line with ITTC recommendations (ITTC - Recommended Procedures and Guidelines, 2011) and detailed in Figure 3.2.

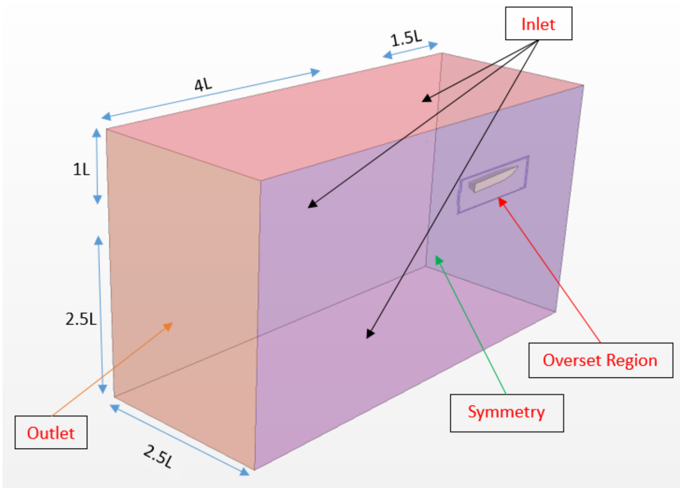

Figure 3.2 - Boundary conditions and domain sizes

In all CFD simulations, the selection of appropriate boundary conditions is vital for both the determination of an accurate solution and the prevention of unnecessary computational costs. The Dirichlet boundary condition was applied, simulating free flow. Only half of the hull is modelled to reduce to computational complexity and demand, with the centreline of the domain being represented by a symmetry plane. This assumption has been shown to have negligible impact upon the calculation of the forces or the free surface elevation aft of the hull (Gray-Stephens, Tezdogan and Day, 2020b). Other boundaries were modelled with velocity inlets as detailed in Figure 3.2. This has been shown to be the least computationally demanding configuration (Gray-Stephens, Tezdogan and Day, 2021).

In addition to selecting an appropriately sized domain, the VOF Wave Damping option was enabled on the side and outlet boundaries to ensure that wave reflections did not impact the solution. The VOF Wave Damping option introduces a vertical resistance to vertical fluid motion and suppresses waves to prevent them reflecting back into the simulation. A damping zone of 1.25 L_{OA}, as recommended by (Tezdogan *et al.*, 2015) was selected.

3.3.3 Computational Grid

The mesh was generated using the automated meshing capability of Star CCM+, which relies upon the Cartesian cut-cell method. The trimmed cell mesher presents a robust and efficient method of producing a high-quality grid, predominantly made up of unstructured hexahedral cells with polyhedral cells next to the surface. Growth parameters ensure that there is a smooth transitioning of the mesh and prevent the introduction of numerical errors.

The prism layer mesher was used in conjunction with the trimmed cell mesher to generate orthogonal prismatic cells next to the hull. Utilising the prism layer mesher generates high-aspect ratio cells that are aligned with the flow next to the wall, allowing the software to resolve high velocity gradients that are associated with the boundary layer and increases the accuracy of the simulation. The initial thickness of the prism layer was calculated as the thickness of the turbulent flow over a flat plate, as given by:

$$\frac{\delta}{x} = 0.37 R_n^{-\frac{1}{5}} \tag{3.4}$$

Where δ is boundary layer thickness, x is plate length, and R_n is the Reynolds number.

A stretching ratio of 1.2 as suggested by (ITTC - Recommended Procedures and Guidelines, 2011) was employed. Care was taken to ensure that there was a smooth transition with similar cell sizes between the outer layer of the prism mesh and the core mesh.

The volume mesh was set up with volumetric controls to progressively refine areas in which flow features of interest and large gradients occurred. Three layers of refinement were used for the free surface, the hull box and the wake region. Additional refinements were included for the bow, the stern, and the free surface upstream of the hull. A further refinement zone increased the resolution of the grid in the area where the flow separated from the step and intersected with the aft hull, ensuring that the grid was capable of modelling the complex phenomena that occur in this region. The refinements can be seen in Figure 3.3 and are detailed in Table 3.3.

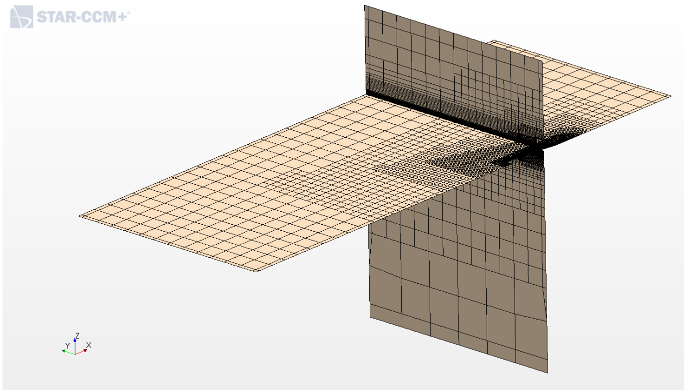

Figure 3.3 – Computational grid

For the generation of the mesh a base size of 0.025m was selected as a function of the vessel length and was 1.25% L_{OA},. This is in line with similar studies, for which base size ranged from 1.3% L_{OA}, to 4.7% L_{OA}, (Tezdogan *et al.*, 2015; De Marco *et al.*, 2017a; Mancini, de Luca and Ramolini, 2017; CD Adapco, 2018). All refinement zones were sized as a percentage of this base size.

Table 3.3 - Refinement Zone Sizes

Refinement Zone	X	Y	Z
Surface Mesh	50%	50%	50%
Hull Box [Near]	50%	50%	50%
Hull Box [Mid]	100%	100%	50%
Hull Box [Far]	200%	200%	100%
Overset Interface	200%	200%	100%
Wakebox [Near]	100%	100%	100%
Wakebox [Mis]	200%	200%	200%
Wakebox [Far]	400%	400%	400%
Freesurface [Upstream]	800%	800%	3.125%
Freesurface [Near]	800%	800%	12.5%
Freesurface [Mid]	800%	800%	25%
Freesurface [Far]	800%	800%	50%
Bow	6.25%	6.25%	6.25%
Stern	6.25%	6.25%	6.25%

The low y^+ meshes were made up of around 8.5 million cells, with the simulations taking between 438 to 1559 core hours to simulate 6 seconds of run time. The high y^+ meshes consisted of 5.8 million cells, taking between 288 to 703 core hours to complete a 6 second simulation. As the HPC nodes were made up of 40 cores, simulations had to run from 7 to 39 hours to return results, depending upon the set up.

3.3.3.1 Mesh Motion

The hydrodynamic field generated by a planing hull is far more complex than that of a conventional displacement hull, with a small error in trim having a large impact upon the total resistance . Modelling the motion of the vessel to ensure that it reaches it equilibrium position is vital to producing accurate results.

The Dynamic Fluid Body Interaction (DFBI) model is used to simulate realistic vessel behaviour in response to the shear and pressure forces exerted by the flow. The DFBI model enables the RANS solver to calculate the force and moments acting upon the vessel before solving the governing equations of rigid body motion to determine the new position of the vessel at every timestep. This model allows a body to have up to six degrees of motion, however, to reduce the complexity of the simulation the vessel was only free to translate in the z-direction and rotate about the y-axis, modelling sinkage and trim.

To facilitate the motions of the hull an overset approach is employed. This has been shown to be well suited to the large motions of a planing hull, producing accurate results (Mancini, de Luca and Ramolini, 2017; Sukas *et al.*, 2017). The overset approach is made up of two regions, one tailored the environment and one tailored to the flow around the body that remains fixed relative to the body as it translates and rotates.

Cells are grouped into active, inactive (passive) and acceptor cells, where the discretised governing equations are only solved for active cells. Inactive cells are those in the background region that are overlapped by the overset mesh, and therefore are not required in the calculation of flow. These cells can however become active if the overset region moves. Acceptor cells separate the active and inactive cells in the background region, and form the boundary of the overset region. They are used to couple the solutions of the two overlapping grids with information passing from the active cells of one region to the active cells of the other through them. Donner cells are the active cells nearest to the acceptor cells from the other mesh, and express values at acceptor cells of the other mesh through interpolation (CD Adapco, 2018). The more computationally demanding linear interpolation scheme was employed in an attempt to minimise interpolation errors.

There is no definitive recommendation made on the sizing of the overset zone. This zone should be large enough to ensure that no large gradients in the flow occur where the field values are interpolated from the donor cells to the acceptor cells. The size of the overset domain was selected to be in line with similar studies. These studies all featured the same length of 1.5L, breadth ranging from 1.5B to 5B, and heights ranging from 2.5D to 6D (Tezdogan *et al.*, 2015; De Luca *et al.*, 2016; Sukas and Gökçe, 2016; De Marco *et al.*, 2017a). The overset region that was generated was 1.75L in length, 4B in width, and 4D in height. It can be seen in Figure 3.4, however due to the density of the mesh it is somewhat difficult to make out the bow, stern, and finest free surface refinements.

Care was taken to follow the overset guidelines as laid out by (CD Adapco, 2018). Of key importance was to ensure that cells in the overlapping region between the overset and background meshes are of similar sizes. This helps reduce any interpolation errors to be of the same order as other discretization errors.

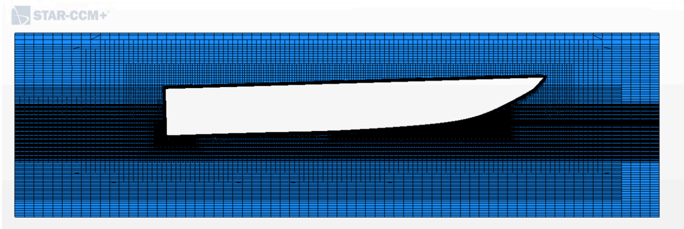

Figure 3.4 - Overset mesh region

3.3.4 Special Considerations for Numerical Ventilation

Numerical Ventilation (NV), or streaking, is a well-known problem that occurs when the Volume of Fluid method is used to model vessels with a bow that creates an acute entrance angle with the free surface, as is typical for both planing hulls and yachts. Numerical Ventilation may be considered one of the main sources of error in numerical simulations of planing hulls (De Luca *et al.*, 2016; De Marco *et al.*, 2017a). Despite the fact Numerical Ventilation is a well-known issue it is rarely discussed in depth by scientific papers (Viola, Flay and Ponzini, 2012), with some studies failing to mention the phenomenon altogether.

Numerical Ventilation occurs when the free surface interface is not properly captured. Particles of air become trapped in the boundary layer in the first few cells nearest the wall and are transported under the hull. The near wall cell contains a non-physical mixture of air and water, which alters the fluid properties, leading to notable effect on the calculation of the shear forces (Viola, Flay and Ponzini, 2012; Olin, 2015). The miscalculation of these forces has a knock-on effect, introducing errors into the trim and pressure resistance of the vessel.

The first cause of numerical ventilation is mesh related. In the bow region the spray thickness tends to zero. At some point the local cell size will not be sufficient to resolve the spray sheet. When this occurs the information in these cells will be supplied under the hull and cause Numerical Ventilation (Olin, 2015).

The second cause of numerical ventilation stems from the interface capturing scheme. Star CCM+'s implementation of the High-Resolution Interface Capturing (HRIC) scheme blends it with the Upwind Differencing (UD) scheme based upon an upper and lower value of the local Courant Friedrichs Lewy (CFL) number. This blending is introduced to bring stability and robustness to the scheme; however it is known that the UD scheme increases numerical diffusion, especially when the calls are misaligned with the flow direction, leading to the free surface becoming smeared (Böhm and Graf, 2014).

During the development of the numerical set up a comprehensive investigation into how numerical ventilation may be minimised was conducted, evaluating a number of parameters and strategies. Quantitative and qualitative analysis was conducted to determine the most successful of these. While the study is not detailed in full in the thesis, the findings were presented at a conference (Gray-Stephens, Tezdogan and Day, 2019) and published in a journal (Gray-Stephens, Tezdogan and Day, 2021). The most successful strategies that were employed by the final numerical set up are detailed in the present section, however for a more details please refer to the referenced papers.

In order to minimise numerical ventilation, the dependency of the HRIC scheme upon the local CFL was removed. While transient methods are employed, calm water resistance simulations seek a steady state solution and as such the robustness of the interface capturing model is not required (Böhm and Graf, 2014). Ensuring that a pure HRIC scheme is used and that no blending with UD scheme results in a much sharper free surface interface, resulting in the minimisation of numerical ventilation. It is also known that this approach has a positive impact on the calculated wave patterns due to the fact there was less interface smearing.

The second strategy that was applied to reduce the level of numerical ventilation was mesh related. Refinements were applied in the bow region and on the upstream freesurface to increase the resolution where the spray sheet tended to zero. The prism layer was reduced in thickness at the point of bow entry. This reduces the number of cells that are misaligned with the freesurface and helps reduce numerical diffusion. Finally, care was taken to ensure that the outer layer of the prism layer was similar in size to the surrounding cells in the core mesh.

An additional strategy that was found to help prevent numerical ventilation was the inclusion of the source tension model, setting the surface tension of water equal to 0.072N/m. This strategy was identified by (Gray-Stephens, Tezdogan and Day, 2020), and supported by the results of (Jesudhas, 2016). The surface tension coefficient expresses how easily two fluids can be mixed, with a higher surface tension represents a stronger resistance to mixture. The coefficient itself is defined as the amount of work necessary to create a unit area of free surface (Ubbink, 1997). For the most part the effects of surface tension are negligible with The ITTC Specialist Committee on Computational Fluid Dynamics stating that they may usually be neglected for ship hydrodynamics problems (Campana *et al.*, 2011).

3.4 Verification

Before any numerical set up may be employed it is first necessary to conduct a verification study so that the level of numerical uncertainty accountable to the spatial and temporal discretization may be quantified and understood, allowing the results to be used with confidence. It is noted that this practice is neglected in several examples of planing hull simulations available in the literature, with validation being conducted by a straightforward comparison of the simulated result and tank testing data. Without conducting a formal verification study there can be little confidence in any results as uncertainty of the simulation has not been evaluated.

Verification is the quantitative assessment of the numerical uncertainty (U_{SN}) and when conditions permit, estimating the sign and magnitude of the numerical error (δ^*_{SN}) and the uncertainty (U_{S_CN}) in that estimate. It is used to determine if a computational simulation accurately represents the conceptual model (AIAA and and, 1998).

Best practice guidelines for Verification in the context of marine CFD are published by the ITTC (Resistance Committee of 25th ITTC, 2008), based upon the work of (Stern *et al.*, 2001). This approach defines errors and uncertainties in a manner that is consistent with experimental uncertainty analysis, where the simulation error is the difference between a simulation result (S) and the truth (T), and is made up of modelling (δ_{SM}) and numerical (δ_{SN}) errors.

$$\delta_S = T - S \tag{3.5}$$

$$\delta_S = \delta_{SM} + \delta_{SN} \tag{3.6}$$

The procedure relies upon Richardson Extrapolation (RE) (Richardson, 1911), which is the basis for existing quantitative numerical uncertainty and error estimates for both grid and timestep convergence (Xing and Stern, 2010). The error is expanded in a power series, with integer powers of grid spacing or timestep taken as a finite sum. When it is assumed that the solutions lie within the asymptotic range it is acceptable that only the first term is considered, leading to a so-called triplet study.

The first step of this approach is to assess the convergence condition using the convergence ratio (R_i), defined as the ratio between $\varepsilon_{i,21} = S_{i,2} - S_{i,1}$ and $\varepsilon_{i,32} = S_{i,3} - S_{i,2}$. Here $S_{i,k}$ refers to the solution obtained from the i^{th} input parameter using the k^{th} refinement. The solutions obtained by systematically coarsening the i^{th} parameter by the refinement ratio, r_k. Four convergence conditions may exist, as defined by (Stern, Wilson and Shao, 2006):

- Monotonic Convergence : $0 < R_i < 1$
- Oscillatory Convergence : $R_i < 0$; $|R_i| < 1$
- Monotonic Divergence : $R_i > 1$
- Oscillatory Divergence : $R_i < 0$; $|R_i| > 1$

For the first condition, Generalized Richardson Extrapolation is used to assess the uncertainty (U_i). The error ($\delta^*_{RE_{i,1}}$) and order of accuracy (P_i) must be calculated:

$$\delta^*_{RE_{i,1}} = \frac{\varepsilon_{i,21}}{r_i^{P_i} - 1} \tag{3.7}$$

$$P_i = \frac{\ln\left(\frac{\varepsilon_{i,32}}{\varepsilon_{i,21}}\right)}{\ln(r_i)} \quad \textbf{(3.8)}$$

The Correction Factor approach was employed, providing a quantitative measure for defining how far a solution is from the asymptotic range, and then approximately accounting for the effects of higher order terms. This is based upon verification studies for 1D wave equations and 2D Laplace equation analytical benchmarks, which showed one-term RE error estimates to be poor when out with the asymptotic range, however that these could be improved by the inclusion of a correction factor. The numerical error is defined as:

$$\delta_i^* = C_i \delta_{RE_{i,1}}^* = C_i \left(\frac{\varepsilon_{i,21}}{r_i^{P_i} - 1}\right) \quad \textbf{(3.9)}$$

The correction factor (C_i) is based upon replacing the observed order of accuracy with an improved estimate which roughly accounts for the effects of higher order terms. This limits the order of accuracy of the first term as spacing size goes to zero and ensures that as the asymptotic range is reached (C_i) tends to zero (Stern, Wilson and Shao, 2006).

$$C_i = \frac{(r_i^{P_i} - 1)}{(r_i^{P_{est}} - 1)} \quad \textbf{(3.10)}$$

Depending how close δ_i^* is to the asymptotic range determines the expression that is used to evaluate the solution uncertainty (U_i):

$$U_i = [9.6(1 - C_i)^2 + 1.1]\left|\delta_{RE_{i,1}}^*\right| \qquad |1 - C_i| < 0.125 \quad \textbf{(3.11)}$$

$$U_i = [2\,|1 - \mathrm{C_i}| + 1]\left|\delta_{RE_{i,1}}^*\right| \qquad |1 - C_i| \geq 0.125 \quad \textbf{(3.12)}$$

3.4.1 Verification Case

Verification studies were performed for both the high and low y^+ approaches, employing Hull C at a speed of $9.21ms^1$ (Froude number of 3.12). This speed was selected as it was in the middle of the speed range to be examined. Verification studies were not undertaken for Hull C1 or Hull C2. It was reasoned that similar levels of numerical uncertainty exist in all simulation provided that the same level of temporal and spatial discretisation was employed under the same physics conditions.

A refinement ratio of √2 was used for the grid study, while a refinement ratio of 2 was employed in the timestep study, as suggested by (Tezdogan *et al.*, 2015),. In all cases resistance, sinkage and trim were shown to displayed monatomic convergence, allowing the uncertainties to be calculated following the correction factor approach. Prior to the undertaking these studies, it was ensured that the iterative uncertainty was negligible and didn't contaminate the results.

The results of the verification study for the high y^+ approach are presented in Table 3.4 Table 3.5 while the results for the low y^+ approach are presented in Table 3.6 & Table 3.7. The numerical uncertainty resulting from the spatial and temporal discretization is then combined to determine the numerical uncertainty, as presented in Table 3.8. Additionally, the experimental uncertainties as reported by the experimental study (Taunton, Hudson and Shenoi, 2010) are presented in Table 3.8.

Table 3.4 - Grid convergence study high y+

Parameter	r_G	EFD	S_1	S_2	S_3	R_G	U_G	U'_G
Cell Count	-	-	6,134,234	2,900,496	1,446,087	-	-	-
$Resistance$ [N]	$\sqrt{2}$	69.98	75.695	76.010	76.442	0.73	1.776	2.54%
$Sinkage$ [m]	$\sqrt{2}$	0.05	0.0483	0.0485	0.0498	0.22	0.0005	0.99%
$Trim$ [Deg]	$\sqrt{2}$	1.75	2.1482	2.1416	2.1267	0.44	0.0065	0.37%

Table 3.5 - Timestep convergence study high y+

Parameter	r_T	EFD	S_1	S_2	S_3	R_T	U_T	U'_T
Timestep [s]	-	-	3.04E-03	4.30E-03	6.08E-02	-	-	-
$Resistance$ [N]	$\sqrt{2}$	69.98	75.695	75.737	75.972	0.18	0.068	0.10%
$Sinkage$ [m]	$\sqrt{2}$	0.05	0.0483	0.0482	0.0481	0.81	0.0005	1.09%
$Trim$ [Deg]	$\sqrt{2}$	1.75	2.1482	2.1464	2.1414	0.36	0.0021	0.12%

Table 3.6 - Grid convergence study low y+

Parameter	r_G	EFD	S_1	S_2	S_3	R_G	U_G	U'_G
Cell Count	-	-	6,134,234	2,900,496	1,446,087	-	-	-
$Resistance$ [N]	$\sqrt{2}$	69.98	70.328	71.215	72.782	0.57	1.676	2.40%
$Sinkage$ [m]	$\sqrt{2}$	0.05	0.0476	0.0474	0.0472	0.63	0.0005	1.04%
$Trim$ [Deg]	$\sqrt{2}$	1.75	2.0075	1.9643	1.8494	0.38	0.0526	3.01%

Table 3.7 - Timestep convergence study low y+

Parameter	r_T	EFD	S_1	S_2	S_3	R_T	U_T	U'_T
Timestep [s]	-	-	3.04E-03	4.30E-03	6.08E-02	-	-	-
$Resistance$ [N]	$\sqrt{2}$	69.98	70.328	70.415	70.557	0.61	0.231	0.33%
$Sinkage$ [m]	$\sqrt{2}$	0.05	0.0476	0.0477	0.0478	0.41	0.0001	0.19%
$Trim$ [Deg]	$\sqrt{2}$	1.75	2.0075	2.0015	1.9916	0.60	0.0130	0.74%

Table 3.8 – Total uncertainties

Parameter	U_d	U_{sn} $High\ y^+$	U_{sn} $Low\ y^+$
$Resistance$	2.30%	2.54%	2.42%
$Sinkage$	2.80%	1.47%	1.28%
$Trim$	1.20%	0.39%	3.10%

In both the high y^+ and low y^+ cases it is seen that there is a higher level of uncertainty associated with the spatial discretisation than the temporal discretisation. The low level of uncertainty stemming from the temporal discretisation indicates that the timestep being employed is appropriate for the conditions being modelled.

Table 3.8 shows the numerical uncertainty for both the high y^+ and low y^+ approaches to be suitably small for all parameters. The numerical uncertainty is of the same order as the experimental uncertainty, allowing a high degree of confidence in all results generated by this numerical set up.

3.5 Results

This section will detail the high and low y^+ results for each of the variant hulls, commenting upon the results of each and providing reasoning for the apparent trends. The results are presented both numerically in tables, and graphically to allow a complete analysis to take place. It should be noted that an attempt has been made to ensure all figures are of a similar scale, however this was not always practical, and care should be taken if directly comparing the figures for each case.

The solution of the CFD simulations considers both the static, buoyant forces and dynamic forces that act upon the hull, with both contributing to the equilibrium position of the vessel. While this also the case for a physical model in a fluid, each experimental run commenced by recording the zero level of each transducer, thereby only measuring the dynamic components for trim and sinkage. As the static values were not provided by the paper, they were calculated by completing a CFD simulation in which the vessel had zero forward speed. The hull geometry was initially positioned with zero trim and a draft of 0.0956m. The static values as calculated by the numerical simulation were utilised, as detailed in Table 3.9.

Table 3.9 – Static position Values

Hull	Static Trim [°]	Static Sinkage [m]
C	0.023	-0.0052
C1	1.125	-0.0059
C2	1.009	-0.0045

The results presented in this section detail the total resistance of the hull, the total trim of the vessel at its equilibrium attitude, and the dynamic sinkage. The running trim is presented as this value if of more interest in the design of planing hulls than the dynamic trim. The dynamic sinkage is presented as the rise of the vessels CG from its static position.

3.5.1 Unstepped Hull

This section presents and discusses the numerical results for the unstepped hull geometry, Hull C. Table 3.10 & Table 3.11 detail the resistance, trim and sinkage as calculated by CFD. Additionally, the comparison error, as given by Equation (3.13) is presented. Each of the calculated values is analysed and discussed separately, before general comments related to the numerical simulation are put forward.

$$Error = \frac{CFD - EFD}{EFD} \tag{3.13}$$

Table 3.10 – Hull C high y^+ numerical results

Speed	Froude Number	Resistance [N]	Trim [°]	Sinkage [m]	Resistance Error	Trim Error	Sinkage Error
5.09	1.58	42.85	3.67	0.0285	10.43%	20.70%	-4.89%
7.11	2.31	54.69	2.87	0.0423	10.26%	23.53%	5.77%
9.21	3.12	75.70	2.15	0.0483	8.17%	22.52%	-3.48%
11.13	3.80	100.86	1.71	0.0513	5.17%	12.75%	2.63%
13.09	4.57	131.30	1.44	0.0535	2.02%	-17.16%	7.09%

Table 3.11 – Hull C low y^+ numerical results

Speed	Froude Number	Resistance [N]	Trim [°]	Sinkage [m]	Resistance Error	Trim Error	Sinkage Error
5.09	1.58	39.90	3.48	0.029	2.83%	15.02%	-3.24%
7.11	2.31	51.10	2.69	0.042	3.02%	16.57%	4.90%
9.21	3.12	70.33	1.98	0.048	0.50%	14.50%	-4.82%
11.13	3.80	93.97	1.54	0.050	-2.01%	3.57%	0.28%
13.09	4.57	123.09	1.27	0.053	-4.36%	-25.68%	5.37%

3.5.1.1 Resistance Results

The mean absolute resistance error values for the high y^+ case was found to be 7.21%, with a range from 2.2% to 10.43%, whereas the low y^+ case was 2.54%, with a range of -4.67% to 3.02%.

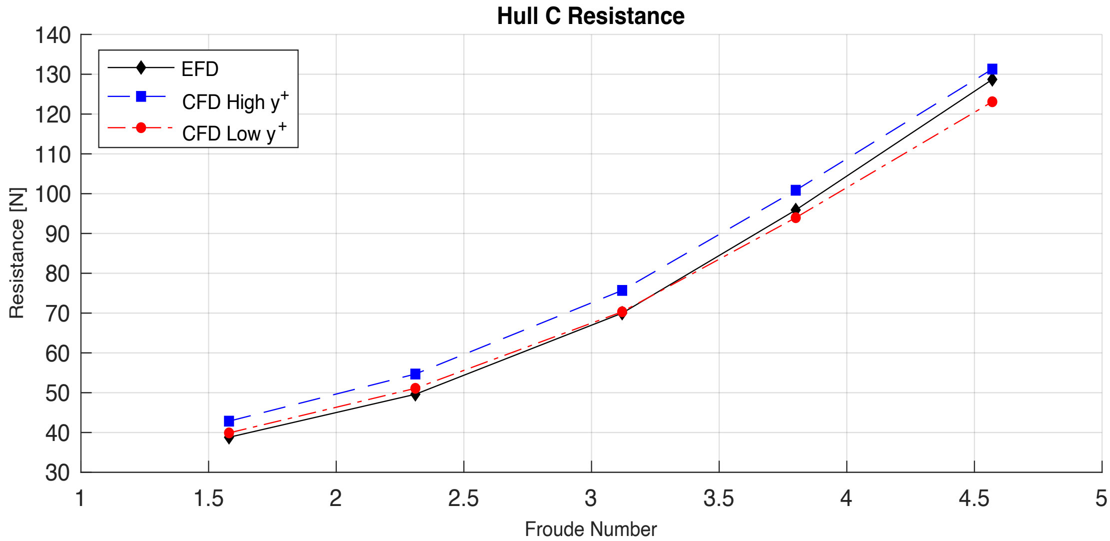

Figure 3.5 - Hull C Resistance

The accuracy of the high y^+ case is in line with the reported findings of similar numerical studies available in the literature, where the average reported prediction error has been in around 7% in recent years, as detailed in Table 2.1 while the present study was not able to decrease this average error, it was able to model the planing hull with a level of accuracy that may considered state of the art for such simulations, providing a suitable analysis tool for further investigation and a baseline for comparison to be made against. As is the case with several studies, the simulation is seen to be considerably more accurate for some speeds than others, with the comparison error decreasing from 10.43% to 2.02%. This highlights the finding that it is possible to develop very accurate simulations capable of modelling the resistance of a complex planing hull for certain speed cases, however the simulation will not hold this level of accuracy across a large speed range. While the accuracy is found to improve as the speed increases, the high y^+ case is seen to be capable of modelling the general trend of the experimental resistance, as seen when plotted in Figure 3.5.

The accuracy of the low y^+ case is considerably higher, proving to be the most capable instance of CFD modelling a planing hull in terms of resistance error of any of the previous studies that were examined during an extensive review of the available literature. The average error of 2.54% is a distinct improvement over the accepted accuracy of 7%, and is considerably superior to the 10% as proposed by (ITTC - Recommended Procedures and Guidelines, 2011). As pointed out by (De Luca *et al.*, 2016), it is well known that marine CFD simulations of planing craft are significantly less reliable than for conventional vessels, however the present study shows this disparity in accuracy to be closing. Analysis of the 2005 Gothenburg Workshop showed the average error for all resistance simulations for displacement ships to be 4.7%, with this decreasing to 2.1% for the entries of the 2010 workshop (Larson, Stern and Visonneau, 2014). The workshop provides an international benchmark for CFD as applied to conventional ships, and the results of this are not applicable to high-speed craft, however a marked improvement in levels of accuracy is seen as numerical techniques are developed over time. The low y^+ case of the present study shows it is now possible to model the resistance of planing hulls with a similar level of accuracy as conventional ships. It should be noted that the Gothenburg Workshop in 2010 comprised of 33 entries modelling the KCS hull over a range of speeds, demonstrating that CFD methods are consistent at producing precise results from a range of practitioners. Comparable level of accuracy has only been obtained for a planing hull in the present study. There is still a way to go before CFD may be relied upon for planing hulls to the same extent as it is for conventional vessels, and robust validation cases are still necessary for all planing hull application, however it shows the continual development and improvement in the ability of CFD to model planing hulls in recent years as previously outlined in Table 2.1.

The key reason attributable to the increase in accuracy in comparison to previous results reported in the literature is the use of the higher fidelity, low y^+ approach to turbulence modelling as opposed to the high y^+ methodology employed by the majority of work in this field. This change in approach improved the accuracy by 4.67%, which is a significant gain. It has been found previously that the choice between a low and high y^+ approach is the numerical set up factor that has the single largest effect upon the accuracy of the calculated resistance, with a previous improvement of 6.01% being demonstrated (Gray-Stephens, Tezdogan and Day, 2020b). This is in line with the present study and shows that switching from a high to low y^+ approach to turbulence typically improves the resistance calculation by around 5%. Under the low y^+ approach the viscous sublayer is directly resolved as opposed to employing wall functions to model the boundary layer, deriving turbulence dissipation and the wall shear stress from equilibrium turbulent boundary layer theory. By ensuring that the whole near wall turbulent boundary layer is resolved, with the transport equations being solved all the way to the wall cell and the wall shear stress being computed as in laminar flows by utilising a low y^+approach, the calculation of forces is more accurate. The downside to this approach is that it requires the centre of the first cell to located in the viscous sublayer, requiring a large number of prism layers and which can be very computationally expensive to run. On average the change from a low to high y^+approach resulted in a 33.16% increase in the overall cell count and a 25.29% increase in the Solver CPU time.

3.5.1.1.1 Resistance Components of Hull C

To develop a more complete understanding of the changes that occur between the high and low y^+ approaches, further analysis of the resistance components was conducted. The use of CFD allow the pressure and shear force components of the wetted area to be extracted, as well as the air resistance acting upon the hull. These force components are plotted in Figure 3.6.

It is seen that the low y^+ approach leads to a reduction in the calculated shear forces. The higher fidelity approach more accurately resolves the boundary layer flow, as it does not rely upon the assumptions and approximations embodied in the wall functions corresponding with the reality of the application. Differences of less than 2% are also observed in the wetted pressure and air resistance components, however these appear minor in comparison to the differences observed in wetted shear. Interestingly, when the resistance components are plotted as a percentage of total resistance as in Figure 3.7, it is seen that the composition of the total resistance of the hull is near identical for both approaches. The maximum difference in component percentage is 0.66% for air, 1.12% for shear, and 1.10% for shear. This indicates that while the frictional resistance appears to be the most effected by the approach to turbulence, this is only because it is the largest component and in fact all of the components are affected in a similar manner.

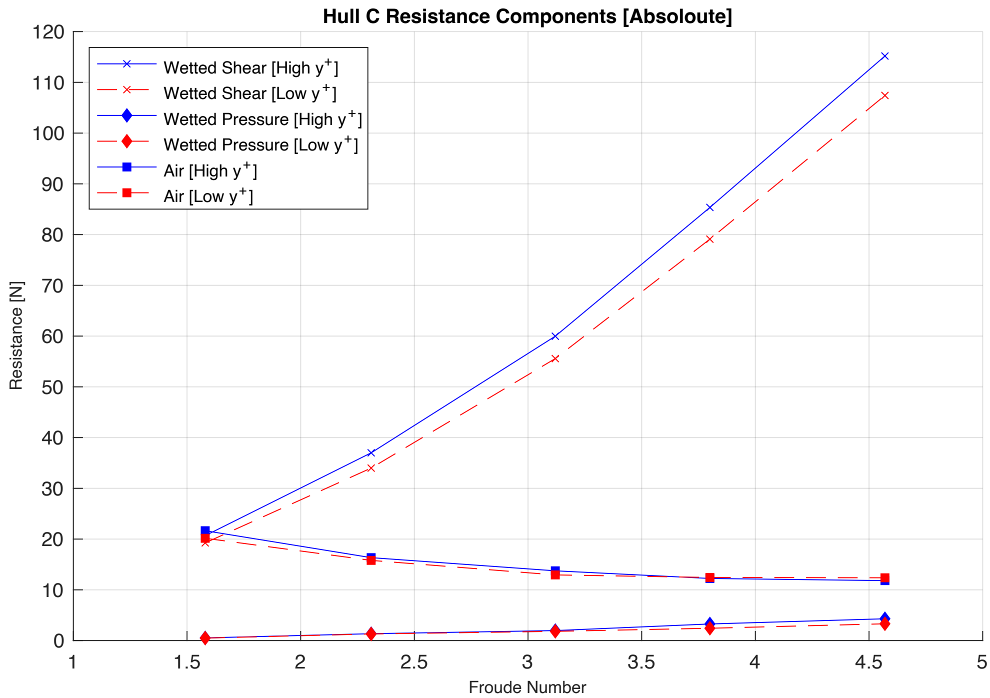

Figure 3.6 - Hull C absolute resistance components

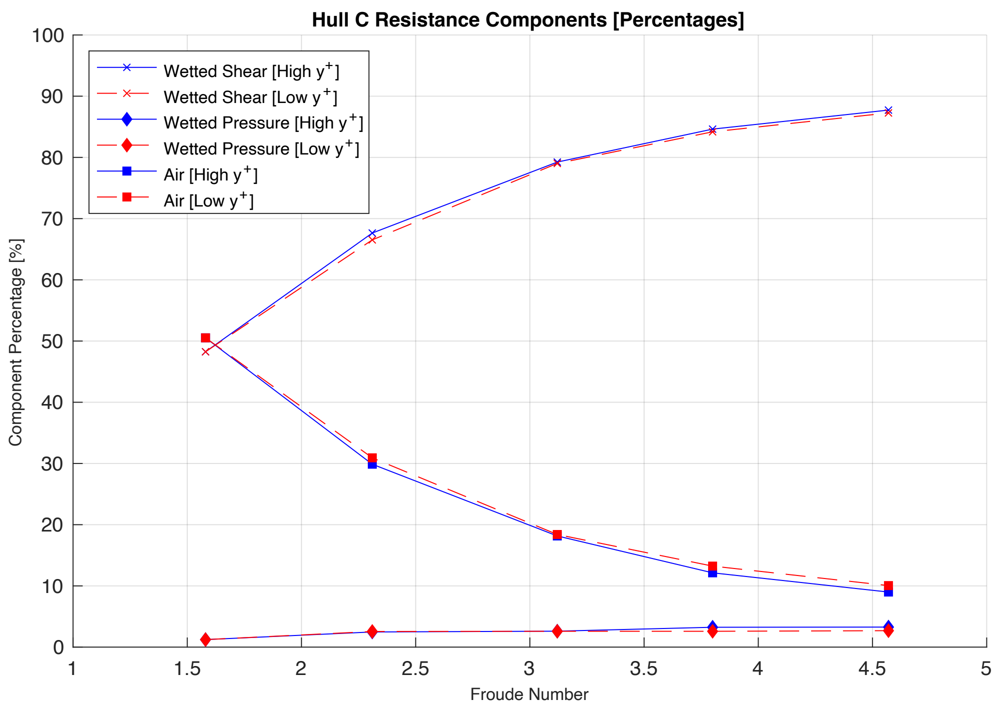

Figure 3.7 - Hull C percentage resistance components

The resistance components of Hull C show the expected trends with the frictional resistance component dominating at higher speeds. The contribution of pressure resistance decreases from 50.52% to 10.05%, whereas the frictional component increases from 48.25% to 87.26%. It is fact that the frictional component of resistance is so large at higher speeds that technologies the attempt to reduce the wetted portion of the hull such as stepped hulls, or hydrofoils are so attractive to the designers of high-speed craft, despite their added complexity. The component of air resistance increases from 1.23% to 2.69%, which is far less significant that the changes seen in the other components. Despite this, the increase shows the need to consider the aerodynamics of the above water portion of the hull as the speed of the vessel increases into the higher Froude number ranges, although this is out with the scope of the current study.

3.5.1.1.2 Numerical Ventilation of Hull C

As has been outlined in Section 3.3.4 Numerical Ventilation is a prominent source of error in simulations of high-speed planing hulls. Figure 3.8 to Figure 3.11 shows the NV for the fastest and slowest speed case of both approaches. It can be seen that the NV in all cases was in line with the levels reported by (Gray-Stephens, Tezdogan and Day, 2020b), showing the strategies proposed by the study to be robust. As the timestep is a function of speed, the NV is seen to be relatively constant for both speed conditions as the courant numbers of both simulations are similar. In any case, previous studies found NV to be more closely linked to the mesh than the timestep. The levels of NV are higher for the low y^+ approach, likely due to the larger number of layers in the prism mesh.

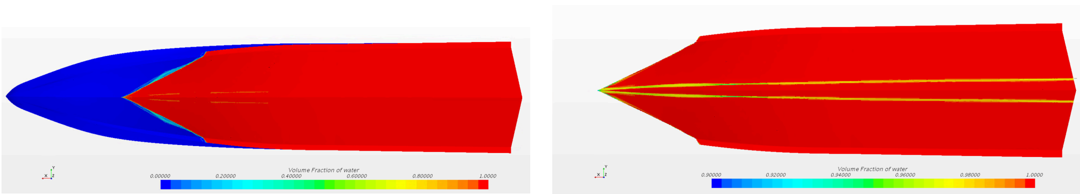

Figure 3.8 – Volume fraction high y+ [Fn = 1.58] (Top: 0% - 100%) (Bottom: 90% - 100%)

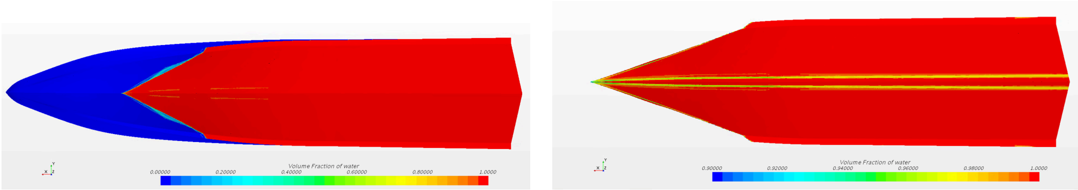

Figure 3.9 – Volume fraction high y+ [Fn = 4.57] (Top: 0% - 100%) (Bottom: 90% - 100%)

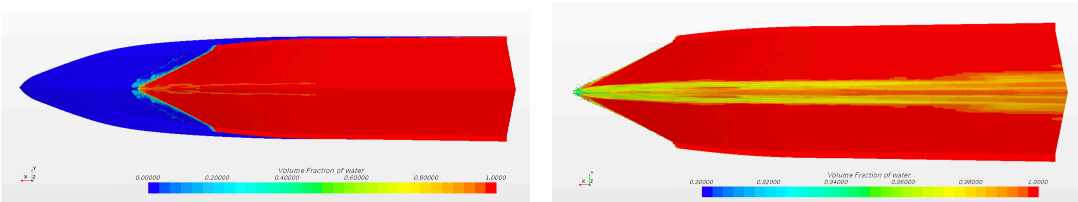

Figure 3.10 – Volume fraction low y+ [Fn = 1.58] (Top: 0% - 100%) (Bottom: 90% - 100%)

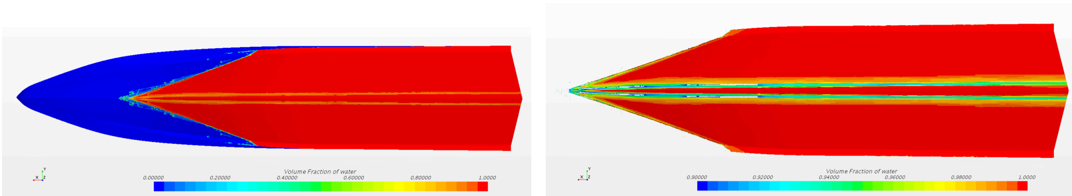

Figure 3.11 – Volume fraction low y+ [Fn = 4.57] (Top: 0% - 100%) (Bottom: 90% - 100%)

While previous studies have produced detailed strategies to minimise Numerical, the key metric in measuring the success of these strategies was the qualitative analysis of VOF plots (Gray-Stephens, Tezdogan and Day, 2020b). No work to date has gone as far as undertaking a quantitative analysis into the effects of numerical ventilation.

For the current study it is possible to evaluate and define the levels of numerical in a more meaningful way through the VOF Phase Replace Model. The model works to eliminate a VOF phase in cells as defined by the user, replacing it with a specified VOF phase. It differs from the artificial suppression method, as detailed by (Viola, Flay and Ponzini, 2012), in that phase replacement is not implemented with source terms to transport equations. Instead, some fields are overwritten prior to the first transport equation being solved within each iteration. The model updates the volume fraction of the phases, updates the mixture density to match the new volume fraction, and finally updates the total enthalpy for the primary and secondary phases, as well as for the mixture. This process ensures that the model does not contribute to the unsteady terms.

The model was applied to the converged solutions, which were then run for a single additional timestep as outlined by (Casalone *et al.*, 2020). The forces calculated on the hull for the final timestep do not include the altered fluid properties resulting from NV. These are compared to the forces of the previous timestep to quantifying the effects of numerical ventilation on resistance. When employing this method it is necessary to ensure that NV has been minimised before it is implemented. The method is only utilised for a single timestep, so the DFBI model is not able to determine the changes to the hulls position as a result of forces without NV. If there are significant levels of numerical ventilation prior to the phase replacement procedure, then the position of the hull may be incorrectly calculated. The incorrect positioning of the hull impacts both the pressure drag and the frictional drag through the incorrect wetted area. While it is possible to eradicate NV through this strategy, great care should be taken as it may give false confidence in the results if employed incorrectly.

The results of the phase replacement strategy applied to both the high and low y+ simulations are detailed in Table 3.12. An average change in error of 0.60% was found for the high y+ case, and 1.23% for the low y+ case. This is in line with the findings of (Gray-Stephens, Tezdogan and Day, 2020b), showing that with the correct strategies the impact of NV may be considered insignificant. The fact that the small amount of air entrapment as seen in Figure 3.11 leads to a 1.32% reduction in resistance does however demonstrate the potential of NV to influence a solution. It is apparent simulations with large levels will have a significant impact on their results.

When a phase replacement strategy is applied for the high y+ approach the average resistance error increases from 7.21% to 7.86%, while for the low y+ approach it decreases from 2.54% to 2.46%. The sinkage and trim results remain unchanged, as discussed. Analysis of the resistance components revealed that for the high y+ approach there was an average change to total resistance of 0.40% accountable to changes in the pressure force, and 0.17% accountable to changes in the shear force. Similarly, for the low y+ case there was an average change to total resistance of 0.67% accountable to changes in the pressure force, and 0.34% accountable to changes in the shear force. In both approaches the impact of NV is around twice as large on the pressure force component than the frictional force component. This shows that for cases in which there is initially only small quantities of numerical ventilation it is not only the skin friction of a hull that is influenced by NV as noted in (Casalone *et al.*, 2020).

Table 3.12 – Hull C phase replacement

Speed $[ms^{-1}]$	5.09	7.11	9.21	11.13	13.09
High y+ Resistance [N]	42.85	54.69	75.70	100.86	131.30
High y+ & Phase Replace Resistance [N]	43.15	55.08	76.10	101.44	131.96
High y+ Difference in Comparison Error	0.70%	0.72%	0.54%	0.57%	0.50%
Low y+ Resistance [N]	38.80	49.60	69.98	95.90	128.70
Low y+ & Phase Replace Resistance [N]	40.03	51.35	71.72	95.86	124.73
Low y+ Difference in Comparison Error	0.33%	0.49%	1.99%	2.01%	1.32%

3.5.1.2 Trim Results

The mean error in the running trim for the high y^+ case was found to be 19.33%, with a range from -17.16% to 23.53%, whereas the mean error for the low y^+ case was 15.07%, with a range of -25.68% to 16.57%. The results are plotted in Figure 3.12.

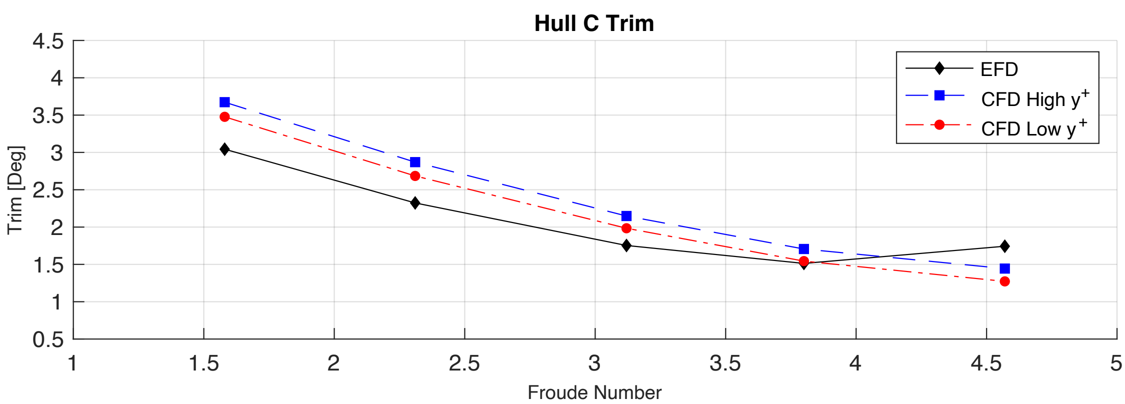

Figure 3.12 - Hull C Trim

The trim was found to produce the highest error of the three numerical metrics used to compare CFD to EFD, although it should be noted that while the percentage values of the error in trim are large, the absolute errors are 0.41° and 0.32° respectively for the high and low y+ approaches. This is typical of simulations of planing hills, as seen in Table 2.1 where the average error in trim was generally found to be below 20%, with a maximum of 25% (Kahramanoglu, Yildiz and Yilmaz, 2018). Mancini et. al. found a similar result, stating that percentage differences of up to 20% may be expected (Mancini, de Luca and Ramolini, 2017). The accurate calculation of trim in planing hulls has proved to be challenging, which is a result of difficulties in identifying the centre of pressure, or generally the pressure distribution on the hull (De Luca *et al.*, 2016). The calculation of the pressure distribution was found to be affected significantly by edge effects, and the percentage of hydrodynamic lift required to sustain the hull.

Both the high and low y+ approaches are seen to follow the same trend of decreasing trim with increasing speed, which is typical of planing hulls. The experimental trim decreases with speed until a Froude number of 3.8, after which point it increases from 1.51° to 1.74°. The experimental data in this region is in contradiction to the trends in trim reported by (Savitsky and Morabito, 2010), who use the well renowned work of (Savitsky, 1964) to show that the equilibrium trim angle decreases with increasing speed. The results of both the high and low y+ approach agree with this finding. Errors of -25.65% for the low y+ case and 17.16% for the high y+ approach are found at a Froude number of 4.57, which are some of the largest reported error. This is the only speed at which CFD was found to underpredict the trim value. (Khazaee, Rahmansetayesh and Hajizadeh, 2019a) modelled Hull C using their CFD set up and Savitsky's method, reporting a similar finding to the present study where the trim is found to continue decreasing at a Froude number of 4.57. Unfortunately, without further access to the experimental data it is not possible to comment upon the reasons for the increase in trim at this highest speed in the experimental results.

Once again, the low y+ approach is seen to produce the most accurate trim results, decreasing the average error by 4.27%. In Figure 3.12 it is seen that the difference between the high and low y+ cases is relatively constant with an average value of 0.18° and a range of 0.16° - 0.20°. This would indicate that there is a constant change in the longitudinal centre of pressure when a low y+ approach adopted, resulting in a similar change in in trim.

3.5.1.3 Sinkage Results

The mean sinkage error for the high y^+ case were found to be 4.77%, with a range from -4.89% to 7.09%, while the mean error for the low y^+ case was 3.72%, with a range of -4.82% to 5.37%. The results are plotted in Figure 3.13.

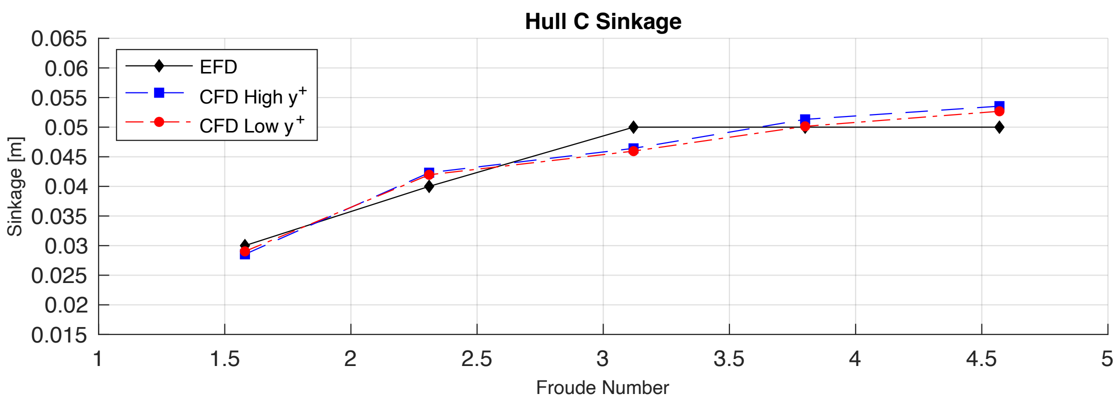

Figure 3.13 - Hull C Sinkage

When previous work in the literature was studied the sinkage error was typically found to be less than 10%, as seen in Table 2.1. The sinkage errors found in the present study were among the most accurate of all the work that was compiled, showing that an average trim error of less than 5% was attainable for both the high and low y+ approaches. In a manner similar to the resistance and trim results, the sinkage results for both the high and low y+ approach are seen to follow the same trend. Of all the metrics examined the sinkage was seen to be the least effected by the approach to turbulence, with only 1.05% difference in the average error being seen between the two. The average absolute difference between the high and low y+ approaches was found to be 0.71mm. Despite the differences between the two approaches being small, it was still seen that once again the low y+ approach produced the more accurate results.

One factor that makes comparison between the experimental and numerical data difficult was the degree of accuracy with which the experimental data is reported. The experimental data was published to two decimal places, or the nearest 0.01m. This results in a unit uncertainty of 0.005m, or 16% for the lowest speed case and 10% for the highest. Indeed, when the numerical data was subject to the same rounding both the high and low y+ results match the experimental results identically. It would normally be expected that the sinkage gradual increases with speed, as seen in the early experimental results of (Gerard Fridsma, 1969), as opposed to increasing up to a point and then plateauing as in the experimental results of (Taunton, Hudson and Shenoi, 2010). Due to this it is not possible to have as high a level of confidence in the comparison that is made between the numerical and experimental sinkage data as in the resistance or trim comparisons. Despite this, there is still seen to be a strong degree of correlation, with the numerical data matching the experimental data satisfactorily.

3.5.2 Single-Stepped Hull

This section presents and discusses the numerical results for the single-stepped hull geometry, Hull C1. Figure 3.14 shows the experimental results of the unstepped hull versus the single stepped hull. The benefit of stepped hulls is immediately obvious, with the single stepped hull exhibiting a lower resistance than the unstepped hull at all speeds. As the speed increases the difference in resistance becomes more pronounced, until at $12.05ms^{-1}$ there is a reduction in resistance of 25.85%. The following section sets out to analyse the effectiveness of CFD in calculating the resistance and running attitude of a single stepped planing hull, and the effects of the approach to turbulence. The CFD results will be analysed in detail to discuss the mechanisms through which the resistance of a single stepped hull is achieves such a large resistance reduction and the effects of numerical ventilation.

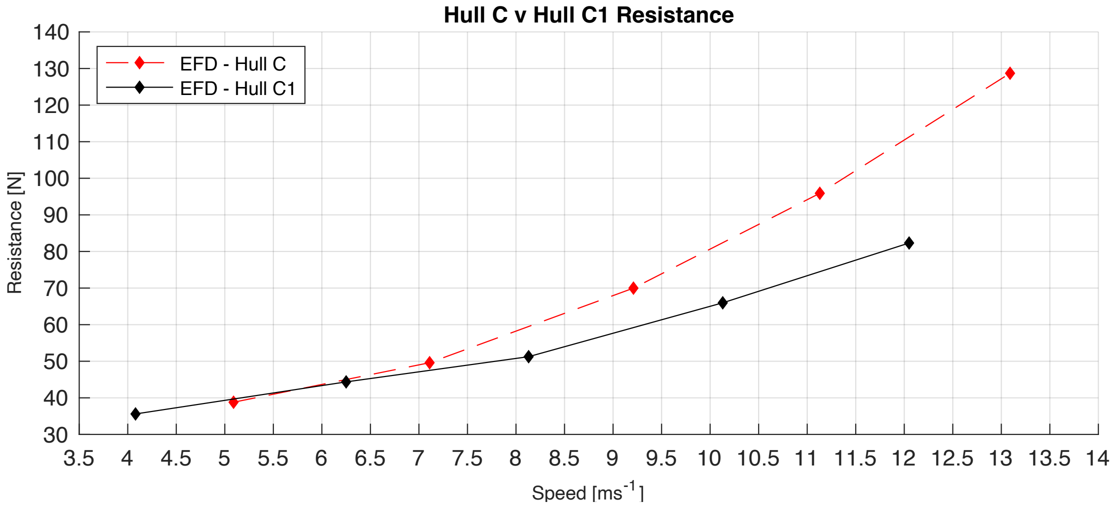

Figure 3.14 - Hull C v Hull C1 resistance

(Taunton, Hudson and Shenoi, 2010) experimentally measured and compared the dynamic trim of the stepped and unstepped hull, finding that while there were some changes the same trends were followed and it was largely the same for all hull variants. However, when the total trim of a stepped hull is considered, as presented in Figure 3.15 it is seen that there is a far larger difference then when only dynamic trim is compared. A stepped hull is seen to have an increased running trim over its unstepped variant. This is due to the increased static trim of the stepped hull, as seen previously in Table 3.9. The unstepped hull was found to have a static trim of 0.02°, whereas the single-stepped hull was found to have a static trim of 1.13°. When a step is added volume in the aft section of the hull is lost, and so the static trim has to increase to make up for this lost buoyancy when in an equilibrium position.

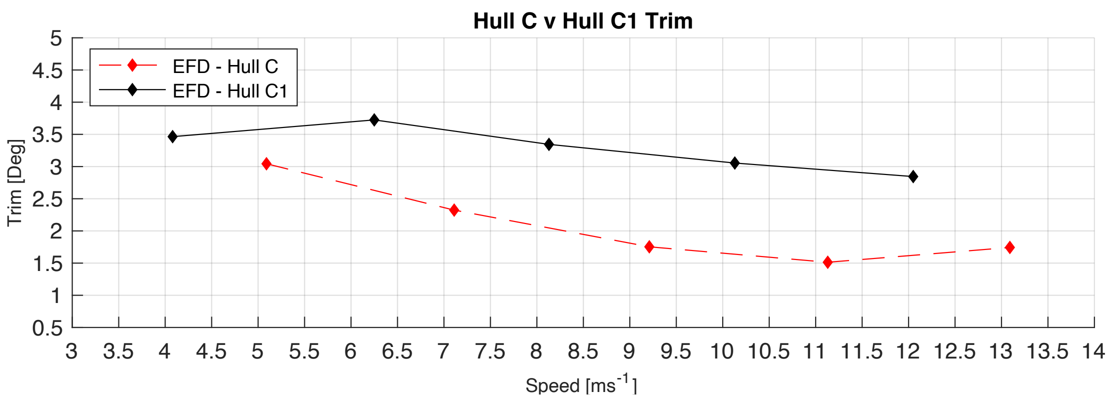

Figure 3.15 - Hull C v Hull C1 Trim

Due to the unit uncertainty in the reporting of the sinkage values, as discussed previously, it is difficult to draw any real conclusions or comment on the comparison of sinkage as presented in Figure 3.16. It does however appear that the rise of the CG for the stepped hull is greater than that of the unstepped hull. When the high y+ CFD results for both hulls is compared, as seen in Figure 3.17, it is confirmed that a stepped hull's rise in CG is larger. This is linked to the fact that the stepped hull has a greater running trim. Increasing the angle of attack of a lifting surface produces more lift. As there is a larger dynamic lift component, the remaining lift component that is produced as by the buoyancy force is not required to be so large to support the weight of the vessel, and the hull may rise further out of the water.

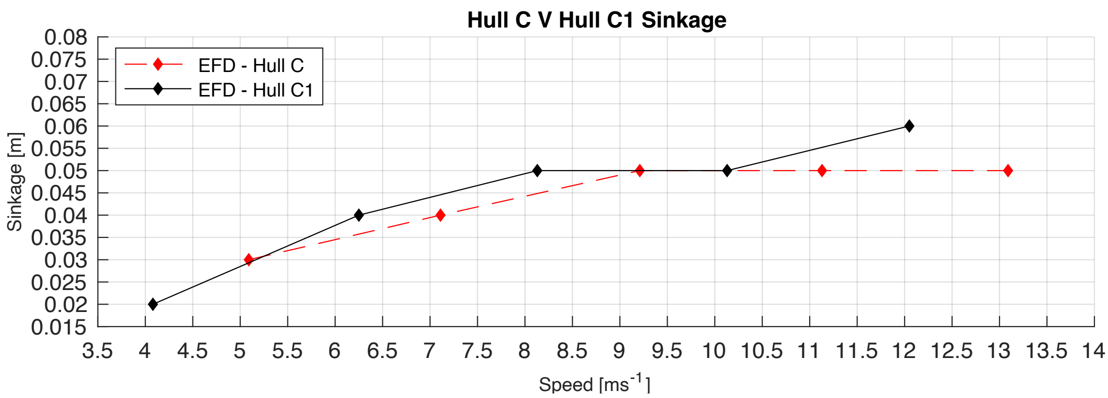

Figure 3.16 - Hull C v Hull C1 sinkage (experimental)

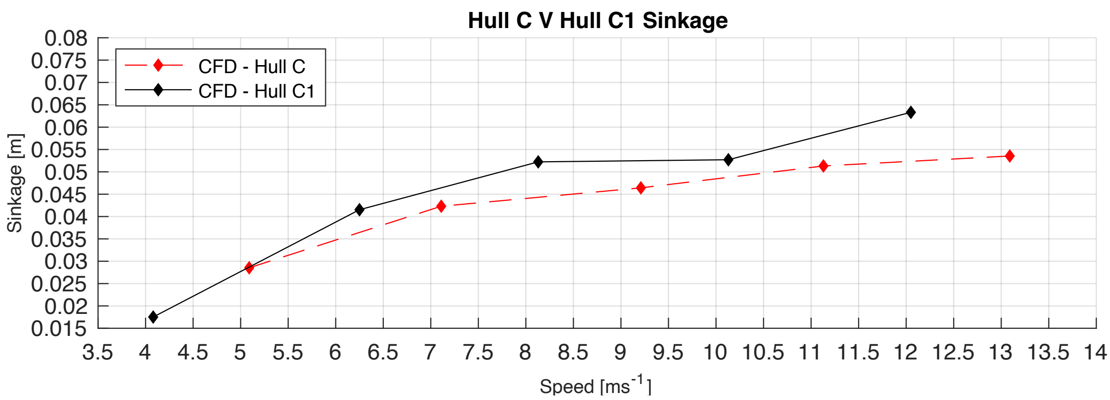

Figure 3.17 - Hull C v Hull C1 sinkage (numerical)

Table 3.13 & Table 3.14 detail the resistance, trim and sinkage as calculated by CFD. Additionally, the comparison error, as given by Equation (3.13) is presented. Each of the calculated values will be analysed and discussed separately, before general comments related to the numerical simulation are put forward.

Table 3.13 – Hull C1 High y^+ Numerical Results

Speed	Froude Number	Resistance [m]	Trim [°]	Sinkage [m]	Resistance Error	Trim Error	Sinkage Error
4.08	1.14	36.82	3.64	0.018	3.44%	5.05%	-12.41%
6.25	1.89	45.88	4.05	0.042	3.43%	8.67%	3.82%
8.13	2.61	49.61	3.81	0.052	-3.19%	13.98%	4.46%
10.13	3.34	63.34	3.44	0.053	-3.98%	12.60%	5.42%
12.05	4.00	71.57	3.17	0.063	-13.05%	11.53%	5.53%

Table 3.14 – Hull C1 Low y^+ Numerical Results

Speed	Froude Number	Resistance [m]	Trim [°]	Sinkage [m]	Resistance Error	Trim Error	Sinkage Error
4.08	1.14	35.30	3.57	0.018	-0.84%	3.01%	-15.39%
6.25	1.89	42.02	3.88	0.041	-5.27%	4.30%	2.86%
8.13	2.61	46.68	3.66	0.063	-8.91%	9.57%	30.28%
10.13	3.34	58.83	3.25	0.060	-10.82%	6.45%	23.62%
12.05	4.00	70.58	2.94	0.074	-14.25%	3.24%	25.56%

3.5.2.1 Resistance Results

The mean absolute resistance values for the high y^+ case was found to be 5.42%, with a range from -13.05% to 3.44%, whereas the mean value for the low y^+ case was 8.02%, with a range of -14.25% to -0.84%. The numerical and experimental data is plotted in Figure 3.18.

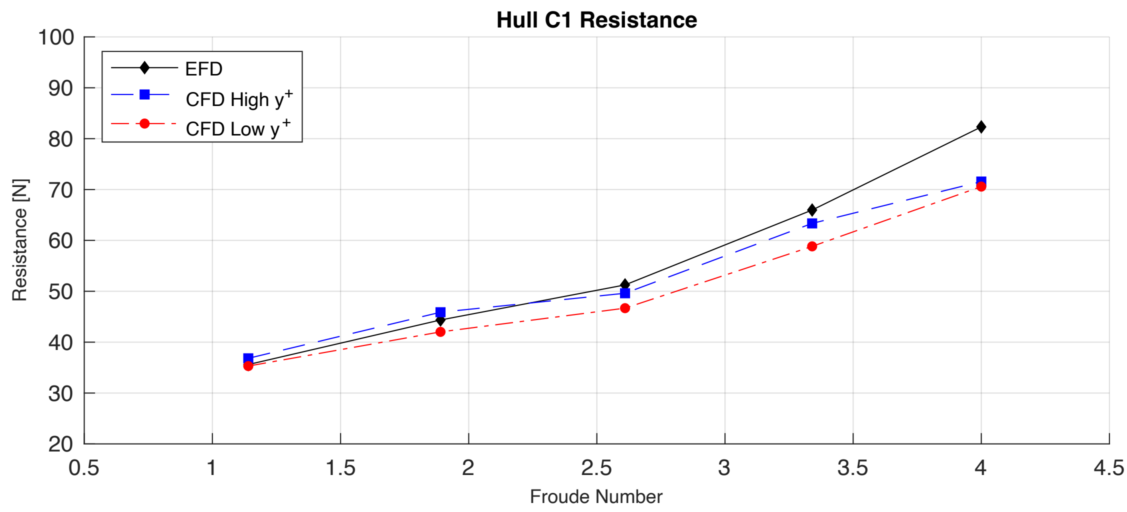

Figure 3.18 - Hull C1 resistance

When the literature was studied it was found that an average resistance error of 8.5% was typical for a numerical simulation of a single stepped planing hull. Four studies were found to have modelled Hull C1, resulting in average errors of approximately 10% (Veysi *et al.*, 2015), 5.25% (Lotfi, Ashrafizaadeh and Esfahan, 2015), 5.91% (Yang *et al.*, 2019) and 7.80% (Dashtimanesh, Tavakoli, *et al.*, 2020). The set up employed by the present study was able to model the resistance with a higher level of accuracy than is typical of single-stepped playing hulls, matching the average resistance error of the study that produced the most accurate results.

The experimental data was well modelled by CFD for both a high and low y+ approach to turbulence. While it was found that for an unstepped hull that a low y+ approach was more capable of calculating the resistance this is not the case for a single-stepped planing hull. It is seen that the high y+ approach is more accurate, reducing the average resistance error by 3.57%. Additionally, it is seen that both approaches tend to underpredict, rather than overpredict the resistance as is typical for simulations of unstepped planning hulls. This may suggest that NV was tainting the simulations, reducing the calculated resistance. It was previously shown that the low y+ approach was better able to model the forces acting on a planing hull, however it was more prone to air becoming trapped in the near wall cells. This further suggests that NV may be an issue in the present simulations.

3.5.2.1.1 Numerical Ventilation of Hull C1

The VOF plots of the hull for both the high and low y+ approaches are presented in Figure 3.19 and Figure 3.20. Numerical ventilation is seen to exist in all cases, however it is seen that the strategies to minimise its effects as outlined in (Gray-Stephens, Tezdogan and Day, 2020b) are seen to perform well when applied to single-stepped planing hulls.

It was seen in all cases there were larger quantities of NV present on the aft hull. This is due to the fact that the forehull is intersecting with calm water, whereas the aft hull is intersecting with the more complex flow that has separated from the step. A more detailed investigation into this may be able to further reduce the amount of numerical ventilation present on the aft hull through further changes to the meshing strategy, however it was deemed that the levels were acceptable for the current application. In both the high and low y+ approaches the level of NV on the forehull does not appear to show a strong correlation with speed. The level of numerical ventilation on the after body does however, appear to show a correlation with speed and larger quantities of air are introduced to the near wall cells as the speed increases. This is especially true for the side wetting that is occurs when the stagnation line crosses the step in the 10.13 ms^{-1} & 12.05 ms^{-1} cases.

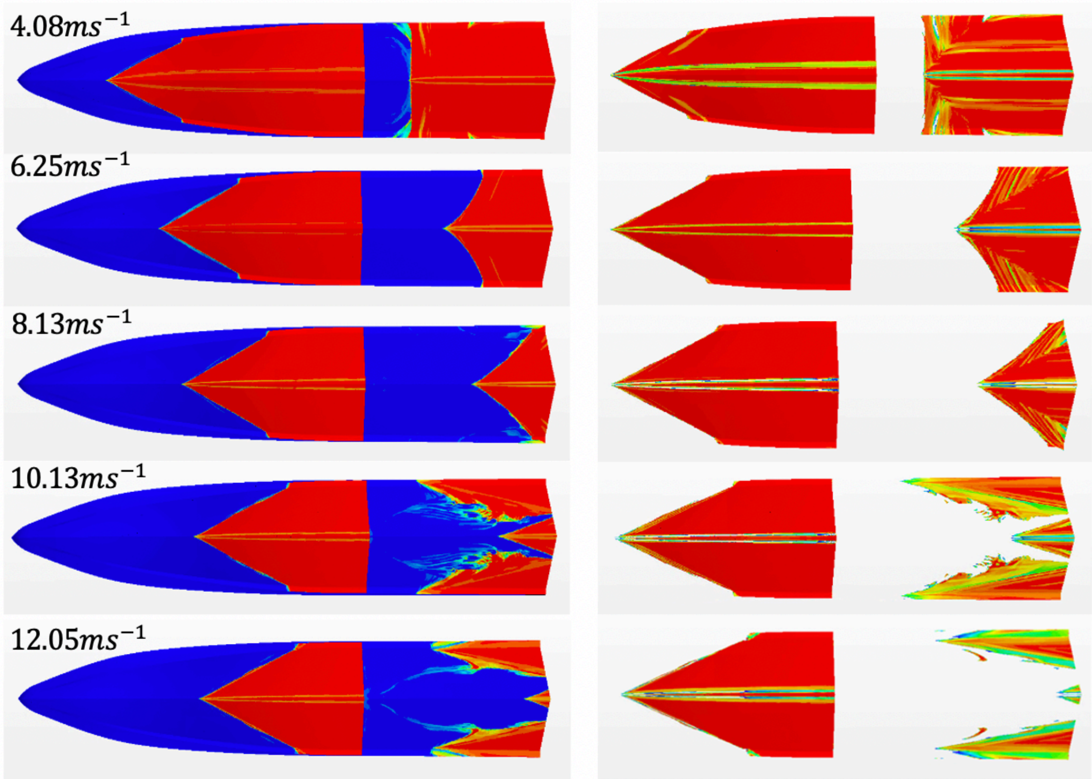

Figure 3.19 – Volume Fraction High y+ (Left 0% - 100%) (Right 90% - 100%)

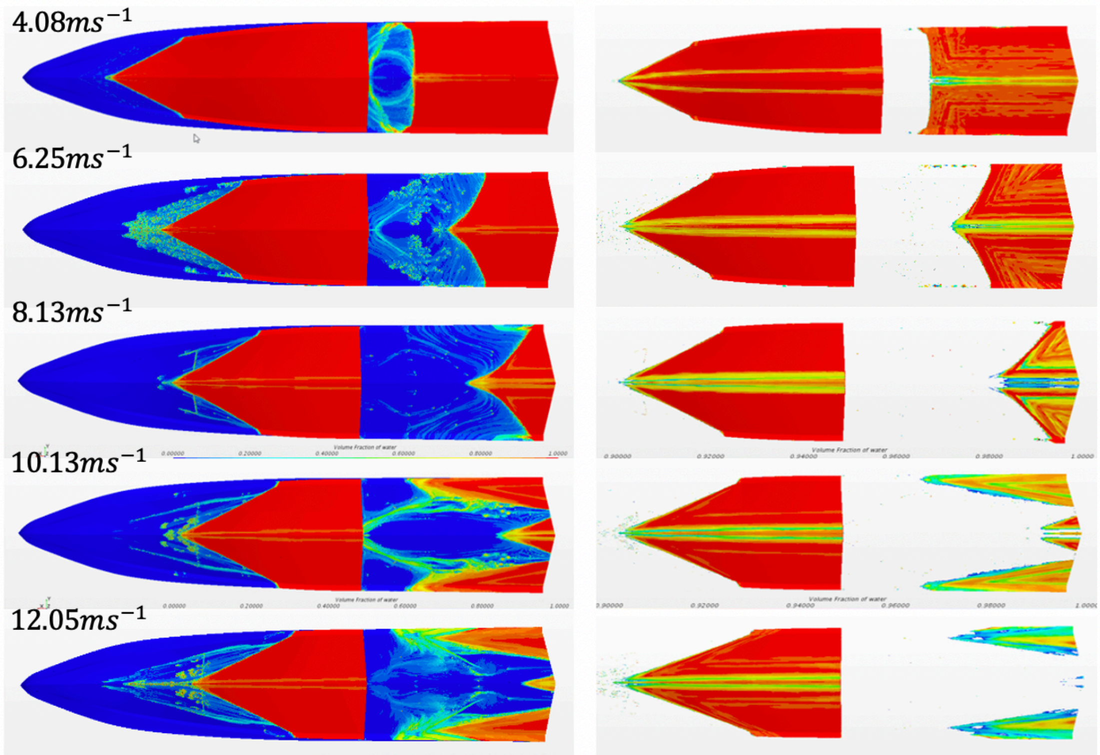

Figure 3.20 – Volume Fraction Low y+ (Left 0% - 100%) (Right 90% - 100%)

Previous work has highlighted potential issues surrounding the applicability of the phase replacement method when applied to stepped hulls due to its inability to differentiate between physical ventilation and NV (Gray-Stephens, Tezdogan and Day, 2020b). While there is a case to be made that there will be some mixture of fluids transported under the hull, it can be seen that the fluid mixture on the aft hull in Figure 3.19 and Figure 3.20 is characterised by two central streaks. This is a clear indication of NV. The side wetting is harder to attribute entirely to numerical ventilation, however it does resemble the second source of numerical ventilation detailed in (Gray-Stephens, Tezdogan and Day, 2020b). Care should be taken to ensure that the fluid mixture on the aft hull is caused due to NV, rather than CFD's attempt at modelling bubbles of air prior to utilising phase replacement. It is likely that in the case that CFD is trying to model physical ventilation and flow with bubbles in it that the percentage of air in the cells would be significantly higher than <10% as is seen here. Finally, photographs of a similar experimental study as conducted by (De Marco *et al.*, 2017b) employing a Perspex hull show these sections to contain no physical ventilation, as seen in Figure 3.21. It was seen that the air and water phases did not physically mix and that there was a clear free surface formed aft of the step. As such it was viable to employ a phase replacement strategy to eliminate the NV, as detailed in Section 3.5.1.1.2.

Figure 3.21 – Flow Pattern of a Similar Experimental Study (De Marco *et al.*, 2017b)

Table 3.15 details the results. The increase in resistance in comparison to the experimental data when NV was supressed for the high y + approach is 2.12%, with a range of 1.54% to 2.86%. This increase is significantly larger than the 0.60% found for the high y+ simulation of the unstepped hull. This result is unsurprising as a comparison of Figure 3.9 to Figure 3.19 shows the single stepped hull was subject to significantly more NV. The average resistance error for the high y+ approach with phase replacement is 4.72%, a 0.69% improvement over the simulations prior to the removal of NV. When the strategy is applied to the low y+ approach the resistance increases by an average of 3.42% in comparison to the experimental data, with a range of 1.01% to 5.76%. Once again, this is considerably larger than the 1.23% found for the unstepped hull. This is far more significant and shows the extent to which low y+ simulations are affected by numerical ventilation. The average resistance error for the low y+ approach decreased from 8.02% to 6.36% once the numerical ventilation had been removed.

Table 3.15 – Hull C1 phase replacement

Speed [ms^{-1}]	**4.08**	**6.25**	**8.13**	**10.13**	**12.05**
High y+ Resistance [N]	36.82	45.88	49.61	63.34	71.57
High y+ & Phase Replace Resistance [N]	37.39	46.67	50.88	64.58	73.61
High y+ Difference in Comparison Error	1.54%	1.72%	2.55%	1.95%	2.86%
Low y+ Resistance [N]	35.30	42.02	46.68	58.83	70.58
Low y+ & Phase Replace Resistance [N]	35.85	42.74	47.87	59.98	72.60
Low y+ Difference in Comparison Error	1.01%	5.76%	4.16%	2.89%	3.26%

Examination of the resistance components of the high y+ case revealed the average change in pressure and shear resistance to be 1.43% and 0.48%, while these were 2.13% and 0.89% for the low y+ case. This agrees with the findings for the unstepped hull, as detailed in Section 3.5.1.1.2, showing the detrimental effects of numerical ventilation to not be limited to then frictional component of resistance. It has been stated previously that calculating the trim of a planing hull is challenging, with both shear and pressure resistance being affected by any errors. It follows that when removing NV leads to a significant change in resistance, the pressure distribution on the hull will be altered and both resistance components will be affected, which may have a significant impact upon the equilibrium trim of the vessel. While it is not possible to determine this new equilibrium position using the phase replacement strategy, it is foreseeable that there will be changes to the induced pressure drag, and the wetted area and thus frictional drag, further impacting the accuracy of the simulation. This highlights how vital it is to ensure that numerical ventilation is minimised prior to replacing the cells containing a mixture of fluids, as otherwise the potential errors compound in the results and there can be less confidence in the numerical solution.

It is not uncommon to see numerical ventilation affecting studies available in the literature. The VOF plot published in Figure 17 of the paper by (Sajedi and Ghadimi, 2020) shows no cells on the wetted hull contain 100% water, while the cells on the aft hull contains a fluid mix of close to 60/40. The study found reasonable results with resistance error of >5%, a sinkage error of 6.5% and a trim error of 9.5%. The work of the present section details the influence of NV on stepped hulls, and outlines the knock on effects arising from the equilibrium position of the hull. Given the prevalence of NV in the aforementioned study, it is highly likely that the results are significantly impacted, and little confidence can be placed in them.

3.5.2.1.2 Resistance Components of Hull C1

It is well established that the addition of a step decreases the resistance of a stepped hull, with the experimental results of (Taunton, Hudson and Shenoi, 2010) demonstrating that there may be a reduction of 25.85% for higher speeds as shown in Figure 3.14. This is achieved through reducing the wetted area of the hull, however a more detailed analysis is required to fully bring the benefits of a stepped hull to light and to understand how best to exploit these to maximise the reduction in resistance. It is difficult to compare the resistance components of a stepped hull experimentally for a number of reasons. Firstly, it is very complex to directly measure the frictional and pressure components. Instead, the frictional resistance must be determined using alternate methods, such as the ITTC '57 friction line, which adds an element of uncertainty. Secondly, and of greater consequence, using these methods requires the wetted area of the hull. This is something that is difficult to determine experimentally for a conventional hull and is even more challenging when considering stepped hulls which are subject to the additional to the complexity determining the intersection of flow with the afterbody. Secondly, as seen in Figure 3.19 the wetted area of the afterbody can comprise of several components. Accurately determining the wetted area of a stepped hull experimentally is extremely challenging, introducing a large element of uncertainty however, without this it is not possible to determine the resistance components.

When performing numerical calculations using CFD the total resistance to be easily broken down into its component parts. This has been done for the high y+ simulations of the unstepped and single-stepped hull variants, with the results plotted on Figure 3.22. The actual breakdown of resistance of a planing hull includes a component of spray resistance, as detailed by (Savitsky, DeLorme and Datla, 2007), which under the present methodology is included in the wetted pressure and shear drag components.

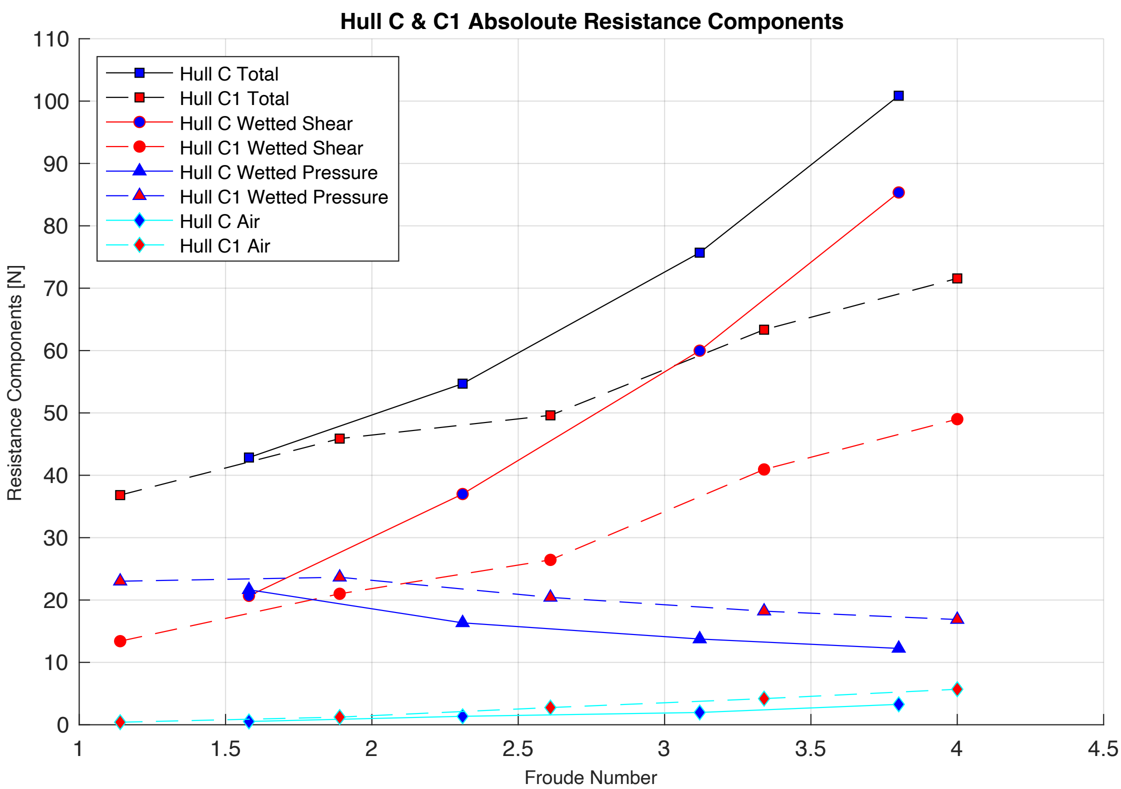

Figure 3.22 – Hull C & C1 Absolute Resistance Components

Figure 3.22 reveals the considerable decrease in the frictional resistance resulting from the addition of steps. In the VOF plots detailed by Figure 3.19 it is seen that the wetted surface of a stepped hull reduces with speed as the ventilation length increases. Frictional resistance increases proportionally with area, and with speed squared. As the Froude number of the vessel increases so too does the difference in frictional resistance, increasing form 12.93%, at a Froude number of 1.58 to 45.52% at a Froude number of 3.80.

The pressure component of resistance is seen to increase by a relatively constant value of about 5N for all speeds. Pressure resistance closely linked to the trim. As the stepped hull is subject to a relatively constant increase in trim, it follows that the increase in pressure resistance would be relatively constant.

Finally, it is seen that the air resistance of a stepped hull is larger than that of an unstepped hull. A contributing factor to air resistance arising from air passing through the inlets and under the hull at the step. Air resistance increases with speed, and so too does this additional component, leading to an growing difference as the speed increases.

The resistance components are plotted as a percentage of total resistance in Figure 3.23. It is seen there is a notable difference in the composition of resistance between a stepped and unstepped hull. This follows from the previous discussion surrounding the decreased frictional, and increased pressure and air components. While the make-up of total resistance is different for a given speed, the general trends are the same for both the unstepped and single stepped hull. As the speed increases the frictional component grows rapidly and dominates the total resistance, while the absolute pressure resistance reduces slightly with the reducing trim, and its percentage contribution to the total resistance reduces significantly.

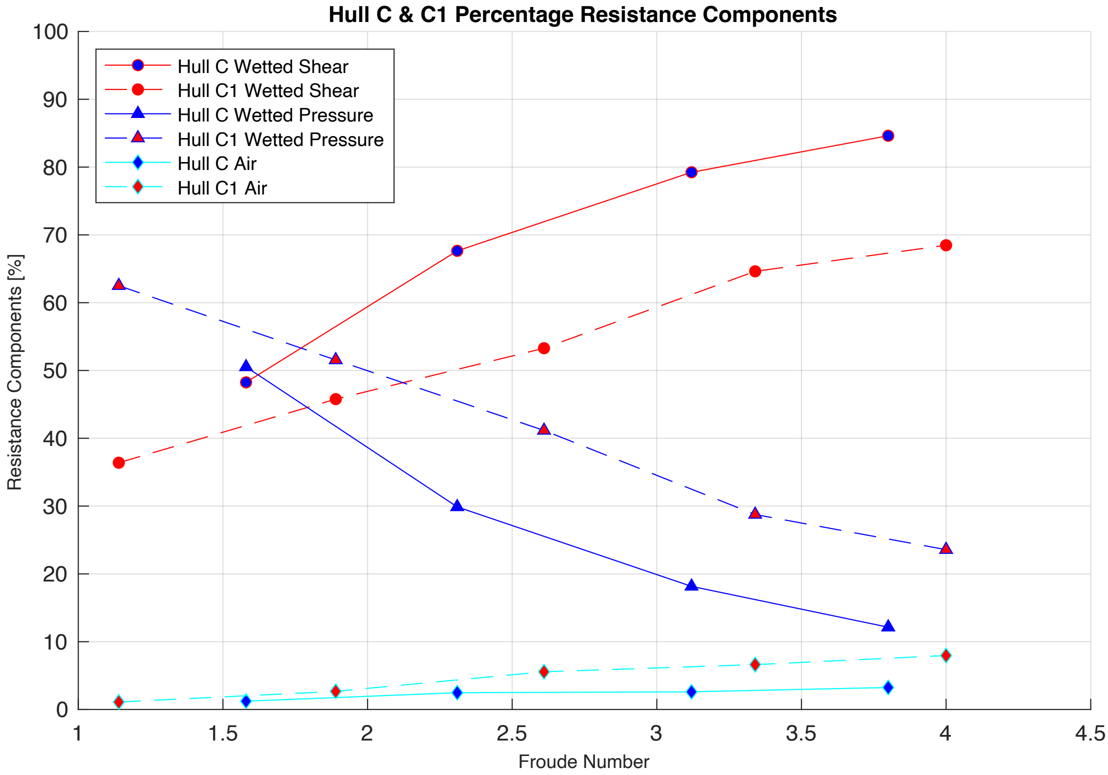

Figure 3.23 – Hull C & C2 percentage resistance components

3.5.2.2 Trim Results

The mean error in the running trim values for the high y^+ case was found to be 10.36%, with a range from 5.05% to 11.53%, whereas the mean value for the low y^+ case was 5.31% with a range of 3.01% to 9.57%. The results are plotted in Figure 3.24.

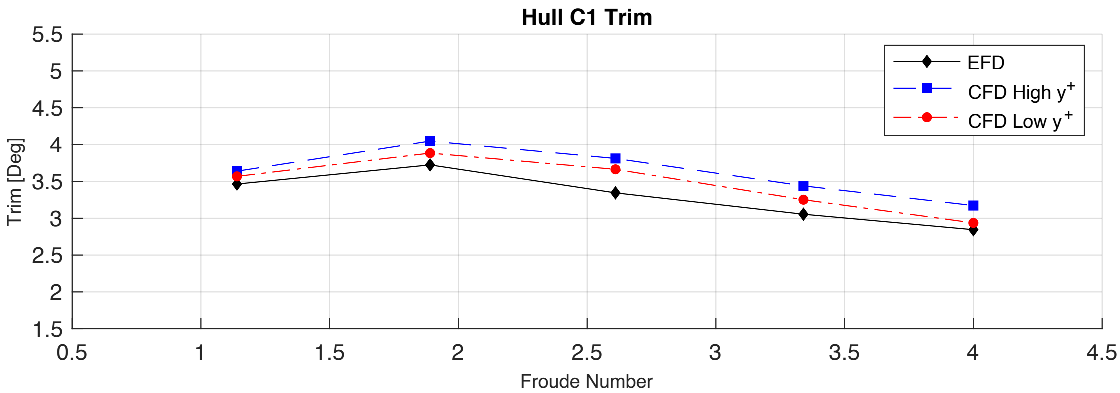

Figure 3.24 - Hull C1 Trim

Both the high and low y+ approaches perform remarkably well in calculating the running trim of a single stepped hull, resulting in low errors and modelling the trends well. An average error of around 10% was found when the in the literature for similar studies, while those specifically investigating Hull C1 found average errors of 12.86% (Lotfi, Ashrafizaadeh and Esfahan, 2015), 11.68% (Yang *et al.*, 2019) and 11.13% (Dashtimanesh, Tavakoli, *et al.*, 2020). It is seen that the present study was more accurate than the previous work investigating this hull.

No previous study was found that investigated the use of a low y+ approach to turbulence as applied to a stepped hull. Initially, it appears as though this is more capable of modelling the trim of a stepped hull than a high y+ approach. This finding should, however, be treated with caution. In Section 3.5.2.1 it was shown that the low y+ approach is less accurate in calculating the resistance, while being subject to changes in error of up to 5.76% due to NV. The low y+ approach is clearly less capable in modelling the forces acting upon the hull and given the sensitivity of the trim calculation this apparent accuracy may be a coincidence. Additionally, due to the larger effects of NV for the low y+ case, the hull is not necessarily in its equilibrium position. As such these results should be treated with caution, and trim results of the high y+ approach may be used with a higher degree of confidence, despite appearing to be less accurate.

3.5.2.3 Sinkage Results

The mean running sinkage error values for the high y^+ case was found to be 6.33%, with a range from -12.41% to 5.53%, whereas the mean error value for the low y^+ case was 19.54%, with a range of -15.39% to 30.28%. The results are plotted in Figure 3.25.

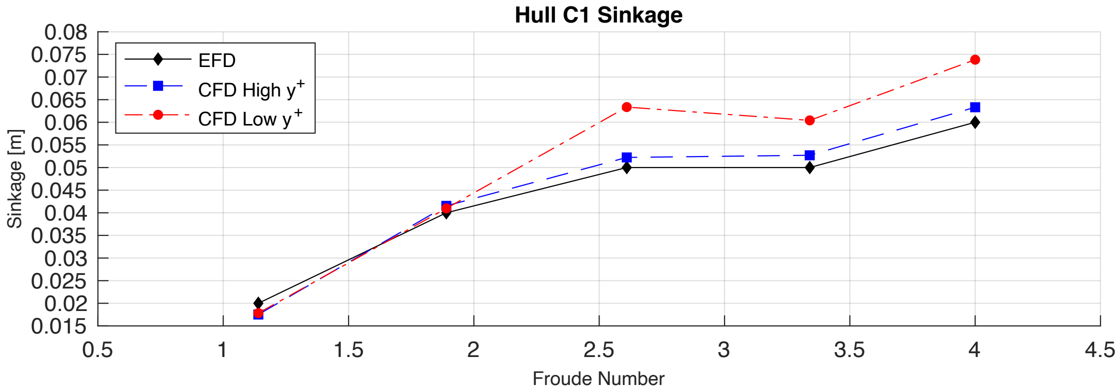

Figure 3.25 - Hull C1 sinkage

It is seen that the trends in sinkage are well modelled by the high y+ approach. The performance of the low y+ approach is considerably less satisfactory, with the general trends are modelled, but subject to an overprediction. This is likely due to the low y+ simulation being more effected by NV. The inaccuracy in sinkage confirms that there is a lower confidence in the results in the equilibrium position of a stepped hull, , as discussed in the previous section.

The largest error arising from the high y+ approach is -12.41% for the slowest condition, where the experimental sinkage is 0.02m. The absolute difference between the experimental and numerical values at this speed condition is in line with the absolute differences for the faster speeds. It is due to the small physical value that the percentage error is significantly larger for this condition. The absolute error at a Froude number of 1.14 is 0.00248m, whereas the average across all speeds is 0.00245m, with a range of 0.00153m to 0.00331m.

The average error of similar studies available in the literature was 14.17%, as seen in Table 2.2. Studies specifically investigated Hull C1 were found to have average errors of 30.62% (Lotfi, Ashrafizaadeh and Esfahan, 2015), 11.23% (Yang *et al.*, 2019) and 3.22% (Dashtimanesh, Tavakoli, *et al.*, 2020). This is a significantly larger range than for the other metrics being examined and shows that the sinkage calculation for stepped hulls to be challenging and sensitive. When looking at sinkage with low absolute values, the percentage errors may be misleading, so caution should be exercised. The present study produced one of the most accurate results in terms of sinkage, showing the high y+ approach to be capable of determining the equilibrium position of a stepped hull.

3.5.3 Double-Stepped Hull

This section presents and discusses the numerical results for the double-stepped hull geometry, Hull C2. Figure 3.26 shows the experimental resistance results of the single-stepped hull versus the double-stepped hull. There is no significant differences in the resistance of the single versus double-stepped hull, with an average deviation of 2.07% and a maximum deviation of 2.56% at a speed of 12.05ms^{-1}. A potential reason for the results of the single and double stepped hulls being near identical is that the step dimensions were very similar. The step length for Hull C1 is 0.62m, with a total step height of 0.02m, while the combined step length for Hull C2 is 0.62m and the combined step height was 0.02m. There was a first step of 0.25m length and 0.01m height for Hull C2. The following section will look at the two hulls in order to identify how the differences in step layout have affected the wetted area and resistance components in order to develop a more thorough understanding of the different step configurations.

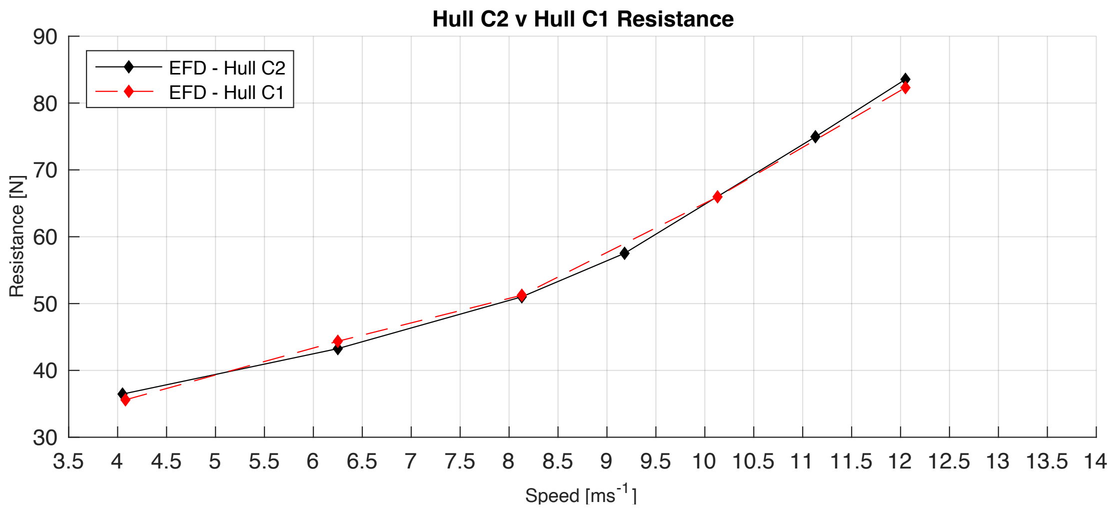

Figure 3.26 - Hull C2 v Hull C1 Resistance

The trim of Hull C2 is slightly less than that of Hull C1, as presented in Figure 3.27. This is a result of the Hulls C2's lower static trim of 1.01°, in comparison to 1.13° for Hull C1. There is less volume removed from the aft hull of the double stepped configuration due to the presence of the lower first step. Therefore, the hull requires a smaller static trim angle to replace the lost buoyancy and reach its static equilibrium position. At the highest speed of $12.05ms^{-1}$ the trim for hull C2 does not follow the trend line. This point is of particular interest in the CFD analysis to see if there is an explanation for this behaviour.

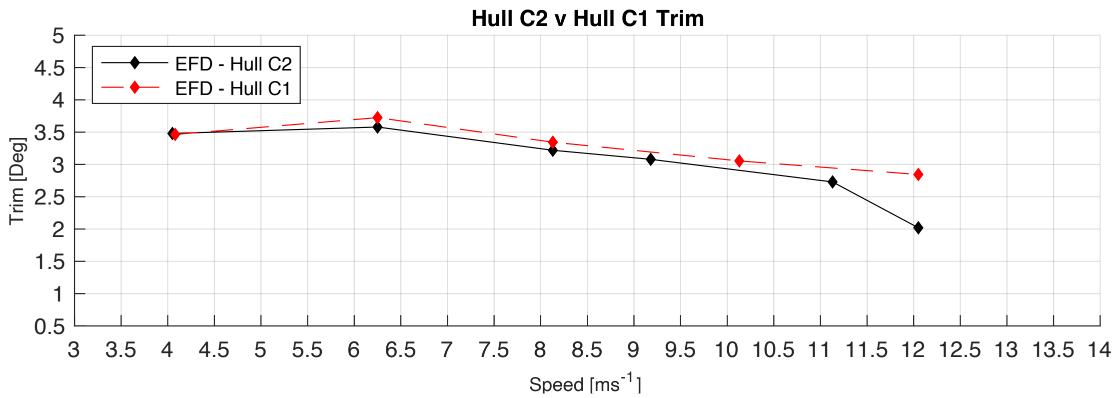

Figure 3.27 - Hull C2 v Hull C1 trim

Once again, due to the unit errors it is difficult to draw any real conclusions or comment on the comparison of sinkage as presented in Figure 3.28. The rise of the centre of gravity for Hull C2 is slightly less than that of Hull C1, which is likely due to the slight decreases in running trim for the double-stepped hull.

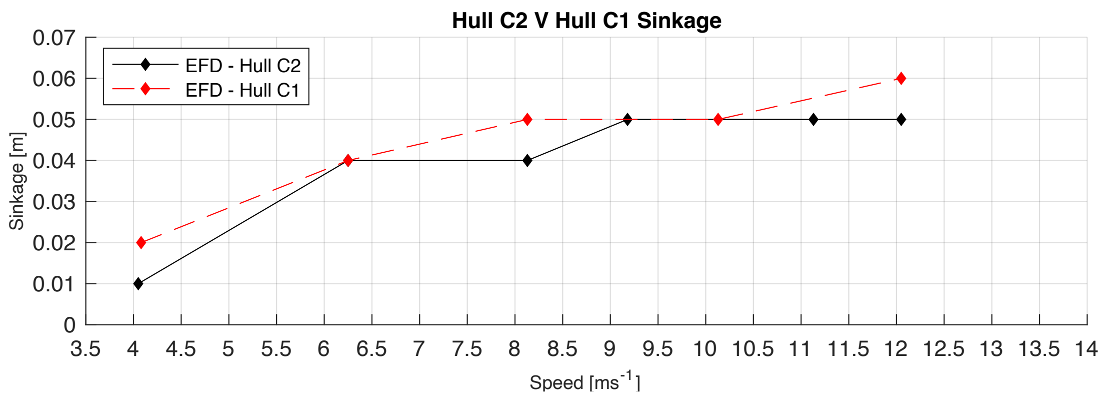

Figure 3.28 - Hull C2 v Hull C1 sinkage

Table 3.16 and

Table 3.17 detail the resistance, trim and sinkage as calculated by CFD. Additionally, the comparison error, as given by Equation (3.13) is presented. Each of the calculated values will be analysed and discussed separately, before general comments related to the numerical simulation are put forward.

Table 3.16 – Hull C2 High y^+ numerical results

Speed $[ms^{-1}]$	Froude Number	Resistance [m]	Trim [°]	Sinkage [m]	Resistance Error	Trim Error	Sinkage Error
4.05	1.14	35.94	3.71	0.009	-1.43%	6.61%	-15.00%
6.25	1.93	44.79	4.00	0.041	3.54%	11.73%	1.25%
8.13	2.62	49.14	3.77	0.041	-3.67%	17.08%	2.50%
9.18	2.99	54.60	3.43	0.054	-5.08%	11.37%	7.00%
11.13	3.77	66.13	3.25	0.050	-11.78%	19.05%	-0.60%
12.05	4.03	73.40	3.14	0.051	-12.15%	55.46%	2.60%

Table 3.17 – Hull C2 Low y^+ numerical results

Speed $[ms^{-1}]$	Froude Number	Resistance [m]	Trim [°]	Sinkage [m]	Resistance Error	Trim Error	Sinkage Error
4.05	1.14	34.18	3.47	0.011	-6.25%	-0.29%	6.00%
6.25	1.93	42.29	3.82	0.041	-2.24%	6.65%	1.32%
8.13	2.62	46.51	3.62	0.040	-8.82%	12.42%	1.00%
9.18	2.99	51.53	3.37	0.053	-10.41%	9.52%	6.45%
11.13	3.77	61.18	3.15	0.058	-18.38%	15.31%	16.35%
12.05	4.03	68.39	3.00	0.059	-18.14%	48.53%	18.51%

3.5.3.1 Resistance Results

The mean resistance error values for the high y^+ case was found to be 6.27%, with a range from -12.15% to 3.54%, whereas the mean error value for the low y^+ case was 10.71%, with a range of -2.24% to -18.38%. The numerical and experimental data is plotted in Figure 3.29.

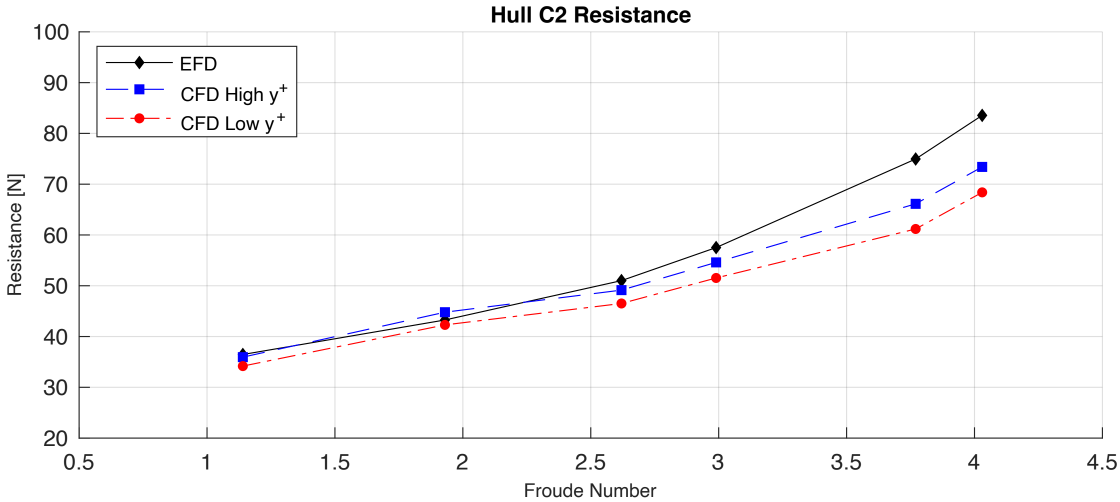

Figure 3.29 - Hull C2 resistance

While there are considerably fewer numerical studies investigating double stepped planing hulls available in the literature an average resistance error of 9.5% was typical. This is slightly larger than the 8.5% typical of a single stepped hull. Three previous studies were found to have modelled Hull C2, reporting average errors of 12% (Mancini *et al.*, 2018), 4.86% (Esfandiari, Tavakoli and Dashtimanesh, 2019) and 6.22% (Esfandiari, Tavakoli and Dashtimanesh, 2019). The work of the present study was able to model the resistance with a higher level of accuracy than is typical of double-stepped playing hulls.

When Figure 3.29 is examined, trends are similar in nature to those found for Hull C1 are seen, as presented in Figure 3.18. These trends are more pronounced for the double stepped hull. Both the high and low y+ approaches are seen to underpredict the resistance, indicating that once again the simulations are likely being affected by NV.

3.5.3.1.1 Numerical Ventilation of Hull C2

The VOF plots of the hull for the high y+ approach can be seen in the left-hand column of Figure 3.30. There is visibly more NV present for the double stepped planing hull. In addition to NV of the form that was seen for Hull C and C1, Figure 3.30 shows dry parts of the hull to be covered in a mixture of fluids, containing mostly air, as seen in the light blue patches. This is likely caused by particles of water getting caught up in the air flow as it is drawn under the step due to the complex nature of the flow.

The phase replacement strategy is once again employed, with the resulting VOF plots presented in the right-hand column of Figure 3.30. The slowest speed case was subject to the most significant NV, with large amounts of fluid mixing upon the hull. Once the phase replacement procedure was applied, the wetted surface was still not representative of the real-world scenario. This highlights one of the issues with using the phase replacement strategy, highlighting the need to be starting from a point in which NV has already been reduced as much as possible.

The strategies employer to minimise NV in the simulations of Hull C & C1 were also applied to the simulations of Hull C2, however they found to be less effective. As the flow becomes more complex aft of the midhull it is more susceptibility to NV. In all cases there is little NV on the forehull, more on the midhull and then the largest amount is present on the aft hull. While the phase replacement strategy is capable of eradicating NV on the fore and mid hulls, streaks of mixed fluid on the aft hull remain in some cases. This is as these areas contain less than 50% water, so the phase replacement procedure does not replace the mixed fluid with 100% water. While the threshold value of 50% can be altered in the user field function this runs the risk of introducing water to cells that should be fully air. As the free surface is defined as 50/50 this is a logical threshold to apply.

Once the phase replacement strategy had been employed the average change in resistance for each of the speed conditions was 2.63%, with individual cases ranging from 1.98% to 3.12%. The average error of the high y+ approach reduced from 6.27% to 4.98%, which is a significant improvement and shows the degree to which a double stepped hull may affected by numerical ventilation. The changes in resistance for all speed cases are presented in Table 3.18

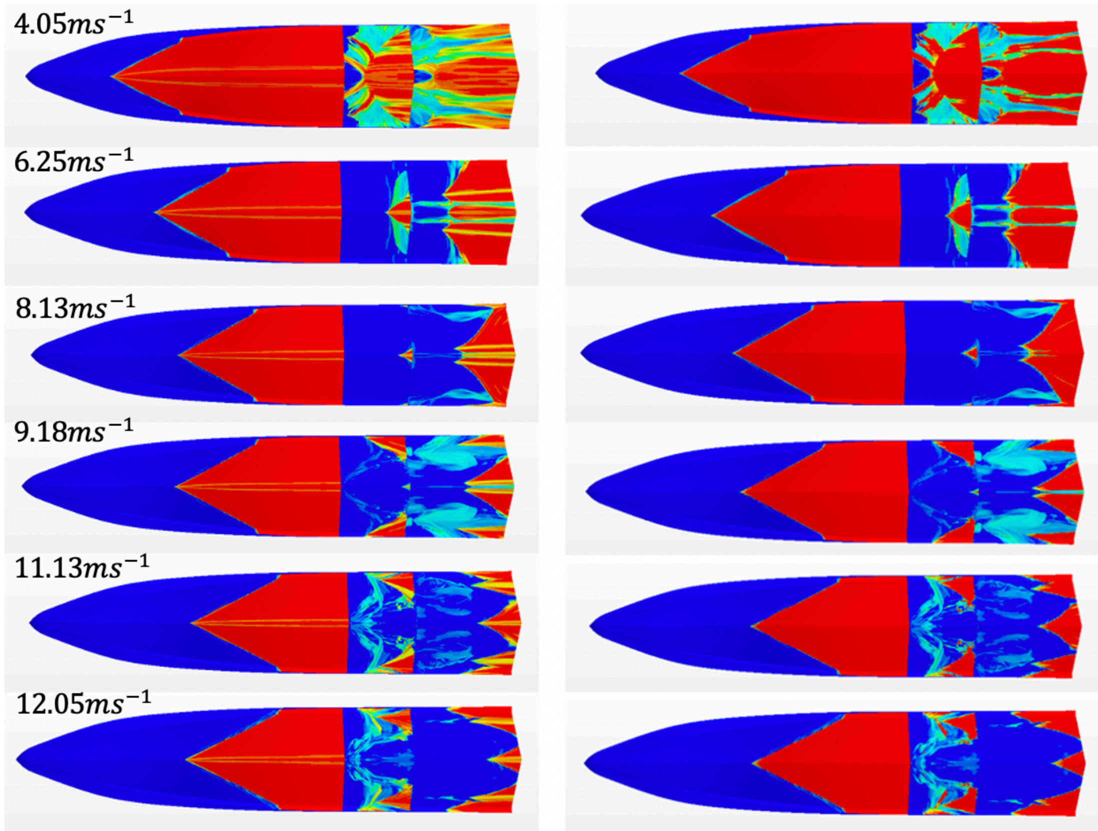

Figure 3.30 – Volume fraction high y+ Hull C2 (Left – No phase replacement) (Right - phase replacement)

Table 3.18 – Hull C2 phase replacement

Speed	4.05	6.25	8.13	9.18	11.13	12.05
High y+ Resistance [N]	35.94	44.79	49.14	54.60	66.13	73.40
High y+ & Phase Replace Resistance [N]	36.65	46.00	50.47	55.85	68.20	75.58
High y+ Difference in Error	1.98%	2.70%	2.72%	2.30%	3.12%	2.97%

The VOF plots of the low y+ case are presented in Figure 3.31. This approach was not capable of modelling the flow and there is a considerable mixing of fluids. The severity of this increases with Froude number and the flow is not clearly defined for the higher speeds. It is not possible to calculate the resistance or equilibrium position with any degree of accuracy when this occurs. The severity of the numerical ventilation for the low y+ case is the reason for the underprediction in resistance, as seen in Figure 3.29.

The low y+ simulations of hull C2 suffered the highest degree of stability issues, requiring large amounts of inner iterations in the initial flow stages to prevent divergence. It was also found that these simulations were very sensitive to the number of cells in the prism layer, which also lead to divergence at times. It may be possible to develop stable, reliable and accurate simulations of a double stepped hull that utilises a low y+ approach to turbulence, but despite considerable effort this was unfortunately not achieved in the present study.

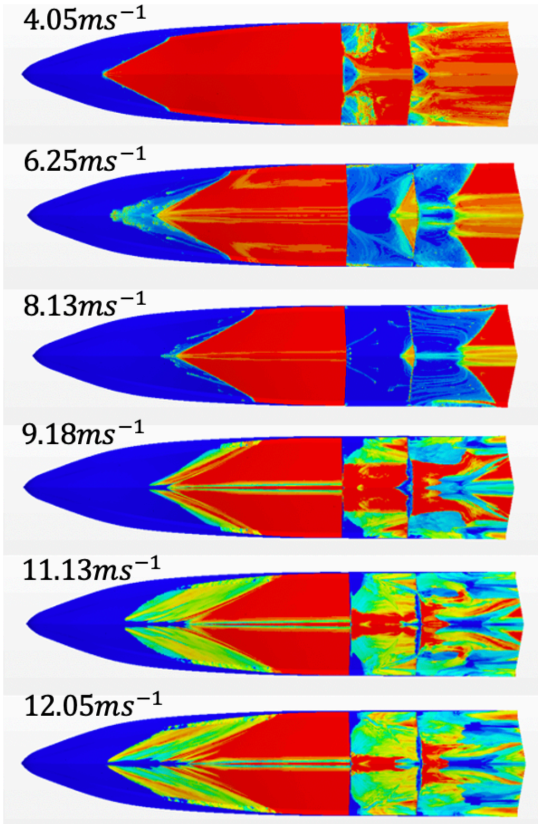

Figure 3.31 – Volume fraction low y+ Hull C2

As a further example to show the importance of ensuring that numerical ventilation levels are satisfactorily low prior to employing a phase replacement strategy to deal with NV, phase replacement was applied to the second highest speed case. The resulting VOF plot is detailed in Figure 3.32, and is seen to be completely unrepresentative of the physical flow.

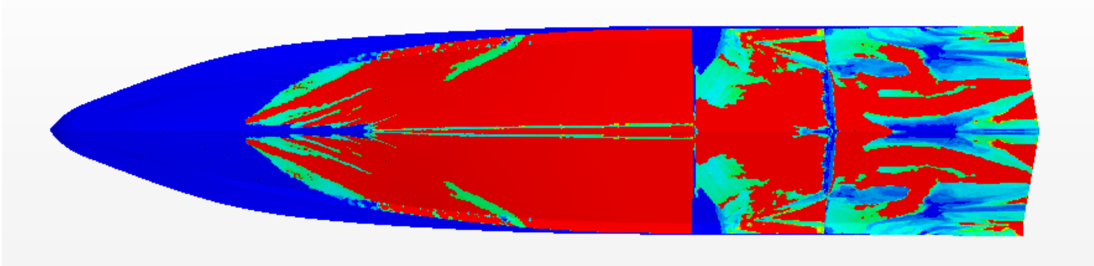

Figure 3.32 - Unsuccessful phase replacement

3.5.3.1.2 Resistance Components of Hull C1

The resistance components of the double stepped hull were examined in the same manner as detailed previously, as presented in Figure 3.33.

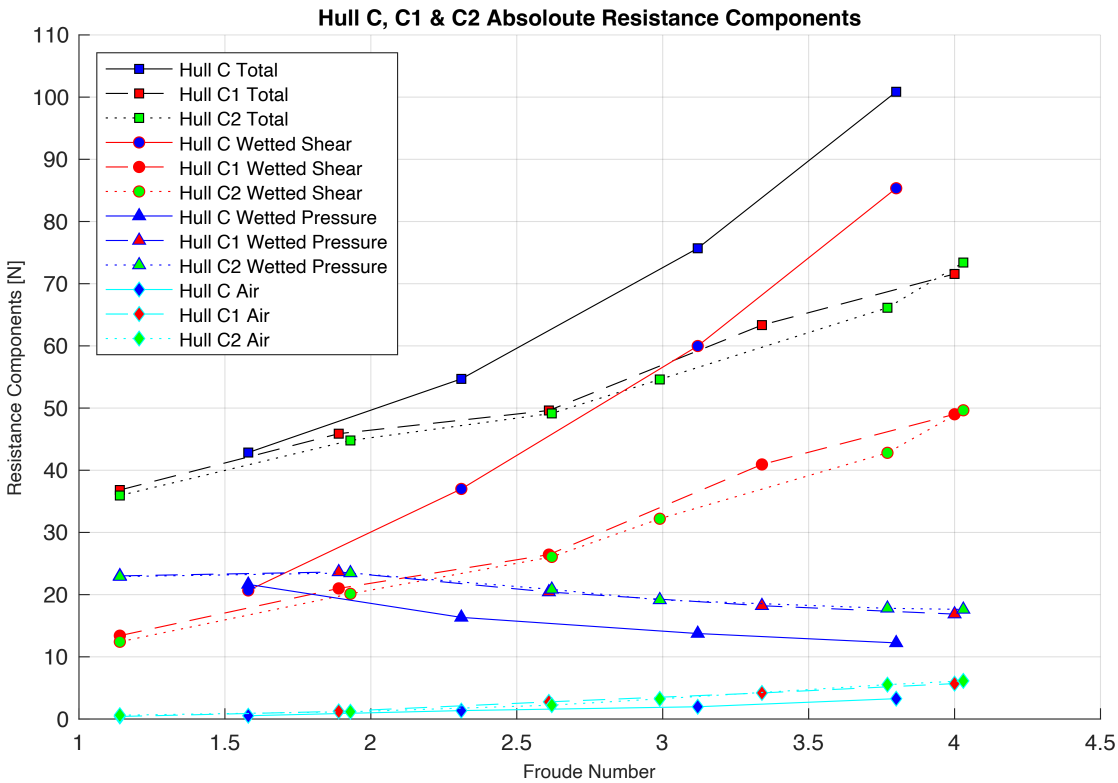

Figure 3.33 – Hull C, C1 & C2 Absolute Resistance Components

Figure 3.33 show the composition of resistance for the single and double stepped hull to be largely the same. In general, the total resistance of the double stepped hull is slightly lower than that of the single stepped hull, which appears to occur due to a reduction in the frictional resistance. The pressure and air resistance components do not change much between the single and double stepped hulls.

3.5.3.2 Trim Results

The mean error in the running trim values for the high y^+ case was found to be 20.22%, with a range from 6.61% to 55.46%, whereas the mean value for the low y^+ case was 15.45% with a range of -0.29% to 48.53%. The results are plotted in Figure 3.34.

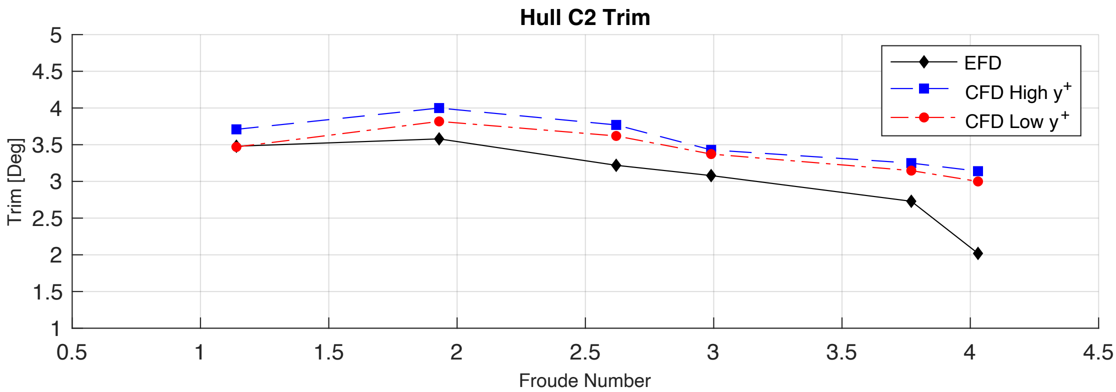

Figure 3.34 - Hull C2 Trim

The largest error is for the highest speed case, where the experimental result is seen to decrease suddenly in comparison to the trend, while both the high and low y+ approaches calculate a trim that follows the trend of the previous points. When this last point is excluded the average error for the high and low y+ reduces to 13.17% and 8.84% respectively. This level of error is acceptable, and the simulation may be considered accurate in this application. Despite the inability of the low y+ approach to calculate the wetted area due to NV, and the resulting underprediction in resistance, the trim follows the trends as calculated by the high y+ approach.

3.5.3.3 Sinkage Results

The mean running sinkage error for the high y^+ case was found to be 4.83%, with a range from -15.00% to 7%, whereas the mean error for the low y^+ case was 8.28%, with a range of 1.00% to 18.51%. The results are plotted in Figure 3.35

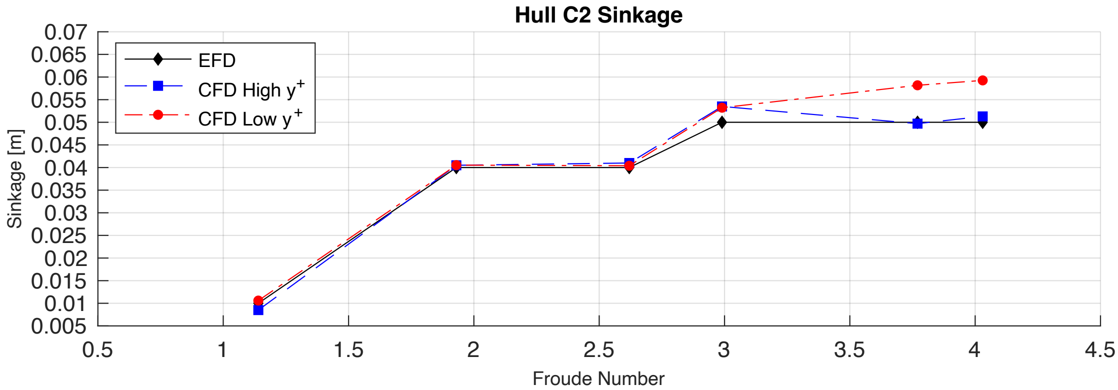

Figure 3.35 - Hull C2 sinkage

Both the high and low y+ approaches were able to satisfactorily calculate the rise in CG, with both modelling the trends of the experimental data well. The high y+ approach was notably more accurate than the low y+ approach, however as discussed previously there were serious failings with the low y+ approach and it should be treated with caution. The high degree of accuracy with which the high y+ approach models the rise in CG shows it to be accurate and robust in calculating the resistance and equilibrium position of a double stepped planning hull.

3.6 Summary

This chapter set out to develop the knowledge of stepped hulls thought numerical modelling and determine the effects that the addition of steps has upon the performance of a planing hull. CFD simulations that were capable of accurately modelling unstepped, single and double stepped hulls were developed. A formal verification study was then undertaken, showing that numerical errors arising from the spatial and temporal discretization to be suitably small and allowing the set up to be used with a high degree of confidence. The three hull configurations were modelled over a range of speeds and a thorough investigation of the results was presented, making comparisons between the hull configurations and evaluating the hydrodynamic performance. Decomposition of the resistance into its pressure and shear components revealed the mechanisms through which stepped hulls achieve a reduction in resistance, and under what operating conditions it is beneficial to employ steps.

Further work was conducted to improve the level of confidence that may be placed in CFD simulations of planing hulls by identifying methods to improve their accuracy and by quantifying the effects of one of the largest sources of error. The approach to wall treatment was identified as one of the most promising means through which the accuracy of simulations modelling planing hulls may be improved. Both the high y^+approach, where the viscous sub layer and the buffer layer are modelled using wall functions, and the low y^+approach, where the transport equations are solved all the way to the wall and the entire near wall turbulent boundary layer is resolved were employed for all cases, allowing a direct comparison between the two approaches over a broad range of conditions. To the best of the authors knowledge only one study has previously employed a low y^+ approach to model an unstepped planing hull, and there were no examples of this being utilised for stepped hulls. Additionally, the effects of numerical ventilation studied and discussed for all cases, with the. Impact on resistance being quantified and presented.

Steps were shown to be beneficial at Froude numbers of 1.93 and above. As the speed increases the benefits of stepped hulls were found to increase, resulting in a resistance reduction of 25.85% at a Froude number of 4.00. Both the single and double stepped hull configurations that were examined in this study were found to produce very similar resistance characteristics, with a maximum difference of 2.56%. The loss in buoyancy in the aft portion of the hull due to the inclusion of steps was found to increase the equilibrium trim position of the hull. Due to a combination of the loss of buoyancy and the increased trim angles, the rise of CG of stepped hulls was less than that of an unstepped hull. Analysis of the resistance components of stepped hulls showed that steps improve the performance entirely through a reduction in the frictional component. Due to the higher trim angles, they were shown to increase the pressure component of resistance. While the increase in the pressure component is relatively uniform over all speeds, the difference in the frictional resistance was closely linked to speed, increasing from 12.93%, at a Froude number of 1.58 to 45.52% at a Froude number of 3.80 for the single stepped hull. As the speed increases the ventilation length of the flow aft of the step increases, resulting in a reduced wetted area. At highter the frictional drag dominates the total drag, contributing up to 85% of the total resistance of an unstepped hull. The addition of steps reduces this to 68%.

It can be concluded from this study that establishing strategies and designing step configurations that reduce the wetted area offer promising means to improve the performance of stepped hulls further and is a key consideration to investigate during the preliminary design phase. Careful attention should be paid to the effects of trim, as excessive increases to the pressure resistance may have negative effects. Designers may need consider additional technologies such as trim tabs or interceptors to remain in control of the trim of stepped hulls.

For all three hull variants, simulations that were either more accurate, or in line with the accuracy of state-of-the-art simulations in the field were obtained, as summarised in

Table 3.19. The accuracy of the low y^+ approach for an unstepped hull was shown to be significantly more accurate than the standard practice of employing wall functions for this type of problem, reducing the errors to levels previously only possible for far less complex conventional displacement vessels. Problems were seen when employing the low y+ approach for a stepped hulls due to the more complex nature of the flow, and the interaction of the aft hull with the forehull wake, resulting in increased numerical ventilation. When a second step was introduced, these problems grew, resulting in an inability to model the flow correctly and rendering this approach to wall treatment unfit for application with double stepped hulls. Despite this, the use of wall functions was shown to produce remarkably accurate results for both the single and double stepped hulls. The more complex nature of the flow when

there were two steps was seen to only be marginally detrimental to the accuracy of the high y+ approach, showing this to be robust and reliable in this application.

Table 3.19 – Summary of simulation accuracy

	Resistance Error	Resistance Error [Phase Replacement]	Sinkage Error	Trim Error
Hull C [High y+]	7.21%	7.86%	4.77%	19.33%
Hull C [Low y+]	2.54%	2.46%	3.72%	15.07%
Hull C1 [High y+]	5.42%	4.72%	6.33%	10.36%
Hull C1 [Low y+]	8.02%	5.76%	19.54%	5.31%
Hull C2 [High y+}	6.27%	4.98%	4.83%	13.17%
Hull C2 [Low y+}	10.76%	n/a	8.28%	8.84%

The effects of numerical ventilation were studied through the phase replacement method, which was shown to be applicable in all cases aside the low y+ double stepped simulation. Minimising the numerical ventilation prior to adopting this strategy was highlighted as essential to minimised errors to the resistance being introduced through positioning errors. The inability of this method to determine the equilibrium position of the hull once numerical ventilation has been removed was found to be one of its major flaws. A quantitative analysis of the effects of numerical ventilation for each of the variant hulls was conducted, with the results summarised in Table 3.20. Numerical ventilation was found to have twice the impact for low y+ cases, confirming the finding that the prism layer mesh is highly influential in the prevention of NV (Gray-Stephens, Tezdogan and Day, 2021). It is also clear that the number of steps impacts the levels of numerical ventilation as the fluid flow contains larger quantities of physical ventilation. Care was taken to minimise numerical ventilation prior to the application of the phase replacement strategy, however these results show the effect that numerical ventilation that remain, and confirm it as one of the largest sources of error in simulations of planing hulls.

Table 3.20 – Summary of effect of phase replacement

Case	Average Increase in Resistance
Hull C [High y+]	0.60%
Hull C [Low y+]	1.23%
Hull C1 [High y+]	2.12%
Hull C1 [Low y+]	4.72%
Hull C2 [High y+}	2.63%
Hull C2 [Low y+}	n/a

It is recommended that a low y+ approach to wall modelling approach is employed for simulations of standard planing hulls, due to the significant increase in accuracy. For stepped hulls the low y+ approach was found to introduce errors due to the complex nature of the forebody flow as it intersects with the afterbody, and as such the use of wall functions was shown to be more reliable and accurate. An area of promising future research is to develop strategies that allow the use of the low y+ approach with stepped hulls, as it was shown to be considerably more accurate for unstepped hulls.

The developed simulations have been shown to be highly accurate and applicable for use in the further study of stepped hulls. Indeed, in this chapter they were employed to examine the resistance components of the different hulls, developing understanding of the precise mechanisms through with stepped hulls are so advantageous. In the following chapters they will be employed to further study the flow under a stepped hull, as well as to investigate how changing the step design effects the hull performance, looking to identify how the performance may be improved.

Chapter 4 – Experimental and Numerical Analysis of Fluid Flow as it Separates Aft of A Step

This chapter develops knowledge of the flow aft of a step through the application of numerical simulations, which will be employed to enhance and accelerate analysis techniques in the subsequent chapter. Developing a thorough understanding of the flow in this region is of key importance to the designers of stepped hulls, who are required to determine how the freesurface flow intersects with the mid and afterbodies.

4.1 Introduction

When a stepped hull is employed, any method of performance prediction must calculate the forces and moments acting on each section of the hull, before summing them to solve for the global forces and moments that establish the total resistance, lift and the equilibrium position of the hull. To calculate these for each of the lifting surfaces, both the wetted area and the relative deadrise angle between the fluid surface and the hull must be known. It is vital to be able to accurately model the free surface flow aft of the step to determine the fluids intersection with the afterbodies. Errors introduced through the incorrect modelling of this freesurface elevation result in differences in the wetted area and relative deadrise, leading to the incorrect calculation of forces and moments acting upon each surface. While the calculation of resistance is negatively affected, it is the calculation of the hulls equilibrium position that suffers the greatest accuracy loss when this happens. This is due to the incorrect distribution of forces arising from the incorrect wetted area and relative deadrise calculations.

For these reasons, establishing a method of reliably and accurately modelling the freesurface elevation aft of a step is crucial to the performance prediction and design of stepped planing hulls. To this end, Savitsky and Morabito performed an extensive model-testing program in 2010, measuring the wake elevation aft of prismatic planing hulls in a number of conditions (Savitsky and Morabito, 2010). The data was used to develop empirical formulae that calculate the longitudinal wake elevation at the Centreline (CL) and the Quarter Beam (QB) longitudinals of a planing hull, given that it fits within certain parameters. To date, Savitsky's work is the only example of an in-depth investigation into the nearfield wake elevation of planing hulls that looks to capture or model the longitudinal freesurface elevation profile directly aft of the hull.

Savitsky's work was limited to investigating the wake elevation aft of a prismatic planing hull and did not measure the freesurface flow aft of a step (Savitsky and Morabito, 2010). Considering the freesurface elevation without the presence of the afterbody changes the physics of the problem and is a considerable simplification. This was, however, necessary as experimentally extracting the wake elevation aft of a step with anything other than photographs of the wetted areas is extremely challenging and is not something that has been achieved by researchers to date.

Researchers attempting to develop an analytical performance prediction method for double stepped planing hulls reported significant inaccuracies introduced to their model through an inability to accurately model the freesurface elevation aft of each of the steps (Dashtimanesh, Tavakoli and Sahoo, 2017). They went on to highlight an urgent need to conduct extensive set of experiments and extract the flow pattern behind each step. Despite this being an extremely challenging task when attempted experimentally, the application of numerical simulations presents a means by which this data may be obtained.

The study reported in this chapter first validates the accuracy of CFD in modelling the longitudinal wake elevation aft of a prismatic hull against experimental results. Due to the lack of available studies in the public domain a tank testing program was undertaken to generate validation data. The work will show CFD to be an accurate and reliably tool capable of modelling the freesurface elevation of separating flow and will justify its use for investigating the flow of a stepped hull for which there is no experimental data.

Having shown CFD to be an appropriate tool the chapter will present a detailed analysis of the numerical simulations developed in Chapter 3 to develop knowledge of the flow aft of a step. The free surface elevation aft of the steps of single and double stepped hulls will be extracted and different methods of modelling this will be analysed. The wetted areas will be examined, looking to establish the different components the aspects of flow that creates them. Finally, methods of determining the wetted area of the afterbody will be investigated so that these may be accurately calculated by analytical models.

4.1.1 Aims

The overall aim of this chapter is to develop the understanding of the flow as it separates aft of a step. This can be analysed to allow analytical models to determine the conditions that the afterbodies are operating in so they may accurately determine the forces and moments of each surface. The chapter also sets out to enhance the knowledge of the wetted area components of a single and double stepped hull, looking at their characteristics, and the aspects of flow that creates them.

In order to achieve these three aims a number of objectives are put forwards:

1. **Develop** validation data by means of an experimental tank testing program
2. **Validate** the accuracy of CFD in modelling the fluid flow as it separates from a prismatic planing body
3. **Evaluate** the flow as it separates at the steps of single and double stepped hulls using numerical simulations
4. **Determine** the accuracy of methods of modelling the free surface elevation aft of a planning hull when applied to fluid separating at a step

5. **Evaluate** the wetted areas of single and double stepped hulls using numerical simulations

4.1.2 Methodology

The work reported in this chapter is broken down into two stages.

In the **first stage** an experimental testing program is conducted at the Kelvinside Hydrodynamics Laboratory to develop a validation dataset. The experimental study utilised sonic probes to determine the elevation of the free surface aft of a prismatic planing hull. A numerical simulation was then developed for the geometry employed in the experimental study following the methodology outlined in Section 3.3. The freesurface elevation profiles aft of the hull at the Centerline and Quarterbeam were investigated to determine if CFD could be considered an accurate and reliable tool in this application. Additionally, a qualitative comparison was made between images of the experimental study and free surface graphics generated by CFD to provide a fuller analysis.

The **second stage** went on to investigate the free surface flow under a stepped hull as it separated aft of a step for both single and double stepped configurations. The numerical simulations reported in the previous chapter were employed as they modelled both a single and double stepped hull over a range of speed conditions, and had been shown to produce accurate results. The wetted area and dynamic pressures of the hulls were examined to develop understanding of causes of each wetted component, and the freesurface elevation aft of the each step was extracted. This data facilitated a comprehensive assessment into the accuracy of the Linear Wake Assuption and of Savitsky's Wake Equations, and was used to provide insight into how best to calculate the wetted areas.

4.2 Experimental Set Up

The purpose of the experimental testing was to develop validation data for the numerical simulation. The set up will be detailed briefly in this section, however for a more in-depth account of the experimental set up, analysis of the results and the full data set please refer to (Gray-Stephens, Tezdogan and Day, 2020a).

4.2.1 The Model

The model was a simple prismatic hull, featuring a constant deadrise, as detailed in Figure 4.1. The model was built by the technicians employed at the Kelvin Hydrodynamics Laboratory. It was constructed of high-density foam that was milled by a CNC machine, before being faired and painted.

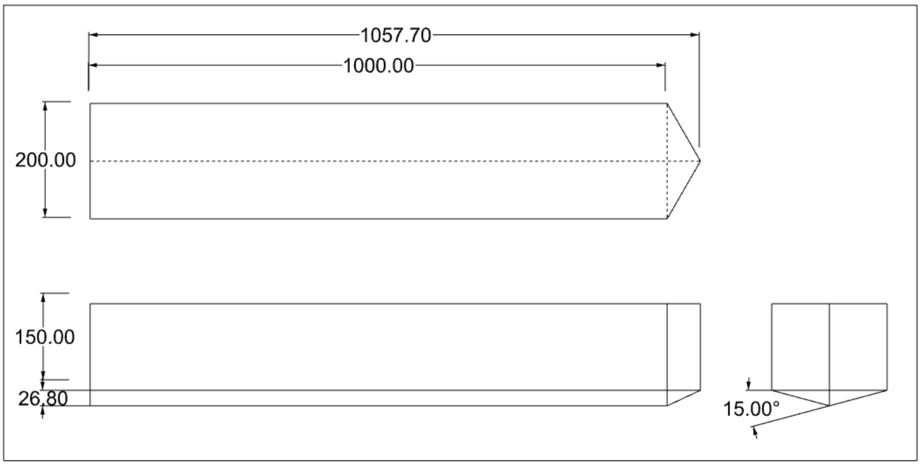

Figure 4.1 - Lines plan of model (linear dimensions in mm)

4.2.2 Test Matrix

An experimental test matrix was defined to cover a broad a range of hull positions. This allowed for a robust validation case across a number of conditions. The matrix comprised of three hull positions being tested at four speeds, ranging from 2 ms^{-1} to 4.5 ms^{-1}. This resulted in 12 test cases for which a total of 175 runs were completed.

4.2.3 Set Up

All tests took place in calm water, with the hull in the fully planing condition. The model was fixed in sinkage and trim to give full control over the hulls position and to reduce the complexity of the numerical set up when the validation took place.

The model was mounted to an Ogawa Seiki 6-Axis Load Cell and test rig via hinged plates, with measurements being recorded and analysed with the Spike 2 software package. Cameras were set up with both photographs and video recordings being taken to allow further post processing.

The free surface elevation aft of the hull was measured using sonic probes mounted on a gantry behind the model. There were a number of challenges in using sonic probes in this application, however they were found to produce accurate results. For full details please refer to (Gray-Stephens, Tezdogan and Day, 2020a). The layout of the gantry and the experimental set up is presented in Figure 4.3. A photograph of the experimental set up is presented in Figure 4.2.

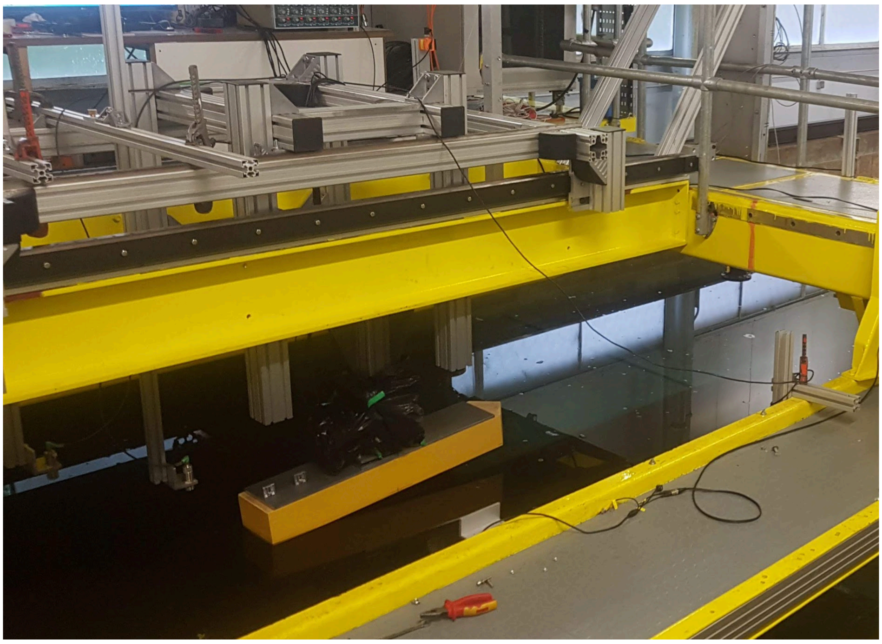

Figure 4.2 – Photo of Experimental Set-Up

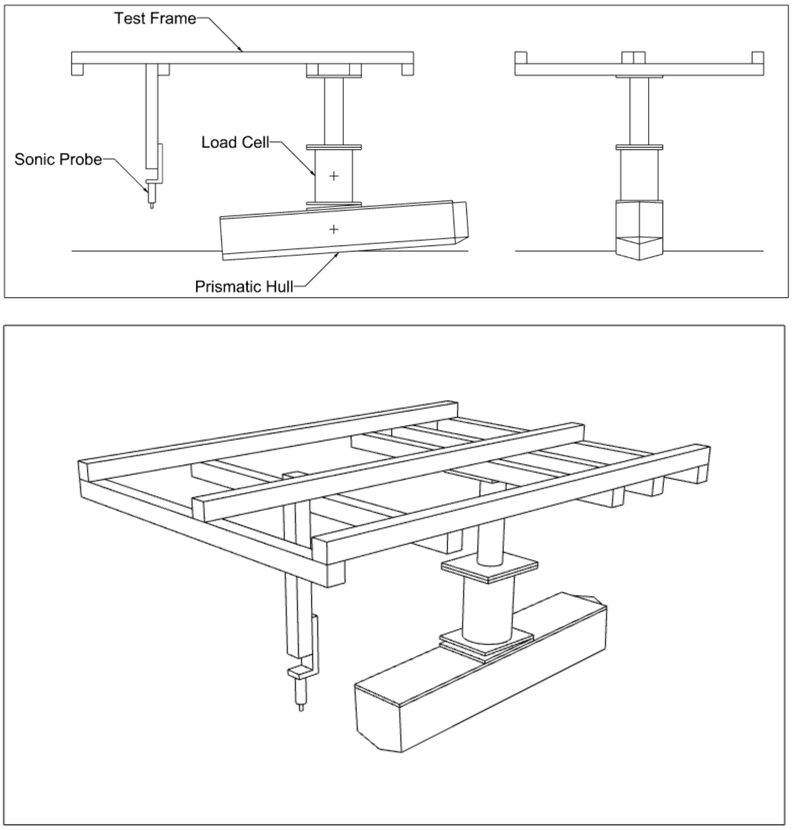

Figure 4.3 - Gantry step up for one sonic probe

4.3 Analysis Methods

Over the course of this chapter several methods are used to evaluate the free surface elevation aft of a prismatic hull or step. Each of these is detailed in the present section.

4.3.1 Computational Fluid Dynamics

CFD is the main analysis tool used throughout this study. The results for Section 4.4 are obtained from a simulation that was set up using the geometry detailed in Figure 4.1 and a similar methodology as detailed in Section 3.3. As the experimental model was fixed there was no need to simulate motion, so a fixed mesh was used and the body was constrained in all degrees of freedom. Full details of this numerical set up may be found in (Gray-Stephens, Tezdogan and Day, 2020b).

The results for Section 4.5 were extracted from the simulations previously described and analysed in Chapter 3.

4.3.2 Savitsky's Surface Wave Contour Equations

(Savitsky and Morabito, 2010) developed empirical equations that quantitatively define the longitudinal freesurface elevation aft of a prismatic planing hull. The equations were developed using physical phenomena that can be associated with the development of the freesurface elevation profile, rather than using computer-based methods to arbitrarily fair the data.

The resulting equations took the following form:

$$H = 0.17(A + 0.03L_k\tau^{1.5}) \sin\left(\frac{\pi}{C_V}\left(\frac{X}{3}\right)^{1.5}\right) \quad \textbf{(4.1)}$$

Where H is the height of the profile for a given location in beams, L_k is the wetted keel length in beams, τ is the trim, C_V is the speed coefficient, X is the distance aft of the transom in beams and A is a constant defined as follows:

- Centreline Profile ($\beta = 10°$): $A = 1.5$
- Centreline Profile ($\beta = 20°$ & 30): $A = 2.0$
- Quarter Beam Profile ($\beta = 10°, 20°$ & 30): $A = 0.75$

The paper in which the equations are first presented sets out a strict set of limits, stating that it is essential that the application of any data-based equations is limited to the range and combination of parameters used by the test program. Whilst this holds true and generally the use of empirical equations out of range should be treated with caution, they may maintain some level of accuracy. This depends how far out of range the equations are being used, with accuracy usually diminishing the further the case is from the original data. Secondly, it depends upon the strength of the relationships used to develop the empirical equations. As physical phenomena were used to develop the Savitsky Wake Equations, they should maintain a higher level of accuracy when used out of range. This was shown to be the case in analysis of the equations conducted by (Gray-Stephens, Tezdogan and Day, 2020a).

These limits are as follows:

- $10° \leq \beta \leq 30°$
- $3° \leq \tau \leq 4°$
- $L_k \geq 0.10 + \frac{\tan\beta}{\pi\tan\tau}$
- $0.017 L_K \tau^{1.5} \geq 0.18$
- $L_K < 3.5B \qquad \beta = 20° \;\&\; 30°$
- $L_K < 2.5B \qquad \beta = 10°$
- $4 \leq C_v \leq 8$
- $X \leq 3B$

4.3.3 Linear Wake Assumption

As outlined in the Critical Review of the literature, the linear wake assumption was originally proposed by Lorne Campbell, and first used by (Danielsson and Strømquist, 2012) to adapt Savitsky's Empirical Method of calculating resistance for application with a double stepped hull. It provides a means of modelling the forebody freesurface elevation profile so that the intersection of forebody flow with the afterbody may be established. The linear wake assumption reasons that at high speeds an incoming hull will 'scrape off' the surface layer of fluid, which is thrown aside as spray, leaving undeflected streamlines remain parallel to the original free surface.

4.4 Validation of CFD

This section investigates the accuracy of CFD in modelling the freesurface elevation aft of a prismatic planing hull, making comparisons to experimental data. For a more in depth reporting of this investigation please refer to (Gray-Stephens, Tezdogan and Day, 2020b).

All wake elevation plots reported in this chapter are presented in a format consistent with (Savitsky and Morabito, 2010), where the origin represents the point where the keel meets the transom (or step) and the horizontal axis in line with the keel, as seen in Figure 4.4.

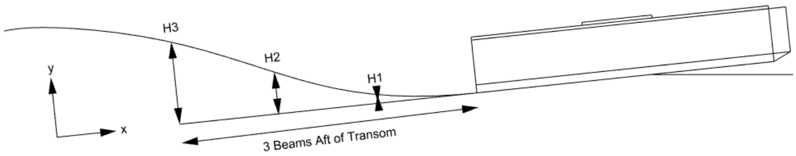

Figure 4.4 - Results reference axis

4.4.1 Centerline Freesurface Elevation Profiles

The results for all the experimental cases will not be presented here as to do so would require 20 individual graphs, which are instead detailed in Appendix A. The data presented in this section has been selected to highlight key findings and trends in the results.

It should be noted that the experimental uncertainty in the measurements of the freesurface elevation profile amplitudes was 0.56mm. This uncertainty is not displayed as error bars on the graphs as they are not visible due to the scale of the graphs. Inspection of the freesurface elevation plots from the temporal and spatial discretisation studies that were undertaken showed there to be insignificant differences so it can be assumed that the numerical uncertainty is negligible.

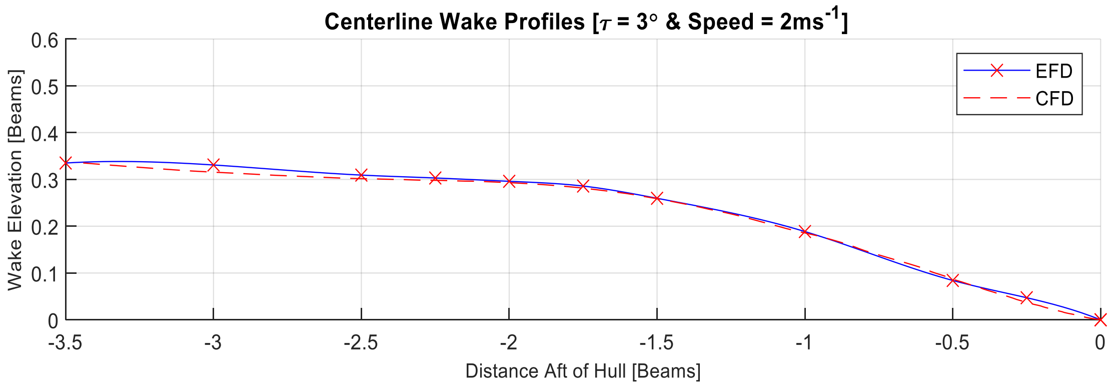

Figure 4.5 - Best-fit CFD results

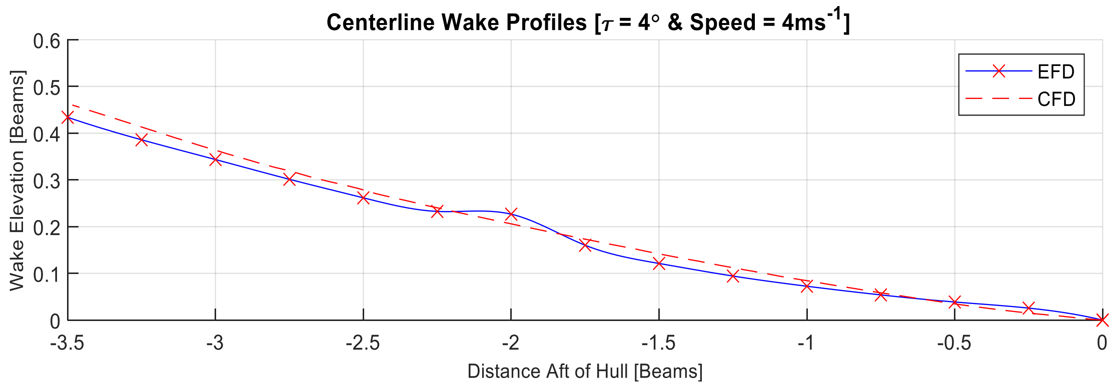

Figure 4.6 – Worst-fit CFD results

In all cases the centreline freesurface elevation profile as calculated by the numerical simulation is shown to have good correlation with the experimental results. It shows CFD to be an accurate and robust method of calculating the flow aft of a planing hull across a range of speed and trim conditions. At the lower speeds of 2 & 3 ms^{-1} the CFD results are seen to marginally under predict the amplitude of the freesurface elevation, however at the larger velocities of 4 & 4.5 ms^{-1} the opposite is true, with the CFD solution featuring a slight overprediction.

Figure 4.5 shows what is considered to be the best-fit result when all cases are compared. As can be seen the CFD profile may be considered an extremely good fit with the experimental data, passing almost exactly through the data points from zero to -2 beams. Following this there is a slight deviation, with a maximum difference of 2.56mm, which has a corresponding comparison error of 3.83%. The best fitting point in this case has a deviation of 0.03mm, or a corresponding comparison error of 0.04%.

Figure 4.6 shows what is considered to be the worst fit of CFD results to experimental data. Despite this, there is still seen to be a very good correlation between the two data sets. The maximum deviation at a single point is 4.72mm, or a comparison error of 10.87%. When the other centreline cases are examined, it is found that the second worst deviation is 4.18mm with a comparison error or 7.37%.

4.4.2 Quarter Beam Freesurface Elevation Profiles

The data presented in this section has once again been selected to highlight key findings and trends in the results. The full data se and comparisons for all conditions is detailed in Appendix A.

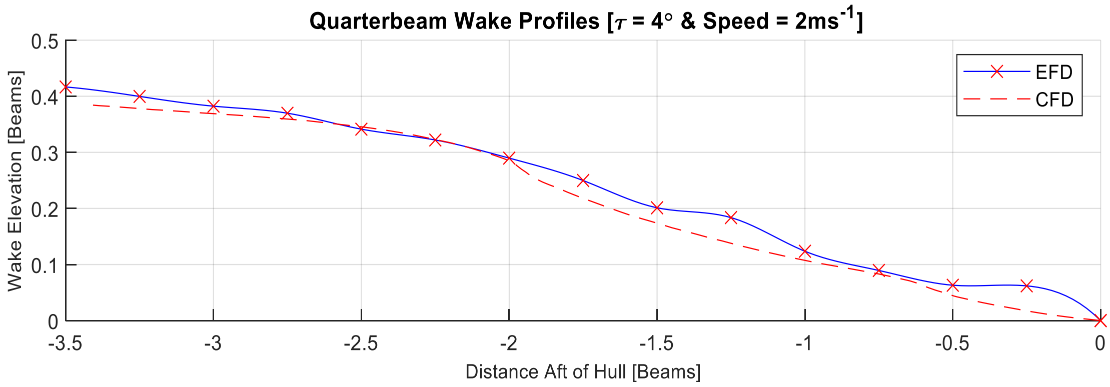

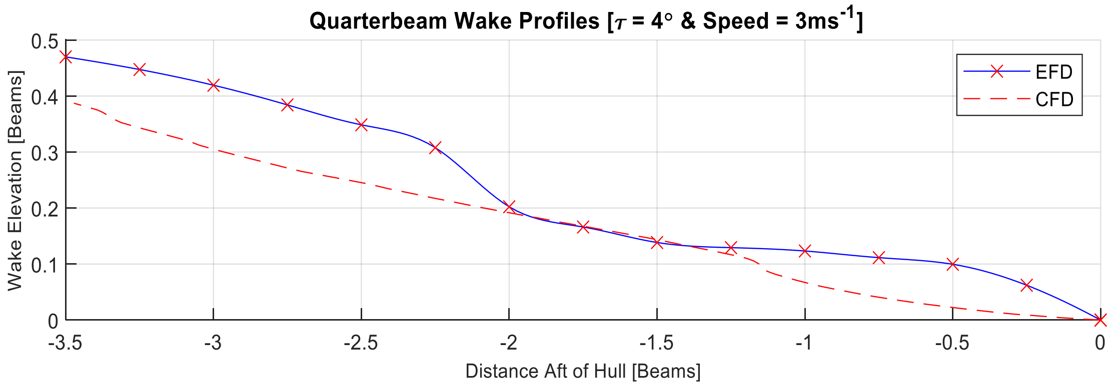

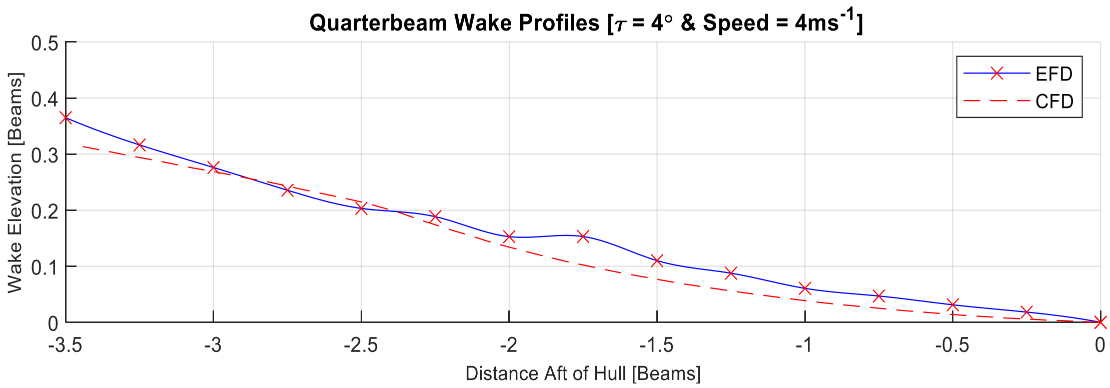

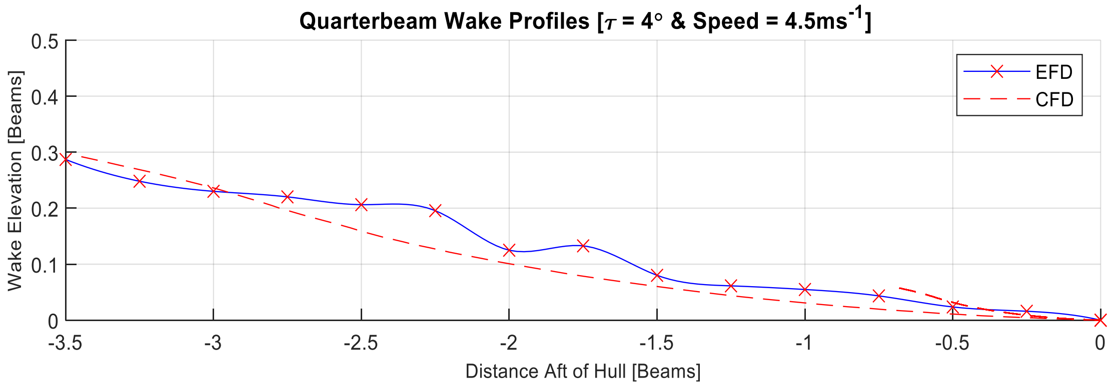

Figure 4.7 - Quarterbeam profiles [τ =4]

The ability of CFD to model the QB freesurface elevation is seen to be strongly related to the speed of the hull. Whilst the trim effects the shape of the wake, it does not appear to influence CFDs capabilities in calculating the freesurface elevation, with the same trends being seen for both the 3° & 4° trim conditions. As speed is found to be influential, plots of QB profiles for all speeds in the 4° trim condition are displayed in Figure 4.7 and will be discussed in this section.

Once again, CFD is shown to be relatively accurate for almost all cases. The case featuring the best fit between CFD and the experimental data is $2ms^{-1}$, where there is a maximum deviation of 6.54mm, however for the most part the difference this is smaller than 3.34mm.

As the speed increases the accuracy of the QB profiles decreases, although it is still considered to be a good fit. As is discussed in the following wake pattern section, it appears that CFD set up as used in this work is incapable of modelling the feature lines that appear between the interacting aspects of flow. These feature lines cause the disturbances in the experimental QB freesurface elevation plots, whilst the inability to model these feature lines is why the CFD profiles are smooth. Cases that have the largest disturbances (3 & 4.5 ms^{-1}) are seen to be the ones that CFD is least capable of modelling. This results in a maximum discrepancy of 12.9mm in the $3ms^{-1}$ case, where the CFD performs poorly for distances over 0.4m from the hull. Despite this for distances less that 2 beams from the hull the CFD result is still considered accurate.

4.4.3 Qualitative Wake Pattern Analysis

In addition to allowing a comparison of quantitative data in the form of freesurface elevation plots, a qualitative comparison of photos taken during the tank testing is made with free surface contour plots from the CFD simulations. The freesurface elevation plots give a far better measure of the accuracy of the CFD, however comparing the wake patterns from both methods offers further insight. One of the key issues when comparing the photos and the elevation plots is that it is impossible to ensure that the views are at the same scale and perspective to allow a valid comparison, so engineering judgment must be employed when making visual comparisons.

Figure 4.8 and Figure 4.9 show these comparisons for the trim angles 4°, 2° & 4.5 ms^{-1}. As can be seen both cases show similar wake patterns, further validating the ability of CFD in calculating the longitudinal freesurface elevation and wave pattern of a planing hull. One of the notable differences is that the experimental photos show far more distinct feature lines, created by the interaction of different aspects of flow. Some of these are visible in the contour plots, however they are far less clearly defined. It is thought to be the inability to accurately model these feature lines from the intersecting parts of flow that leads to the loss of accuracy in some of the quarter beam freesurface elevation profiles, as mentioned previously. In general, aside from these pronounced feature lines the CFD is very capable of modelling the wake elevation.

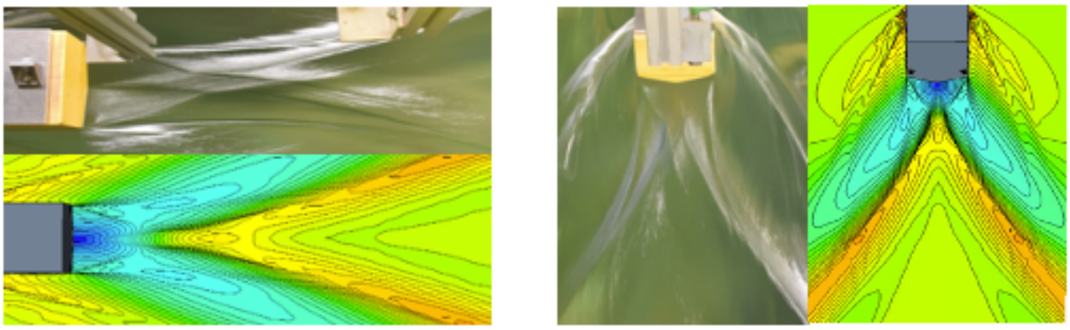

Figure 4.8 - Wake pattern comparison [$\tau = 4°$ & speed =$2ms^{-1}$]

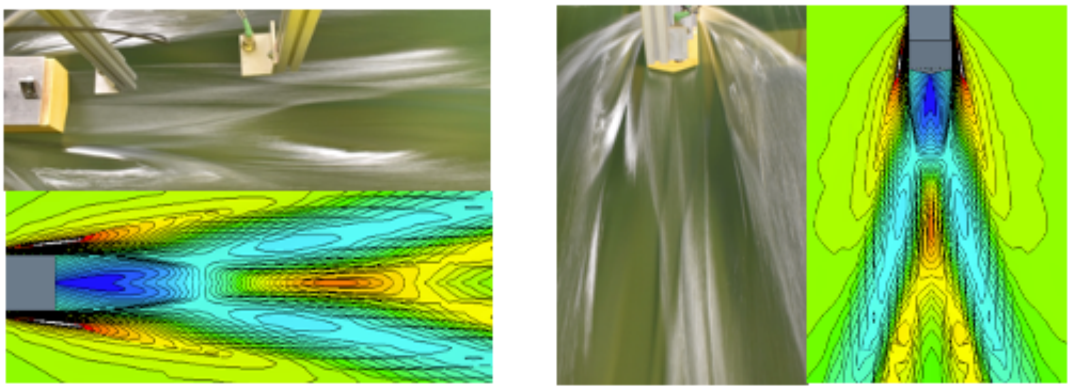

Figure 4.9 - Wake pattern comparison [$\tau = 4°$ & $speed = 4.5\ ms^{-1}$]

Finally, it is possible to compare the spray patterns of the two methods, as presented fo the 4° trim at 4.5 m/s case in Figure 4.10. As can be determined from the visual comparison the spray pattern appears to be well captured.

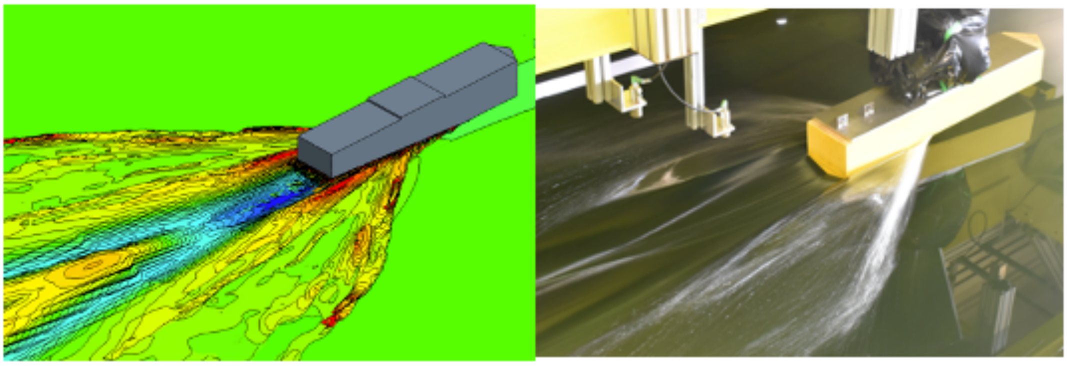

Figure 4.10 - Spray sheet [$\tau = 4°$ & $speed = 4.5\ ms^{-1}$]

4.4.4 Conclusion

The comparison of experimental centreline freesurface elevation plots to those calculated numerically validates the use of CFD in this application, good correlation being seen for all conditions.

Comparison of experimental quarterbeam freesurface elevation plots showed CFD to be less accurate in this application, however there was still a relatively good correlation with the experimental data. Qualitative analysis of the wave patterns showed CFD was incapable of modelling the feature lines visible in the wake patterns at higher speeds. CFD performed well in the region closer to the hull before the feature lines impact the profile, however, it is still able to model the trends of the profiles where feature lines impact the results. In the case of a stepped hull the flow being analysed will always be in this region close to the point of separation in which CFD was shown to be accurate.

4.5 Freesurface Flow Aft of a Step

Having verified CFD as an accurate tool in calculating the free surface elevation aft of a planing surface, further analysis of the numerical simulations conducted in Chapter 3 is undertaken to develop knowledge of the flow aft of a step. The validation of the previous section allows us to confidently use the numerical results to analyse the fluid flow, and to assess the accuracy of analytical models using these as the baseline. This section initially investigates a single stepped hull, before extending the analysis to a double stepped hull.

4.5.1 Single Stepped Hull

The further analysis conducted for a single stepped hull will first analyse the wetted area of the afterbody and its composition, before extracting the free surface elevation aft of the step and investigate how accurately the Savitsky Wake Equations and the LWA can model this flow.

4.5.1.1 Wetted Area

When calculating the resistance of a planing hull it is essential that the wetted area is accurately modelled. As such, the wetted area of the single stepped hull is evaluated. Its composition is broken down to ensure that mathematical models for performance prediction may employ this knowledge to ensure they are capable of modelling this accurately.

In the case of a planing surface with zero deadrise the water rises in front of the surface. This causes the wetted length of a surface which is producing hydrodynamic lift to be larger than the length of the intersection of the undisturbed water surface with the underside of the surface. This rise of water in front of a planing surface is termed the wave rise. At some point in this wave rise there will be a stagnation point at which the flow has no x-component of velocity. It is at this point that the highest pressures occur, and therefore where the majority of the lift is generated. At some point in front of the stagnation point the flow will blend into a thin sheet of water flowing forward along the planing surface, forming whisker spray (Savitsky, DeLorme and Datla, 2007). The region that is the origin of this thin sheet is termed the spray root. The spray root is slightly forward of the stagnation point and all flow aft of the spray root exerts pressure on the hull generating lift. This is sometimes termed the pressure area (Savitsky, 1964). A planing hull's wetted area is composed of this pressure area, generating lift and contributing to the resistance, and the whisker spray area, which does not provide lift yet contributes to the frictional resistance.

Prior to presenting the wetted areas of a single stepped hull, it is first necessary to explain the figures that are presented. For all cases the overlaid graphic as seen in Figure 4.11 will be presented, detailing an overlay of the VOF plot showing the wetted area of the hull as seen in Figure 4.12 (right) and the pressure distribution on the hull as seen in Figure 4.12 (left).

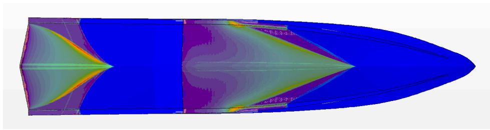

Figure 4.11 – Overlay of VOF and pressure plots for Hull C1

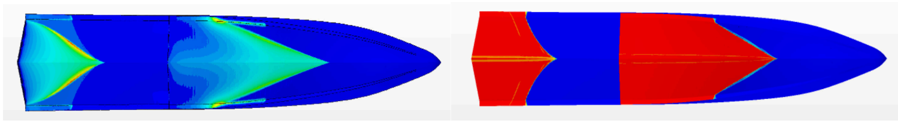

Figure 4.12 –Pressure distribution plot of Hull C1 [left], VOF plot of Hull C1 [right]

While the VOF plot of the hull details the wetted area, the pressure distribution is necessary to determine the location of the spray root, and therefore to identify the whisker spray area and pressure area of the wetted surface. These areas are more clearly defined by the representations as seen in Figure 4.13, where the wetted areas for all speed cases are presented.

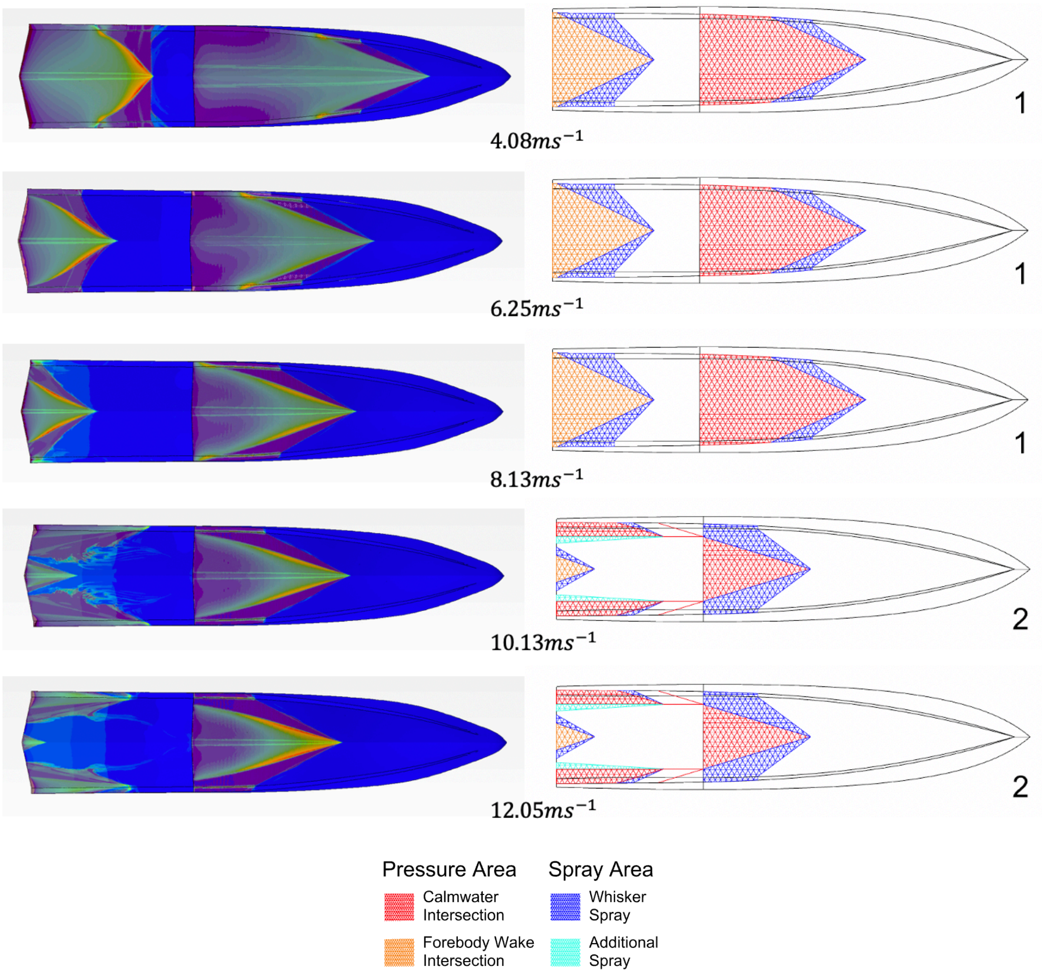

Figure 4.13 – Wetted area composition of Hull C1

For the single hull there are two possible conditions for the wetted area of the hull, as labelled 1 and 2 in Figure 4.13. These are characterised by whether the spray root of the forebody crosses the step. Cases where the spray root does not cross the step are referred to as the 'chine's wet' condition, while cases where the spray root does cross the step are referred to as 'chine's dry' condition. These two distinct cases are pointed out in (Savitsky and Morabito, 2010), and again in (Lotfi, Ashrafizaadeh and Esfahan, 2015), with the experimental and numerical results of (De Marco *et al.*, 2017a) showing agreement, however there is no analysis of which wetted areas may be considered pressure areas, and which are spray areas.

The chine's wet condition is the most straight forward case. In this condition the spray root line intersects with the chine of the forehull and does not cross the step. In this condition the composition of the afterbody wetted area is identical to the forebody, forming a 'triangle' region, made up of both pressure and spray components.

The chine's dry condition is seen to be more complex, with side wetting in addition to the standard wetted triangle of the first condition. While previous papers have noted the existence of this side wetting, none have examined its composition so that it may be included in mathematical models. This side wetting is caused by the afterbody intersecting with the undisturbed, level free surface. This is due to the fact that in the chine's dry condition the forebody only intersects with the incoming free surface to the location at which the spray root crosses the step as opposed to the full beam. When this side wetting area is examined in the pressure and VOF plots it is seen that it comprises of a pressure and spray area, the composition of which is detailed in Figure 4.13. The pressure area is the region in which the afterbody intersects with the undisturbed free surface, and the spray area forms in a manner similar to the standard whisker spray, however there is no means through which the spray area may be quantified. The spray area is relatively small however, so it will have a minimal impact upon the total resistance.

The additional side wetting of the chines dry condition generates lift and contributes to the pressure and shear components of resistance, so it is important that any analytical model for the performance prediction of stepped hulls is capable of accounting for the effects of these areas.

4.5.1.2 Modelling the Freesurface Elevation Aft of the Step

In order to calculate the wetted area of the afterhull the flow as it separates from the forehull must be modelled accurately. The two existing methods of undertaking this are Savitskys Wake Equations, and the Linear Wake Assumption.

To the best of the authors knowledge, the only study that has previously extracted the freesurface elevation aft of a step and compared the results of the Savitsky wake equations was (Lotfi, Ashrafizaadeh and Esfahan, 2015), who make a brief comment upon this for a single speed. No studies set out to verify the accuracy of methods of calculating the freesurface elevation, primarily due to the challenges of experimental obtaining this data. Savitsky's wake equations were developed with the assumption that the afterbody has negligible impact on the forebody wake. Some authors have suggested that the equations are not applicable for flow under a stepped hull due to this fact, however conducted no analysis to support this claim (Dashtimanesh, Tavakoli and Sahoo, 2017). Others have found that the difference between the numerical freesurface elevation profile and the Savitsky freesurface elevation profile is 20% on average (Lotfi, Ashrafizaadeh and Esfahan, 2015). A recent experimental study investigating the reattachment point of the centreline profile determined that there was approximate accordance achieved between the experimental results of reattachment length against the extracted results from Savitsky empirical formulations (Najafi *et al.*, 2019).

Section 4.4 validated the accuracy of the numerical set up in modelling the nearfield freesurface elevation profile of a prismatic planing hull. It is therefore reasonable to assume that the simulated flow aft of a step will be modelled with a similar degree of accuracy, allowing comparison of the freesurface elevation profile under a stepped hull with that as calculated with Savitsky's Wake Equations. The freesurface elevation profiles for the flow aft of the step of hull C1 as calculated numerically is detailed in Figure 4.14 and Figure 4.15.

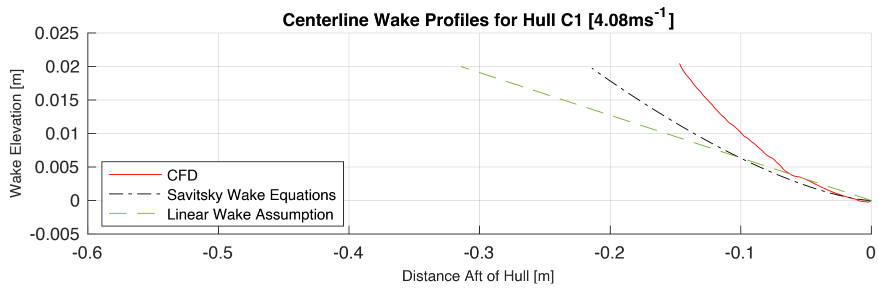

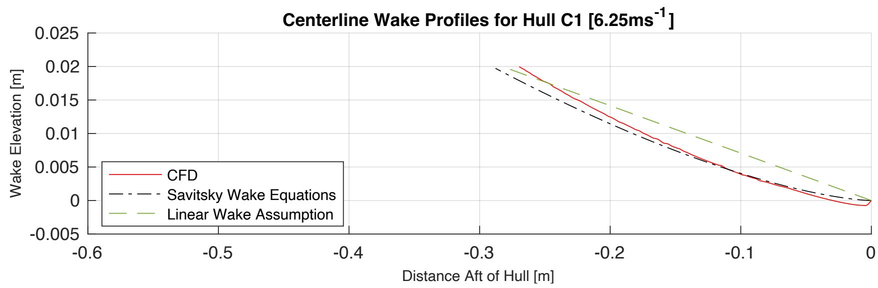

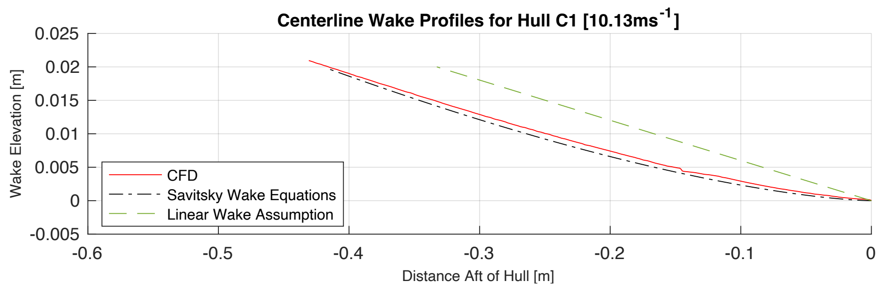

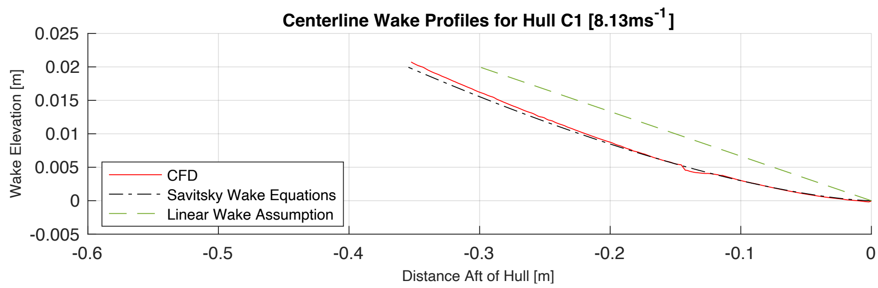

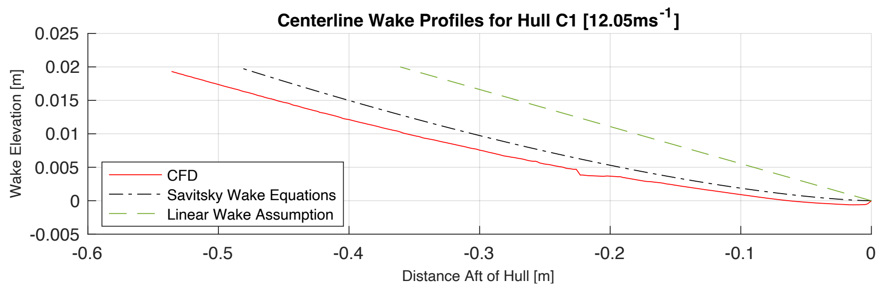

Figure 4.14 - Centreline freesurface elevation profiles aft of step Hull C1 (Note: Vs=0.02)

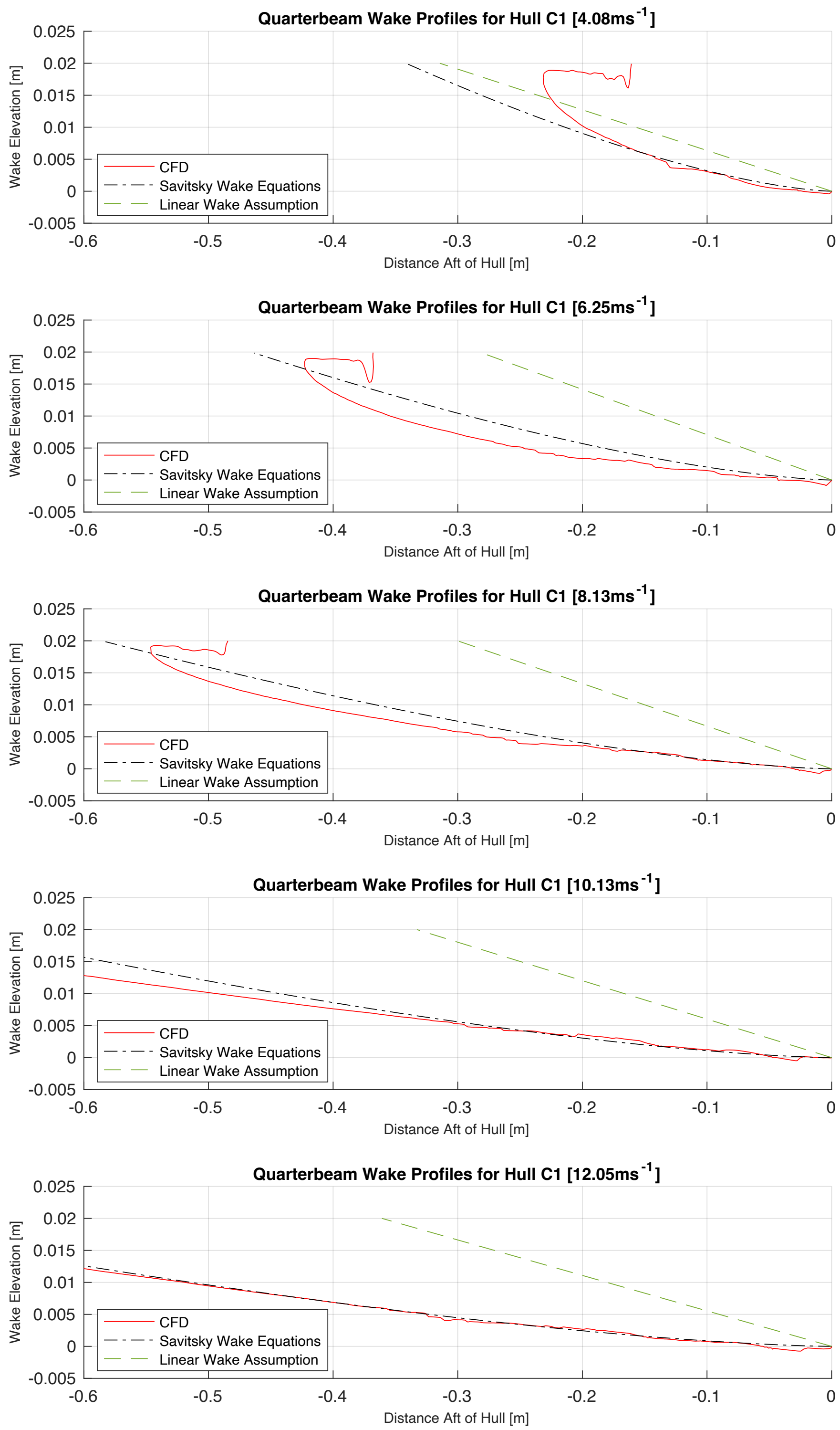

Figure 4.15 - Quarterbeam freesurface elevation profiles aft of step Hull C1 (Note: Vs=0.02)

In addition to the plotting the numerical flow aft of the step of Hull C, Figure 4.14 and Figure 4.15 plot the freesurface elevation as calculated by Savitsky's Wake Equations and the linear wake assumption. It is seen that Savitsky's Wake Equations model the flow well in almost all cases aside for the slowest speed condition and may be considered accurate. The linear wake assumption displays considerably less accuracy in all cases. In order to quantitively analyse the accuracy of each of the methods the ventilation length was determined by the point of intersection with the afterbody. These results are presented in Table 4.1. When the profiles of the 4.08, 6.25 and $8.13ms^{-1}$ are examined in Figure 4.15 the wetted area, due to the whisker spray as detailed in (Savitsky, DeLorme and Datla, 2007), is seen where the profile reverses direction along the afterbody. For these cases the point of intersection is taken to be the location at which the profile reverses direction and the whisker spray is ignored. No data is presented for the quarterbeam intersection of the 10.13 and $12.05ms^{-1}$ cases as the quarterbeam freesurface elevation profile does not intersect with the afterbody at these speeds.

Table 4.1 - Intersection locations Hull C (Error percentage is the different between the empirical method and the CFD)

Speed [ms^{-1}]	**4.08**	**6.25**	**8.13**	**10.13**	**12.05**
CFD CL intersection [m]	0.146	0.268	0.351	0.430	0.534
Savitsky Wake CL intersection [m]	0.214	0.288	0.355	0.418	0.477
LWA CL intersection [m]	0.314	0.283	0.300	0.333	0.361
Savitsky Wake Error	46.73%	7.20%	1.09%	-2.84%	-10.66%
LWA Error	115.49%	5.27%	-14.41%	-22.59%	-32.47%
CFD QB intersection [m]	0.23	0.42	0.55	n/a	n/a
Savitsky Wake QB intersection [m]	0.34	0.46	0.58	n/a	n/a
LWA QB intersection [m]	0.31	0.28	0.30	n/a	n/a
Savitsky Wake Error	47.12%	9.56%	6.64%	n/a	n/a
LWA Error	35.87%	-33.16%	-45.06%	n/a	n/a

When Figure 4.14 and Figure 4.15 are examined it is apparent that neither method is capable of modelling the flow aft of the step for the slowest speed of $4.08ms^{-1}$, producing errors of 46.73% for the CL point of intersection and 115.49% for the LWA. For the QB point of intersection these errors are 47.12% and 35.87%. The speed coefficient for this condition is 2.20, while the lower limit of the range of applicability for the Savitsky Wake Equations is 4. While it was concluded that the Equations displayed a remarkable level of accuracy when applied out with their limits by (Gray-Stephens, Tezdogan and Day, 2020b), it was noted that they were not applicable at lower speeds where there was a large deviation from the equations range. This conclusion is reinforced by the 6.25ms^{-1} condition for which both the Cl and QB profiles are seen to be well modelled, while still outwith their applicability range with a speed coefficient of 3.37. Excluding the 4.08ms^{-1} case, the Wake Equations have an average accuracy of 5.45% for the CL point of intersection and 8.10% for the QB. This is once again in line with the findings of (Gray-Stephens, Tezdogan and Day, 2020b), where the equations were more accurate in modelling the CL profile than the QB.

It is seen that the LWA is not capable of accurately modelling with the CL or QB profiles for the flow under a stepped hull. Excluding the 4.08ms^{-1} case, the method produced average errors of 18.68% and 39.11% for the CL and QB locations of intersection. (Gray-Stephens, Tezdogan and Day, 2020b) found that the accuracy of the LWA increased with speed and this was highlighted as an area for further investigation, however in the present results this is seen to not be the case. It is actually seen that the accuracy of the LWA deteriorates with speed.

From this analysis of the flow under a single stepped hull it is concluded that the Savitsky Wake Equations do hold true, and are very capable of accurately modelling the flow provided the speed coefficient is not too far out of range. The level of accuracy is shown to be in line with the accuracy with which they can model the flow aft of a prismatic planing hull as reported in (Gray-Stephens, Tezdogan and Day, 2020b).

4.5.1.3 Calculating the Afterbody Wetted Area

The pressure area of a planing hull includes the wave rise, as discussed previously, and the calm water intersection with a planing surface does not account for the wave rise. (Wagner, 1932) determined the wave rise for a 2-dimensional wedge penetrating a fluid surface vertically to be $\pi/2$ times the width defined by the calm water intersection with the wedge. (Savitsky, 1964) then derived the following expression to determine the difference between wetted keel length and wetted chine length for a prismatic planing surface:

$$L_1 = L_k - L_c = \frac{b \tan \beta}{\pi \tan \tau} \tag{4.2}$$

In this expression the wetted chine length is defined as the location where the spray root intersects the chine of the hull. The relationship between the waterline intersection with a hull and the spray root line are detailed in Figure 4.16.

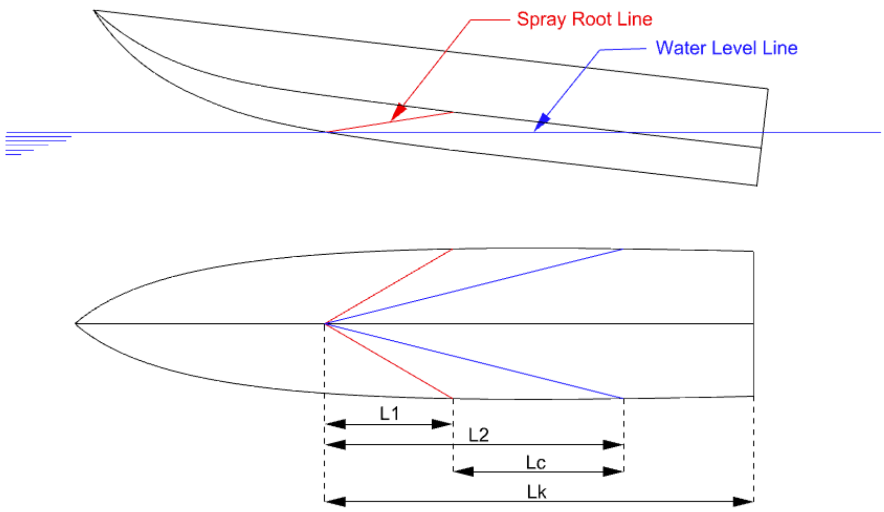

Figure 4.16 – Waterline intersection and spray root (Adapted from (Savitsky, 1964)**)**

The calm water intersection length, L2 is defined by (Savitsky, 1964) as:

$$L_2 = \frac{b \tan \beta}{2 \tan \tau} \tag{4.3}$$

It is necessary to establish if wetted area of the afterbody is subject to the wave rise in the same manner as a hull intersecting with calm water as detailed by (Wagner, 1932), and if Equation (4.2) is appropriate to model this. If this was the case then the wetted area of the afterbody may be calculated by determining its intersection with the wake from the forebody, which would represent the 'calm water intersection' in Savitsky's definition, and then including calculating the area due to wave rise using an equation similar to (4.2). As the afterbody is not subject to level water it is necessary to orient it relative to the wake hollow through the use of local values, as will be outlined in Section 5.2.2 so Equation (4.2) is therefore modified to become Equation (4.4).

$$L_{1_{Aft}} = L_{k_{Aft}} - L_{c_{Aft}} = \frac{b_L}{\pi} \frac{\tan \beta_L}{\tan \tau_L} \tag{4.4}$$

Savitsky Wake Equations were shown to be capable of modelling the flow aft of the step, so using these it is possible to determine the afterbody's intersection with the wake from the forebody, or L2. Using local values, it is then possible to calculate the wave rise and determine L1. It is only possible to determine L1 from CFD as there is no way to extract the afterbody's intersection with the incoming flow without the effect of wave rise. Comparison between the CFD L1 values, and the L1 values as calculated using Equation (4.4), and the L2 values as calculated by Savitsky's wake equations is presented in Table 4.2.

Table 4.2 – Wave rise of the afterbody (Error percentage is the different between the empirical method and the CFD)

Speed $[ms^{-1}]$	4.08	6.25	8.13	10.13	12.05
L1 CFD [m]	0.21	0.32	0.45	0.64	0.78
L2 Savitsky Wake Equations [m]	0.18	0.32	0.44	0.56	0.68
L2 Savitsky Wake Equations Error	-12.86%	0.61%	-3.22%	-11.94%	-13.46%
L1 Eqn (4.4) [m]	0.12	0.20	0.28	0.36	0.43
L1 Eqn (4.4) Error	-44.52%	-35.95%	-38.39%	-43.94%	-44.91%

It was found that calculating the wave rise using Equation (4.4), based upon the work of (Savitsky, 1964) and (Wagner, 1932) resulted in an L2 value with an average error of 41.54%. This equation was developed for a prismatic planing hull's intersection with the undisturbed, level free surface. It was shown to not be applicable for cases where the afterbody is intersecting with the wake of the forebody. Using this method will result in an overcalculation of the wetted area of the afterbody.

Interestingly, it was found that the taking L1 as the intersection with the forebody wake (L2) and neglecting to add any wave rise resulted in an average error of 8.17%. This suggests that there is very little wave rise when the afterbody is operating in the forebody wake. Physically, there will be some amount of wave rise, but this value is considerably smaller than that as calculated by Equation (4.4), and ignoring its presence results in a good approximation to calculate the wetted area of the afterbody.

Once ventilation lengths at the CL and QB are known, as detailed in Figure 4.17, it is simple to determine the wetted area of the afterbody through basic mathematics, depending on whether the afterhull is operating in the chines dry condition or not. This process will be discussed in more detail in Section 5.3.

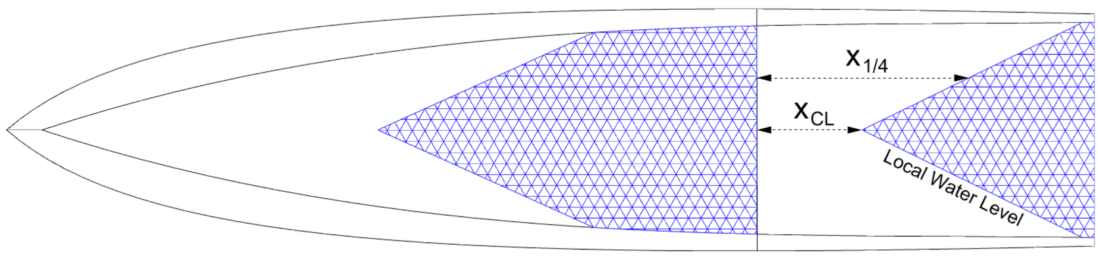

Figure 4.17 – Ventilation lengths at the CL and QB locations

4.5.2 Double Stepped Hull

The further analysis conducted for a double stepped hull follows the same structure as Section 4.5.1.

4.5.2.1 Wetted Area

The analysis of the wetted area of a double stepped planing hull followed the same methodology as that of the single stepped hull. The composition was broken down into pressure and spray areas, and the characteristics of each are discussed. The wetted areas for all speeds simulated in Chapter 3 are presented in Figure 4.18. The numbers 1 – 5 indicate the possible wetted area configurations for a double stepped hull.

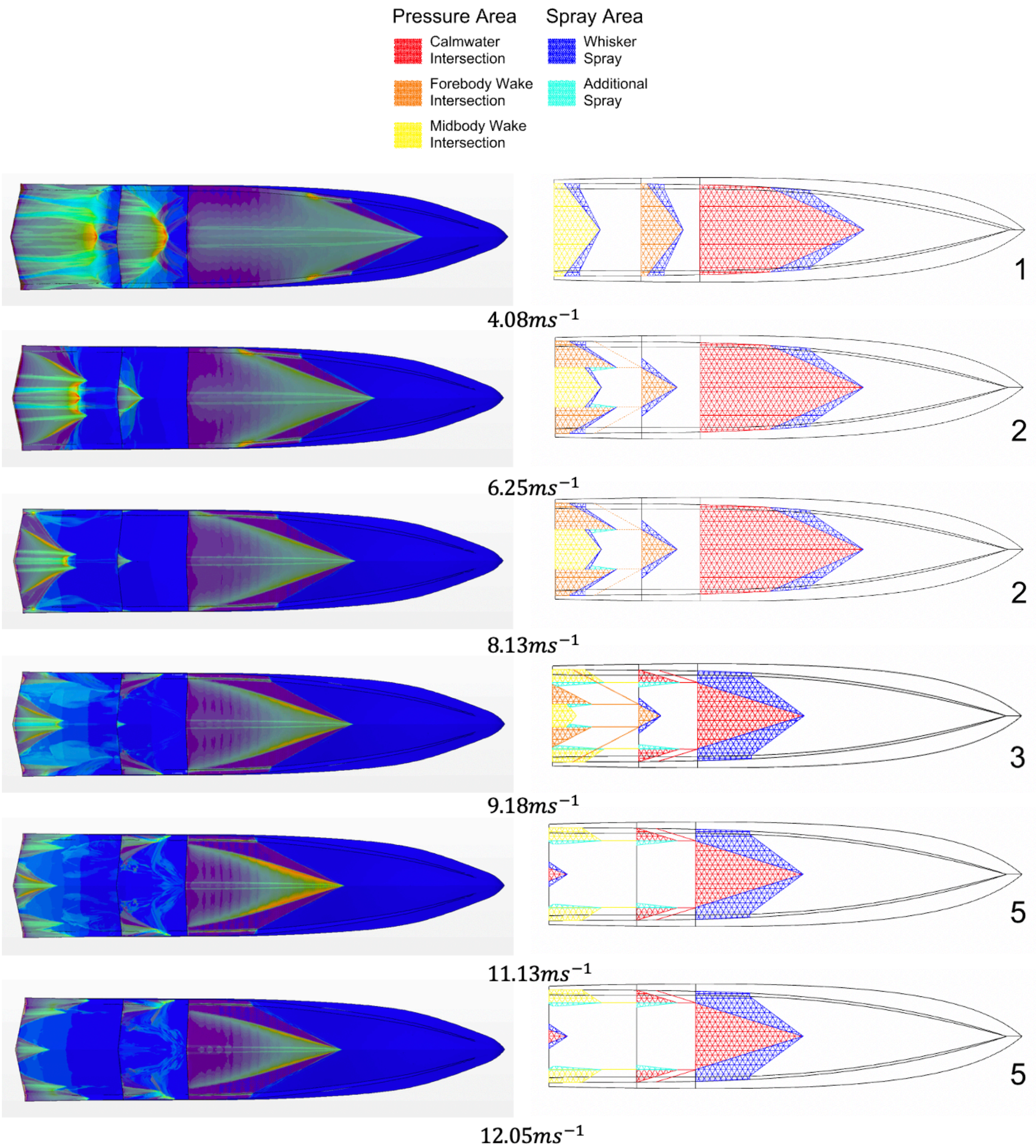

Figure 4.18 – Wetted area composition of Hull C2

The addition of the second step makes the wetted area considerably more complex. Despite this, the phenomena that are occurring are an extension of the flow characteristics that were apparent for the single stepped hull. For the 4.05ms^{-1} case both the forebody and midbody are operating in the chine's wet condition. As such the wetted area of the midbody and afterbody forms a 'triangle' region. For the 6.25 and 8.13 ms^{-1} cases the forebody is in a chine's wet condition, so there is no side wetting on the midbody and the wetted area forms a triangle region. The midbody is however in a chine's dry condition and as such there is both side wetting and a triangle region present on the afterbody. For the 9.18ms^{-1} case both the forebody and the midbody are operating in the chine's dry condition. This introduces a new component of wetted area that contributes to the pressure area of the afterbody, arising from the flow from the side wetting of the midhull as it separates at the second step. The afterbody in this case is made up of three components:

- The triangle region where the flow of the midbody intersects (yellow triangle Figure 4.18)
- The side wetting, where the flow of the forebody intersects, due to the chine's dry condition of the midhull (orange Figure 4.18)
- The outside side wetting, where the side wetting on the midhull due to the chine's dry condition of the forehull separates at the second step and intersects with the afterbody (yellow sides Figure 4.18)

For the 11.13 and 12.05ms^{-1} cases ventilation length of the forebody wake is large enough that it does not actually intersect with the midbody, instead intersecting with the afterbody. The forebody is in the chine's dry condition so there is side wetting present on the midbody where it intersects with the undisturbed free surface. There is also additional side wetting on the afterbody where the midhull side wetting separates at the step. There is a final condition that it is possible for the double stepped hull to be operating in, even though it was not demonstrated by the cases presented. It is shown in Figure 4.19, and occurs when the forebody is operating in the chine's wet condition, yet the ventilation length is such that the wake does not intersect with the midhull at all.

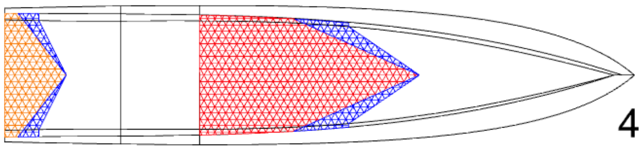

Figure 4.19 – Additional possible wetted area composition of Hull C2

The 12.05ms^{-1} shows the importance of and analytical model being able to model the side wetting. There is no intersection of the forbody flow with the midbody, and the triangle region formed by the intersection of the forebody wake with the afterbody is small. Therefore, the majority of the lift and resistance for the mid and afterhull must come from the side wetting, and if these areas are not correctly modelled then the performance prediction model will not be accurate.

The analysis of the possible configurations of wetted area for a double stepped hull show that long ventilation lengths are possible, causing the forebody flow to miss the midbody. Where (Danielsson and Strømquist, 2012) found their performance prediction model for double stepped model that attempted to incorporate Savitsky's wake equations to fail due to 'unreasonably long ventilation', it is possible that this was not the case, and the model was just incapable of dealing with this possibility. A mathematical performance prediction model must be formulated with an understanding of the wetted area scenarios that can occur and how to model them correctly, or it will not produce accurate results.

4.5.2.2 Modelling the Freesurface Elevation Aft of the Steps

The centreline and quarterbeam freesurface elevation profiles were extracted from the CFD simulations of the double stepped hull so that Savitsky's Wake Equations and the LWA may be verified for the flow aft of each step. There were no examples in the literature of the flow under a stepped hull being analysed in this manner. The results of the centreline profiles are presented in Figure 4.20 while the quarterbeam profiles are presented in Figure 4.21 and Figure 4.22. When the hull is operating in the chine's dry condition the quarterbeam location is taken using the pressure beam as the spray root crosses the step rather than the physical beam. As the pressure beam is different for the forebody and the midbody the quarterbeam is different for each flow regime, as detailed in the title of each of the plots. In Figure 4.21 the quarterbeam profile from the forebody flow is presented, while the quarterbeam profile from the midbody flow is presented in Figure 4.22. Both centreline profiles are presented on the same graph as the location of the profile is identical for both cases. The point of intersections for each of the methods is given in Table 4.3.

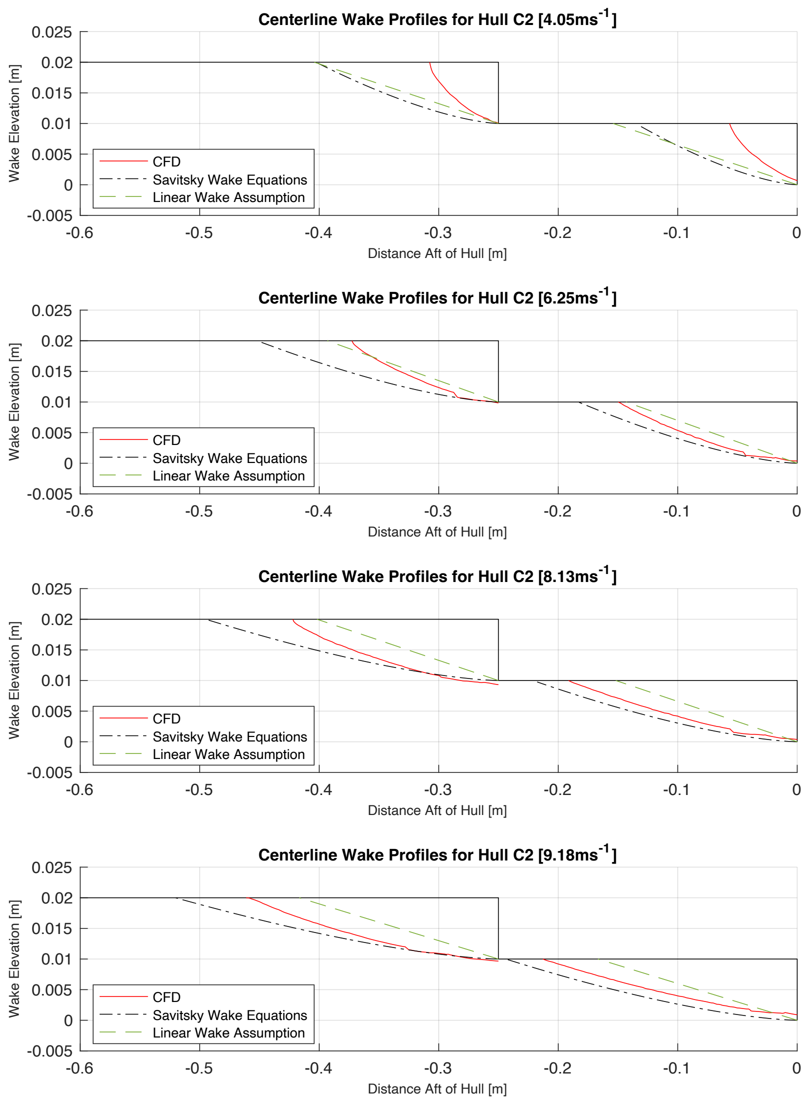

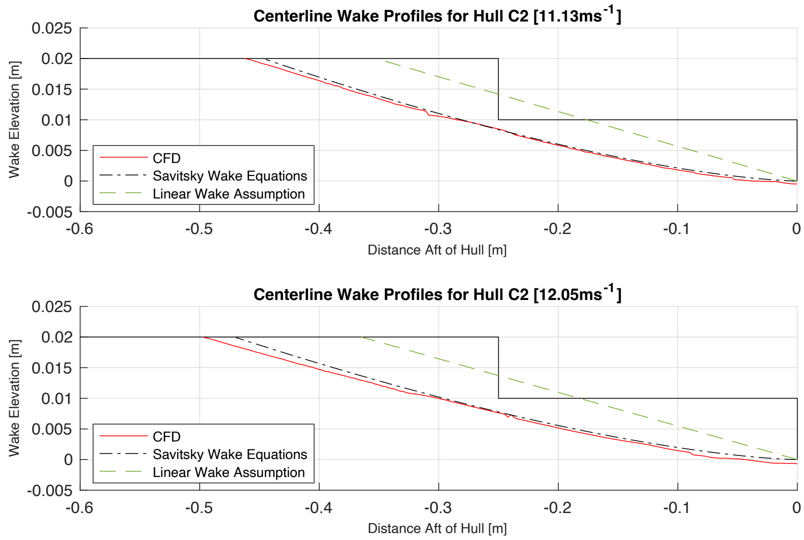

Figure 4.20 – Centreline freesurface elevation profiles aft of step Hull C2

Table 4.3 - Intersection locations of centreline profile Hull C2

Speed [ms^{-1}]	**4.05**	**6.25**	**8.13**	**9.18**	**11.13**	**12.05**
Forebody CFD CL intersection [m]	0.06	0.15	0.19	0.21	0.46	0.50
Forebody Savitsky Eqn CL intersection [m]	0.13	0.18	0.22	0.24	0.44	0.47
Forebody LWA CL intersection [m]	0.15	0.14	0.15	0.17	0.35	0.36
Forebody Savitsky Eqn Error [%]	135.71	21.92	13.73	13.42	-3.69	-5.52
Forebody LWA Error [%]	172.29	-4.36	-20.65	-21.67	-23.65	-26.64
Midbody CFD CL intersection [m]	0.06	0.12	0.17	0.21	n/a	n/a
Midbody Savitsky Eqn CL intersection [m]	0.15	0.20	0.24	0.27	n/a	n/a
Midbody LWA CL intersection [m]	0.15	0.14	0.15	0.17	n/a	n/a
Midbody Savitsky Eqn Error [%]	162.51	64.40	39.53	27.88	n/a	n/a
Midbody LWA Error [%]	167.99	16.76	-11.73	-21.04	n/a	n/a

Figure 4.20 shows that, once again, neither method is applicable to the 4.05ms^{-1} case. As discussed, this is as the speed coefficient is below the limits of applicability of the equations. As such, the 4.05ms^{-1} case is excluded from all following discussion.

The Savitsky Wake Equations are once again shown to be capable of modelling the forebody flow with an acceptable degree of accuracy. This was to be expected given they were shown to be accurate for the single stepped hull, and the physics of this problem is the same. The average error for the point of intersection calculated using the Savitsky Wake Equations is 11.66%. The linear wake equation is again shown to be less capable of modelling the centreline freesurface elevation profile of the forebody, resulting in an average error of 19.40%.

When the CL freesurface elevation aft of the midbody was examined, an issue arose for three cases (6.25, 8.13 and 9.18ms^{-1}) as the beam of the spray root as it crossed the second step, or pressure beam was very small (0.14m, 0.04m and 0.02m, respectively). The Savitsky Wake Equations are only capable of modelling the flow for three beam lengths aft of a step. This is not sufficient to determine the point of intersection with the after hull. As a work around, the physical beam was input to the Wake Equations, which appeared to create a reasonable extension of the profile. This practice is however questionable, and it is likely this contributed to the increased error of the Savitsky Wake Equations when modelling the midbody flow. The average error was found to be 43.94%, a considerable increase when compared to the forebody flow. As such the Savitsky Wake Equations cannot be said to be accurate in this application. The Linear Wake Assumption was seen to be notably more accurate, resulting in an average error of 16.51% for the intersection point.

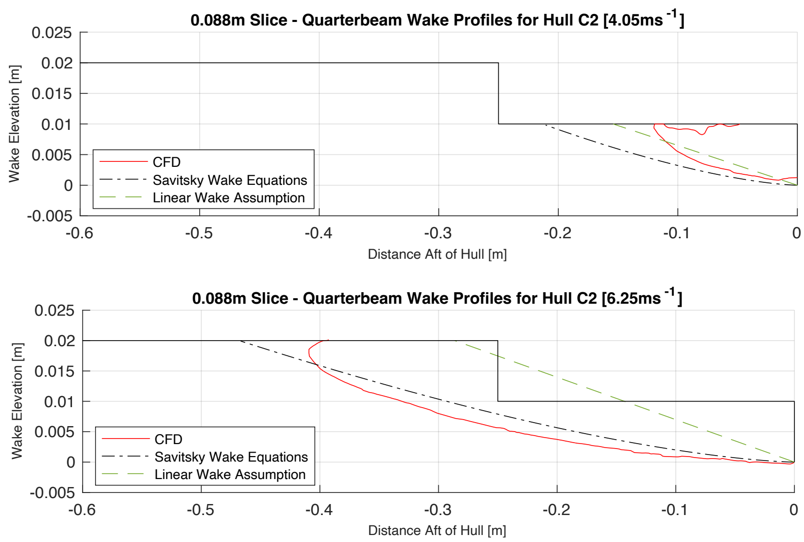

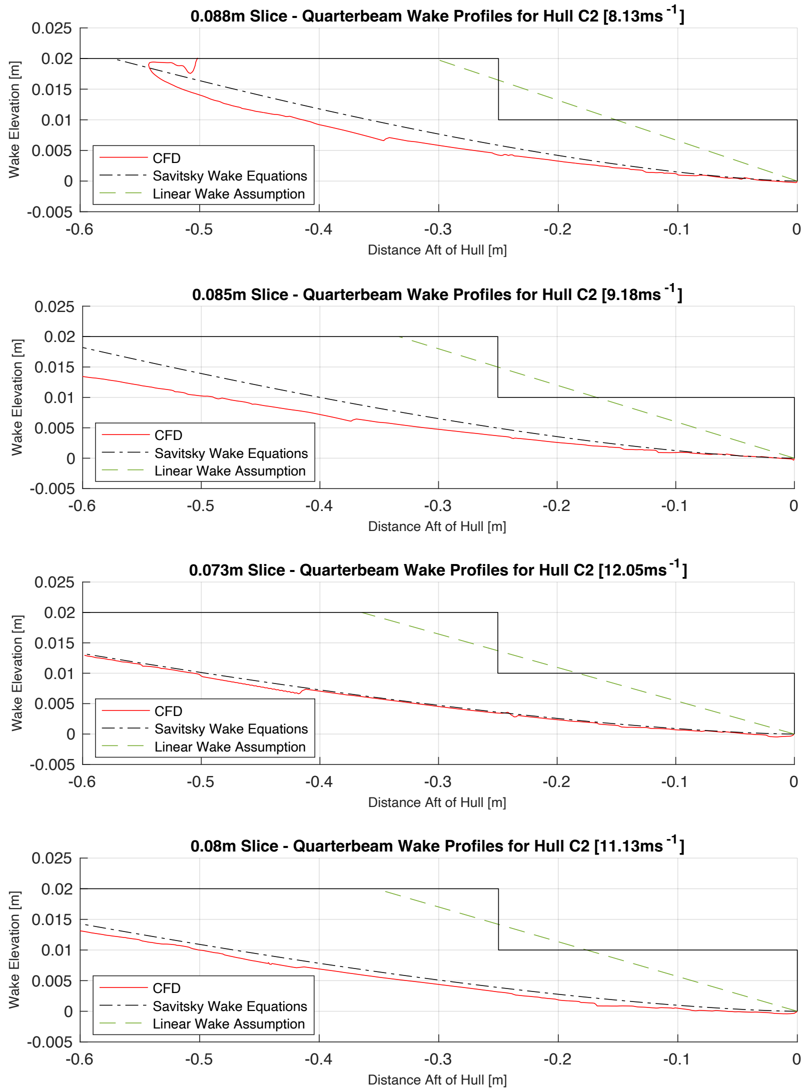

Figure 4.21 – Quarterbeam freesurface elevation profiles aft of first step Hull C2 (Forebody flow)

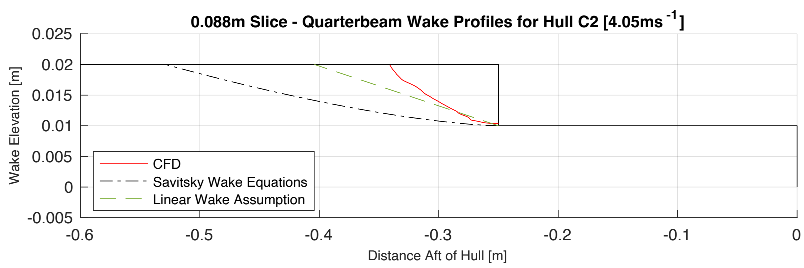

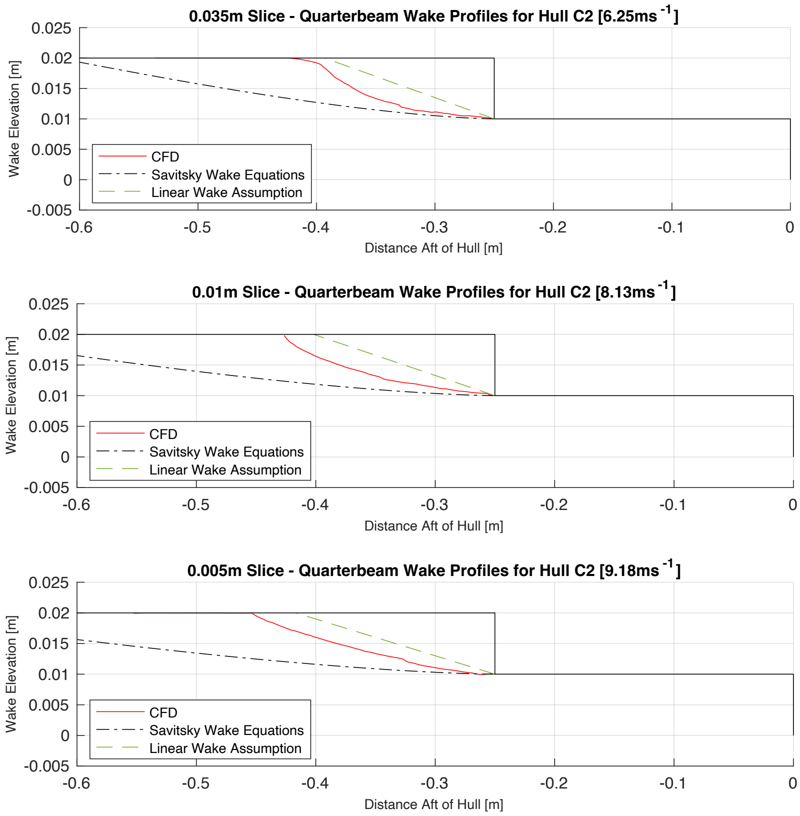

Figure 4.22 – Quarterbeam freesurface elevation profiles aft of second step Hull C2 (Midbody flow)

Table 4.4 - Intersection locations of quarterbeam profiles Hull C2

Speed [ms^{-1}]	**4.05**	**6.25**	**8.13**	**9.18**	**11.13**	**12.05**
Forebody CFD CL intersection [m]	0.12	0.41	0.54	n/a	n/a	n/a
Forebody Savitsky Wake CL intersection [m]	0.21	0.47	0.57	n/a	n/a	n/a
Forebody LWA CL intersection [m]	0.15	0.15	0.16	n/a	n/a	n/a
Forebody Savitsky Wake Error [%]	75.62	14.06	5.41	n/a	n/a	n/a
Forebody LWA Error [%]	28.49	-30.02	-44.07	n/a	n/a	n/a
Midbody CFD CL intersection [m]	0.09	0.17	0.18	0.21	n/a	n/a
Midbody Savitsky Wake CL intersection [m]	0.28	0.37	n/a	n/a	n/a	n/a
Midbody LWA CL intersection [m]	0.15	0.14	0.15	0.17	n/a	n/a
Midbody Savitsky Wake Error [%]	205	121.3	n/a	n/a	n/a	n/a
Midbody LWA Error [%]	69.4	-13.58	-14.81	-20.12	n/a	n/a

Similar trends are apparent for the Quarterbeam profiles, as presented in Figure 4.21. Results detailing the point of intersection with the mid and aftbody are presented in Table 4.4. The ventilation lengths as such that for several cases in which no intersection occurs. The Savitsky wake equations are once again seen to be capable of accurately modelling the forebody flow, resulting an average point of intersection error of 9.73%. The linear wake equations are shown to be inaccurate, resulting in an average error of 37.05%.

Modelling the midbody profiles using Savitsky's wake equations face raises the same issues in relation to the small pressure beam as discussed previously. When they are extended using the physical beam, it is found that they are not capable of modelling the quarterbeam profiles of flow aft of the midbody, resulting in large overpredictions of the points of intersection. The linear wake assumption is it is seen to be relatively accurate in modelling the quarterbeam profile, resulting in an average point of intersection error of 16.17%. This is in line with the findings of the centreline profile for midbody flow. While it is physically not the case that the centreline and quarterbeam wake will have the same profiles, this is not an unreasonable assumption for cases where the pressure beam is narrow, and therefore the separation between the two profiles is very small.

The reason for the Savitsky Wake Equations being accurate when modelling the forebody flow, yet producing unreasonable results for the midbody flow is the large differences in the wetted area of both surfaces impacting the flow characteristics. The forebody flow is fully developed having been in contact with a large area of the hull. This influences the flow as it separates at the first step and means that the Savitsky Wake Equations are applicable. In comparison, the wetted area of the midbody is very small. The flow does not develop with characteristics imparted from the midhull due to its small area. The underlying assumption of the LWA is that the hull 'scrapes' off the top layer of water, leaving the underlying streamlines parallel to the free surface. It is found that this assumption is reasonable when only a small portion of the hull in contact with the fluid, and the flow does not develop into the traditional wake hollow. The application of the Savitsky freesurface elevation profiles to the midhull flow violated several of the applicability criteria of the equations, as detailed in Section 4.3.2, so it unsurprising that the profiles they model are not considered applicable.

4.6 Conclusions

This chapter set out to develop knowledge of the flow as it separates aft of a step that may be employed to develop enhanced analytical models through analysing results of numerical simulations. Experimental data was generated and employed to validate CFD as an accurate tool in modelling the freesurface elevation aft of a planing surface. The composition of the wetted area, methods of modelling this, and the free surface elevation aft of a step were then considered and analysed for both a single and double stepped hull. A large amount of understanding was developed, and key factors to consider when developing analytical performance predication models were highlighted.

The comparison of experimental data to the results of the numerical simulation for the free surface elevation aft of a prismatic hull showed that there was good correlation for cases. The CL profiles were found to be extremely accurate. There were larger errors for the QB profiles, although the corelation was still considered good and the accuracy increased as the distance aft of the transom reduced. CFD may be considered accurate in modelling the fluid flow aft of a planing surface.

Analysis of the numerical results of the single stepped case showed there to be two possible operating conditions, resulting in two distinct wetted area compositions. Accurately accounting for the additional side wetting of the chines dry condition was highlighted as an important aspect of any analytical model as this area generates lift and contributes to the pressure and shear components of resistance. The Linear Wake Assumption was shown to be inappropriate at modelling the free surface elevation aft of the step. Savitsky's Wake Equations however, were capable of accurately modelling the flow provided the speed coefficient is not too far out of range, resulting in an average error of 5.45% for the CL point of intersection and 8.10% for the QB.

There was found to be little wave rise when the afterbody intersected with the wake hollow of the forehull, and ignoring its presence results in a good approximation to calculate the wetted area of the afterbody.

Analysis of the numerical results of the single stepped case showed the composition of the wetted area to be far more complex with four possible configurations. An analytical model must be capable of accounting for all aspects of wetted area, and determining which configuration the hull is operating in. Savitsky wake equations were shown to be accurate in calculating the freesurface elevation aft of the first step, resulting in an average point of intersection error of 11.66% for the CL profile, and 9.73% for the QB. They were found to be inaccurate in calculating the freesurface elevation aft of the second step. As there was very little of the midhull in contact with the fluid, it was seen to 'scrape off' the top layer rather than influencing the flow characteristics. As such, the Linear Wake Assumption was shown to be relatively accurate, resulting in an average point of intersection error of 16.51% for the CL and 16.17% for the QB.

This chapter successfully developing a large amount of knowledge of the fluid flow as it separates at a step that will be employed to enhance and accelerate analytical performance prediction methods in Chapter 5.

Chapter 5 – The Development of an Analytical Mathematical Model for the Performance Prediction of Stepped Hulls

This chapter sets out to develop enhanced semi-empirical models for the performance prediction of single and double stepped hulls that reduce the level of error when compared to the existing models of (Svahn, 2009) and (Dashtimanesh, Amirkabir and Sahoo, 2016). This will be achieved by applying the knowledge developed of the fluid flow aft of a step in Chapter 4 through the analysis of numerical simulations. The developed models will be used to model Hull C1 and C2, with the results being compared to the experimental data of (Taunton, Hudson and Shenoi, 2010) and the CFD results of Chapter 3 in order to evaluate and comment upon the accuracy of each.

5.1 Introduction

Over the past decade there has been a significant effort devoted to the study of stepped planing hulls by marine researchers (Bakhtiari and Ghassemi, 2017). These studies have employed a number of analysis techniques of varying complexity and with very different computational demand requirements. Experimental testing programs have been undertaken, physically testing model hulls at hydrodynamic laboratories and providing insight into the complex nature of these hulls (Taunton, Hudson and Shenoi, 2010). Crucially, these EFD studies develop validation data that may be employed to verify the accuracy of other analysis methods. Researchers have development mathematical models based upon semi-empirical methods (Svahn, 2009; Savitsky and Morabito, 2010; Danielsson and Strømquist, 2012; Dashtimanesh, Amirkabir and Sahoo, 2016). Others have employed more complex numerical methods based on 2D+T theory (Bilandi *et al.*, 2018). Finally, there are many researchers who turn to Computational Fluid Dynamics to solve the Reynolds Averaged Navier Stokes equations, capable of fully modelling three-dimensional flow and non-linearities associated with this.

While it is generally accepted that CFD is the most robust and accurate of these methods, it is the most computationally demanding. CFD simulations require considerable time to run, complex software and at times, specialist computing facilities. The development of an accurate, yet simple mathematical model for the performance prediction of stepped hulls is an attractive prospect, as it allows designs to be evaluated quickly and easily without the need for specialist training or facilities.

The most famous such model was developed by (Savitsky, 1964), for unstepped planing hulls. The study developed empirical equations to calculate the hydrodynamic characteristics of a planing hull, based on the results of an extensive systematic experimental testing program. A computational procedure was proposed that utilised these equations to determine the resistance and equilibrium position of a planing hull. While these equations were successful, they were not applicable to stepped hulls as there was no practical way to determine how the flow from the forebody intersected with the afterbody. To this end, (Savitsky and Morabito, 2010) conducted a series of model tests, developing empirical equations that quantitatively define the centreline and quarterbeam freesurface elevation profile aft of a planing hull, allowing designers of stepped planing hulls to determine how the flow aft of a step intersects with the afterbody. (Svahn, 2009) then went on to develop a new mathematical model for the performance prediction of a single stepped hull, based upon the empirical resistance equations of (Savitsky, 1964) and employing the work of (Savitsky and Morabito, 2010). Svahns model contains numerous limitations and ambiguities. One of the key issues with its implementation is the lack of proper validation against experimental data (Mancini *et al.*, 2018). (Danielsson and Strømquist, 2012) attempted to extend Svahn's method for application with a double stepped planing hull. They were unsuccessful in implementing the Wake Profile Equations as developed by (Savitsky and Morabito, 2010), finding the resulting model to be overly complex. Instead, they employed the Linear Wake Assumption to model the fore and midbody flow.

This chapter sets out to further investigate the use of semi-empirical mathematical models in modelling stepped hulls, addressing the limitations and concerns surrounding the existing models. Savitsky's method has been shown to be capable of robust, accurate, and most notably, rapid calculations of the resistance and trim of planing hulls (Khazaee, Rahmansetayesh and Hajizadeh, 2019b). The development of such rapid evaluation tools is very valuable to the initial design phases, where higher fidelity, yet more time-consuming methods are not always practical is abundantly clear. This chapter will implement the enhanced knowledge of the flow characteristics of stepped hulls that was developed in Chapter 4.

5.1.1 Aims and Objectives

It is the main aim of this chapter is to develop enhanced mathematical models for the performance prediction of single and double-stepped planing hulls. These models should address the limitations of existing models, resulting in a more robust and accurate design tool.

In order to achieve this aim a number of objectives are put forwards:

- **Evaluate** the accuracy of Savitsky's Model for Hull C
- **Evaluate** the accuracy of Svahn's Model for Hull C1
- **Address** the limitations of Svahn's Model, **Enhancing** its accuracy
- **Develop** a new method for the performance predication of double stepped hulls
- **Evaluate** the accuracy of the developed methods for Hull C1 & C2

5.1.2 Methodology

Existing Semi-Empirical models are coded in MATLAB and used to model the geometries experimentally tested by (Taunton, Hudson and Shenoi, 2010). Savitsky's Method (Savitsky, 1964) will first be used to model the Hulls C to provide a baseline in the expected accuracy of such methods. Following this, Hull C1 will be modelled with Shahn's Method (Svahn, 2009), providing a better understanding of the model and its limitations, while highlighting further areas in which it may be improved.

A series of modifications will then be made to Svahn's Method to extend its range of applicability, making it more robust and capable of modelling more realistic wetted areas. These alterations will be based on the knowledge of flow as it separates at a step and the composition of the wetted area that was developed in the previous Chapter. The two proposed alterations are to develop a strategy that allows the model to deal with the chine's dry planing condition, and to develop a means through which the wetted area employed by the model is more physically representative of the real-world condition. The Modified version of Svahn's method will be compared against the original formulation, using the experimental baseline data.

An attempt will then be made to expand the modified version of Svahn's model for application with double stepped hulls. The extension of the model will employ the same logic, however this will be extended to include the third lifting surface. This proposed model will once again employ the detailed knowledge of flow and composition of wetted areas that was developed. The developed method will then be assessed with the results being analysed and commented upon.

5.2 Mathematical Models

This section will briefly detail the mathematical models developed by (Savitsky, 1964) and (Svahn, 2009) so that the procedures may be understood, and the modifications that are proposed the following section are given some context.

5.2.1 Savitsky's Method for Planing Hulls

Savitsky's method is a semi-empirical technique to evaluate the hydrodynamic performance of planing hulls in a simple and rapid manner. It was derived from an extensive set of experimental data on prismatic planing hulls (Savitsky, 1964). The study analysed the elemental hydrodynamic characteristics of a prismatic planing surface, utilising the results of systematic model tests to developed empirical formulas that describe the lift, drag, wetted area, centre of pressure and proposing stability of planing vessel as a function of speed, trim, deadrise angle and loading. A a computational procedure was proposed that utilised these equations to predict the resistance, trim, draft and proposing stability of a prismatic planing hull. The empirical equations and the computational procedure will be briefly presented in this section so that the means by which it is adapted to stepped hulls is better understood, however for full details of the method please refer to (Savitsky, 1964).

Savitsky's method investigates the pitching moment equilibrium of a planing vessel. It is assumed that the vessel is in a steady state as seen in Figure 5.1, and as such the forces must be balanced (Equation (5.1) and (5.2)) and the moment must be zero (Equation (5.3)). The trim angle is systematically varied until trim values that result in a positive moment and a negative moment are found. Linear interpolation is then used applied to these trim values to find the running trim that results in zero moment and is thus the equilibrium position of the hull.

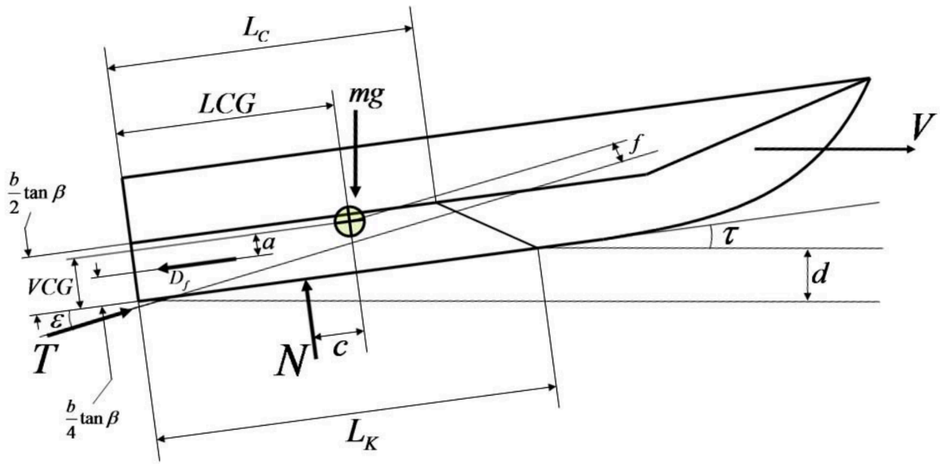

Figure 5.1 - Steady state planing hull (As presented in (Svahn, 2009)**)**

The steady state force and moment equations are:

$$Vertical\ Force: \quad N cos\tau + T sin(\tau + \epsilon) - mg - D_f sin\tau = 0 \tag{5.1}$$

$$Horizontal\ Force: \quad Tcos(\tau + \epsilon) - Nsin\tau - D_f cos\tau = 0 \tag{5.2}$$

$$Moment: \quad (N * c) + \left(D_f * a\right) - (T * f) = 0 \tag{5.3}$$

It is known that as the deadrise of a planing surface increases less lift is produced due to the reduction in stagnation pressure at the leading edge. The first empirical equation developed by Stavisky relates the lift of a deadrise surface to the lift of a flat plate of identical values of τ, λ and C_v, as detailed in Equation (5.4).

$$Cl_\beta = Cl_0 - 0.0065\beta Cl_0^{0.60} \tag{5.4}$$

Following this the empirical equation relating the lift of a flat planing surface to its aspect ratio and angle of attack is used to determine the wetted beam to length ratio that produces the required lift, as presented in Equation (5.5). The formulation of the empirical lift equation is based on a combination of both static and dynamic lift and in effect determines the vertical position of the hull for the given position.

$$Cl_0 = \tau^{1.1}\left(0.0120\lambda^{0.5} + \frac{0.0055\lambda^{\frac{5}{2}}}{C_v^2}\right) \tag{5.5}$$

The frictional resistance coefficient of the hull may then be determined using the ITTC 1957 friction line. The component of frictional drag acting in the horizonal orientation is determined by Equation (5.6).

$$D_f = \frac{1}{2}\frac{\rho V_m^2 \lambda b^2}{cos\beta}(C_f + \Delta C_f) \tag{5.6}$$

The pressure resistance, or induced resistance is then calculated for a frictionless fluid using Equation (5.7).

$$D_p = \Delta \tan\tau \tag{5.7}$$

The centre of pressure may be determined by separate evaluation of the static and dynamic lift, where the dynamic force acts 75% of the mean wetted length forward of the transom, while the buoyant force acts 33% forward of the transom. The empirical expression detailed in equation (5.8) was derived to calculate this.

$$C_p = \frac{l_p}{\lambda b} = 0.75 - \frac{1}{5.21\, {C_v^2}/{\lambda^2} + 2.39} \tag{5.8}$$

Equations (5.4) - (5.8) may be employed in the procedure detailed in Figure 5.2, allowing the hydrodynamic performance of a planing hull to be determined based upon its principal dimensions, mass, and centre of gravity.

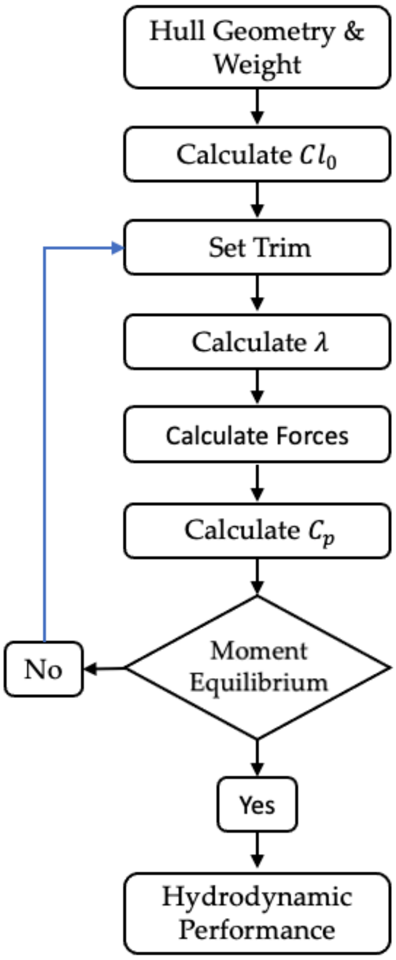

Figure 5.2 - Computational procedure for Savitsky's Method

5.2.2 Svahn's Method for Single Stepped Hulls

Svahn went on to extend Savitsky's method for application with single stepped planing hulls (Svahn, 2009). The methodology treated the hull in front of the step and the hull aft of the step as separate lifting surfaces, using Savitsky's method to determine the forces acting upon each as if they were two regular hulls following each other closely. The equilibrium equations were derived for this multi-body model, and solved to find the steady state position of the hull and its associated resistance.

In this model the forebody follows the same theory as a normal planing hull intersecting with the calm level water surface. The afterbody, however, does not as it is operating in the wake of the forehull as opposed to the calm water level. Savitsky's method has no practical way to input the geometry of the freesurface elevation of the wake, so instead a methodology to interpret the afterbody hull shape relative to the wake surface was developed. The novelty that Svahn introduced to his method was the addition of local deadrise, beam and trim values to calculate the forces on the afterbody. These values orient the perspective of the afterbody relative to the wake in a way that allows the standard Savitsky equations to be used to calculate the forces as for calm water. By doing so the wake of the forehull is viewed as level, and Savitsky's method may be applied to the afterbody. In order to determine the intersection of the forebody wake with the afterbody the Savitsky Wake Equations, as outlined in Section 4.3.2 are employed.

Another issue that Svahn's method address is that the weight distribution between the fore and afterbody's is initially unknown. The location of the centre of pressure, and magnitude of force acting on each lifting surface varies with speed and trim, while the centre of gravity remains constant. The weight distribution is solved iteratively by locking the trim and varying the vertical position of the vessel, and therefore the wetted lengths of both surfaces, until the vertical force equilibrium equation is satisfied. Svahn's Method then goes on to investigates the pitching equilibrium of the stepped planing vessel.

This section details the modifications that were made by Svahn to adapt Savitsky's method for application with single stepped planing hulls. New parameters will be explained, and the computational procedure and logic will be briefly presented so that the reader has an overview of the method and may understand how it is modified in the following sections. This is not intended to detail the method in full however, and for a comprehensive procedural description please refer to (Svahn, 2009).

The vessel is assumed to be in a steady state position, with a force diagram as presented in in Figure 5.3. It is seen that the addition of the step complicates the force diagram in comparison to that of a standard planing hull, as seen in Figure 5.1. The force and moment equations are thus updated, as detailed in Equations (5.9) - (5.11).

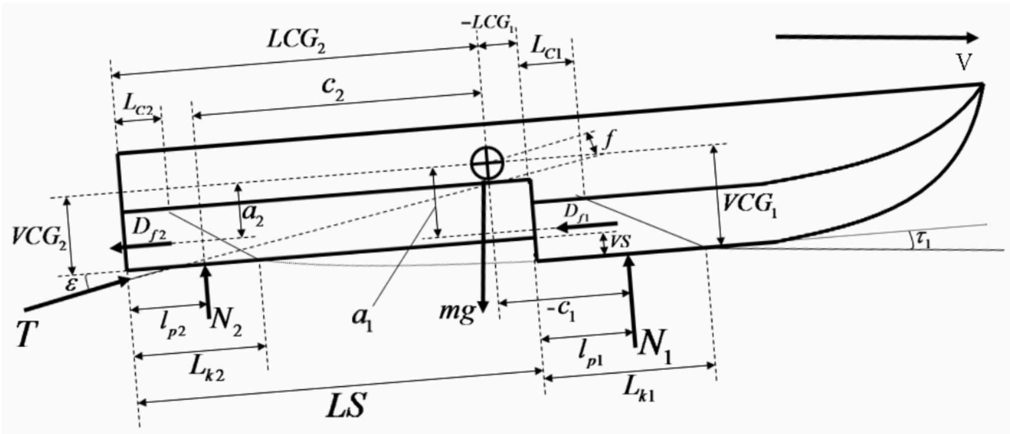

Figure 5.3 - Steady state planing hull (As presented in (Svahn, 2009)**)**

The steady state force and moment equations are:

$$Vertical\ Force: \quad N_1 cos\tau_1 + N_2 cos\tau_2 + Tsin(\tau + \epsilon) - mg - D_{f1} sin\tau_1 - D_{f2} sin\tau_2 = 0 \tag{5.9}$$

$$Horizontal\ Force: \quad Tcos(\tau + \epsilon) - N_1 sin\tau_1 - N_2 sin\tau_2 - D_{f1} cos\tau_1 - D_{f2} cos\tau_2 = 0 \tag{5.10}$$

$$Moment: \quad (N_1 * c_1) + (N_2 * c_2) + (D_{f1} * a_1) + (D_{f2} * a_2) - (T * f) = 0 \tag{5.11}$$

The shape of the wake of the forehull is modelled using Savitsky's Wake Equations (Savitsky and Morabito, 2010). These equations allow the freesurface elevation at the centerline and the quarter beam line to be calculated, and thus the intersection of the forebody flow the afterbody, the wetted area and forces acting upon the afterbody. A straight line connecting the two intersection points forms the local mean water level line, as detailed in Figure 5.4. Despite the difference caused by the shape of the wake, it is assumed that the fluid behaves in the same manner when hitting the afterbody as it does for the forebody.

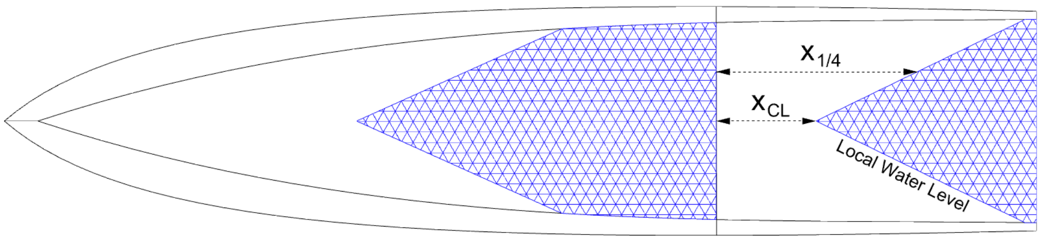

Figure 5.4 – Intersection of forebody flow with the afterbody (Adapted from (Svahn, 2009)**)**

Local deadrise, beam and trim are then introduced to orient the afterbody with the wake in a way that represent it intersecting calm level water so that Savitsky equations to be used to calculate the forces. The wake of the forehull is a V-shaped hollow that flattens out as the distance aft of the step increases. As such the afterbody is no longer intersecting with level water and the deadrise between the hull and the water surface is reduced. The term 'local deadrise' is introduced to account for this new orientation. As the wake shape varies with distance aft of the step a mean value is taken at the quarter beam line. In Savitsky's method beam is taken as the horizonal projection of the hull onto the level water line. Once again due to the shape of the wake the term local beam is introduced, which is the projection of the hull onto the inclined water surface subject to the local deadrise. The local deadrise and beam are detailed in Figure 5.5

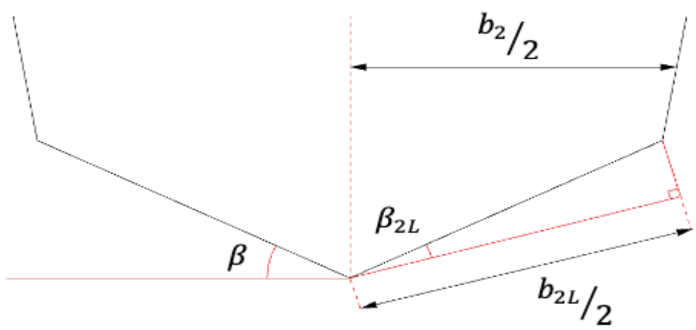

Figure 5.5 – Local deadrise and local beam (Adapted from (Svahn, 2009)**)**

A final local value for the trim must be introduced to account for the fact that the lift force is calculated perpendicular to the water surface as it meets the aft hull, while the wake this is no longer level, as shown in Figure 5.6. The mean value is once again taken at the quarter beam line.

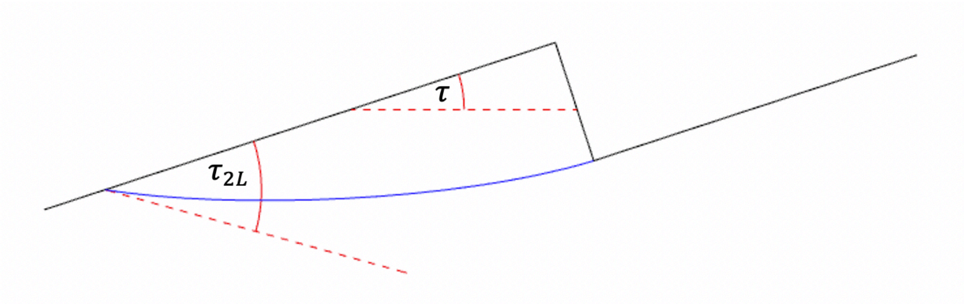

Figure 5.6 – Local trim (Adapted from (Svahn, 2009)**)**

Having determined the wetted areas of the fore and afterbody's and introduced local values to orient the afterbody in such a way that Savitsky's method is applicable, the forces on each surface are calculated. Following this, the weight distribution must be solved iteratively by locking the trim and varying the vertical position of the vessel until the vertical force equilibrium equation is satisfied. This is done through the introduction of the term Ω, which is the percentage of weight carried by the forebody. To initiate the process an initial guess that 60% of the total weight being supported by the forebody is made. The following equations are then introduced to determine the lift of the forebody surface, the vertical equilibrium, and a new value of weight distribution should the vertical equilibrium not be less than a given tolerance.

$$F_{L1} = \Omega\mathrm{mg}\,, \quad \text{where } 0 \leq \Omega \leq 1 \qquad \textbf{(5.12)}$$

$$F_{L1} + F_{L2} - mg = \gamma \qquad \textbf{(5.13)}$$

$$if\ |\,\gamma| > tol\,, \quad \Omega_{\mathrm{n+1}} = \frac{1}{2} + \frac{F_{L1} - F_{L2}}{2mg} \qquad \textbf{(5.14)}$$

Svahn's Method sets a trim and then calculates the forces acting on the forebody using Savitskys Method. The intersection of the afterbody with the forebody wake is then determined using Savitsky's Wake Equations. The local values as introduced by Svahn then allow the calculation of the forces on the afterbody. The weight distribution is iterated until vertical equilibrium is reached. Following this the pitching moment equation is solved. A new trim is then set, and the procedure is repeated until a positive and negative pitching moment are found, and then the final trim and resistance values are determined through linear interpolation. The computational procedure as described is illustrated in Figure 5.7.

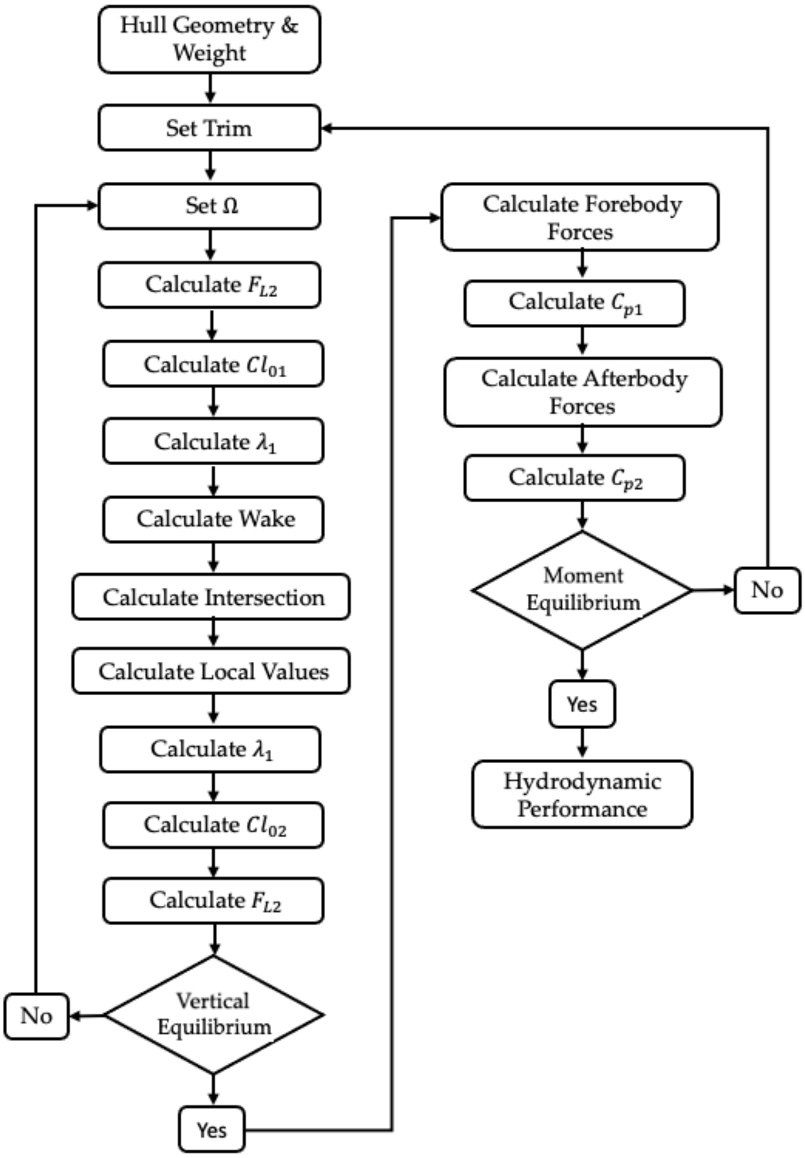

Figure 5.7 - Computational procedure for Svahn's Method

5.2.3 Extension for Double Stepped Hulls

To develop a method to model a hull with two steps the same logic employed by Svahn's method is applied to the additional planing surface. Local deadrise, beam and trim will be used to orient the midbody and the afterbody with the wake in a way that represent it intersecting calm level water so that Savitsky equations to be used to calculate the forces on both these surfaces.

The steady state force and moment equations for hulls with more than one step (where n is the number of steps) become:

$$Vertical\ Force: \quad \sum_{i=1}^{n} N_{\mathrm{n}} cos\tau_{\mathrm{n}} + Tsin(\tau + \epsilon) - mg - \sum_{i=1}^{n} D_{f\mathrm{n}} sin\tau_{\mathrm{n}} = 0 \tag{5.15}$$

$$Horizontal\ Force: \quad Tcos(\tau + \epsilon) - \sum_{i=1}^{n} N_{\mathrm{n}} sin\tau_{\mathrm{n}} - \sum_{i=1}^{n} D_{f\mathrm{n}} cos\tau_{\mathrm{n}}\ 0 \tag{5.16}$$

$$Moment: \quad \sum_{i=1}^{n} (N_n * c_n) + \sum_{i=1}^{n} (D_{fn} * a_n) - (T * f) = 0 \tag{5.17}$$

5.3 Modified & Extended Mathematical Models

Having developed a more comprehensive knowledge of the flow characteristics under both the single and double stepped hulls, as well as a detailed understanding of the composition of the wetted area in Chapter 4 it is possible to improve Svahn's Method for single stepped hulls and extend it for application with double stepped hulls. This section will detail the modifications to Svahn's Method for single stepped hulls and the logic behind each of them. It will then go on to discuss how this is extended to application for a double stepped planing hull. The results will be presented and discussed in the following section.

5.3.1 Single Step

Two key aims set out to enhance Svahn's Method for the rapid evaluation of single stepped hulls:

- **Improve** the accuracy of the model through the application of knowledge developed from the evaluation of the numerical result
- **Develop** the method so that it can cope with a hull operating in a chine's dry condition

This section will set out each of these is achieved, initially developing a methodology that will allow Svahn's method to deal with the chine's dry condition for the afterbody. Following this a methodology for the chine's dry condition for the forebody will be put forward. Additionally, knowledge of the flow and wetted area of the afterbody developed in Chapter 4 will be implemented to enhance the accuracy. The results of each of the modifications will then be evaluated and discussed.

5.3.1.1 Modification to the Wave Rise Calculation

The first change to be implemented was in relation to the calculation of the wetted area of the afterbody. In Svahn's method the difference between the wetted keel and wetted chine, or L1, is calculated using the methodology put forward in (Savitsky, 1964), and presented in Equation (4.4). In Section 4.5.1.3 this method was shown to not be applicable for cases where the afterbody is intersecting with the wake of the forebody. Instead, it was found that setting L1 to be equal to the intersection of the chine with the forebody wake (L2) and neglecting to add any wave rise was more appropriate. This finding is confirmed by (Najafi *et al.*, 2019)who showed that the wetted area of the afterbody calculated using the intersection of the forebody flow and not accounting for wave rise produced good corelation with experimental data. As such, Equation 2.09 in (Svahn, 2009) is replaced with Equation (5.18)

$$L_{1_{Aft}} = L_{2_{Aft}} \tag{5.18}$$

The effect of this modification is to reduce the wetted area of the afterbody as calculated for any given condition.

5.3.1.2 Methodology for Chine's Dry Afterbody Conditions

The method presented in (Svahn, 2009) has no means of determining if the spray root of the afterbody crosses the transom. This condition was shown to be highly likely at higher speeds in Section 4.5.1.1. In Svahn's method it is assumed that the wetted area is in the shape of a right trapezoid, and as such the wetted length to beam ratio for the afterbody, λ_2, can be calculated using Equation (5.19).

$$\lambda_2 = \frac{L_{k_2}}{b_2} - \frac{L_{1_{Aft}}}{2b_2} \tag{5.19}$$

If there was a chine's dry condition for the afterbody then $L_{1_{Aft}}$ is larger than L_{k_2}, resulting in the incorrect calculation of λ_2, and in some cases a negative value for λ_2. This introduces inaccuracies into the wetted area calculation, and in cases where λ_2 becomes negative, causes the method to fail. For cases when the afterbody is operating in the chine's dry condition it is proposed to implement the following procedure in place of Equation (5.19):

$$if\ Ls < L_{1_{Aft}} + x_{CL} \tag{5.20}$$

$$L_w = Ls - x_{CL} \tag{5.21}$$

$$\lambda_2 = \frac{L_w}{2b_2} \tag{5.22}$$

This accounts for the fact that the wetted area is for the afterbody in the chine's dry planing condition is in the shape of a triangle, with a wetted length that stops at the transom.

5.3.1.3 Methodology for Chine's Dry Forebody Conditions

Savitsky's method does not take into consideration the chine's dry condition as the empirical equations were developed using experimental data for which the hull was in a chine's wet condition. As no alternate approach is available it is assumed that the equations are applicable for the chine's dry condition, however as pointed out by (Svahn, 2009) there may be a loss of accuracy due to this assumption.

The proposed methodology that accounts for the chine's dry forebody condition does so through the inclusion of the additional side wetting of the afterbody, where it intersects with the undisturbed level water surface. This component of the wetted area is discussed in some detail in Section 4.5.1.1. Svahn's method, like all current mathematical models of stepped hulls, is only capable of modelling the triangular wetted region of the afterbody and does not consider this additional side wetting.

(Savitsky and Morabito, 2010) note the presence of side wetting, making the recommendation that such a condition is avoided. The authors reason that this additional wetting is purely accountable to spray, and that the increased wetted area results in increased frictional resistance whilst not contributing to the performance of the hull. Section 4.5.1.1 conducted analysis of the wetted area using CFD as opposed to underwater experimental photographs and able to investigate with considerably more detail. It was found that this additional side wetting contained high pressure regions and contributed to pressure area of the hull, generating lift. The side wetting components form high aspect ratio lifting surfaces and therefore have a low lift to drag ratio. While this is undesirable and is not considered and efficient lifting surface, these areas are not always avoidable as seen in Chapter 4 and pointed out by (Svahn, 2009).

To modify the model so that it is capable of modelling a stepped hull operating in a forebody chines dry condition, calculating the area of the side wetting and including its effects the following procedure is proposed:

1. Determine the vertical depth of step edge, at the keel, below water surface

$$depth = \left(\frac{(\lambda_1 b_1) + (b_1 \tan\ \beta_1)}{2\pi tan\tau}\right) sin\tau \qquad \textbf{(5.23)}$$

2. Project the depth onto the step edge

$$d = \frac{depth}{\cos\tau} \quad \textbf{(5.24)}$$

3. Determine the wetted beam at the first step

$$b_{wave\_rise} = \frac{2d}{tan\beta_1} * \frac{\pi}{2} \quad \textbf{(5.25)}$$

4. If $b_{wave\_rise} < b_1$ then the forehull is in a chine dry condition. Determine the beam of the side wetting

$$b_{ad} = b_1 - b_{wave\_rise} \quad \textbf{(5.26)}$$

5. Determine the intersection of the undisturbed free surface with the afterbody at a longitudinal taken where the spray root crosses the step

$$x_{int} = \frac{Vs}{tan\tau} \quad \textbf{(5.27)}$$

6. Determine the L1 value of the additional wetting

$$L_{1_{ad}} = \frac{b_{ad}}{\pi} * \frac{tan\beta_2}{tan\tau} \quad \textbf{(5.28)}$$

$$if\ L_{1_{ad}} + x_{ad} > Ls \qquad L_{1_{ad}} = ls - x_{ad} \quad \textbf{(5.29)}$$

7. Determine the wetted length of the additional wetting at the longitudinal taken where the spray root crosses the step

$$L_{ad} = Ls - x_{ad} \quad \textbf{(5.30)}$$

8. Determine the length to beam ratio of the side wetting

$$\lambda_{ad} = \frac{L_{ad}}{b_{ad}} - \frac{L_{1_{ad}}}{2b_{ad}} \quad \textbf{(5.31)}$$

Initially it was attempted to calculate the lift of the side wetting following Savitsky's Empirical Equations. It was found that the narrow beam (b_{ad}) lead resulted in wetted length to beam ratio's (λ_{ad}) that were out with the range of the equations and the results were unrealistic. For cases in which b_{ad} is large, and λ_{ad} falls within the range of Savitsky's Empirical Equations it is recommended that they are employed to calculate the lift. For other cases, an alternate recommendation is proposed, making the assumption that the side wetting generates an equivalent lift per unit beam as the triangle region, and as such lift can be calculated as follows:

$$Lift_{ad} = \frac{b_{ad}}{b_2} * F_{l_2} \tag{5.32}$$

The calculated lift is included in the vertical equilibrium equation to determine the sinkage for a given trim. Once vertical equilibrium is achieved and the algorithm solves the force loop, the frictional resistance of the side wetting may be calculated following the same procedure as for the triangle region, as outlined by Savitsky's Method. This force can then be included in the moment equilibrium equation.

5.3.1.4 Results

This section presents the results of each of the modifications in order to evaluate the impact upon accuracy and to validate the proposed changes. The full analysis and discussion of the results generated by the final method is presented in Section 5.4 later in this chapter. In this section the annotation represents the following:

- Svahn –Svahn's original method as outlined in (Svahn, 2009)
- Svahn Mod 1 – Modification to the wave rise calculation of the afterbody as outlined in Section 5.3.1.1 and methodology to for chine's dry afterbody as outlined in Section 5.3.1.2
- Svahn Mod 2 – Svahn Mod 1, with the methodology for chine's dry forebody conditions implemented as detailed in Section 5.3.1.3

The resistance as calculated by each of the mathematical models for Hull C1, as tested by (Taunton, Hudson and Shenoi, 2010) is presented by Figure 5.8 while the trims are presented by Figure 5.9.

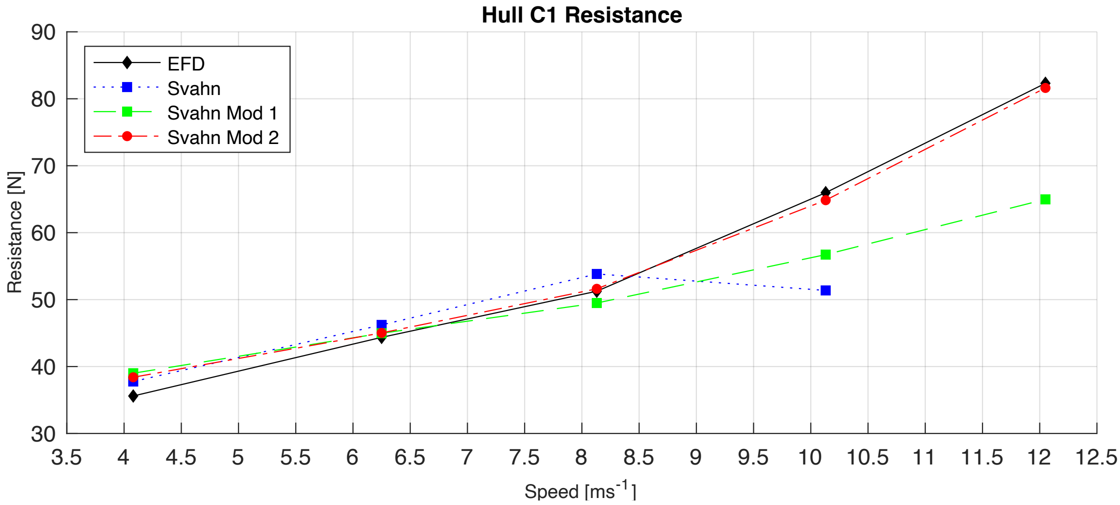

Figure 5.8 – Resistance comparison of modified Svahn Models

Svahn's original method is seen to be accurate in calculating the resistance for the lower speeds, resulting in an average error of 5.10% for speeds up to 8.21ms^{-1}. For the 10.13ms^{-1} case it was inaccurate, while for the 12.05ms^{-1} case it failed. The reason for this is the fact that for these cases the afterbody is operating in the chine's dry condition, as seen in Figure 4.13 and as discussed Svahn's original method is not capable of resolving this condition. Svahn Mod 1 is seen to have rectified this failing and is capable of generating results for the whole speed range, showing the chines dry afterbody methodology to have been successful. Additionally, Svahn Mod 1, calculates a lower resistance than the original Svahn method, increasing the accuracy for the 6.25 and 8.11ms^{-1} cases and indicating that the changes to the calculation of $L_{1_{Aft}}$ enhanced the model. For the higher speeds where side wetting was seen to occur this model underpredicts the resistance considerably. When the methodology for the chines dry forebody condition is implemented to account for the lift and resistance of the side wetting components, as seen in Svahn Mod 2, the accuracy for the higher speed cases is seen to improve significantly, and the model may be considered accurate. The average error in resistance of Svahn Mod 2 is 2.50%. The improvement in the accuracy due to the inclusion of the side wetting shows how vital it is to accurately model the correct composition of the afterbody wetted area.

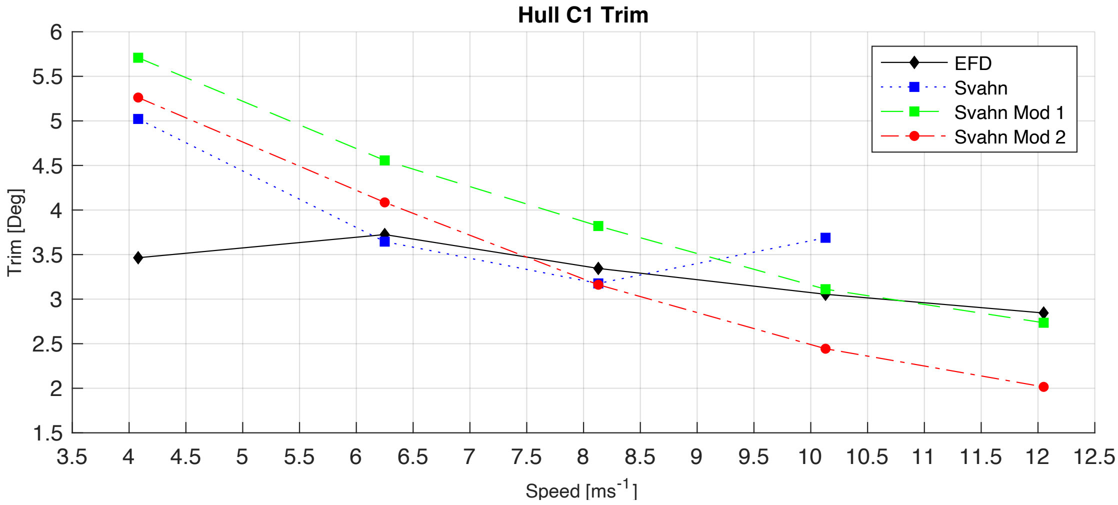

Figure 5.9 – Trim comparison of Modified Svahn models to EFD (Taunton, Hudson and Shenoi, 2010)

All the models struggle to accurately calculate the attitude of the stepped hull. The results for the 4.05ms^{-1} case should be treated with caution as it has been shown that the Savitsky Wake Equations are not accurate for this case. It is seen that the error in trim is linked to whether the wake equations under or over predict the ventilation length aft of the step. In cases where the ventilation length is overpredicted, the aft wetted area is under predicted, and as a result the trim is overpredicted to increase the aft wetted area. It is also seen that for the two cases for which side wetting exists Svahn Mod 2 underpredicts the trim. This would suggest that the afterbody is generating too much lift, and may be as a result of the assumption made in the lift calculation for the side wetting as outlined in Equation (5.32). Unfortunately, no other means of calculating this are available, however reducing the proportion of assumed lift may improve the accuracy. This is highlighted as a topic for future work.

Over the course of this section both the accuracy and range of applicability of Svahn's original model have been enhanced significantly, removing its limitations and allowing it to consider a single stepped hull in all possible operating conditions. This has been achieved through in-depth analysis of the flow under a stepped hull, made possible through numerical simulation. The application of the knowledge and understanding developed has created a model that runs in seconds and is capable of modelling a single stepped hulls resistance across a broad speed range with an average error of 2.50%.

5.3.2 Double Step

Following the successful modification of Svahn's Method extending its range of applicability and increasing its accuracy, the same logic is applied to develop a model for double stepped planing hulls. The same methodology is followed, utilising the enhanced knowledge of flow characteristics and wetted areas of a double stepped hull, developed from the analysis of CFD results.

The strategy proposed to develop the Double Stepped Model follows the same logic as Svahn's Method in applying Savitsky's Empirical Equations to multiple planing surfaces. The methodology that is applied aft of the step in Svahn's method is repeated to account for the surface aft of the second step. The wetted area of each planing surface is determined, and the local values proposed by Svahn are calculated to orient the surface to the incoming wake in a manner that allows the forces be calculated using Savitsky's Empirical Equations. The equilibrium equations for the vertical forces and the pitching moment are then solved in an iterative procedure to determine the equilibrium position. The full procedure with individual equations are not detailed in this section, as it is not a complex process to add a duplicate set of equations to Svahn's method to account for the second lifting surface. Instead, the novel aspects of the proposed model will be highlighted and discussed. Additionally, the computational procedure will be presented.

In the literature the examples of semi-empirical models for the performance prediction of a double stepped planing hull only account for the triangular wetted regions and rely upon the linear wake assumption to determine where the flow intersects with the midbody and afterbody. The analysis conducted in Section 4.5.2.2 showed that the Linear Wake Assumption was sufficient in modelling the flow aft of the midbody due the small wetted area of the midbody. It also determined that the

Savitsky Wake Equations were far more suited in modelling the forebody flow, as the large wetted area meant that the flow was fully developed. As such, the proposed model will model the flow of the forebody as it separates at the first step using the Savitsky Wake Equations, while the LWA will be used to model flow as it separates at the second step.

The analysis of the numerical data showed the composition of the wetted area of a double stepped planing hull to be complex in nature, comprising of several distinct portions arising from intersections with individual components of flow. Unless all three lifting surfaces were operating in the chine's wet condition, which was shown to only occur at low speeds, modelling the wetted areas as only the triangular region is an inadequate oversimplification. The importance in correctly modelling the distinct wetted areas that occur due to the chine's dry condition was highlighted by the significant increase in accuracy of the Svahn Mod 2 model in Section 5.3.1.4. As such, a novel procedure is proposed to determine each of these wetted areas so that the forces acting upon each may be determined. This procedure became complex to implement with several variables, but is necessary to accurately model the wetted surface of the double stepped planing hull.

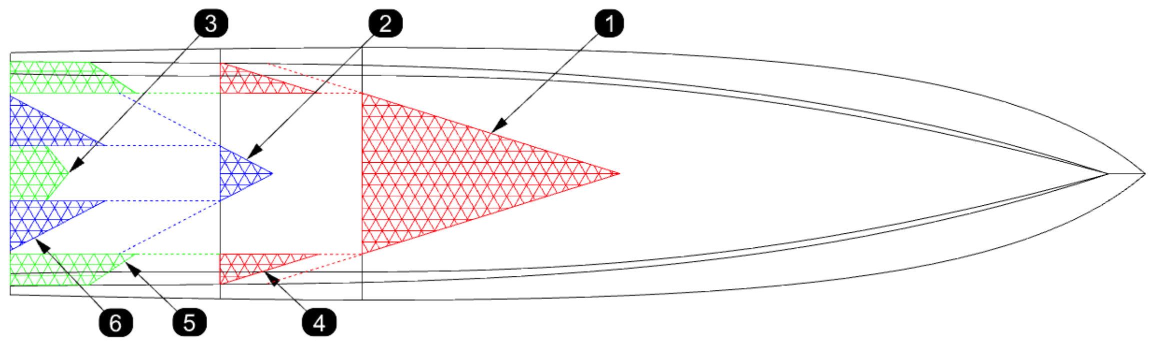

Figure 5.10 – Wetted area composition of a double stepped Hull (Areas defined in following section)

The possible distinct wetted portions of the hull are detailed in Figure 5.10. These can occur in a number of combinations depending on the condition of the hull. The wetted portions on the afterbody may arise from intersection with either the forebody flow or the midbody flow, further complicating matters. The computational procedure that was developed to calculate each of these is presented in Figure 5.11.

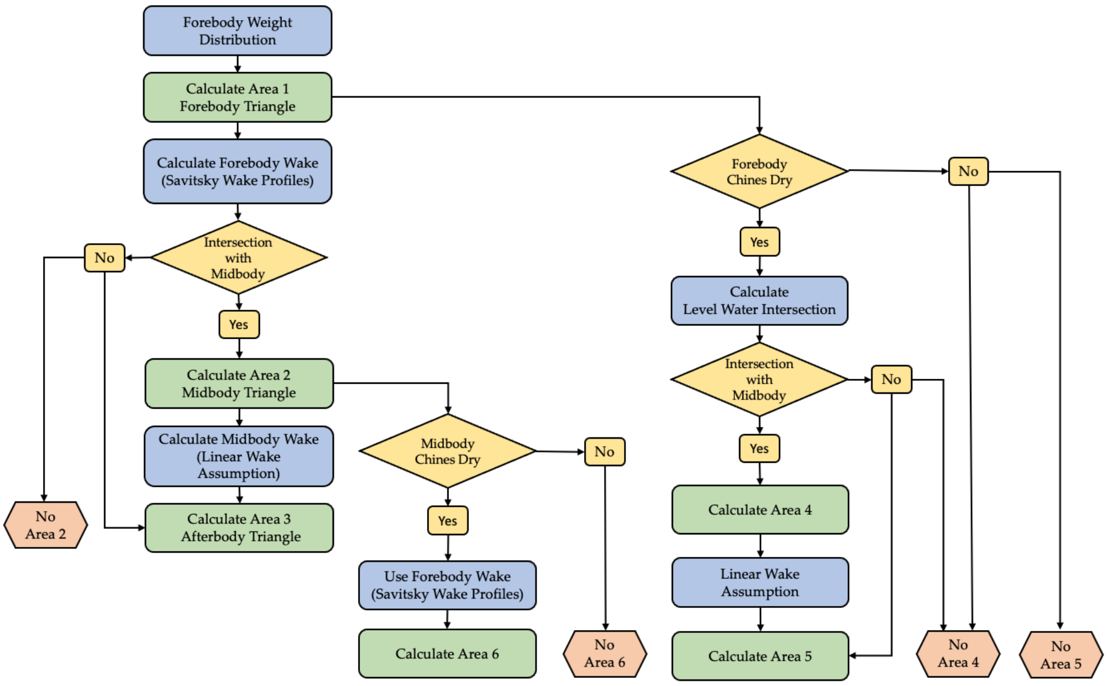

Figure 5.11 – Wetted area calculation procedure of a double stepped hull

The following section discusses the procedure outlined in Figure 5.11 and provides further details. It should be noted that instead of calculating the physical wetted area, the calculation determines the wetted length to beam ratio, λ. This is in effect the aspect ratio of the lifting surface and may be used to determine the wetted area using Equation (5.33).

$$A_{WS} = \lambda b^2 \qquad \textbf{(5.33)}$$

Area 1: This wetted area is due to the intersection of level water surface with forebody and is calculated in the same manner as outlined by Svahn's Method for the forebody.

Area 2: This wetted area is due to the intersection of forebody flow with the midbody. The same procedure as outlined for single stepped hulls is followed, however this is modified to account for the possibility that the forebody flow does not intersect with the midbody. As previously stated, the Savitsky Wake Equations are used to model forebody flow.

1. Calculate the centreline freesurface elevation profile using Savitsky's Wake Equation's
2. Calculate if it intersects with the midbody
3. If <u>NO</u> then Area 2 does not exist, skip Area 3
4. If <u>YES</u> calculate the quarterbeam intersection point
5. Calculate L1 using the CL and QB intersection points. Assume no wave rise as detailed previously in the Single Step Model.
6. Calculate λ_2, applying the chine's dry methodology as outlined in the modified Svahn model if applicable

<u>Area 3:</u> This wetted area is due to either the intersection of forebody or midbody flow with the afterbody:

- If Area 2 does exist, the intersection is with midbody flow. Employ the LWA
- If Area 2 does not exist, the intersection is with midbody flow. Employ the Savitsky Wake Equations
- Once the points of intersection for the centreline and quarterbeam are determined is possible to calculate λ_3
- It is assumed that there is no wave rise
- If the spray root crosses the transom, then the chine's dry methodology is applied

<u>Area 4:</u> If the forebody is operating in the chine's dry condition, then this component will exist if the midbody intersects with the water surface at the longitudinal location where the spray root crosses the first step. The procedure is the same as for the additional side wetting that is added to the Svahn Mod 2 Model.

Area 5: This wetted area occurs if the forebody is in the chine's dry condition. If Area 4 is present, then this is due to the flow aft of the side wetting. If this is the case, then the Linear Wake Assumption is used to determine the points of intersection. If Area 4 does not exist, then this is due to the intersection of afterbody with the level water surface at the longitudinal location where the spray root crosses the first step.

Area 6: This wetted area occurs if the midbody intersects with the forebody flow and is in the chine's dry condition. Area 6 is causes by the intersection of the forebody flow with the afterbody, between the chine and the longitudinal location where the spray root crosses the second step.

Once all the wetted area components have been established, each is treated as an individual, joined lifting surface. The forces and moments attributable to each are calculated separately and then applied to the vertical equation and the pitching moment equation to determine the equilibrium position of the hull, and its total resistance. The lift for each area is determined as follows:

- **Area 1:** Svahn's Weight Distribution – Equation (5.12)
- **Area 2:** Savitsky Empirical Equations – Equation (5.4) & (5.5)
- **Area 3:** Savitsky Empirical Equations – Equation (5.4) & (5.5)
- **Area 4:** Assumed the side wetting generates the equivalent lift to beam ratio as the triangle region – Equation (5.12)
- **Area 5:** Assumed the side wetting generates the equivalent lift to beam ratio as the triangle region – Equation (5.12)
- **Area 6:** Savitsky Empirical Equations – Equation (5.4) & (5.5)

The frictional drag for each surface is calculated using the standard ITTC 1957 friction line, while the centre of pressure of each surface is found using Savitsky's Empirical Formula. The computational procedure that that is followed is outlined in Figure 5.12. The results of this method will be presented and analysed in the following section.

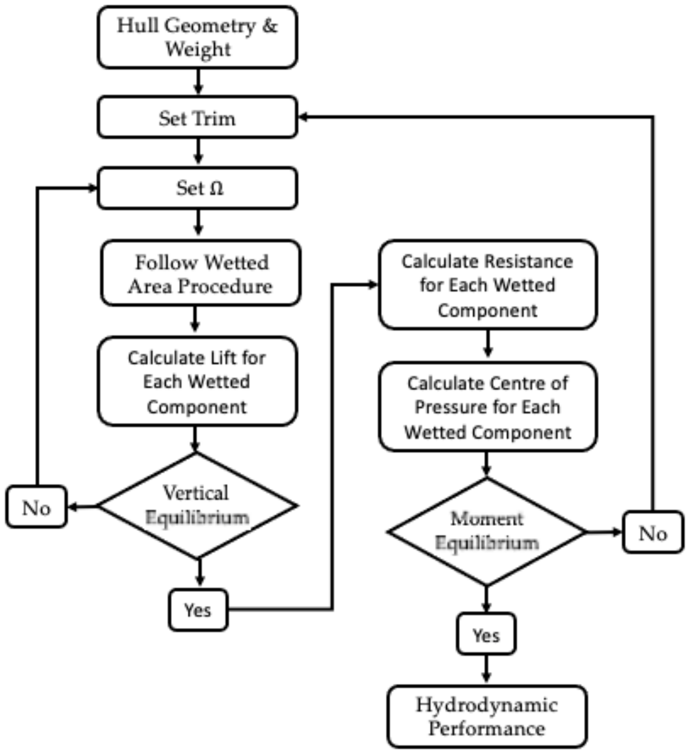

Figure 5.12 - Computational Procedure for Proposed Double Step Method

As the problem being modelled by the mathematical model became more complex due to the addition of steps, so too did the MATLAB scripts that were developed to solve them. The script that was written for Savitsky's method contained 400 lines, Modified Svahns Method contained 600 lines, and the Proposed Method for double stepped hulls contained 1000 lines of code. All three MATLAB programs were capable of calculating the resistance and trim of in under 5 seconds, which is considerably faster than the 12 hours required to complete a CFD simulation.

5.4 Results

This section details the results of the semi-empirical methods for the stepped, single stepped and double stepped planing hull models as experimentally tested by (Taunton, Hudson and Shenoi, 2010) and numerically modelled in Chapter 3.

5.4.1 Hull C

This section presents the results of Savitsky's Method as applied to the unstepped model, Hull C.

Savitsky's Method was coded in MATLAB, and benchmarked against the case study presented in (Savitsky, 1964), for barehull resistance to ensure there were no bugs in the developed script. The results were found to be in agreement with each other, as presented in Table 5.1, confirming that the method had been programmed correctly. The 0.14% variation in resistance is due to the compounded effects of rounding errors.

Table 5.1 - Benchmarking Developed MATLAB Code of Savistky's Method

	Resistance [N]	Trim [Deg]
(Savitsky, 1964)	40456.58	~ 2.3
MATLAB Code	40399.03	2.26

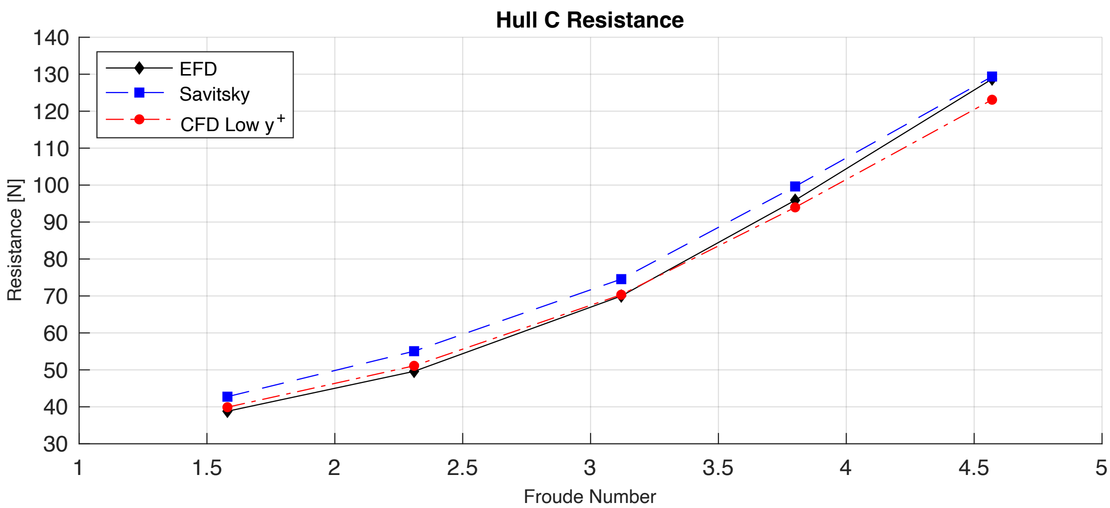

Figure 5.13 - Hull C resistance

As can be seen in Figure 5.13 Savitsky's Method was capable of modelling the resistance of the unstepped hull, with the accuracy improving with speed. The average comparison error with respect to EFD was 6.42%, with a range of 0.52% - 11.00%. Although less accurate than the low y+ CFD approach, the results were in line with the accuracy of the high y+ CFD simulation, and of other numerical results as reported in the literature, as seen in Table 2.1

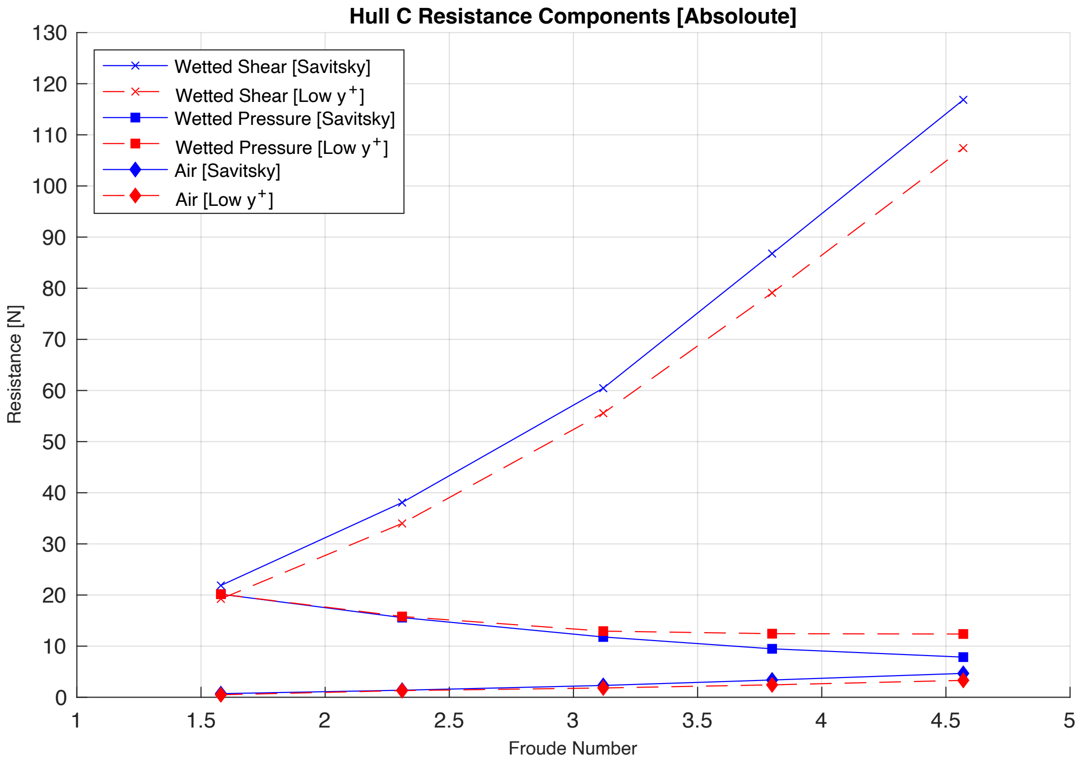

Figure 5.14 - Hull C resistance components (absolute)

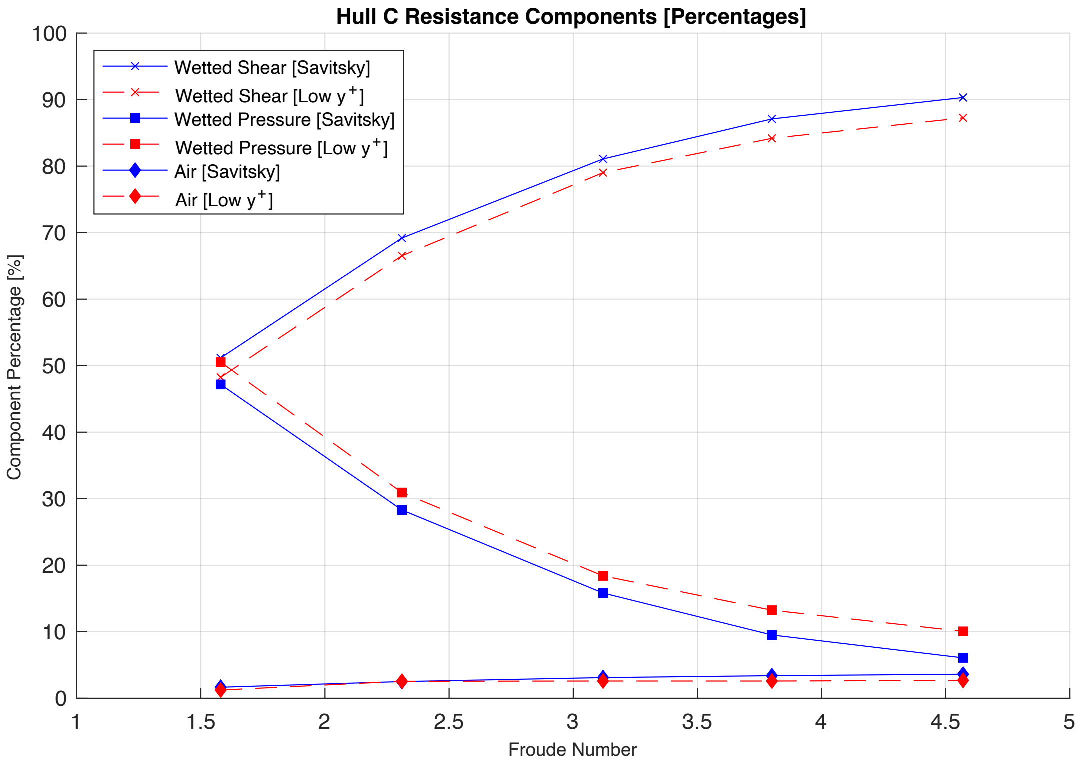

Figure 5.15 - Hull C resistance components (percentage)

As Savitsky's Method systematically calculates each resistance component it is possible to compare these to the numerical values obtained in Chapter 3. It is seen in Figure 5.14 that Savitsky's method has a tendency to overpredict the frictional resistance and underpredict the pressure resistance. This finding was also seen in the results of (Sukas *et al.*, 2017), who used Schoenherr's formula to calculate the frictional resistance, yet still determined that the frictional component was too large across the entire range of Froude numbers studied. The aerodynamic resistance model as presented by (Savitsky, DeLorme and Datla, 2007) shows good correlation with the numerical results. When the resistance components' percentages of the total resistance are examined in Figure 5.15, it is seen that the overcalculation of frictional resistance is consistent in across the whole speed range, with an average value of 2.71%. The undercalculation of pressure resistance is also to be relatively constant, with an average value of 3.25%

The frictional resistance in Savitsky's Method is calculated using the ITTC 1957 friction correlation line, which is based upon Hughes version of a turbulent flat plate friction line, developed from experimental data (ITTC, 2011). This may have overpredicted the frictional component as the Hull C model had a wetted length of 1.27 – 1.45m, and as such the portion of laminar flow will make a relatively larger portion of the flow.

The pressure component is determined using equation (5.7), which is seen to depend entirely upon the trim of the vessel. As is seen in Figure 5.16, Savitsky's method was found to overpredict the trim of Hull C. It is this overprediction in trim that resulted in the underprediction of the pressure component.

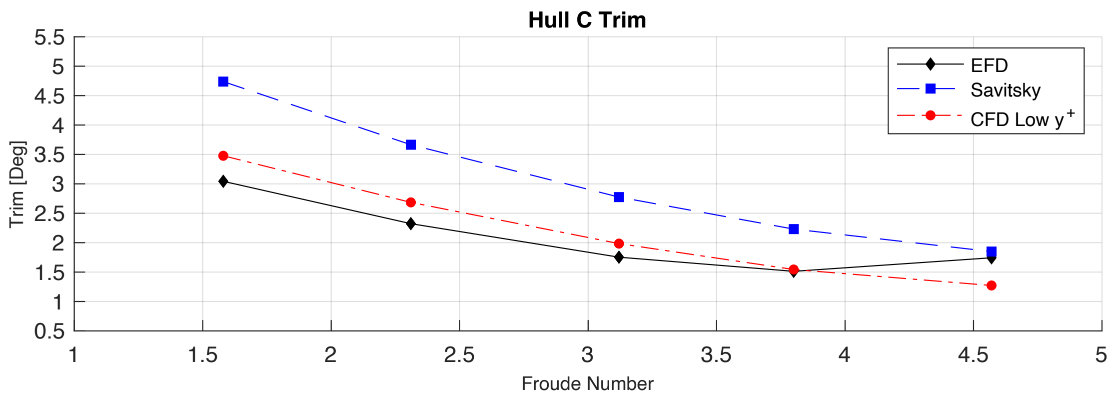

Figure 5.16 - Hull C trim

It was found that the trim calculation was less accurate, resulting in an average error of 45.04%. As the thrust line passed through the Centre of Gravity due to the experimental set up only two forces applied a moment to the hull. These are the lift force acting at the centre of pressure, and the frictional resistance force acting on the wetted hull. Of these four variables, the lift force and the location of the wetted area are fixed. This indicates that the overcalculation of trim is accountable to errors in either the frictional resistance, or the location of the centre of pressure. It is known that Savitsky's method as applied to this case overestimates the frictional resistance, but it is also very likely that the location of the centre of pressure causes the error in trim. It was seen previously that numerical methods were very sensitive in the trim calculation due to changes in the pressure acting upon the hull. This shows the large effect that small changes may have on the trim of a planing hull.

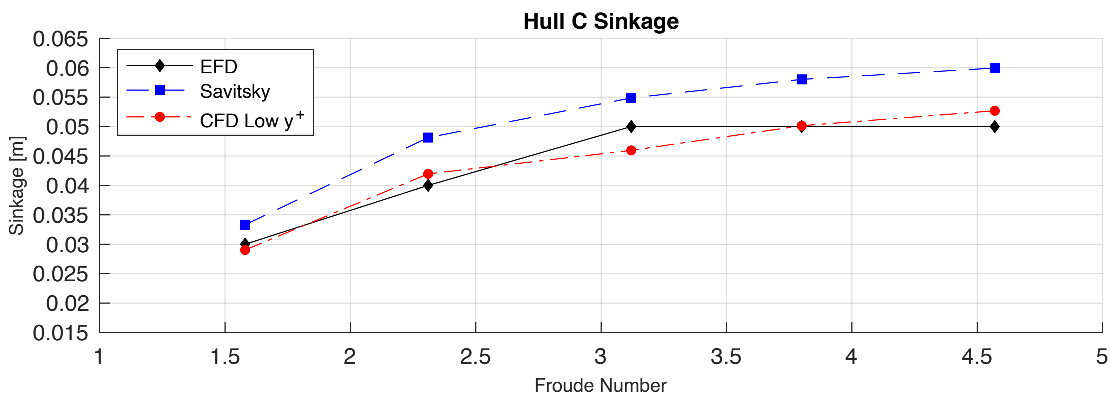

Figure 5.17 - Hull C Sinkage

The sinkage of Hull C is presented in Figure 5.17, where it is seen that there is an average error of 15.41%. The trim as calculated using Savitsky's method can be seen to follow the trend of the CFD results, once again indicating that the experimental data is subject uncertainty introduced through the precision of measurements, as discussed in Section 3.5.1.2. The sinkage has a tendency to be overpredicted, which is linked to the overprediction in trim. Lifting surfaces operating with larger angles of attack produce more lift. As the trim is larger than it should be, the hull is producing a larger quantity of lift and as such it rises further out of the water to reach its equilibrium position.

5.4.2 Hull C1

While the results of the modified Svahn's methods are presented previously in Section 5.3.1.4, the purpose of this was to verify the modifications that were implemented, and the model was shown to be a significant improvement over Svahn's original model. In the present section the results of Svahn Mod 2, which will from here on be termed the Modified Svahn Method, are discussed in more depth and analysed in a manner similar to Savitsky's method in Section 5.4.1.

It should be noted that before any modifications were implemented, the Svahns original model was coded in MATLAB and benchmarked against the case study presented in (Svahn, 2009). The results were found to be in agreement with each other, as presented in Table 5.2, confirming that the method had been programmed correctly.

Table 5.2 - Benchmarking Developed MATLAB Code of Svahn Method

	Resistance [N]	**Trim [Deg]**
(Svahn, 2009)	5229	~ 4.4
MATLAB Code	5226.15	2.26

Following the confirmation that Svahn's Method had been correctly programmed, the modifications as outlined in Section 5.3.1 were applied. The results of the

Modified Svahn Method are presented in Table 5.3, while they are presented graphically in Figure 5.18 and Figure 5.19.

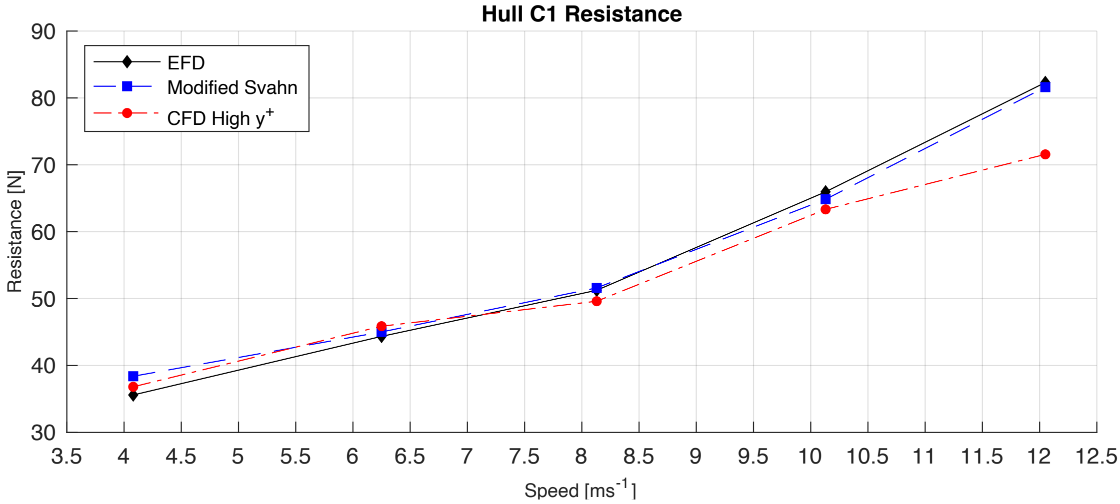

Figure 5.18 - Hull C1 resistance

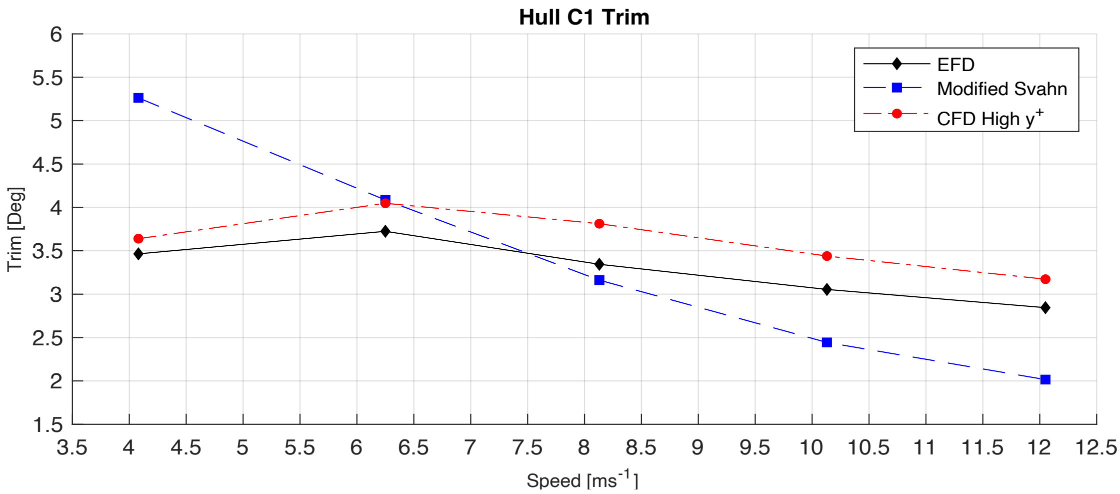

Figure 5.19 - Hull C1 trim

Table 5.3 – Results of Modified Svahn model

Speed [ms^{-1}]	4.08	6.25	8.13	10.13	12.05
Taunton Exp Resistance Hull C1	35.60	44.36	51.25	65.97	82.31
Mod Svahn Resistance [N]	38.40	45.02	51.61	64.85	81.62
Mod Svahn Resistance Error	7.86%	1.49%	0.70%	-1.70%	-0.84%
Taunton Exp Trim Hull C1	3.46	3.72	3.34	3.05	2.84
Mod Svahn Trim [Deg]	5.26	4.09	3.16	2.44	2.02
Mod Svahn Trim Error	52.02%	9.95%	-5.39%	-20.00%	-28.87%

In Figure 5.18 and Figure 5.19 it is seen that the developed model is least accurate at modelling both the resistance and trim for the slowest speed case. The Savitsky Wake Equations were previously shown to be inaccurate for this slow speed as the speed coefficient was significantly below the lower limit of applicability for the equations. These equations determine the intersection of the forebody flow with the afterbody, and thus the afterbody wetted area. The effects of calculating these factors incorrectly is shown to be significant by this slow speed case. Caution is advised when using either the Savitsky Wake Equations, of the Savitsky Empirical Resistance Equations when out with their ranges of applicability. The further from their accepted ranges they are applied, the greater the loss of accuracy will be.

The average resistance error of the modified Svahn method was 2.50%, which was less than the 6.42% error of Savitsky's Method when applied to the Hull C. The average trim error for the Modified Svahn Method was 23.24%, or 16.05% when the $4.05ms^{-1}$ case is excluded. This is considerably less that the 45.04% established for Savitsky's method when applied to a Hull C. This increase in accuracy is possibly due to the fact that lift is generated by multiple wetted surfaces for the stepped hull. If there are inaccuracies introduced through the empirical equations for the centre of pressure as proposed as previously suggested, the fact these surfaces are smaller means that there is a smaller absolute error in the calculated centre of pressure in comparison to the absolute error introduced for the single, considerably larger wetted surface of the unstepped hull. As such, the centre of pressures as calculated for the stepped hull are each closer to the physical locations, and the equilibrium trim will be more accurate, as is seen in the results.

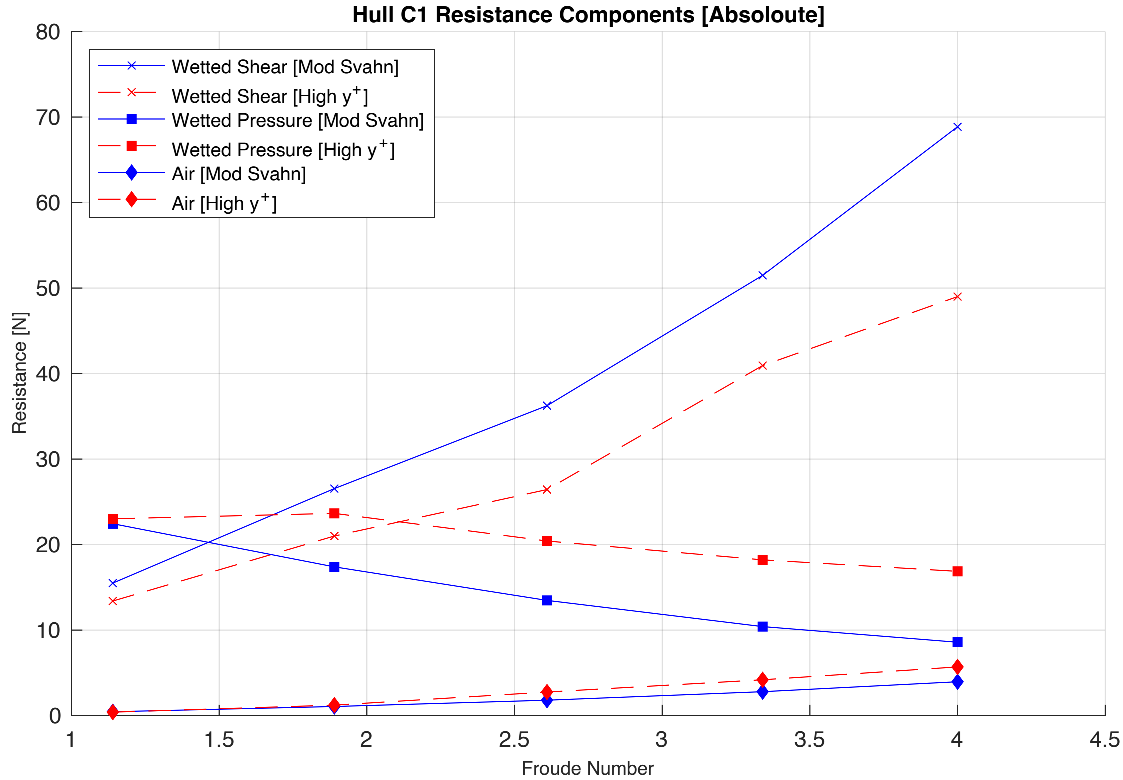

Figure 5.20 - Hull C1 resistance components (absolute)

As with Savitsky's Method, the Modified Svahn's Method systematically calculates each resistance component, so it is possible to compare these to the numerical values obtained in Chapter 3. These are plotted on Figure 5.20, where it is seen that the Modified Svahn Method has a tendency to overpredict the frictional resistance and underpredict the pressure resistance. This trend was also apparent for Savitsky's method previously; however the Modified Svahn Method is subject to a greater level of error.

Both models utilis the same method of calculating pressure resistance, so it would be logical that the error due to this should be similar. Instead, it is seen that the Modified Svahn Method has a larger difference between the numerical and semi-empirical values. In Section 3.5.2.1.2 it as found that for the same Froude number the stepped hull variant was subject to a larger pressure resistance that the unstepped hull. This was attributed to the fact that the running trim of a stepped hull is larger and pressure resistance is closely linked to trim. The modified Svahn method underpredicts the trim, which leads to this underprediction in pressure resistance.

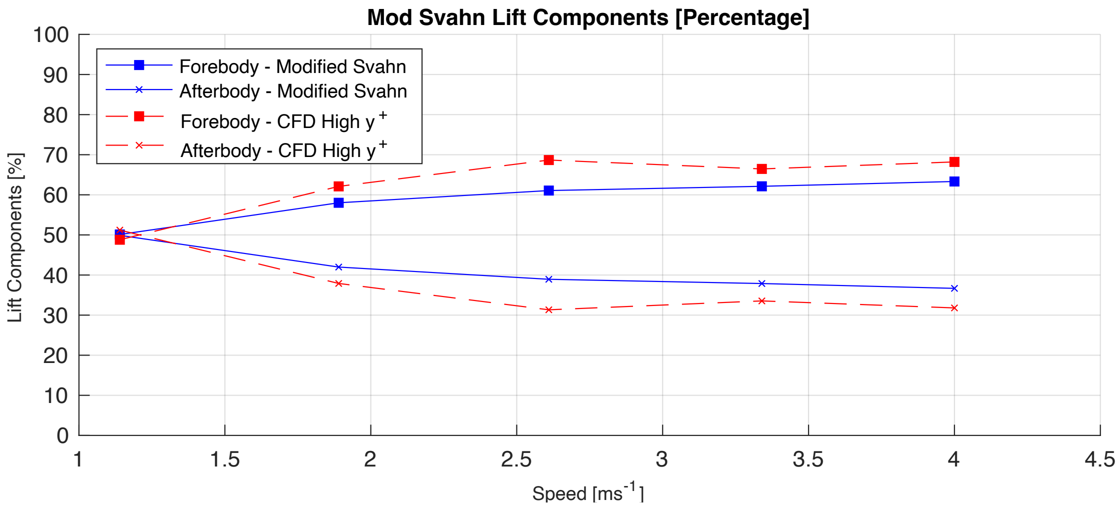

Figure 5.21 – Modified Svahn lift components (percentage)

In addition to the resistance components, it is possible to extract the lift force acting upon the forebody and afterbody from the CFD solution. This is compared to the lift acting upon the two surfaces by the Modified Svahn Model in Figure 5.21. As no experimental data is available it is impossible to say which result is the most accurate, however due to the higher fidelity of the numerical solution this should be the more reliable solution. It is seen that the results of both methods follow the same trends and are in agreement with each other for all speed cases, with a maximum difference of 9.47%. It is established that as the speed increases, the percentage of lift generated by the forebody increase. The split between the two lifting surfaces is seen to be around 65/35. This is in line with the proposal of (Svahn, 2009), who stated that in a normal case it is reasonable to assume that 70% of the weight is carried by the forebody. (Savitsky and Morabito, 2010) suggest this value is approximately 90% and this assumption should be made by the designers of stepped hulls, however this analysis shows that this assumption to be an overprediction.

5.4.3 Hull C2

As the proposed method for the double stepped hull was developed over the course of this study there was no benchmarking of the MATLAB code against previous reports of the model. Instead, it was validated purely against the experimental data of (Taunton, Hudson and Shenoi, 2010). Following the development of the MATLAB script following the methodology outlined in Section 5.3.2, the full range of speed conditions of Hull C2 were modelled. The results and the error of each is presented in Table 5.4.

Table 5.4 – Results of Proposed model

Speed [ms^{-1}]	**4.08**	**5.1**	**6.25**	**7.11**	**8.13**	**9.18**	**10.13**	**11.13**	**12.05**
Taunton C2 EFD Res [N]	36.46	40.07	43.26	46.89	51.01	57.52	65.62	74.96	83.55
Proposed Model Res [N]	50.61	47.68	43.16	46.35	54.11	58.90	67.12	75.03	83.18
Proposed Model Res Error	38.81%	18.98%	-0.22%	-1.14%	6.08%	2.40%	2.29%	0.10%	-0.44%
Taunton C2 EFD Trim [Deg]	3.48	3.82	3.58	3.41	3.22	3.08	2.84	2.73	2.02
Proposed Model Trim [Deg]	9.69	8.31	5.01	4.13	3.16	2.84	2.57	2.34	2.13
Proposed Model Trim Error	178.42%	117.59%	39.90%	21.29%	-1.80%	-7.80%	-9.64%	-14.22%	5.67%

The resistance results for the proposed model are compared to the experimental data, and the CFD results of Section 3.3 in Figure 5.22.

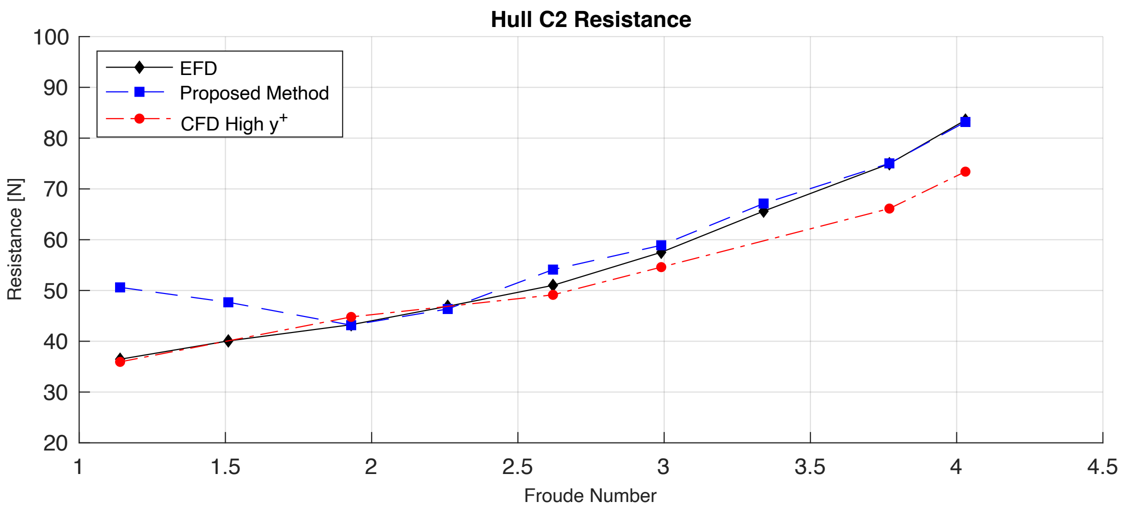

Figure 5.22 - Hull C2 resistance

It can be seen in Figure 5.22 that the model is once again least accurate at modelling the resistance at the lower speed cases, producing resistance errors of 38.81% and 18.96%. This occurs for the same reasons as for the Modified Svahn Model, however, the loss of accuracy is significantly worse for the double stepped hull. In the previous Chapter analysis of the flow under the double stepped hull showed that neither the Savitsky Wake Equations, or the Linear Wake Assumption were valid for the slower speed ranges. Due to the inability of the model to accurately calculate the profile of the flow as it separates at the step, and therefore its inability to calculate the intersection and wetted area, the model is unable to determine the forces of moments with any degree of validity. The accuracy of the model is seen to improve significantly for the $6.25ms^{-1}$ case. This is the speed for which the Modified Svahn Model's accuracy was seen to improve. This is once again because at this speed the Savitsky Wake Equations and Linear Wake Assumption have been shown to be capable of modelling the flow, as discussed in Section 4.5.2.2, allowing the model to determine the forces and moments correctly. This finding highlights the importance of correctly determining the wetted areas of each lifting surface. Excluding the results for which the model is shown to be invalid, the average error was found to be 1.29%. This result shows that the correlation between the model and the experimental results is extremely good, and the proposed method is well capable of modelling the resistance of a double stepped planing hull. It proves that the assumptions made in developing the model are all valid and shows that due to the enhanced knowledge of the flow under a stepped hull it was possible to develop a model with a very high degree of accuracy. It also shows that the Savitsky Resistance Equations are fundamental for all hydrodynamic lifting surfaces and are applicable in conditions that are very different for those they were conceived for.

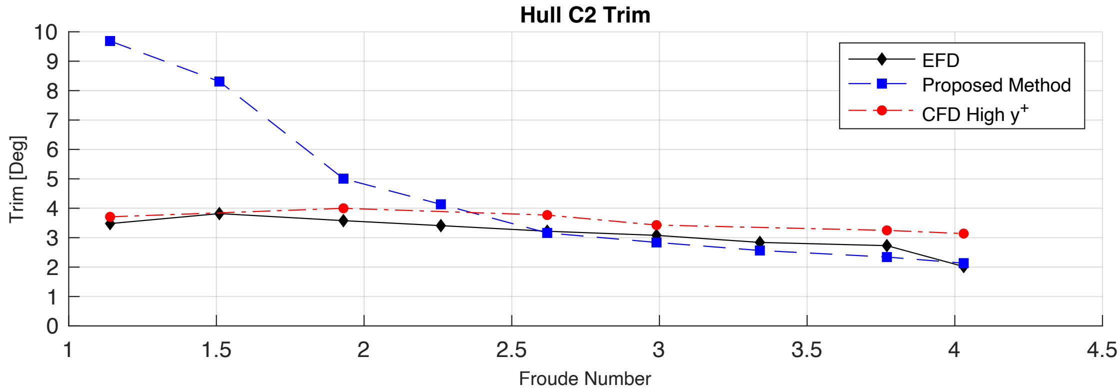

Figure 5.23 - Hull C2 trim

The trim as calculated by the Proposed model is presented in Figure 5.23. For the lower speed cases the model is completely unable to model the trim correctly. This is for the same reasons as discussed for the resistance. For speeds of 6.25ms^{-1} and over the model is seen to be more accurate, producing an average error of 14.33%. This is in line with the average error of 16.08% for the Modified Svahn Method.

The model that was previously developed to extend Savitsky's method for double stepped planing hulls employing the Linear Wake Assumption by (Dashtimanesh, Tavakoli and Sahoo, 2017) achieved an average resistance error of 9% and average trim error of 17%. In addition to employing the LWA their model only accounted for the triangular wetted regions (Area 1, 2 and 3). It employed a similar logic to the proposed model in calculating the forces acting upon each surface and then solving the equilibrium equations iteratively, however the computational procedure and implementation was different. The Proposed Model was more complex due to the inclusion of additional wetted regions, and the use of the Savitsky Wake Equations, however this was shown to significantly enhance the accuracy.

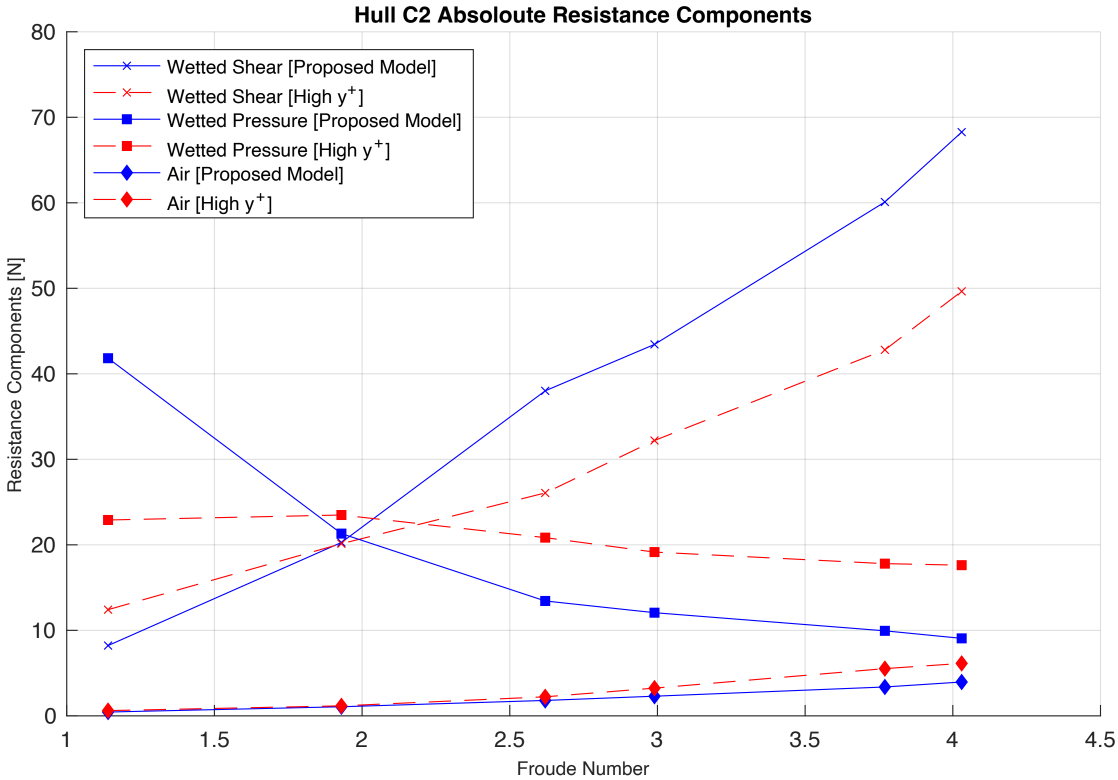

Figure 5.24 - Hull C2 absolute resistance components

The proposed method systematically calculates each resistance component, so it is possible to compare these to the numerical values obtained in Chapter 3. These are plotted on Figure 5.24. When the 4.05ms^{-1} case is investigated it is seen that the large overprediction in total resistance is due to the overprediction of the pressure resistance component, as a result of the unrealistically large trim value. When the rest of the speed range is evaluated it is seen to follow the same trends as the resistance components of the Modified Svahn Method. The frictional resistance is once again over predicted, while the pressure resistance is underpredicted.

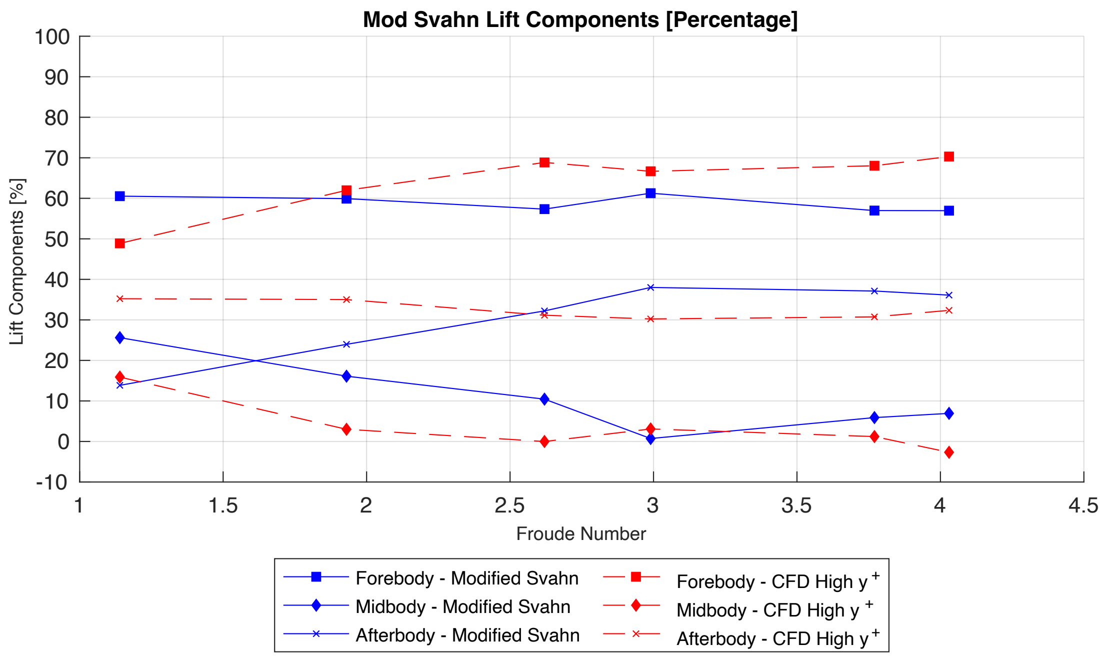

Figure 5.25 - Hull C2 lift components

Finally, it is once again possible to evaluate the lift components of each of the lifting surfaces as presented in Figure 5.25. As no experimental data is available these are compared to the CFD solution.

The forebody produces the largest lift, which is in line with the proportion of lift produced by the forebody of the single stepped hull. The remaining portion of lift is split between the mid and afterbodies, with the midbody producing the lowest value. At the lower speeds more of the midbody is in contact with the water, so it produces larger lift forces. For Froude number 3 and over the forebody flow does not intersect with the midbody. There is side wetting due to the forebody operating in the chine's dry condition. It is seen that there is very little lift calculated for the midbody by either the proposed model or the CFD solution. Interestingly, at the highest speed the midbody of the CFD solution produces negative lift, indicating that there is a suction force acting upon it. This suction is a result from the high-speed flow of air passing between the midbody and the water surface, causing a low-pressure area. There is still lift being created by the side wetting as seen in the proposed method, however the suction force is large enough to produce a net negative force. There is no way of modelling this in the Proposed method. For speeds below Froude number 3 the forebody flow intersects with the midbody, producing more lift. It is seen that the proposed method over predicts the lift of the midbody in these cases. It is also seen that it underpredicts the lift of the afterbody in these cases. While there are some differences in the lift as calculated by each of the methods, they broadly follow the same trends, indicating that the procedure for calculating the wetted area of the double stepped hull has been successful.

5.5 Summary & Conclusion

This chapter set out to develop enhanced mathematical models for the performance prediction of single and double-stepped planing hulls that addressed the limitations of existing models and reduce the level of error. This was achieved by employing knowledge developed from numerical simulations in Chapter 3, which allowed more representative models to be conceived. Two successful models were developed, displaying very high degrees of accuracy in modelling both single and double stepped hulls.

The previous analysis of the wetted areas of stepped hulls showed the components to be complex, resulting from several aspects of flow. The lifting surfaces often operate in the chine's dry condition causing side wetting. This side wetting was shown to contribute to the total lift of the hull and the importance of including these areas and fully modelling all wetted hull components was highlighted when developing the Modified Svahn Model. Novel methods to account for the hull operating in a chine's dry condition were proposed and shown to be successful for the single step model. This methodology was then developed into a procedure to calculate the complex wetted area of a double stepped hull.

The Modified Svahn Model was developed for the performance prediction of a single stepped hull, successfully extending the range of applicability and increasing the accuracy of the Original Svahn Model. For speeds of $6.25 ms^{-1}$ and over, the Modified

Svahn Model calculated the resistance with an average error of 2.50% and the trim with an average error of 16.08%. The Proposed Model for double stepped hulls was shown to once again be accurate for the speeds of $6.25ms^{-1}$ and over, resulting in an average error in resistance of 1.29% and in trim of 14.33%. This was a significant improvement over existing models, showing that the application of knowledge developed from numerical simulations had been successful. The accuracy of both models was shown to be in line with the Savitsky Method as applied to an unstepped hull, showing Savitsky's Semi-Empirical Equations to be versatile in their application. They may be considered fundamental for all hydrodynamic lifting surfaces and are applicable in conditions that are very different from those they were conceived for.

Table 5.5 – Summary of accuracy

Model	Average Resistance Error	Average Trim Error
Hull C - CFD	2.46%	15.07%
Hull C - Savitsky's Method	6.42%	45.04%
Hull C1 - CFD	4.72%	10.36%
Hull C1 - Modified Svahn's Method	2.50%	16.08%
Hull C2 - CFD	4.98%	13.17%
Hull C2 - Proposed Method	1.29%	14.33%

A summary of the accuracy of each method is shown in Table 5.5. For both single and double stepped hulls the developed analytical models calculated trim more accurately than the CFD simulation developed in Chapter 3. The same however, cannot be said for the trim, although the error in the results is comparable. This high level of accuracy demonstrates the value of the developed models in the design of planing hulls, however, it should be remembered that they rely upon assumptions and empirical equations rather than calculating the physical flow. They may be employed for the initial design stages and are a valuable tool due to their ability to rapidly model large numbers of prospective designs, but it is vital that the final hull form is evaluated using a higher fidelity analysis technique such as CFD or EFD to ensure confidence in the design.

Chapter 6 – A Study into Improving the Hydrodynamic Performance of Stepped Hulls

The final research chapter of this thesis investigates how the hydrodynamic performance of single and double stepped hulls in calm water may be improved. This is achieved by coupling the enhanced analysis techniques developed in Chapter 4 and Chapter 5 with a fully-automated parametric optimisation workflow. Analysis of the large data-sets produced determines trends and relationships that reduce the resistance, and may be applied to improve the hydrodynamic performance in the design of any stepped hull.

6.1 Introduction

The interest in stepped hulls amongst the research community been seen to increase significantly in recent years as methods to accurately model such hull forms have been developed and become more widely available (Sajedi and Ghadimi, 2020). Having dedicated much time and effort in developing these numerical techniques and models, researchers are able to employ them in the study of stepped hulls to develop the understanding of the phenomena that are occurring and improve their performance.

The main motivation behind the adoption of a stepped hull is generally to take advantage of the reduced resistance, with the incorporation of steps to the design of a planing hull typically leading to a speed increase of 10 – 15% over the unstepped variant (Loni *et al.*, 2013). Analysis of the experimental results of (Taunton, Hudson and Shenoi, 2010) undertaken in Chapter 3 showed the inclusion of steps to reduce total resistance by 25.85% for the highest speed case (with a Froude number of 4.00). With considerable performance improvements being shown to be possible, conducting further study to understand how to take full advantage of the stepped hull form and maximise these gains is required.

To date several authors have undertaken limited studies to this end, as outlined and discussed in the Critical Review. This work provides some insight into the design of stepped hulls and some of the strategies which minimise the resistance further. They show the significant influence that step design has upon the performance of a hull and indicate the potential resistance reductions that may be achieved through determining the correct step configuration. Undertaking more thorough studies with a larger scope to further develop this understanding will reveal the level of performance improvement that may be achieved by a near optimal hull, and reveal the desirable design trends that lead to this resistance reduction.

All the work available in the literature follows a Design of Experiments (DOE) methodology. This is a systematic method in which the relationship between factors effecting a process and the output of that process is determined in a systematic way. The DOE methodology is used to determine cause-and-effect relationships, for instance how the location of a step influences the resistance. While this methodology is good for finding simplistic relationships, which may be used to improve designs, it does not determine the optimum design of a stepped hull.

The performance of a stepped hull is governed by a range of parameters, forming a large and complex multi-dimensional design space. While it is possible to determine relationships from systematic variation with small sample sizes, as has been done previously, these are not able to consider all the complex interactions between the different parameters. In order to develop understanding of the configuration that results in the lowest resistance, a fully parametric optimisation study, in which an optimisation algorithm enhances the design based up previous results is required. This chapter sets out to undertake such a study, employing both numerical and analytical models in conjunction with a fully automated, parametric optimisation procedure to determine the optimum step configurations for Hull C1 and Hull C2 as experimentally tested by (Taunton, Hudson and Shenoi, 2010). Analysis of the large data-set is used to investigate how the hydrodynamic performance of single and double stepped hulls may be improved.

In addition to investigating how the hydrodynamic performance of stepped hulls may be improved, there is significant merit in developing a useful and validated optimisation workflow that fully take advantage of the developed analysis tools, as pointed out by (Nazemian and Ghadimi, 2021). While the present chapter only considers the step configuration in the calm water condition due time constraints, the presented workflow is equally applicable to other aspects of hull shape optimisation and even seakeeping analysis, provided it is coupled with an accurate and efficient seakeeping CFD simulation. The integration of a parametric CAD model, a CFD solver and optimisation algorithms into a unified workflow allows both academics and industry to make significant design improvements and is a topic that is going become more feasible in the coming years due to the ever-increasing availability of computational power.

6.1.1 Aims

The main aim of this chapter is to investigate how the hydrodynamic performance of single and double stepped hulls may be improved. The study will look to establish design trends that lead to a reduced resistance, investigating the relationship between design parameters so that the trends may be employed by designers of stepped hulls. A secondary aim of this chapter is to determine the extent to which the performance of stepped hulls varies with step configuration and establish the level of improvement that is possible through an optimisation workflow. In addition, this will reveal the extent to which performance is lost through poor step design.

In order to evaluate these aims a number of objectives are proposed:

- **Develop** an automated optimisation workflow managed by the HEEDS MDO software package

- **Optimise** single stepped hulls using the Modified Svahn Model as an analysis tool
- **Optimise** double-stepped hulls using CFD as an analysis tool
- **Evaluate** the workflow and the merits of both analysis tools
- **Evaluate** the data-set to reveal how the hydrodynamic performance of single and double stepped hulls may be improved
- **Quantify** level of improvement that is made possible though enhanced step configuration
- **Develop** design trends that lead to reduced calm water resistance

6.1.2 Methodology

The enhanced and accelerated analysis techniques developed in chapter Chapter 4 and Chapter 5 are employed to improve the hydrodynamic performance of single and double stepped hulls. The analysis models drive a fully automated parametric optimisation workflow, developing a large dataset of different designs. Analysis of the dataset determines the design characteristics that improve hydrodynamic performance in calm water, as well as determining the optimal design.

To undertake the optimisation work, the software HEEDS MDO ("HEEDS MDO User Guide Version 2019.2.2," 2019), developed by Siemens is utilised. HEEDS is a piece of powerful design space exploration and optimisation software, capable of integrating and managing geometry models, analysis models and optimisation algorithms. It facilitates the development of automated analysis workflows, leveraged over a distributed network of computational resources. The software's optimisation algorithm efficiently explores the design space for optimised solutions, and its post processing capabilities allow the analysis of data.

The optimisation of the single stepped is driven using data from semi-empirical Modified Svahn Model. The model was shown to be able to calculate the resistance of a single stepped hull with an average error of 2.50% and is capable of rapidly generating results. The rapid nature of this analysis tool allows a large dataset to be developed, consisting of thousands of prospective designs. Analysis is conducted for multiple speeds allowing the effect of speed on the design traits that lead to an improved hydrodynamic performance to be investigated.

The optimisation of the double stepped hull is driven by data from the high-fidelity RANSE CFD simulation. The CFD set up was shown to be robust and accurate, capable of calculating the resistance of a double stepped hull with an average error of 4.98%. As this analysis technique is considerably more computationally expensive to run, only a single speed is investigated. A parametric model of the double stepped hull was developed using the Grasshopper plug in for Rhino to develop 3D geometries to fed into Star CCM+.

Following the optimisation procedure, the dataset that has been developed is evaluated to determine the design trends and correlation between the parameters and reduced resistance. This analysis will aim to determine the characteristics that lead to an improved hydrodynamic performance.

6.2 Optimisation Procedure

This section details the optimisation workflow that was employed for this study. More in-depth information related to the optimisation set-up is made available in Appendix B to act as an aid to researchers looking to employ this this workflow for their own studies.

The software HEEDS MDO was selected due to the versatility offered by the software, allowing the integration of numerous other modelling and analysis programs. HEEDS acts as an interface, managing connections between data models and allowing an automated workflow to be developed while removing the need for custom scripting to manage software connections. In addition, the software leverages different hardware investments and facilitates the combined use of multiple computational resources, connecting hardware and feeding information in both directions. Geometry modification and the optimisation algorithm can be processed on a local windows PC, while the computationally demanding CFD simulations are performed on a HPC Linux cluster, such as Archie WeST.

A Parameter Optimization study was undertaken to identify optimal solutions and develop the dataset of candidate designs. A hybrid search algorithm was employed, taking advantage of the strengths of several optimisation strategies to facilitate an efficient search of the design space (Chase, Rademacher and Goodman, 2010).

6.2.1 SHERPA Search Algorithm

SHERPA (Simultaneous Hybrid Exploration that is Robust, Progressive, and Adaptive) is an exclusive search technology to HEEDS, which is used to simultaneously leverage multiple global and local search strategies. SHERPA has been shown to outperform other algorithms by a factor of two in the number of evaluations required to fully converge to the optimal solution. In cases where the number of evaluations is limited, it has been shown to progress rapidly toward the optimal solutions, with the average solution being found to be twice as good as that found by other methods (Chase *et al.*, 2010).

Over the course of a single parametric optimisation study, SHERPA employs elements from multiple search methods simultaneously (not sequentially) in a unique blended methodology. This allows the best attributes of each model to be exploited, resulting in a very robust and efficient search algorithm. The internal tuning parameters of each participating approach are updated through the course of the search utilising the knowledge gained about the nature of the design space (Red Cedar Technology, 2014). The evolving knowledge of the design space is used to determine the degree of which each approach contributes to the search, allowing SHERPA to learn about a problem and adapt in a manner that ensures it is effective and efficient. SHERPA is a direct optimisation algorithm, so all function evaluations are performed with the actual model as opposed to an approximate response model.

For further information about the SHERPA search algorithm please refer to Appendix B and (Red Cedar Technology, 2014).

6.2.2 Single Stepped Hull Optimisation Set-Up

The design variables under investigation were the step length (Ls) and height (Vs). Constraints were put in place to define the design space, as detailed in Table 6.1. The objective function of the optimisation was the resistance of the vessel, to be minimised by the SHERPA search algorithm. Hull C1, as tested by (Taunton, Hudson and Shenoi, 2010), was selected as the baseline design. The workflow that was automated using HEEDS is presented in Figure 6.1.

Table 6.1 – Constraints for the Hull C1 optimisation

Input Variable	Minimum	Maximum	Baseline
Step Length [m]	0.20 m	0.75 m	0.62 m
Step Length [Loa]	0.10 Loa	0.38 Loa	0.31 Loa
Step Height [m]	0.001 m	0.060 m	0.020 m
Step Height [T]	0.01 T	0.03 Loa	0.01 Loa

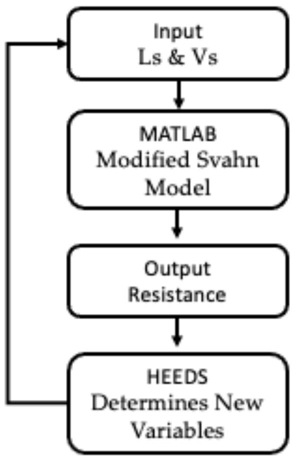

Figure 6.1 - HEEDS process for Hull C1

Conducting performance analysis of prospective designs using the Modified Svahn Model as coded in MATLAB is not a computationally intensive process. Both the performance prediction and the optimisation procedure took place on a local PC. It was ensured that the evaluations had converged upon an optimal solution. Between 250 and 1000 design evaluations were undertaken for each speed that was investigated. The results of this optimisation, and analysis of the factors effecting the performance of a single stepped hull will be presented and discussed later in this chapter.

6.2.3 Double Stepped Hull Optimisation Set-Up

The set-up of the Double Stepped Hull analysis was more complex. While the same process logic was applied as for the single-stepped hull workflow, employing CFD as the design tool led to a far more complicated optimisation procedure. Additionally, it resulted in a considerably more computationally intensive process with an analysis time of around 12 hours per design as opposed to 30 seconds. A brief description of the set-up is provided in this section, with further details presented in Appendix B.

The workflow is detailed in Figure 6.2. To provide the CFD simulation with geometries a parametric model was developed in Rhino Grasshopper. Geometries were defined using variables for the first step location, the first step length, and the height of the first and second step. The geometry was developed on a local PC before it was transferred to the HPC Linux cluster, where it was imported to the CFD simulation. Once the simulation was converged the results were extracted and transferred back to the local PC where the optimisation algorithm analyses them, using the previous data to develop the input variables for the next design evaluation.

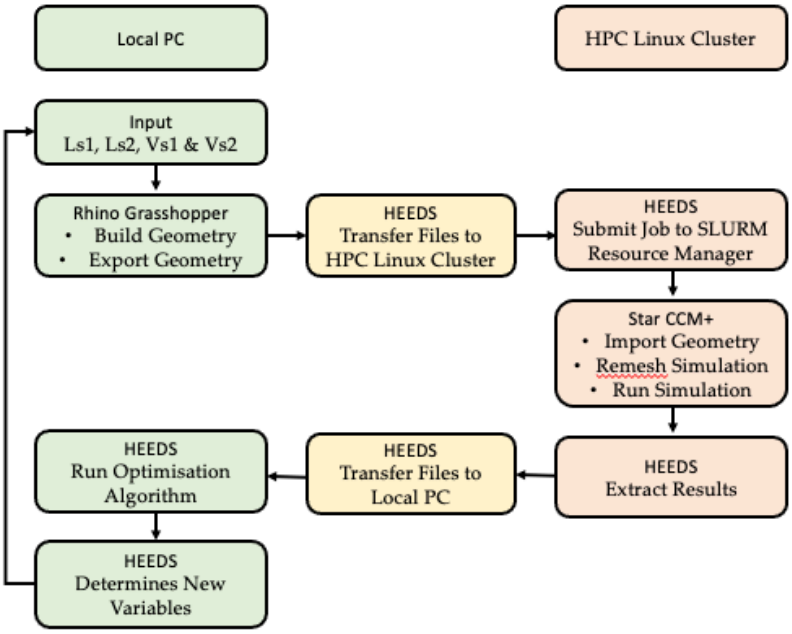

Figure 6.2 - HEEDS process for Hull C2

The input variables under investigation and the constraints are outlined in Table 6.2. The resistance was set as the objective function to be minimised by the SHERPA method. Additionally, a further constraint as outlined in Equation (6.1) was included to ensure that the minimum possible second step length was 0.05m. The baseline design was set to the dimensions of Hull C2 as tested by (Taunton, Hudson and Shenoi, 2010).

Table 6.2 - Input variables for the Hull C2 optimisation

Input Variable	Minimum	Maximum	Baseline
First Step Location from Transom (m)	0.0 m	0.69m	0.62 m
First Step Location from Transom (Loa)	0.0 Loa	0.35 Loa	0.31 Loa
First Step Length (m)	0.1 m	0.7 m	0.25 m
First Step Length (Loa)	0.05 Loa	0.35 Loa	0.125 Loa
First Step Height (m)	0.0011 m	0.03 m	0.01 m
First Step Height (Loa)	0.0006 Loa	0.015 Loa	0.005 Loa
Second Step Height (m)	0.0011m	0.03 m	0.01 m
Second Step Height (Loa)	0.0006 Loa	0.015 Loa	0.005 Loa

$$\text{First Step Location} + \text{First Step Length} < 0.65m \qquad \textbf{(6.1)}$$

As this method was far more time consuming and computationally expensive to generate results with, only one speed was optimised. The $8.13ms^{-1}$ speed case was selected. This equates to a full scale speed of 35.34 knots if the 2m Hull C2 model was representative of a 10m full scale vessel, and a full scale speed of 43.28 knots if it were representative of a 15m vessel. These are two typically sized stepped hull vessels with a full-scale speed that is in an appropriate range for stepped hulls. In addition to only running the study a single speed, the number of evaluations was reduced to 68. It had been shown in the single stepped optimisation that the SHERPA algorithm was capable of finding a near optimal solution in under 50 evaluations, as will be discussed in Section 6.3.1, so this number of evaluations was deemed appropriate. This finding was inline with previous studies that set out to evaluate the effectiveness of the search algorithm (Chase, Rademacher and Goodman, 2010).

6.3 Results – Hull C1 Investigation using Modified Svhan Method

In this section the results of the single stepped hull study will be analysed to investigate how the performance of a single stepped hull may be improved. First the dataset developed by each of the optimisation cases are presented, before the data is analysed and discussed. Finally, the optimal and worst-case hull for each speed are detailed.

6.3.1 Overview of Results

Optimisation studies were undertaken for five speeds, as experimentally tested by (Taunton, Hudson and Shenoi, 2010). A total of 2850 designs were evaluated. Candidate hulls were defined by two input variables, with 11 response variables recorded for each design evaluation, resulting in 37050 data points. A study of 1000 candidate hull evaluations took around 4 hours to run on a desktop PC. Cases in which the forebody wake did not intersect with the afterbody were considered invalid. The total number of design evaluations for each speed case, the number of valid designs, and the number of evaluations to reach the optimum solution is detailed in Table 6.3. Additionally, the best and worst-case solution are presented for each speed case, where the percentage increase or decrease in resistance is relative to the baseline design.

Table 6.3 - Optimisation study of Hull C1

Speed [ms^{-1}]	**4.08**	**6.25**	**8.13**	**10.13**	**12.05**
Number of Evaluations	300	300	1000	1000	250
Number of Valid Evaluations	271	246	693	621	129
Number of Evaluations to Find Optimum	145	33	98	141	227
Optimum Resistance [N]	37.79	42.19	43.37	47.97	53.47
Optimum Resistance Percentage Reduction	2.12%	7.31%	17.36%	27.44%	35.86%
Worst Case Resistance [N]	48.87	59.88	80.90	109.49	153.74
Worst Case Resistance Percentage Gain	26.57%	31.55%	54.15%	65.62%	84.41%

The results in Table 6.3 show that for all speed cases the optimisation workflow improves the baseline design, decreasing the resistance. The level of improvement is correlated with speed, with a 2.12% decrease for the lowest speed, while there is a 35.86% improvement for the highest speed condition. This is due to the fact that stepped hulls are more beneficial at higher speeds, as detailed in Chapter 3. At higher speeds resistance is dominated by the frictional component, so reductions in wetted area resulting from an improved step configuration have a greater impact upon total resistance. The worst-case result for each speed condition features a significant increase in resistance, the impact of which again correlates with speed.

To visualise the full dataset as developed for each speed condition, the resistance of each candidate hull is plotted against its respective evaluation number in Figure 6.3 - Figure 6.7. Additionally, the red line on the graphs shows the path to the optimal solution, beginning at the baseline design and then connecting each subsequent best-case design as it is evaluated.

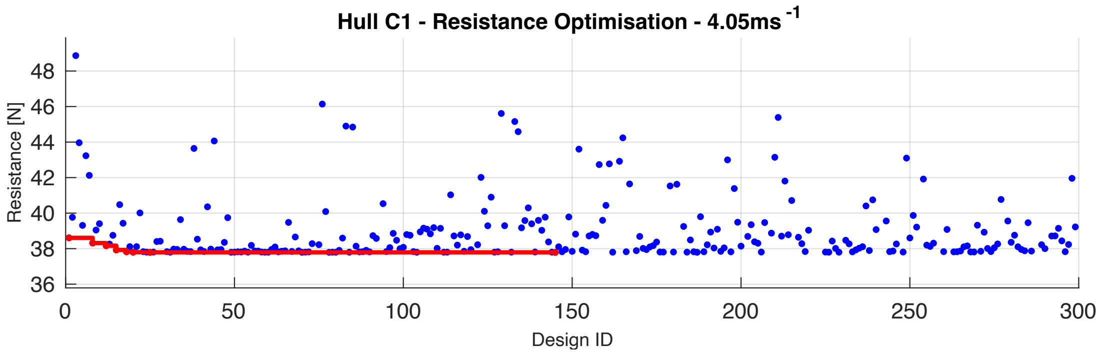

Figure 6.3 - Resistance history for Hull C1 optimisation [$4.05 ms^{-1}$]

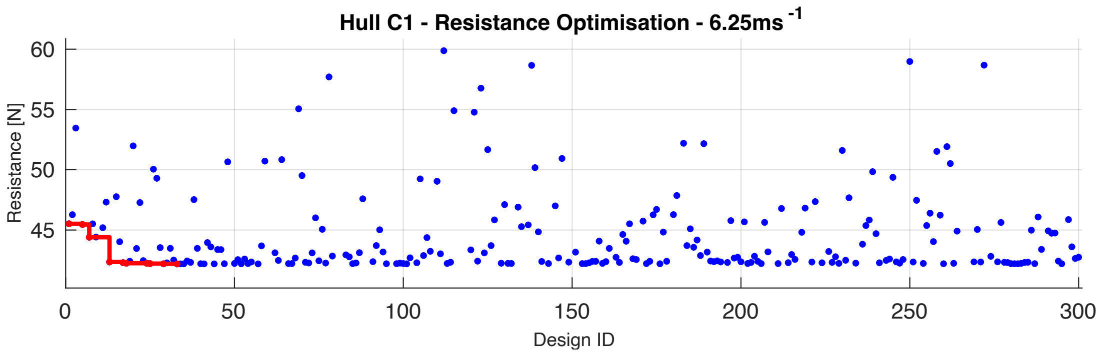

Figure 6.4 - Resistance history for Hull C1 optimisation [$6.25 ms^{-1}$]

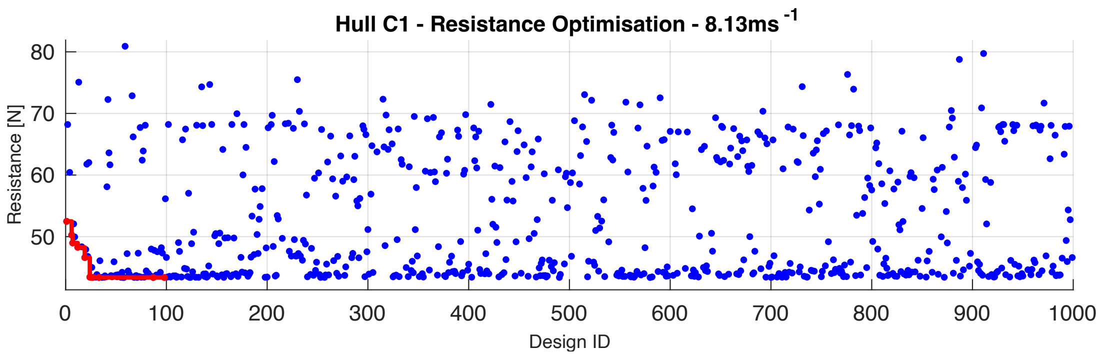

Figure 6.5 - Resistance history for Hull C1 optimisation [$8.13 ms^{-1}$]

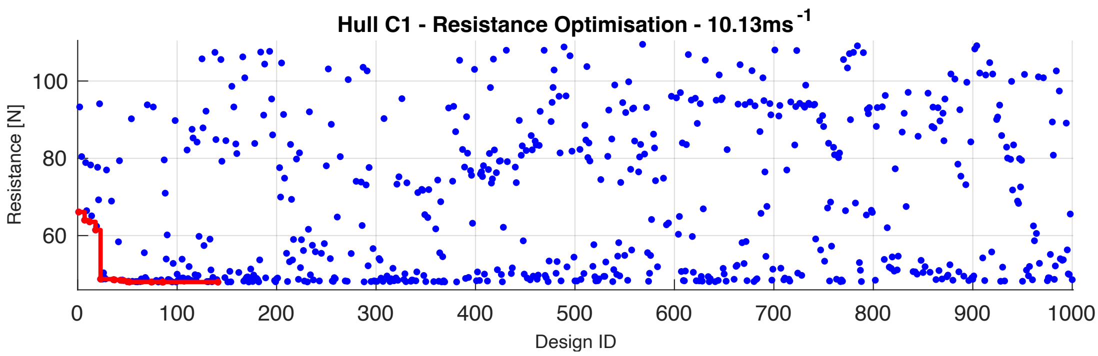

Figure 6.6 - Resistance history for Hull C1 optimisation [$10.13 ms^{-1}$]

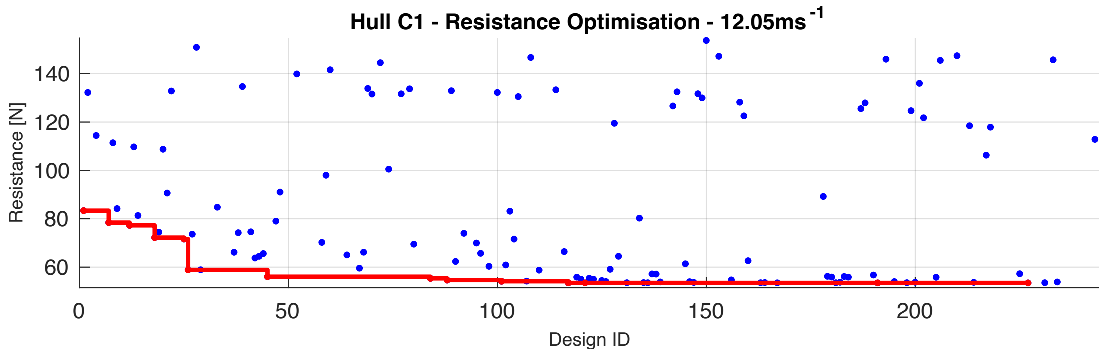

Figure 6.7 - Resistance history for Hull C1 optimisation [$12.05ms^{-1}$]

Figure 6.3 - Figure 6.7 show a large range in resistance for each speed condition as a result of the different geometries. The fact that there is such variation in hull performance highlights the importance of determining the best step configuration for the vessels operating conditions. While it may not always be feasible to undertake such optimisation studies, analysis of the data developed from the present study reveals general design trends that led to improved hydrodynamic performance.

In all speed cases a large population of near optimum hull designs have been found by the optimisation algorithm. The path to the optimal solution for each speed has been plotted against the design performance in Figure 6.8, which is taken as a resistance percentage relative to the baseline result. The SHERPA method is seen to be extremely efficient, finding a near optimal solution for all speed cases in less than 50 evaluations.

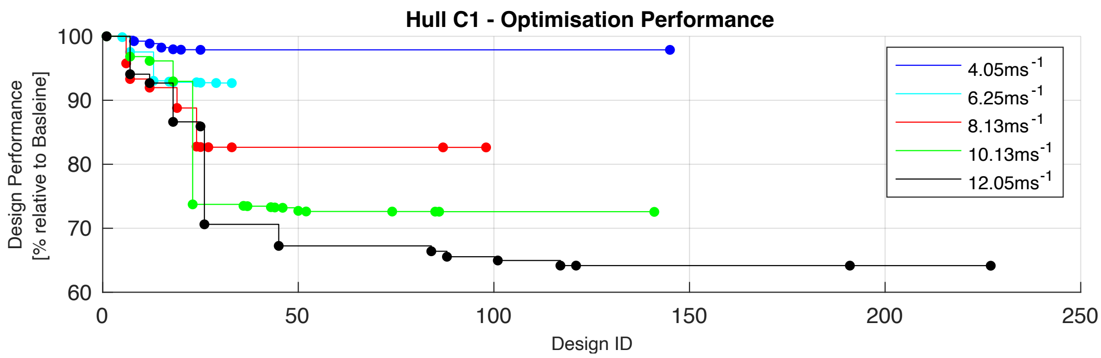

Figure 6.8 – Optimisation performance for Hull C1

6.3.2 Design Trends of a Single Stepped Hull

This section details the analysis of the data set for each speed condition to determine how the hydrodynamic performance of single stepped hulls may be improved. As several speeds were examined it is also possible to investigate how desirable design traits vary with speed.

As an enormous amount of data points were produced over the course of this study it is difficult to condense this data and present it in a concise and meaningful manner. For the sake of consistency this section will first present the design trends for the $8.13ms^{-1}$ case, before presenting the results from all speed cases and expanding the discussion. The $8.13ms^{-1}$ case was selected for individual discussion as it is placed in the middle of the speed range. Additionally, there was a large dataset of 1000 design evaluations for this speed.

The section first investigates the input variables and their impact upon resistance. These are variables that the optimisation algorithm had control over and was able to update in each successive design evaluation. The section will then go on to investigate the response variables and their impact upon the resistance. The response variables are factors that are physical properties of the hull, however they were not directly changed. By investigating these it is possible to determine the reasons for decreased resistance and establish what traits are beneficial in the design of a single stepped hull.

The input parameters are non-dimensionalised by hull length so that the trends developed for this study may be utilised in the design of any stepped hull. Total resistance is plotted as opposed to the non-dimensional resistance coefficient as differences in the wetted area mean the resistance coefficient plots are misleading, as detailed in Section 6.3.2.1.

6.3.2.1 Influence of Input Variables on Resistance

As there were two input variables (step length and step height) and one objective (resistance), 3D scatter graphs are used in this analysis, as seen in Figure 6.9 and Figure 6.12. These allow the resistance design space to be easily visualised and analysed, with resistance trends that are linked to this multivariant problem becoming apparent. In order to further visualise the trends and assist with the analysis the 3D scatter graphs are broken down and viewed in 2D from the X & Y perspectives, so that the effects of an individual input variable may be understood. These are presented in Figure 6.10 and Figure 6.13. Additionally, the non-dimensional resistance coefficient is presented in the same 2D format in Figure 6.11 and Figure 6.14.

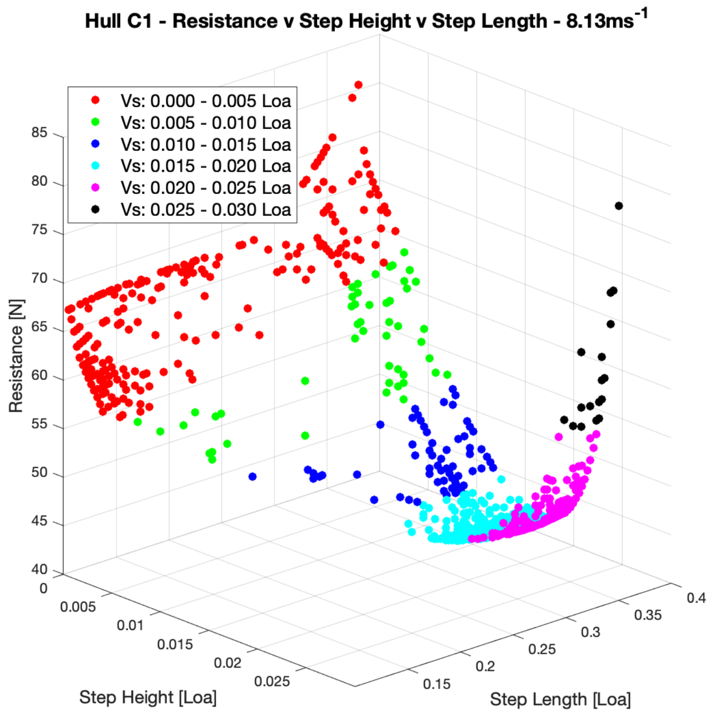

Figure 6.9 - 3D scatter graph of the resistance design space for $8.13ms^{-1}$

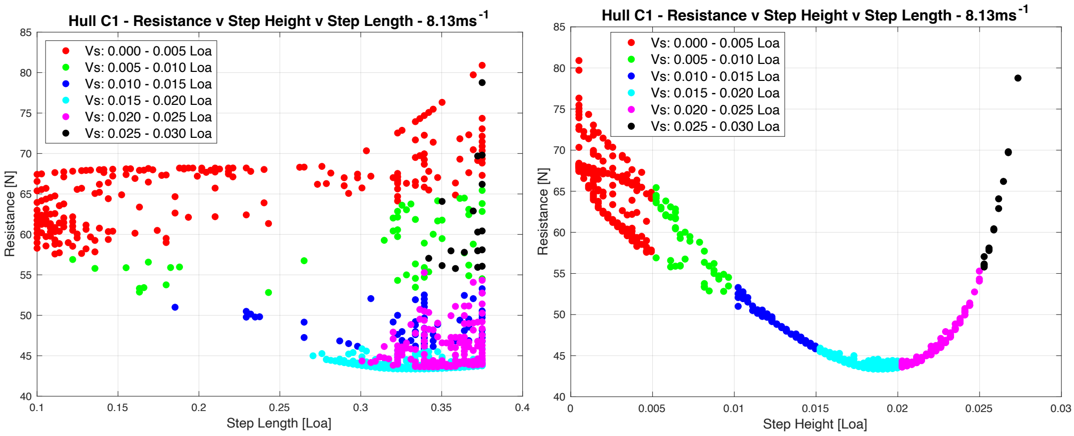

Figure 6.10 – 3D scatter graph of the resistance design space for $8.13ms^{-1}$ (viewed in 2D from the X & Y perspectives)

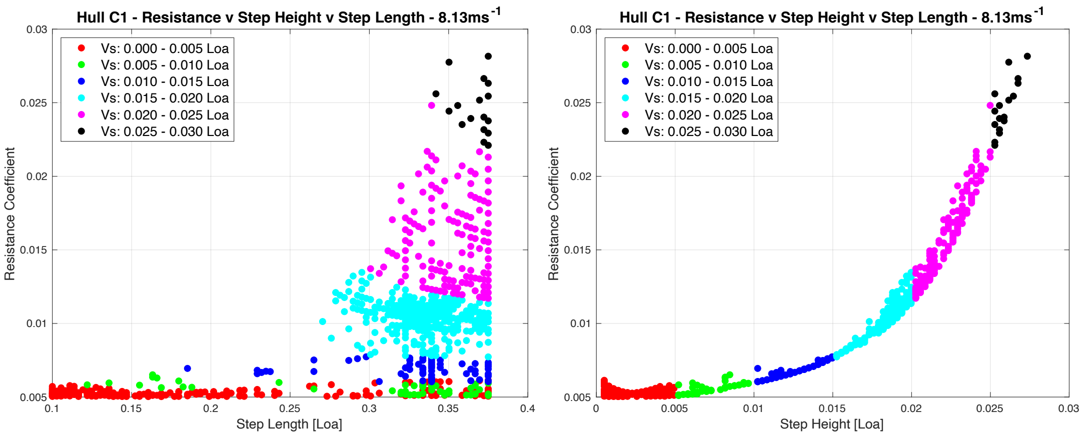

Figure 6.11 – Non-dimensional 3D scatter graph of the resistance design space for $8.13ms^{-1}$ (viewed in 2D from the X & Y perspectives)

The data points from the 693 valid design evaluations for the $8.13ms^{-1}$ speed case are plotted in Figure 6.9. The 3D design space is seen to form a curved triangular shape, with a single trough in resistance. As step height increases, the valid options for step length decrease, forming the point of the triangle (as plotted by the black points). For smaller step heights there is a large range of step lengths that constitute valid designs (as plotted in red). The reason for the formation of this triangular shape is that as the step height increases, so too will the reattachment length of the forebody flow with the afterbody. For a design to be considered valid the flow must intersect, so large step heights require larger step lengths to ensue this intersection of forebody flow with the afterbody.

Two distinct resistance peaks are seen to form, and one resistance trough. The first peak is formed where there is a large step length and a very small step height. This results in a geometry that is similar to an unstepped planing hull, with short ventilation lengths and a large wetted area. Unstepped hulls result in a significantly higher resistance than a single stepped hull. The second peak occurs for cases with a large step height and step length. Increasing the step height increases the ventilation length, reducing the wetted area of the aft hull which and reducing the lift produced by the aft hull. To satisfy the moment equilibrium balance the trim of the hull must therefore increase. A larger trim reduces the ventilation length, increasing the wetted area and therefor lift of the aft hull until the moment equation is balanced. As a result of the increased trim the induced drag is significant. The minimum resistance occurs at a step height of around 0.019 Loa, where all valid step lengths produce a similarly low resistance forming a trough.

Figure 6.10 breaks Figure 6.9 down into two separate 2D graphs, showing the relationship between the individual input variables and resistance. It is immediately obvious that the step height is the key factor in reducing the resistance of a stepped hull. This is in line with the findings of (Najafi *et al.*, 2019). It is seen that as the step height increases the resistance gradually decreases until it reaches a minimum value. As step height increases beyond this, the resistance rises sharply. This is due to the larger trim of these designs, resulting in an increase induced drag.

While the step length had a large influence on whether a design was valid or not, it does not appear to have a large influence on the resistance. For the smaller step heights there is seen to be more of a resistance range accountable to step length, as seen plotted by the red and green markers. In this range the resistance increases gradually as the step length increases. Once the step height is larger than 0.01Loa the resistance variation with step length is seen to reduce significantly, nearly collapsing to a single line on the height vs resistance graph. When this is investigated further it is found that for step heights over 0.01Loa, if the step height is fixed there is some variation in resistance with step length, however this is considerably less significant than the variation due to step height.

Figure 6.11 is analogous Figure 6.10, plotting non dimensional resistance coefficient as opposed to total resistance. Resistance coefficient is lowest for small step heights, increasing with step height. This shows designs that have the largest total resistance to have the lowest resistance coefficient, which is somewhat misleading. This occurs due to significant differences in wetted area between the design evaluations, with small step heights having over four times the wetted area of the large step heights. For this reason, the results for the remainder of this chapter will use resistance as opposed to resistance coefficient.

In Figure 6.12 - Figure 6.14 the data from all speeds under investigation is presented in the same format. In these graphs the different colours are used to distinguish between speeds

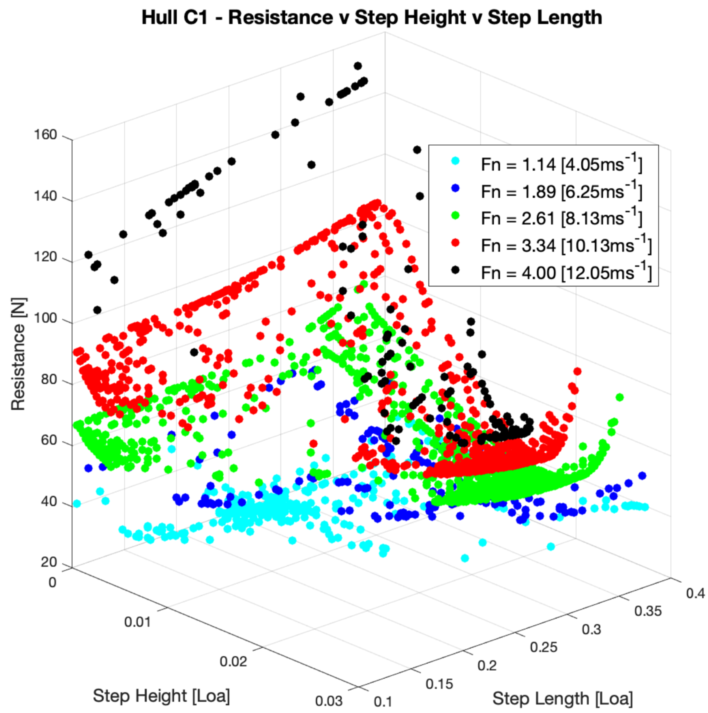

Figure 6.12 - 3D scatter graph of the resistance design space for all speeds

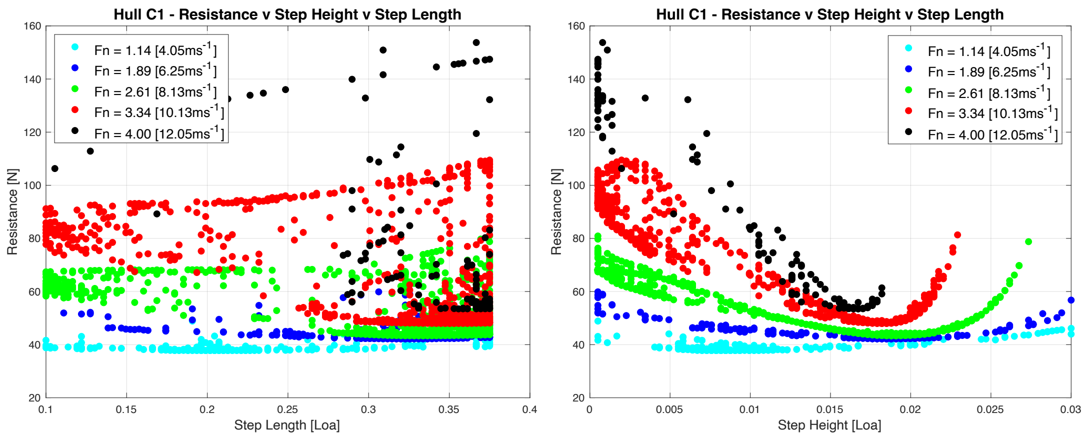

Figure 6.13 – 3D scatter graph of the resistance design space for all speeds (viewed in 2D from the X & Y perspectives)

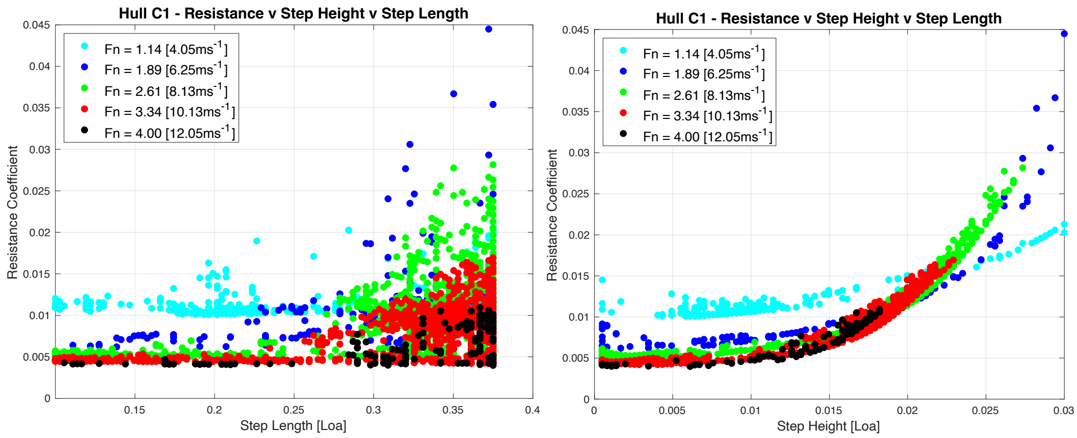

Figure 6.14 – Non-dimensional 3D scatter graph of the resistance design space for all speeds (viewed in 2D from the X & Y perspectives)

The design space for all speeds is seen to be similar in nature in Figure 6.12, forming the two resistance peaks and a single trough as discussed previously. In all cases the largest resistance peak is attributable to a geometry with a large step length and a small step height. The optimisation study for all speeds revealed a resistance trough that is closely linked to step height, which was once again shown to be the most important variable in minimising resistance in Figure 6.13. The range in resistance is far more significant for the higher speeds, with the data for lower speeds appearing condensed. When each is investigated individually however, the same traits as previously discussed are exposed. As the speed increase the step height at which the minimum resistance occurs decreases.

6.3.2.2 Influence of Input Variables on Trim

This section investigates the effects of the design variables on the trim of the vessel, following the same format as the previous section.

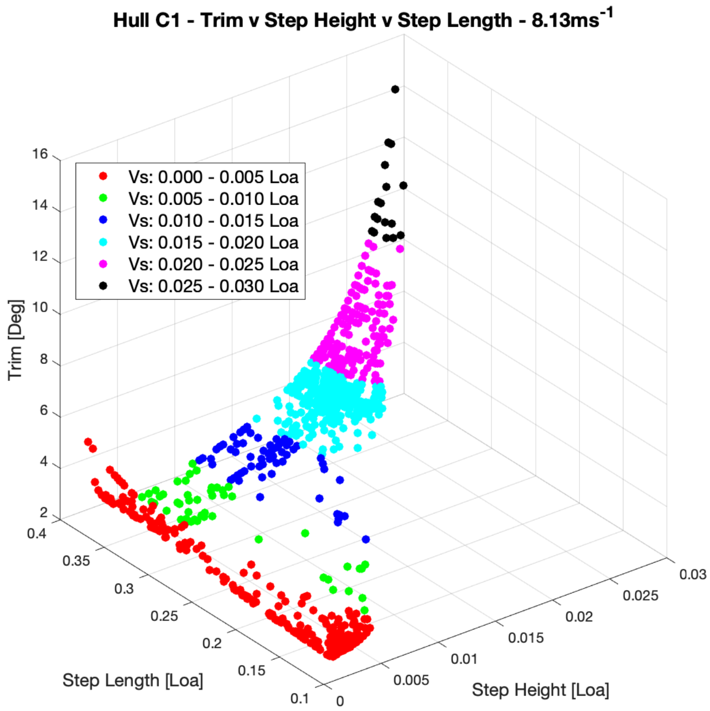

Figure 6.15 - 3D scatter graph of the trim design space for $8.13ms^{-1}$

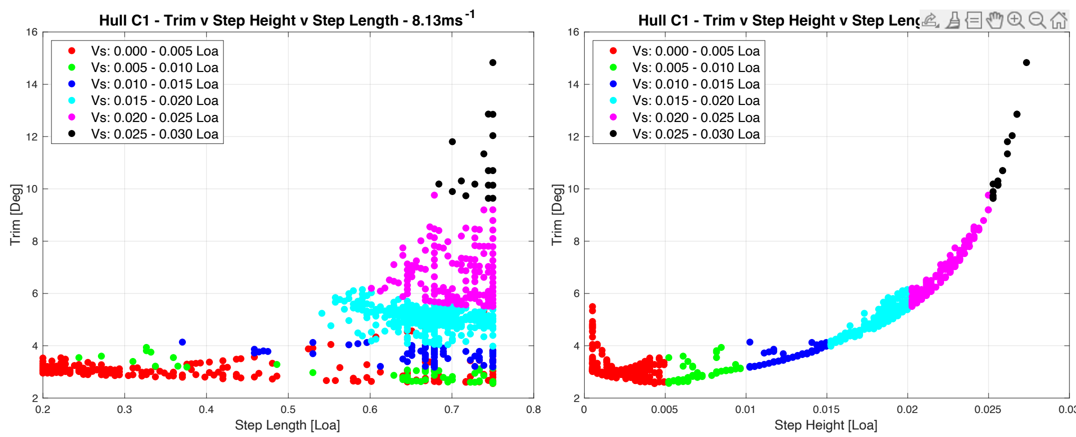

Figure 6.16 – 3D scatter graph of the trim design space for $8.13ms^{-1}$ (viewed in 2D from the X & Y perspectives)

Figure 6.15 and Figure 6.16 detail the trim design space, which is seen to form a triangular shape, for the reasons as previously discussed. Trim is seen to vary slightly with step length, tending to reduce for larger step lengths. As the step length increases the wetted area of the afterbody increases, providing a larger proportion of lift and reducing the trim of the hull. Step height is once again the dominant variable, and the large variations in trim revealing why it was so influential in resistance previously. As the step height increases the trim also increases. This is due to two factors; the first of which is that as the step height increases there is buoyancy lost form the aft portion of the hull, and the static trim has to increase to account for this. This effect was seen in Chapter 3 where the unstepped hull had a static trim of 0 degrees, and the stepped variant had a static trim of around 1 degree. The second reason for the increased trim with larger step heights is that ventilation length increases with step height. A larger trim is therefore required to ensure that the forebody flow intersects with the afterbody.

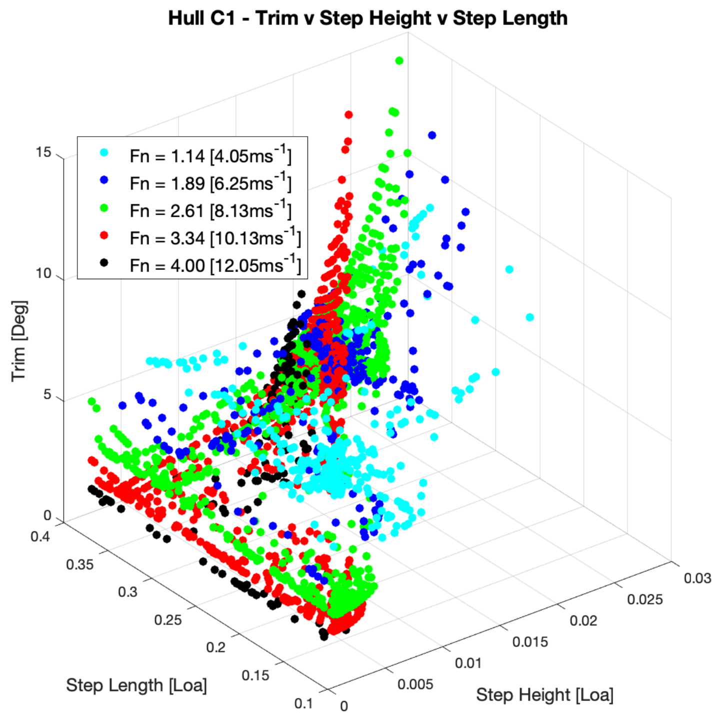

Figure 6.17 - 3D scatter graph of the trim design space for all speeds

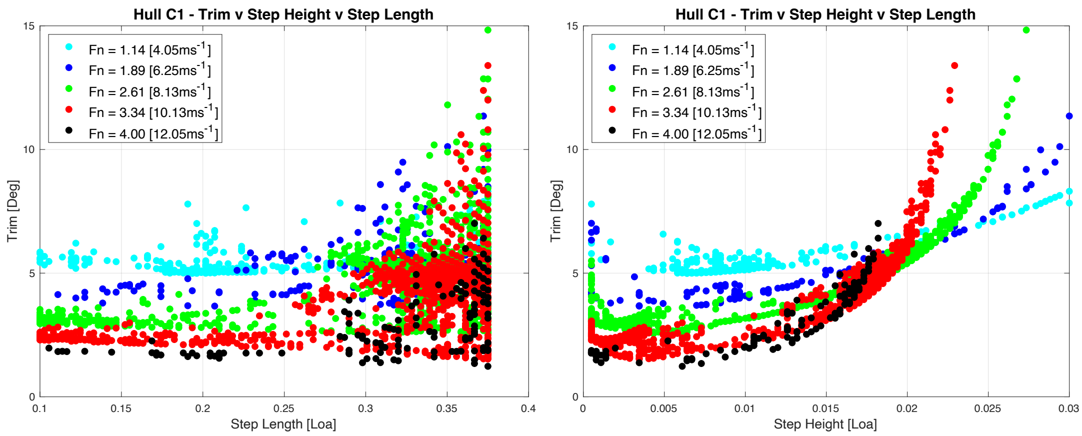

Figure 6.18 – 3D scatter graph of the trim design space for all speeds (Viewed in 2D from the X & Y perspectives)

In Figure 6.17 and Figure 6.18 the data from all speed cases is presented. The same trends as found in Figure 6.15 and Figure 6.16 are visible for all speed conditions. Step length is seen to have a minor influence on the trim in all cases, while the step height is the most influential variable. As is typical of planing hulls, as the speed increases the trim decreases. As the speed increases the gradient with which the trim increases with step height is also seen to increase.

6.3.2.3 Influence of Input Variables on Wetted Area

The effect of the design variables upon the wetted area was investigated. A reduction in the wetted area is the mechanism through which a stepped hull achieves a reduction in resistance in comparison to a conventional planing hull. As such, this parameter is of great importance, and understanding how it may be minimised is beneficial in the design of stepped hulls.

The data is plotted on 3D scatter graph, as presented in Figure 6.19, which are then broken down and viewed in 2D in Figure 6.20.

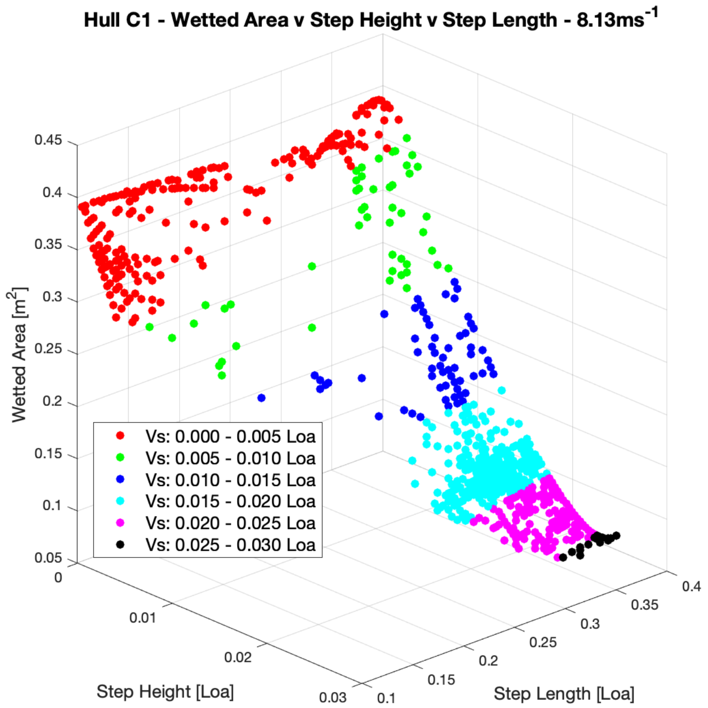

Figure 6.19 - 3D scatter graph of the wetted area design space for $8.13ms^{-1}$

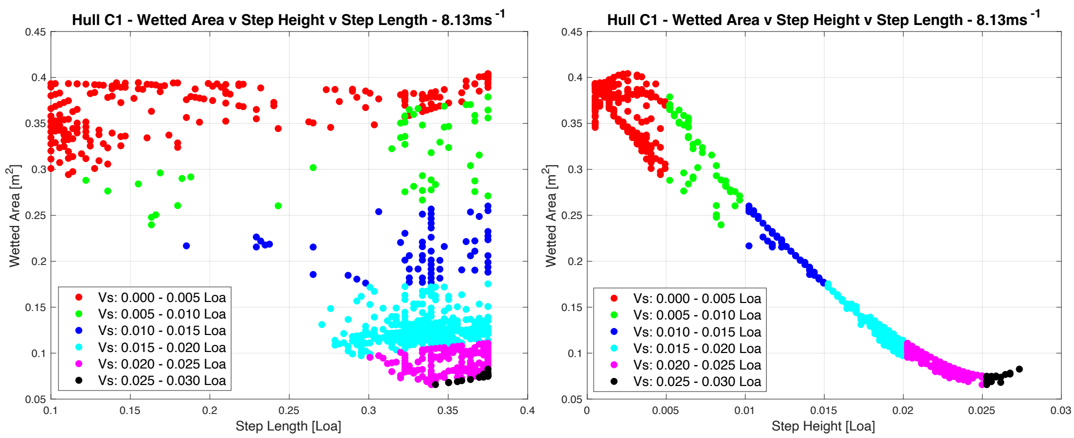

Figure 6.20 – 3D scatter graph of the wetted area design space for $8.13ms^{-1}$ (Viewed in 2D from the X & Y perspectives)

Once again, the familiar triangular point cloud is formed in Figure 6.19, with step height being found to be the most influential parameter. Step length is shown to have a small effect upon the wetted area of the single stepped hull. When Figure 6.20 is consulted it is seen that the step length has a larger impact at smaller step heights, as plotted in red and green. The relationship between step height and wetted area is almost linear, however it does not follow this trend for the large and small extremes.

This trend reveals why increasing step height tends to reduce resistance, as the frictional component of resistance is reduced due to the smaller wetted area.

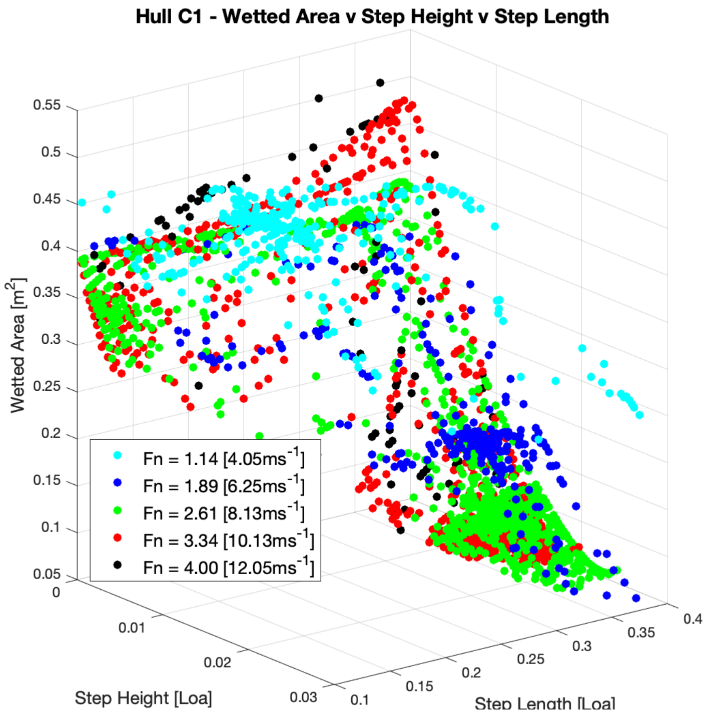

Figure 6.21 - 3D scatter graph of the wetted area design space for all speeds

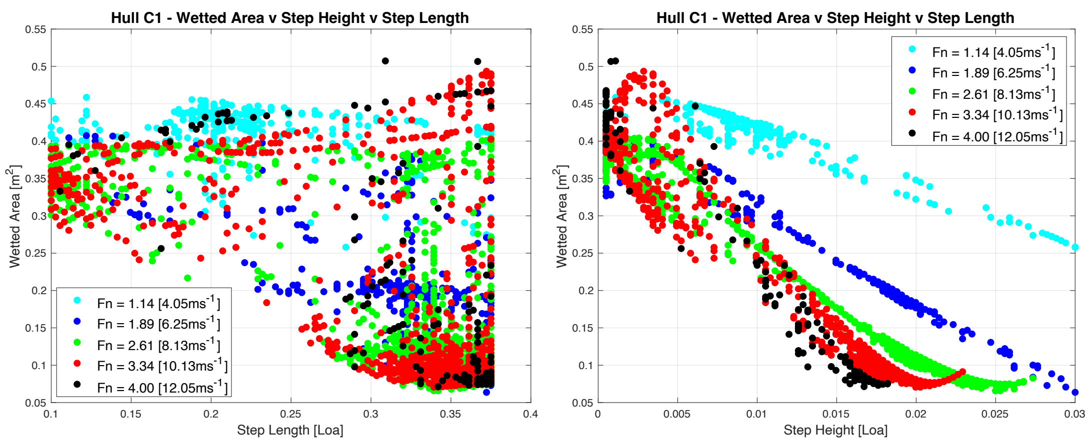

Figure 6.22 – 3D scatter graph of the wetted area design space for all speeds (Viewed in 2D from the X & Y perspectives)

In Figure 6.21 and Figure 6.22 the data from all the speed cases is plotted. These figures how reveal that the trends are similar for all speed conditions. As the speed increases the rate at which the wetted area decreases with step height increases. This is due to the fact that at higher speeds the rate of trim was seen to change more rapidly with step height, and the two factors are closely related.

Comparison with the analysis conducted on the resistance and trim shows that while reducing the wetted area is an important factor, this is not the only factor in play when minimising the resistance. The designs that produce the minimum wetted area are not seen to produce the minimum wetted resistance. They are found to produce a very high equilibrium trim position, increasing the pressure resistance. It can be seen that improving the hydrodynamic performance of stepped hulls is subject to many factors and is a complex multi-dimensional problem.

6.3.2.4 Influence of Response Variables on Resistance

To further explore the complex multi-dimensional problem the influence of the response variables on the resistance is investigated. This will help develop understanding of how these parameters are interlinked and reveal the trade-offs that must be considered when looking to reduce the resistance of a stepped hull.

While the input variables are factors that may be directly changed by the optimisation algorithm, affecting the hull geometry and influencing the resistance in this way, the response variables cannot be directly modified by a naval architect. They are instead the physical properties of the stepped hull in its equilibrium position. Studying these and their correlation with the resistance will offer insight into the desirable attributes of a stepped hull design that will reduce the resistance. The plots in this section are all considerably less complex than the 3D scatter graphs previously, so all speed conditions are presented simultaneously.

Trim is the first response variable to be investigated, as presented in Figure 6.23. It should be noted that this analysis differs from the previous discussion on trim which looked at the input variables affect the trim as opposed to the influence of trim on the resistance. The profile of trim against resistance follows the same trend for each speed. For the slower speeds this is compressed and for the higher speeds it is stretched. As the trim decreases so too does the resistance, until it reaches a minimum. If the trim reduces after it has reached this minimum the resistance increases rapidly, following an almost exponential profile. The initial decrease in resistance with reducing trim is due to a reduction in induced drag, whereas the sharp increase in resistance as trim decreases past its optimum value is accountable to the rapid increase in wetted area associated with low values of trim. This can be seen in Figure 6.25. The optimum trim value to minimise resistance is a balance between reducing the wetted area and reducing the induced resistance of the hull.

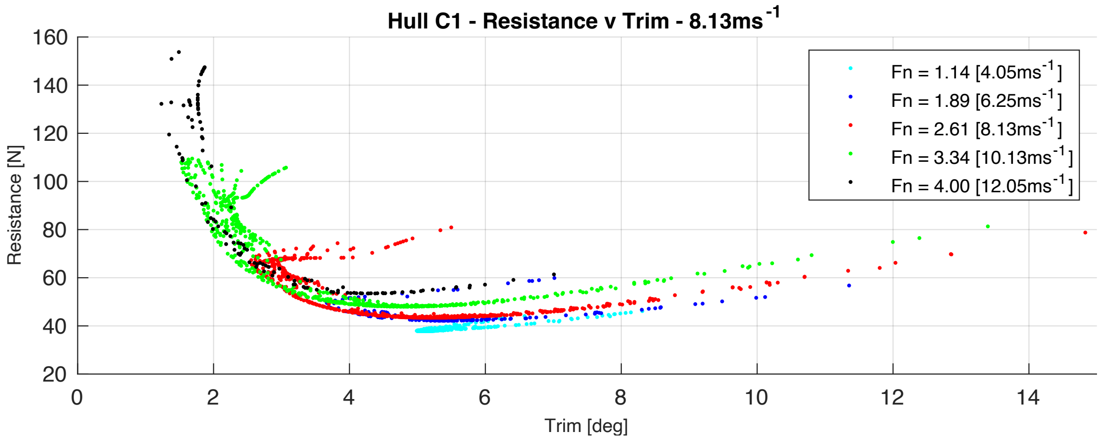

Figure 6.23 - Resistance vs trim Hull C

The second response variable to be investigated is the wetted area, as presented in Figure 6.24. As expected, it is seen that as wetted area reduces the resistance also reduces until it reaches a minimum value. After this minimum value the resistance is seen to rapidly increase. This is in-line with the previous analysis in which it was seen that the region in the design space that resulted in the minimum wetted area was also the location in which a resistance peak occurred. Reducing the wetted area has a far larger effect on the resistance at higher speeds. This is because frictional resistance is proportional to speed squared, so as the speed increases so too does the impact.

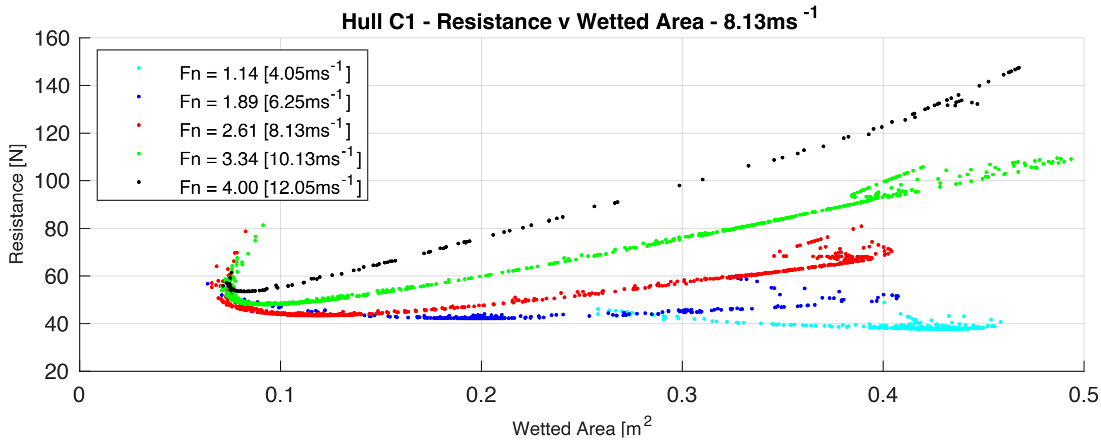

Figure 6.24 - Resistance v wetted area Hull C1

The corelation between trim and wetted area is detailed in Figure 6.25. This reinforces the finding that reducing the wetted area of a stepped hull is not the only objective when determining the step configuration, and instead a balance between pressure and shear drag has to be found.

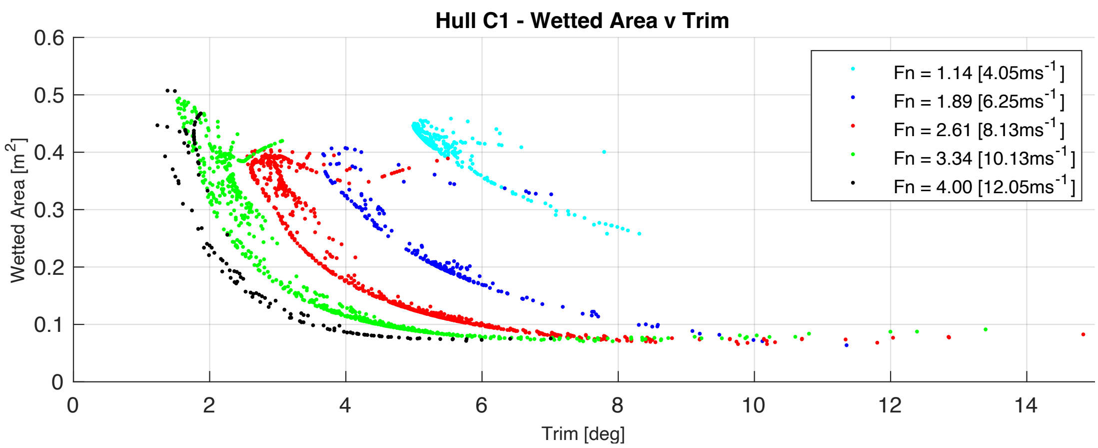

Figure 6.25 - Trim v wetted area Hull C1

In Figure 6.26 the effect contribution of the frictional component to total resistance is plotted. The size of the frictional resistance is measured as a percentage of total resistance. In general, the contribution of the frictional resistance component is seen to increase with speed, as has been found and discussed in Section 3.5.2.1.2. As the frictional resistance components relative size increases, the total resistance decreases to a minimum point. After this, as the frictional component continues to increase in relative size, the total resistance also increases. This is once again explained by the previously discussed play off between induced drag and wetted area. If the frictional component is relatively small, then the pressure component is relatively large indicating that the trim is large. As the trim reduces the size of the pressure component decreases, but this causes the wetted area to increase. There is an optimum point after which reducing the trim further, causes the wetted area to increase, therefor increasing the frictional components relative size. This leads to an increased total resistance.

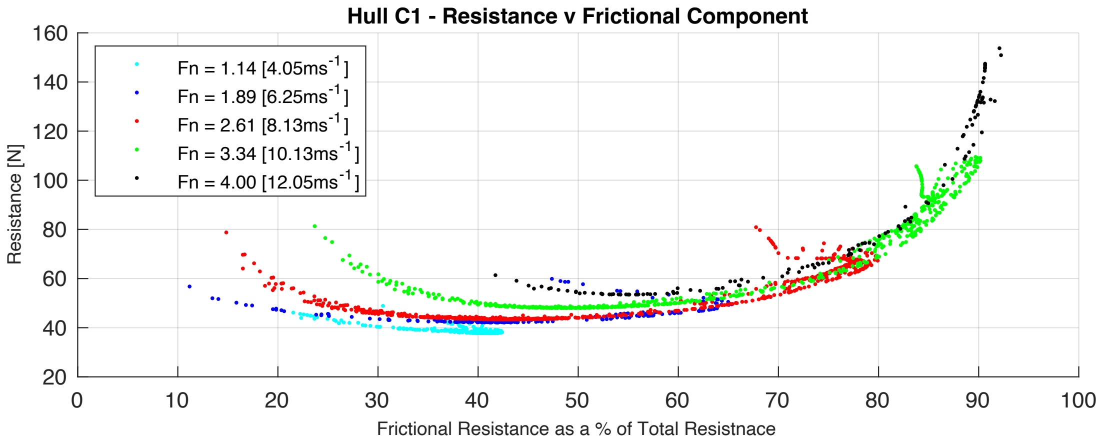

Figure 6.26 - Resistance v frictional resistance component Hull C1

6.3.2.5 Optimum and Worst-Case Hull Geometries

This section investigates the physical geometries that led to the optimum and worst-case solutions for each speed case. This reveals how the optimal design changes with speed, allowing designers to adapt a preliminary design to different design speeds. The properties of each hull are outlined in Table 6.4, while the geometries are presented in Figure 6.27 - Figure 6.31.

Table 6.4 – Variables for optimum & worst case single stepped hulls

	Total Resistance [N]	Gain / Loss [%]	Trim [deg]	Wetted Area [m^2]	VS [m]	VS [Loa]	LS [m]	LS [Loa]
Fn = 1.14 Baseline	38.61		5.26	0.42	0.020	0.01	0.62	0.31
Fn = 1.14 Optimum	37.79	-2.12%	5.06	0.43	0.016	0.008	0.40	0.2
Fn = 1.14 Worst Case	66.23	71.55%	12.14	0.35	0.001	0.0005	0.60	0.3
Fn = 1.89 Baseline	45.52		4.08	0.31	0.020	0.01	0.62	0.31
Fn = 1.89 Optimum	42.19	-7.31%	5.38	0.20	0.037	0.0185	0.65	0.325
Fn = 1.89 Worst Case	59.88	31.55%	7.02	0.33	0.001	0.0005	0.61	0.305
Fn = 2.61 Baseline	52.48		3.18	0.26	0.020	0.01	0.62	0.31
Fn = 2.61 Optimum	43.37	-17.36%	5.20	0.12	0.038	0.019	0.67	0.335
Fn = 2.61 Worst Case	80.90	54.15%	5.50	0.39	0.001	0.0005	0.75	0.375
Fn = 3.33 Baseline	66.11		2.46	0.24	0.020	0.01	0.62	0.31
Fn = 3.33 Optimum	47.97	-27.44%	4.80	0.09	0.036	0.018	0.70	0.35
Fn = 3.33 Worst Case	109.49	65.62%	1.69	0.49	0.004	0.002	0.75	0.375
Fn = 4.00 Baseline	83.37		2.03	0.23	0.020	0.01	0.62	0.31
Fn = 4.00 Optimum	53.47	-35.86%	4.38	0.08	0.033	0.0165	0.71	0.355
Fn = 4.00 Worst Case	153.74	84.41%	1.49	0.51	0.002	0.001	0.73	0.365

While the extent of the gain or loss in performance relative to the baseline design is seen to vary significantly with speed, the optimum and worst-case hulls have similar input parameters for all cases. It was noted in Chapter 6 that the Modified Svahn Method produced the least accurate results for the $4.05ms^{-1}$ speed case due to the Savitsky Wake Equations being far out of their range, and incapable of accurately modelling the longitudinal profile of the flow as it separated at the step. As such the results for this speed should be treated with caution. The step length for this speed is significantly shorter than that found for all other speed cases, however, follows the same trend of decreasing in length as the speed decreases. The step height for this speed is also seen to be significantly different than all other cases.

It is seen that in general a step height of 0.0165 – 0.019 Loa (0.033 – 0.038 m) and a step length of 0.325 – 0.355 Loa (0.65 – 0.71 m) results in the minimum resistance. In all cases the trim of the best-case design is larger than that of the baseline, however this follows the same trend of decreasing with speed. The increase in trim results in an increased pressure resistance for all cases.

In all cases the improvement in hydrodynamic performance results from a reduction in the wetted area that reduces the frictional drag components (as previously seen in Figure 6.24), while balancing the resulting increase in trim and thus pressure resistance. This is the key factor that influences the resistance of the stepped hull. When Figure 6.21 was previously analysed, it was found that the step height was the input parameter that has the largest influence over the wetted area, and therefore the resistance.

The worst-case hull for all speeds was found to have a small step height combined with a large step length. This combination maximised the wetted area and was the closest configuration to an unstepped hull that was possible given the constraints that were in place.

Figure 6.27 – $4.05ms^{-1}$ speed case (Left – Optimum, Right – Worst Case)

Figure 6.28 – $6.25ms^{-1}$ speed case (Left – Optimum, Right – Worst Case)

Figure 6.29 – $8.13ms^{-1}$ speed case (Left – Optimum, Right – Worst Case)

Figure 6.30 – $10.13ms^{-1}$ speed case (Left – Optimum, Right – Worst Case)

Figure 6.31 – 12.05ms^{-1} speed case (Left – Optimum, Right – Worst Case)

6.3.3 Summary of Design Trends of a Single Stepped Hull

From this investigation some key findings were made to improve the hydrodynamic resistance of a single stepped planing hull. Additionally, some recommendations are made as a starting point for the preliminary design of a single stepped hull.

- Step height had a greater impact on resistance than step length. This is the key parameter in improving performance and designers should carefully consider and investigate it.
- As the design speed increases, the step height that results in the lowest resistance decreases. The step length should increase with design speed.
- Step height has the largest influence on trim. Step length does have some influence and may be used to tune the trim of the vessel.
- Trim becomes more sensitive to step height as design speed increases.
- Step height is the most influential parameter on wetted area. Step length also has some influence on wetted area.
- The same trends are apparent at all speeds

To improve the hydrodynamic performance of a stepped hull the designer should look to reduce the wetted area of the hull. This has to be balanced with the resulting increase in trim, which will increase the pressure resistance. The optimum design is found by balancing the reduction in frictional resistance with the increase in pressure resistance.

Based on the analysis from this study it is recommended that a step height of 0.0165 – 0.019 Loa and a step length of 0.325 – 0.355 Loa be used as a starting point in the design of a single stepped hull operating between Froude numbers of 1.14 and 4.

These values were found to result in designs that performed well in calm water, with reduced resistance over other designs. As the design speed increases the design should be feature a reduced step height and increased step length.

6.4 Results – Hull C2 Investigation using CFD

The optimisation study for the double stepped hull considered a single speed, performing 67 design evaluations. A considerable data set of 1261 data points was developed. CFD is a computationally intensive performance prediction tool, with each analysis taking around 12 hours to complete. The automated workflow was hindered by limitations to a single Star CCM+ license and restrictions in use of the ARCHIE West HPC imposed upon academic users. These restrictions resulted in queue times of between 12 and 36 hours between runs due to extensive use of the computational resources and led to the study taking 3 months to complete. It should be noted that were the workflow be employed in combination with multiple Star CCM+ licenses and priority access to HPC facilities, as is standard in industry, a study may be completed in a feasible timeframe.

Candidate designs that were subject to proposing were identified by large oscillatory motions in the trim data and were considered invalid. In total 37 design evaluations were considered valid. The percentage increase or decrease in resistance as compared to the baseline design of the optimum and worst-case solutions are detailed in Table 6.5.

Table 6.5 - Optimisation study of Hull C2

Speed [ms^{-1}]	**8.13**
Optimum Resistance [N]	48.83
Optimum Resistance Percentage Reduction	5.61%
Worst Case Resistance [N]	67.46
Worst Case Resistance Percentage Gain	38.93%

The study successfully improved the performance of the double stepped planing hull by 5.61%. The baseline design, Hull C2, was based on the Union Internationale

Motonautique (U.I.M) Powerboat P1 racing boats (Taunton, Hudson and Shenoi, 2010). As Hull C2 is based upon an existing, production double stepped racing vessel, it is reasonable to assume that the design has already undergone significant design work to ensure it is a hull that performs well. A reduction of 5.61% in calm water resistance of racing hull is a significant improvement, showing that the application of the tools developed in this thesis may be employed to improve the hydrodynamic performance of stepped hulls.

The resistance of each candidate hull is plotted with its respective evaluation number in Figure 6.32. The red line on the graph shows the optimum design path for that evaluation. It starts at the baseline design and then connects each subsequent optimal design until the final solution is found.

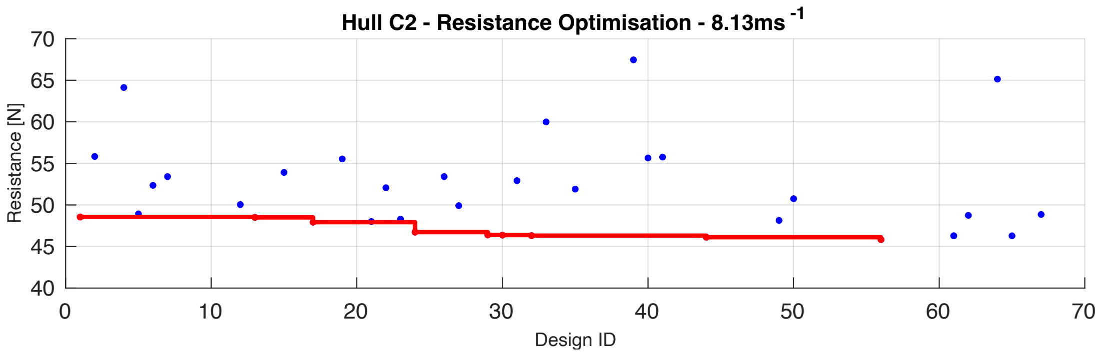

Figure 6.32 - Resistance history for Hull C2 optimisation

What is very notable from when analysing Figure 6.32 is the range of resistances. The worst-case design resulted in a resistance gain of 38.93%, and several other candidate hulls that resulted in an increased resistance. This really highlights the need to undertake a design study, and if possible, an optimisation study to ensure that an appropriate design is found.

Figure 6.33 presents the search path of the optimisation algorithm, plotting design performance of the best hull as the optimisation progresses against the evaluation number. The SHERPA method is seen to once again be extremely efficient, resulting in major resistance reductions in 30 evaluations. After these, smaller incremental gains are found. As only 67 evaluations were carried out it is not reasonable to consider the final solutions to be the optimal design. Had more evaluations been possible it is likely that further small incremental gains would have been made. Given the performance of the SHERPA search algorithm in the more extensive single step optimisations (as detailed in Figure 6.8), is reasonable to consider the final design to be near optimal.

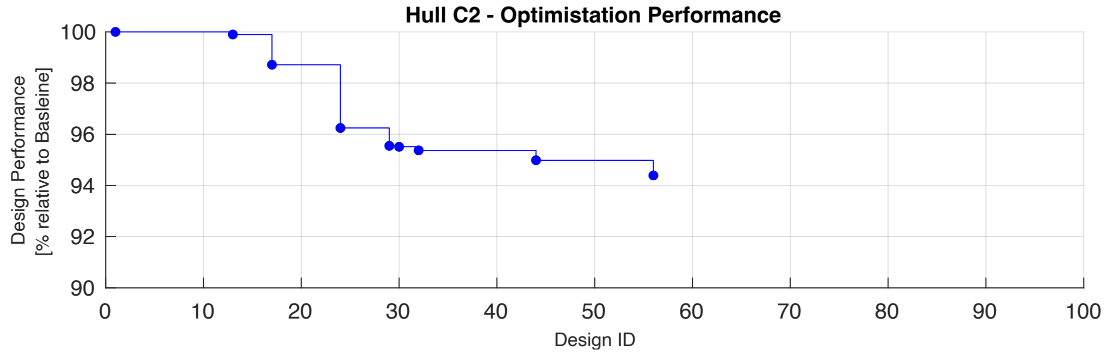

Figure 6.33 – Optimisation performance for Hull C2

6.4.1 Design trends of a double stepped hull

The analysis of the design trends investigates the same factors as for the single stepped hulls, however the plots and figures presented are not the same. This is for two reasons; firstly, there is fewer design evaluations for the double stepped hull and only one speed case was considered. Secondly, while there was two design variables for the single stepped hull, there are four design variables for the double stepped hull. For the single stepped case 3D scatter graphs were used to visualise the design space, plotting the response variable against the two input variables. In the present study parallel coordinate plots are employed due to the increased number of input parameters. These are an effective method of visualising and analysing high-dimensional datasets.

The section will first investigate the input variables and their impact upon resistance, trim and wetted area, before going on to study the response variables and their effect upon the resistance.

6.4.1.1 Influence of Input Variables on Resistance

The four input variables (first step length, second step length, first step height, and second step height) and the one objective variable (resistance) are plotted on a parallel coordinate plot for all valid design evaluations in Figure 6.34. This allows the resistance design space to be easily visualised and analysed, with trends in the resistance that is linked to this multivariant problem becoming apparent. In order to further visualise the trends, the results are broken down into their performance quartiles, and coloured appropriately. The full dataset is ranked by resistance, and then broken down into four new data sets each containing 25% of the design evaluations. The first quartile of these contains the most successful designs, while the fourth quartile contains the least successful. Additionally, the baseline design and optimum design are plotted.

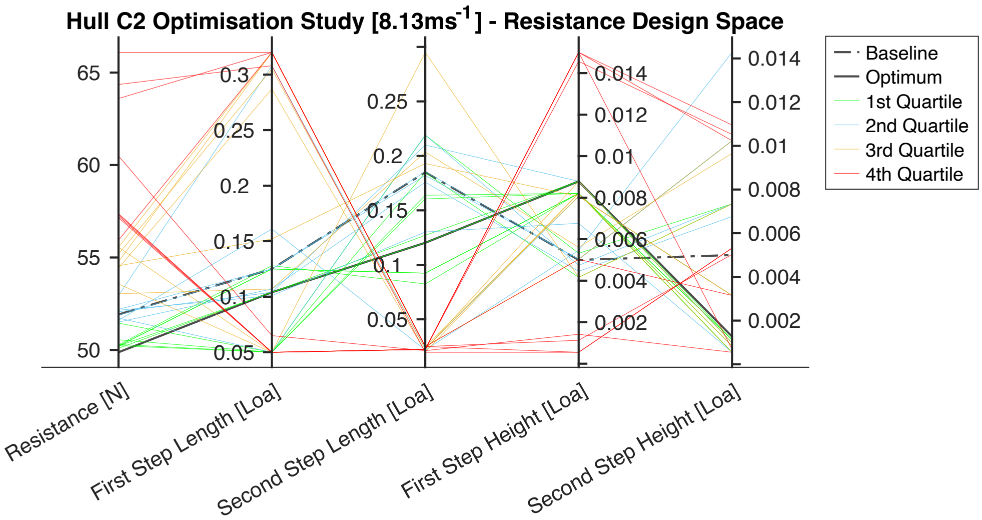

Figure 6.34 – Input Parameters v Resistance [Hull C2]

Figure 6.34 shows the relationship between the resistance and the input variables. It can be seen that the top 25% of design evaluations (plotted in green) tend to follow the same design principles, with similar values for each parameter. The same cannot be said for the lower ranked designs, for which there is considerable variation in input variables that result in a similar level of performance. As the performance decreases, the spread in variables is seen to grow, so it can be said that as the optimisation progresses and better designs are found, the input parameters converge to an extent and there is less spread.

It is not possible to associate particulate trends in individual input variables with resistance. For instance, it can be seen that while the some of the better performing designs have a very small first step length, so too do some of the worst performing designs. The interaction between the four variables is very complex and an optimum design may not be found by focusing upon one of them individually. To demonstrate this further, 2D plots for each the resistance against each individual input parameters are presented in Figure 6.35 to Figure 6.38. These are similar to the 2D relation plots presented for the single stepped optimisation, in which clear relationships were seen. In the present figures there is no obvious relationships seen for the individual input variables.

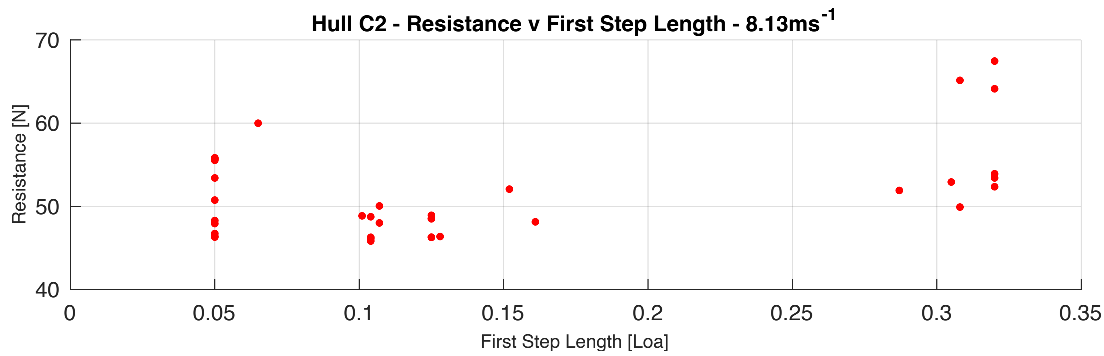

Figure 6.35 - Resistance vs first step length [Hull C2]

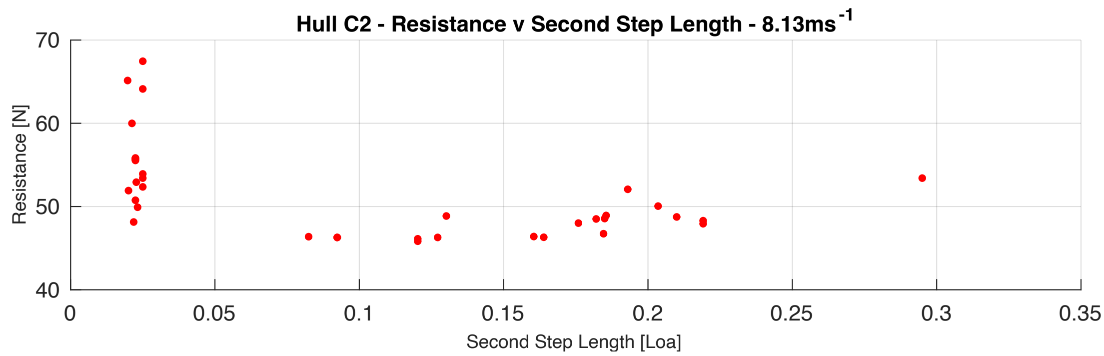

Figure 6.36 - Resistance vs second step length [Hull C2]

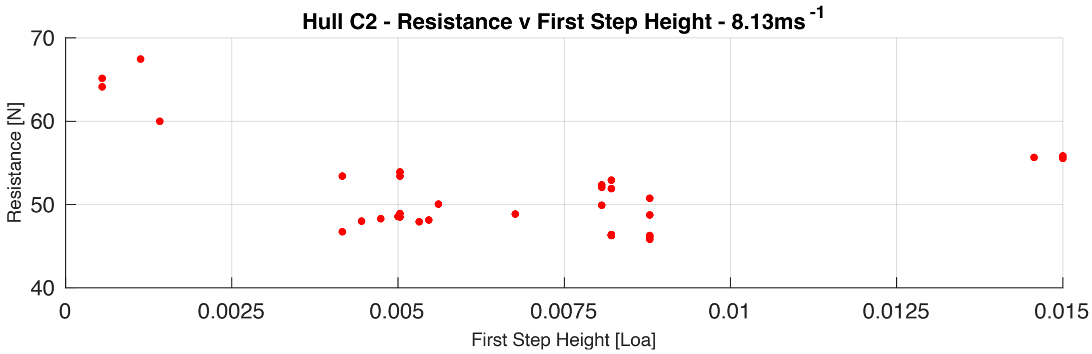

Figure 6.37 - Resistance vs first step height [Hull C2]

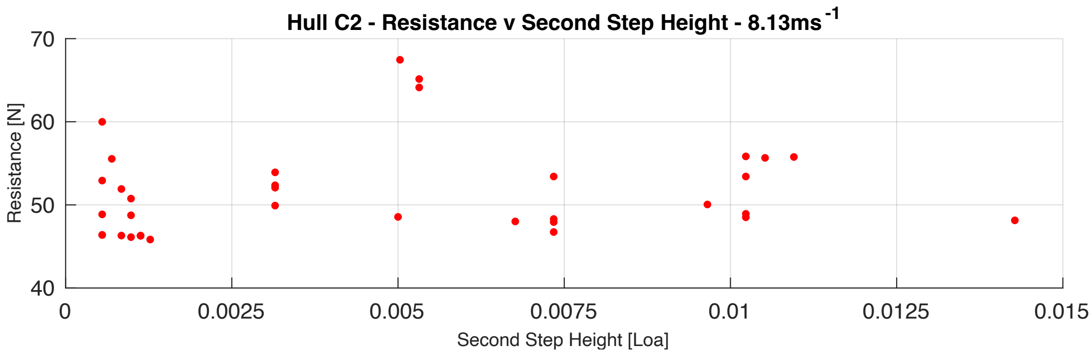

Figure 6.38 - Resistance vs second height [Hull C2]

As no clear relationships were apparent in the analysis of the input variables it was difficult to comment on the influence of each, and determine which ones were key to improving the performance of double stepped hulls. More detailed analysis was undertaken by employing a Boruta analysis to determine the relative influence of each input parameter. The Boruta analysis is an intelligent algorithm for finding 'all relevant variables' that have influence within a dataset. For further details on this algorithm please refer to (Kursa and Rudnicki, 2010). The analysis provides insights into variable sensitivities for better understanding of the design and the design space and allows the determination of the extent to which each design variable affects the response. The Boruta analysis calculates importance values, where higher values indicate more importance, or more effect on the response. It should be noted that these importance values are only significant relative to each other.

This analysis was undertaken for the resistance design space, with the results presented in Table 6.6. The most influential parameter was found to be the first step height. This is in line with the findings of the single stepped hull where it was seen that step height resulted in the largest variations in resistance. The second most influential is the length of the second step. This factor determines the location of the second step and will have a large impact upon how the flow intersects with the afterbody. All importance values were above the threshold value of -0.26, indicating that they all some effect upon the resistance.

Table 6.6 – Boruta importance analysis – Resistance

Input Variable	Importance Value
First Step Length	-0.25
Second Step Length	0.66
First Step Height	2.00
Second Step Height	-0.22

To simplify the complex relationships between each of the individual input variables and produce some insight which may be applied by designers, more global design traits were studied. This allows the identification of traits that may be produced through the multiple different combinations of the individual parameters to produce the similar results. To this end, the input variables were simplified to combined step length, and combined step height and presented in Figure 6.39. Additionally, the aspect ratio of each of the steps is plotted against resistance in Figure 6.40.

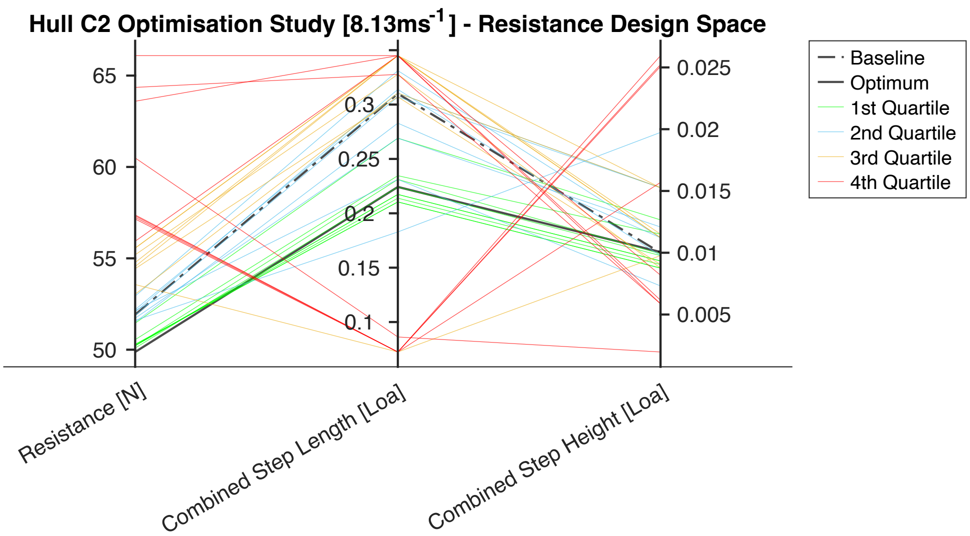

Figure 6.39 – Combined Input Parameters v Resistance [Hull C2]

When Figure 6.39 it examined it is seen that considering combined step height and length reveals design traits that improve the hydrodynamic performance, which may be produced by the multiple combinations of the individual variables. The results of the fourth quartile are ignored in this discussion as they do not follow these trends.

The combined step length is an important factor, with a clear influence on resistance. Reducing the combined step length lowers the resistance of the hull. This increases the trim of the hull and achieves a reduction in resistance by decreasing the wetted area of the hull, as presented in Figure 6.41. When the outliers of in the fourth quartile are ignored, there is no data available for combined step lengths of less than 0.2 Loa. At values lower than this the trim angle required for the forebody flow to intersect with the afterbody becomes too large and introducing longitudinal instability to the hull, resulting in porpoising. Designs that were subject to porpoising were considered invalid and are not included in the analysis. This imposes a limit on the reduction in resistance that is available by reducing the combined step length. When employing this strategy to improving the performance of double stepped hulls designers should take care to conduct appropriate analysis to ensure that it does not result in a hull that is prone to porposing.

The relationship between combined step height is less clear, however reducing the step height generally results in a lower resistance. It is noted that these relationships are linked to each other, and as the search algorithm homed in on specific designs. As a result, several combinations have not been created and it is not possible to comment upon them, aside from the fact that as the optimisation has avoided them it is unlikely that they would produce favourable results.

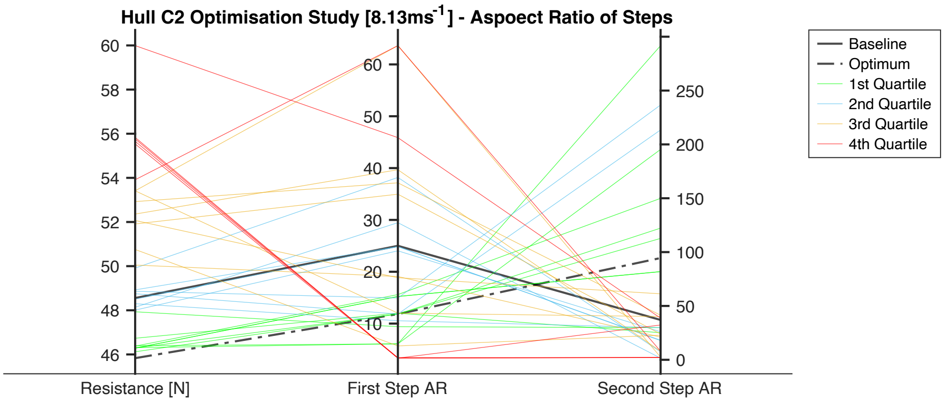

Figure 6.40 – Step Aspect Ratio v Resistance [Hull C2]

$$AR = \frac{Step\ Length}{Step\ Height} \tag{6.2}$$

Figure 6.40 simplifies the complex relationships between each of the individual input variables by reducing them to aspect ratio for each of the steps, as defined by Equation (6.2). The configuration of the first step was far more influential on the resistance, with a clear trend showing that reducing the aspect ratio of the first step reduces the resistance. This relationship is due to the fact that the first step has a large influence over the portion of the midhull that is wet. Reducing this wetted area of the midhull improves the performance of the double stepped hull by decreasing the frictional resistance component. The aspect ratio of the second step is far less influential.

6.4.1.2 Influence of Response Variables on Resistance

The final variables to be investigated to determine their relationship was the response variables. These are not directly modified by the optimisation algorithm, however analysing them reveals the conditions that are desirable to minimise the resistance. These conditions are achieved through the appropriate choice of geometry, as defined by the input variables.

The effect of trim and wetted area upon resistance is plotted in Figure 6.41. This figure shows that as the trim increases the resistance tends to decrease. This is not a linear relationship, and after an optimum value of trim the resistance increases again. The critical trim above which porpoising occurs is around 5.8 degrees for this case.

Wetted area is revealed to be the key parameter in minimising resistance, and it very desirable to design a hull that has small wetted area. The lowest wetted area's however, do not result in the lowest resistances. This is similar to the trends that were identified for the single stepped hull, where the reduction in wetted area has to be balanced with the increased pressure resistance resulting from the increase in trim.

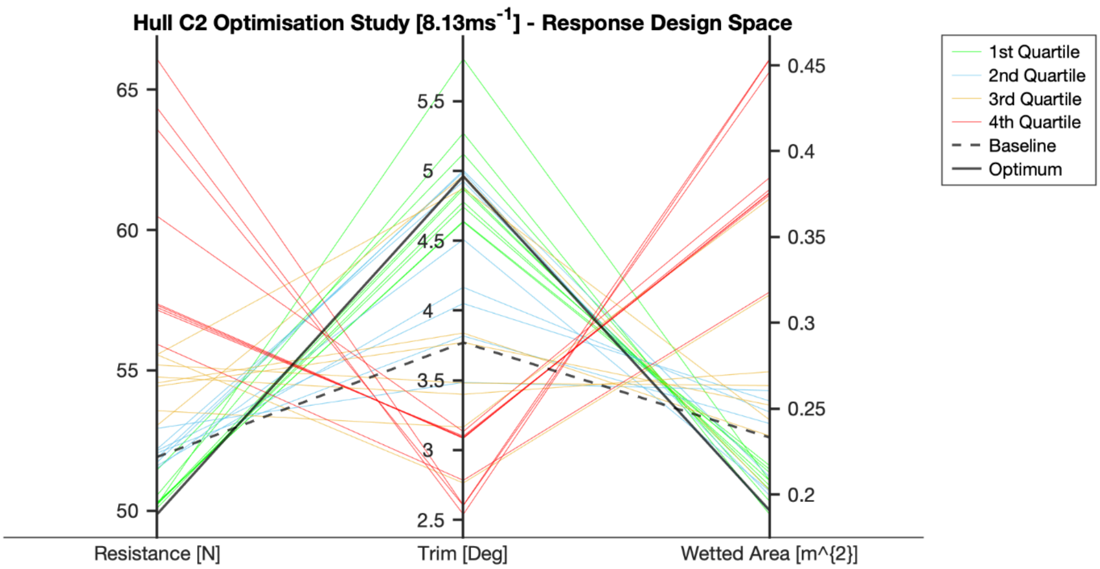

Figure 6.41 –Resistance against Response Variables [Hull C2]

6.4.1.3 Optimum and Worst-Case Hull Geometry

The final section of the analysis investigates the physical geometries that led to the optimum solution, and to the worst-case solution. Each of the hull's properties are outlined in Table 6.7, while the geometries and their associated wetted hulls are presented in Figure 6.42 and Figure 6.43

Table 6.7 – Variables for optimum & worst case double stepped hulls

Input Variable	Optimum Hull	Worst Case Hull
First Step Length [m]	0.21	0.61
Second Step Length [m]	0.24	0.04
Combined Step Length [m]	0.45	0.65
First Step Height [m]	0.018	0.001

Second Step Height [m]	0.003	0.011
Combined Step Height [m]	0.020	0.012

The optimisation of the double stepped hull resulted in a total resistance reduction of 5.61%. This was achieved through an 18.24% reduction in the wetted area, which led to a 14.21% decrease in the frictional resistance. As a result of the changes the trim increased from 2.74 degrees to 3.94 degrees, leading to an increase in the pressure resistance of 4.20%.

The geometry that resulted in the lowest resistance for this specific hull at this specific speed operated in a mid-body dry condition, functioning as a single stepped hull would and detailed in Figure 6.42.

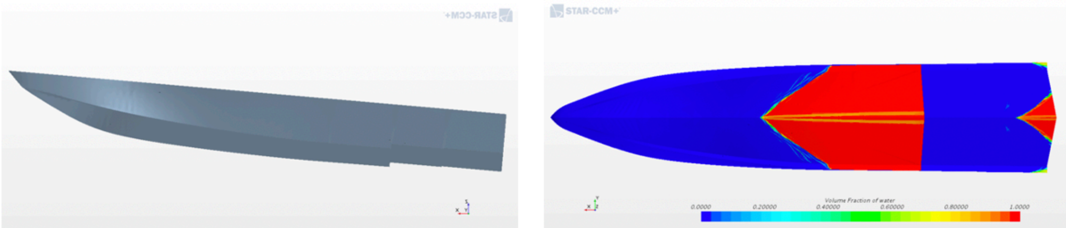

Figure 6.42 - Optimum geometry – double step optimisation

The first step length and second step height such that the forebody flow did not intersect with the midbody. When the hull is operating in this condition it is the combined step length and height that should be considered as the mid-body does not contribute to the hydrodynamic performance of the hull. A first step with a low aspect ratio is likely to result in this condition, or to reduce the wetted area of the midbody in cases in which it does intersect with the forebody flow.

The experimental data of the baseline hull showed there to be little difference in the resistance of the single and double stepped configurations for the $8.13ms^{-1}$ speed case (Taunton, Hudson and Shenoi, 2010), producing a total resistance of 51.25N and 51.01N, respectively. Numerical analysis in Section 4.5.2 revealed that the forebody flow of Hull C2 only marginally intersected with the midbody. One of the reasons for selecting this speed case for the present study is that the search algorithm could increase or eradicate the wetted portion of the midbody, establishing the step configuration that may be considered optimum. The single stepped configuration was found to produce the best case results in this case. In a study of nine double stepped hull variants by (Di Caterino *et al.*, 2018) the authors concluded that reducing the first step length, and increasing the step height produced the lowest resistance. This is the configuration that either eradicates, or minimises wetted area of the midbody and is in agreement with the finding of the present study.

The worst-case configuration resulted in a resistance increase of 34.15%. The frictional resistance increased by 74.25% as a result of a 94.40% increase in wetted area while the pressure resistance reduced by 11.61% as a result of the decreased trim.

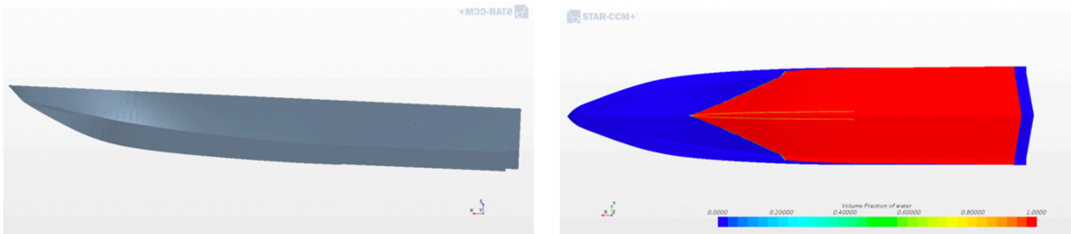

Figure 6.43 – Worst case geometry – double step optimisation

The worst-case hulls geometry closely resembles the geometry of an unstepped hull, as seen in Figure 6.43, however there are some key changes that degrade the performance further. The unstepped variant of the baseline hull (Hull C), had a resistance of 59.07N at a speed of $8.13ms^{-1}$ where this worst-case variant had a resistance of 65.14N. This design was not a desirable configuration and was a product of the constraints that were put in place.

The second step was located near the aft of the hull with a large step height. As a result, the midbody flow didn't not intersect with the afterbody. The first steps height was the smallest allowable height of 0.0005 Loa. The flow did not separate separate at the first step as the inlets to be covered by the wake. This sharp discontinuity introduces large degrees of turbulence and vorticity in the flow, increasing the resistance significantly.

6.4.2 Summary of Design Trends of a Double Stepped Hull

From this investigation some key findings were made that may be employed by designers looking to improve the hydrodynamic resistance of double stepped planing hulls.

Due to the number of variables and the interaction between these there are several combinations that may achieve the same resulting conditions. The height of the first step height was the most influential on the resistance, however variables should not be considered individually, and the global effects of a specific combination of parameters should be considered in all cases.

The best strategy to improve the hydrodynamic performance of double stepped hulls in calm water is to reduce the wetted area. This is achieved by increasing the ventilation lengths, which increase the trim of the vessel. The key to finding the best performing hull is to balance the reduction in wetted area with the increased trim.

It is also found that proposing impacted a large number of prospective designs and was a limiting factor. Designs that had a trim larger than a critical value were subject to porpoising. This is an important aspect and the longitudinal stability of any prospective design must be investigated appropriately.

The wetting of the midbody was found to be an important factor. It is controlled through the aspect ratio of the midbody. Where calm water performance is the sole focus, a midbody dry condition results in lowest resistance for the hull that was studied. A complete design process should consider the effects of this upon the seakeeping and manoeuvring characteristics of the hull, and there will be a need to make further design compromises. In cases where the length to beam ratio is larger midbody wetting is a powerful tool to control the trim of the vessel while reducing the wetted area. In such cases operating with a single step configuration would require excessively large step heights, and thus large trim angles to achieve sufficient ventilation lengths to minimise the wetted area.

The relationships that were established by simpler single stepped study were all seen to hold true for the double stepped case, and the same underlying principles should be utilised to improve the hydrodynamic performance.

6.5 Conclusion

This chapter set out to establish how the hydrodynamic performance of single and double stepped hulls in calm water may be improved. The analysis tools developed in the previous chapters were coupled with a fully automated optimisation workflow. Large-scale studies of the design space were conducted, providing valuable data whist also determining a best-case design for each condition. Analysis of the large dataset and the step configurations that resulted in the lowest resistance allowed design trends to be identified that improve the hydrodynamic performance. The knowledge developed in this chapter may be employed by designers of stepped hulls to improve upon an existing design, or as a starting point to quickly develop a preliminary hull form that performs well.

In every case the investigation was able to determine a step configuration that that reduced the resistance in comparison to the baseline design. The hydrodynamic performance of a single stepped hull was improved by between 2.12% and 35.86% over a range of speeds, while a double stepped hull was improved by 5.61% for a single speed.

Analysis of the large dataset for the single stepped hull study revealed that to improve the hydrodynamic performance of a stepped hull the designer should focus upon reducing the wetted area of the hull. Strategies that reduced the trim tended to increase the trim, and it is important to balance these two factors to prevent the increase in pressure resistance outweighing the decrease in frictional resistance. Step hight has a more significant impact on resistance than step length as this parameter directly controls the ventilation length, and thus the wetted area of the afterbody. As the design speed increases, the step height that results in the lowest resistance decreases as the ventilation length elongates with speed, while the step length should increase with design speed. Based on the analysis from this study it is recommended that a step height of 0.0165 – 0.019 Loa and a step length of 0.325 – 0.355 Loa be used as a starting point in the design of a single stepped hull operating between Froude numbers of 1.14 and 4.

For the double stepped hull there were four design variables as opposed to two, with the interaction between these meaning that there are several combinations which may achieve similar resulting conditions. It was found that it was more beneficial to consider the global effects of a specific combination of parameters as opposed to the individual parameter. Similar trends were found for the double stepped hull to those established for the single stepped hill, and it was once again revealed that step hight was the most influential design parameter. Midbody wetting was shown to be an important factor which was controlled through the aspect ratio of the midbody. Where calm water performance is the sole focus, a midbody dry condition results in lowest resistance for the hull that was studied. It was also noted that porpoising effected many the prospective designs. This is identified as a topic worthy of further investigation in future studies as the longitudinal stability is an import design consideration.

The same underlying principles may be applied to improve the performance of any given stepped hull, however the specific changes to the step configuration that will achieve these principles may vary from hull to hull.

In all cases there was a very large variation in the performance of different step configurations, with large numbers of candidate hulls performing worse than the base line design. This spread in performance really highlights the importance of evaluating a number of to ensure that the design is suitable.

Employing both the modified Svahn method and CFD highlighted the benefits of each of these tools. The modified Svahn method was fast, allowing many designs and conditions to be evaluated. A large amount of data was developed, and it was easy to establish trends from these large data-sets. CFD on the other hand was very computationally expensive and time consuming. The analysis took considerably longer to compete, and the dataset was far smaller. In the preliminary design phases it is recommended to employ a rapid analysis tool such as the modified Svanh method to establish a suitable baseline design, before utilising higher fidelity tools such as CFD to give a comprehensive analysis of prospective designs and improve the hydrodynamic performance further.

Chapter 7 – Conclusions and Future Research

This chapter summarises the main findings and outcomes of each of the studies completed over the course of this thesis. The contribution each chapter makes to the existing knowledge is discussed, and a clear demonstration detailing how the research aims and objectives have been achieved is provided. Finally, recommendations are presented outlining interesting topics for future research that became apparent over the course of this thesis.

7.1 Conclusions

The research question that this thesis set out to address was:

"How can we enhance and accelerate analysis techniques for stepped hulls through knowledge developed from numerical simulations and can hydrodynamic performance be improved through the application of these tools."

It was found that by developing knowledge of stepped hulls through analysis of numerical simulations, it was possible to enhance and accelerate analysis techniques. This was achieved by developing novel approaches to model the interaction of forebody flow with the afterbodies, ensuring the complex wetted area, and thus the fluid forces, were modelled accurately. Analytical models were proposed for single and double step configurations, which were subsequently evaluated against experimental data. The proposed model for single stepped hulls calculated the resistance with an average error of 2.50%, while the proposed model for double stepped hulls achieved an average error of 1.29%. This is a significant improvement over the accuracy of models currently available in the literature.

It was shown that it was possible to apply these tools to improve the hydrodynamic performance of stepped hulls, with significant reductions in resistance being achieved. By using the analytical and numerical tools developed over the course of this thesis to drive an automated optimisation workflow, the hydrodynamic performance of a single stepped hull was improved by between 2.12% and 35.86% over a range of speeds, while a double stepped hull was improved by 5.61% for a single speed. While determining the degree to which the performance of a stepped hull may be improved through optimisation was interesting, the real value of this work lies in the large data set that the procedure produced. The data generated was analysed, developing relationships between the design parameters and establishing trends in step design that are linked to better performance. This knowledge and the relationships may be applied by the designer of any stepped hull to improve the performance.

By seeking the answers to the research question significant contributions were made to the available knowledge of stepped hulls and the main aim of this thesis was achieved:

"To develop enhanced analysis techniques for stepped hulls and apply these tools to determine how the hydrodynamic performance may be improved"

To accomplish this main aim, a number of research objectives had to be addressed through the novel studies within each chapter. The first of these specific objectives was achieved in Chapter 2.

"To ***conduct*** *a review of the available literature on analysis and performance prediction of unstepped and stepped planing hulls"*

The Critical Review put forward in Chapter 2 addressed this objective, presenting a broad ranging review of the current methods for the hydrodynamic analysis, performance prediction and strategies to improve the performance of stepped and unstepped hulls. A discussion on each of the analysis techniques was presented, with the historical development of research into unstepped and stepped planing hulls being detailed. In addition, a focused literature survey detailed the specific areas to be examined by the studies presented throughout this thesis. During this literature review gaps in the available literature were identified and presented, with the following studies of this thesis setting out to address these gaps

The second objective was achieved in Chapter 3:

*"To **enhance** the accuracy with which stepped and unstepped hulls may be modelled by unsteady RANS simulations, employing this tool to **develop** understanding of the flow characteristics of stepped hulls"*

In Chapter 3 a CFD unsteady RANS set-up that was capable of accurately modelling unstepped, single and double stepped hulls that was developed. This tool was employed in Chapter 3, 4 and 6 to study stepped hulls and develop understanding of their flow characteristics. Exploring the use of more computationally expensive wall treatments to resolve the entire near wall turbulent boundary layer was identified as a promising method to enhance the accuracy of these simulations. A broad study was conducted, concluding that for unstepped planing hulls a low y+ approach significantly increases the accuracy, lowering the average error from 7.21% to 2.54% when validated against experimental data. The low y+ aproach enhanced the accuracy as the transport equations are solved all the way to the wall cell with the wall shear stress being computed as in laminar flows as opposed to relying upon empirical equations to satisfy the physics of the flow in the near wall region. Before employing this approach, the impact to the computational expense must be considered as the extra resolution required in the prism layer mesh increased the total cell count by 33.16%, and the overall solver CPU time by 25.29%. For stepped hulls it was found that the low y+ approach introduced errors though an increased level of numerical ventilation. The error in the resistance calculation increased by an average of 2.60% for single stepped hulls and 4.49% for double stepped hulls.

The third objective was achieved in chapter 3:

*"To **quantify** the effects of Numerical Ventilation and **develop** understanding of how the phenomena influences the results of a simulation"*

Numerical Ventilation was identified as one of the largest sources of error in numerical simulations of planing hulls, yet the phenomena is not addressed by the research available in the literature. A study was undertaken to quantify the impact of numerical ventilation, giving users of CFD a reference for how much the resistance is reduced by this phenomenon. By quantifying the effects of this error more confidence is gained in the same manner as assessing the numerical errors arising from temporal and spatial discretisation in the verification process. The resistance of well set up high y+ simulation of an unstepped hull, in which strategies were employed to minimise numerical ventilation, was found to increase by an average of 0.60% when numerical ventilation was eradicated, despite there being no visible streaking in the VOF plots. Simulations of stepped hulls were found to contain more numerical ventilation, with the high y+ simulations of single stepped hulls being increased by 2.12% when numerical ventilation was irradicated, while the increase for double stepped hulls was 4.72%. Stepped hulls are more susceptible to numerical ventilation due to the fact that the mid and aft hulls are intersecting with disturbed flow and there is a much greater change of air being transported into the near wall cells. The low y+ approach was found in all cases to increase the level of numerical ventilation, with an average impact on resistance of 4.72% for a single stepped hull. This increase arises from the greater number of prism layers required to ensure that the centre of the wall cell is located in the viscous sublayer. Prism layer cells are not aligned with the flow, with the freesurface crossing them at an angle. This results in increased numerical diffusion, which is aggravated by increasing the number of prism layer cells. This finding is in agreement with the conclusions of (Gray-Stephens, Tezdogan and Day, 2021).

The fourth objective was achieved in chapter 3:

*"To **evaluate** the effects that the introduction of steps has upon the performance of a planing hull and **investigate** the mechanisms through which a reduction in resistance is achieved"*

To properly take advantage of stepped hulls the mechanisms through which they achieve a reduction in resistance must be properly understood. A study into the hydrodynamic characteristics of stepped and unstepped hulls was undertaken using the previously developed CFD tool. Steps were shown to be beneficial at Froude numbers of 1.93 and above, with the benefits of stepped hulls increasing with speed. A reduction of 25.85% in resistance was found at a Froude number of 4.00, the maximum speed that was examined. The performance improvement was achieved entirely through a reduction in the shear forces, while the pressure forces were found to increase. The reduction was dependent upon speed, increasing from 12.93% at a Froude number of 1.58 to 45.52% at a Froude number of 3.80 for the single stepped hull. At higher speeds the ventilation length of the flow aft of the step is larger as the longitudinal profile of the free surface elevation elongates, reducing the wetted area of the aft hull. It was concluded that establishing strategies and designing step configurations to minimise the wetted area offered promising means to improve the performance of stepped hulls further, and is a key consideration to investigate during the preliminary design phase

The fifth objective was addressed in Chapter 4:

*"To **extract** and **analyse** the fluid flow as it separates aft of a step, investigating the accuracy of various means of modelling this"*

Researchers attempting to develop an analytical performance prediction method for stepped hulls have reported significant inaccuracies introduced to their models through an inability to accurately model the freesurface elevation aft of each of the steps, highlighting this as an active area that requires further research. Modelling the flow aft of a step is essential to determine the wetted area of the afterbody and calcite the subsequent forces that are acting upon the hull. An experimental study was conducted to generate validation data and it was shown that CFD was an accurate and robust tool in modelling the freesurface elevation aft of a planing surface. The fluid flow under a stepped hull then extracted from CFD simulations and an investigation into the freesurface elevation of the fluid as it separates aft of a step and the interaction of forebody flow with the mid and afterbodies was undertaken. Two methods of modelling the free surface elevation aft of a step were evaluated. Stavisky's Wake Equations were shown to be accurate in calculating the freesurface elevation of the fluid flow aft of the fore hull, resulting in an average error of 5.45% for the CL point of intersection and 8.10% for the QB for the single stepped case, while this increased to 11.66% for the CL profile, and 9.73% for the QB for the double stepped case. Additionally, Savitsky's Wake Equations were shown to be capable of accurately modelling the flow when applied out with their intended range. The speed coefficient was found to be the limiting parameter, with the accuracy decreasing below a speed coefficient of 3.37. These equations were not appropriate for calculating the flow aft of the second step, however it was noted that the wetted portion of the mid hull was small for the geometry in this study, so the flow was not fully developed. Flow aft of the second step was well modelled by the Linear Wake Assumption, resulting in an average point of intersection error of 16.51% for the CL and 16.17% for the QB.

The sixth objective was addressed by Chapter 4 & 5:

*"To **enhance** the knowledge of the composition of the wetted area of a single and double stepped hulls, **proposing** procedures to calculate each wetted component"*

Further analysis of the fluid flow extracted from the CFD simulations revealed that for single stepped hulls there were two possible operating conditions, resulting in two distinct wetted area compositions. The flow of double stepped hulls was far more complex, with four possible operating conditions. Accurately modelling the wetted area of a stepped hull and accounting for the additional side wetting of the chines dry condition was highlighted as an important aspect of any analytical model as this area generates lift and contributes to the pressure and shear components of resistance. Analysis showed there to be little wave rise where the afterbody intersected with the wake hollow of the forehull and ignoring its presence results in a good approximation to calculate the wetted area of the afterbody. Procedures that were capable of modelling the wetted area of both single and double stepped hulls were developed, considering the interaction of all aspects of flow. These were shown to provide good accuracy when adopted by the proposed analytical performance prediction developed in chapter 5, showing them to be successful.

The seventh objectives were achieved by Chapter 5:

*"To **propose** and **evaluate** novel semi-empirical performance prediction methods through the application of the developed understanding of the flow characteristics of stepped hulls"*

Chapter 5 outlined the development of novel semi-empirical models for the performance prediction of single and double stepped hulls. These models utilised the knowledge of the flow and wetted areas of stepped hulls as developed over the course of this thesis. This ensured that the appropriate methods were used to determine the freesurface elevation aft each of steps and that that the models were capable of considering all possible operating conditions of stepped hulls, and accounted for additional components of the wetted hull, such as the side wetting. Due to the inability of the Stavisky Wake Equations to accurately model the flow for speed coefficients of less than 3.3, the proposed models were inaccurate for the lowest speed evaluated. For all other speeds however, both the single and double step models were shown to be extremely accurate, calculating the resistance with an average error of 2.50% and 1.29% respectively. This is a significant improvement in accuracy in comparison to existing models. Additionally, the methodology applied in the development of the new models improved the robustness in comparison to existing models. The high degree of accuracy for both of the developed models showed this strategy to have been very successful, producing a valuable early design tool capable of rapidly evaluating large numbers of prospective designs.

The final two objectives were achieved by Chapter 6:

"To ***improve*** *the hydrodynamic performance of stepped hulls through the application of the tools developed by this research"*

"To ***determine*** *design trends and relationships that may be applied universally to improve the performance of stepped hulls"*

In the final chapter the analysis tools that were developed over the course of this thesis were applied to investigate how the performance of stepped hulls may be improved. Both the analytical model for single stepped hulls and the CFD simulation for double stepped hulls were used to analyse prospective designs and provided data to drive an optimisation algorithm. Both approaches were successful at finding designs with improved hydrodynamic performance in comparison to the baseline geometry, demonstrating the value of these tools and the workflow. Analysis was then conducted of the considerable data set to determine trends and relationships between the design variables that improve the calm water performance of single and double stepped hulls. The key means through which the resistance was reduced was through the reduction of wetted area. The most influential parameter on the wetted area was the step height. Increasing the step height also increased the trim, and thus the pressure resistance. It is vital to balance these two factors to determine the best-case design.

7.2 Discussion

This thesis was comprised of three distinct sections: first developing knowledge of the hydrodynamic flow and how this may be modelled using a number of methods, then employing this knowledge to develop performance prediction tools using state-of-the-art CFD methods and more rudimentary semi-empirical methods, and finally going on to use these tools to study stepped hulls further, investigating how the performance of stepped hulls may be enhanced. The key findings of the studies that were undertaken have been summarised and discussed in the previous section.

The unsteady RANS approach was employed as a fundamental tool throughout the thesis. CFD has been seen to be an increasingly popular tool within the naval architecture community in the past two decades, with the levels of accuracy and scope of studies increasing significantly. Over the course of this thesis CFD was shown to be robust and accurate and results with considerably lower comparison errors with experimental data than previously reported were produced. It is known that simulations of the complex flow associated with planing hulls is more challenging than for conventional displacement vessels, however, it was shown to be possible to reduce resistance errors to a similar level. This is in line with the trend of decreasing level of comparison error that is apparent when previous studies are considered, in which the accuracy is seen to steadily improve over the years.

While conducting the numerical studies presented in this thesis, a number of problems were encountered, the majority of which stemmed from the pre-processing stage during which the CFD simulations were developed. Prior to a study being conducted using CFD, exploratory studies were required. These set out to determine the most feasible numerical set up that was capable of modelling the physical problem in an acceptable manner. A number of factors need to be considered during this stage, including the physics set up, the approach to turbulence modelling and the spatial and temporal discretisation of the continuum. Following this, the accuracy of the solution and the effects of the set up must be considered, before being altered in an appropriate manner to improve the solution accuracy. This process was very time consuming, with the individual set up, runtime and analysis taking up to a week for a single prospective set up. The initial work that was undertaken during these exploratory studies encountered problems related to Numerical Ventilation, prompting an in-depth study into the problem to determine how best to minimise its effects which was then published in (Gray-Stephens, Tezdogan and Day, 2021). This study was not factored into the initial project plan and took considerable time to complete, however, the benefits of this are apparent as the accuracy was shown to improve significantly. Another factor that was found to cause issues throughout the thesis was simulations failing to converge satisfactorily, or divergence. This was found to be a particular problem for the low y^+ simulations, which were found to be incredibly sensitive to the grid-spacing, particularly of the prism-layer and its interface with the core mesh. In almost all cases this occurred during the initialisation of the simulation and the very first 0.5 seconds of runtime. Initially when this occurred the mesh topology was adjusted prior to the simulation being rerun. Eventually it was found that increasing the number of iterations at each timestep for the early stages of the run helped the simulation to converge, however, this was a time-consuming and laborious process. The large number of iterations had to be slowly ramped down, requiring careful monitoring of the simulation and manual adjustments. After each of these adjustments, the file had to be resubmitted to the HPC queue which took 12 – 48 hours before the simulation continued to run. The use of custom java run macros to control the simulations offers a potential solution to the need to manually control the simulation.

While the application of CFD can be beneficial to the study containing a large number of factors, its use is severely limited by the availability of computational resources. As stated previously, queueing jobs for submission with the HPC considerably increased the time required to undertake a study. Without access to the Archie-WeST HPC at the University of Strathclyde, it would not be possible to have conducted the work presented in this thesis. Over the course of the separate studies around 200,000

CPU hours were used. On the 40 core nodes of the supercomputer this corresponds to 208 days of continuous run time. The availability of computational resources is increasing giving more people increased access, for less cost, however, this is still a restrictive factor on the utilisation of CFD.

Despite the results generated by CFD becoming more reliable as the methods advance and the research community gains collective expertise in its use, they cannot be accepted without real world validation data. This is required to ensure that the Navier-Stokes equations are being solved accurately and that all the physical phenomena that are occurring are being correctly modelled by the solver. It is due to this need for validation that experimental testing still plays an important role in numerical studies. This was highlighted during the study of free surface elevation aft of a step in with the lack of validation data for the CFD model led to the undertaking of a novel small scale experimental testing program. This experimental work proved to be extremely challenging and time consuming, with a large degree of difficulty associated with the correct positioning of the model and the measurement devices. Whether numerical or experimental means are used as a tool in a study, both present their own unique set of challenges that must be considered carefully in order to be overcome. It is the opinion of the author that despite the considerable challenges associated with CFD, it undoubtedly offers several advantages over experimental testing in the hydrodynamic analysis of high-performance hulls. These advantages arise entirely from the post-processing capabilities of CFD, in which any number of parameters may be visualised and measured, which is often not possible experimentally.

The development of rapid performance prediction methods based on semi-empirical equations may be less robust than CFD and allows only a restricted analysis of only the resistance and trim of the vessel. Despite this, these tools offer a considerable advantage over both CFD and experimental methods in the early design stages, provided that they are shown to be accurate. The advantages of such tools became apparent when HEEDS was employed to optimise single and double stepped hulls. When CFD was used as a performance prediction tool to drive the optimisation search it was severely limited in the number of design evaluations that could be conducted and the run time became so large it was almost impractical. The semi-empirical models that were developed allowed the evaluation of a considerably larger number of prospective designs, in a far more manageable time period. While the results may not be as accurate as those of the higher fidelity CFD method, the larger number of design evaluations in the preliminary design stages is clearly advantageous. Following this, CFD may be used to develop and analyse the best candidate hulls that are established through the rapid evaluation methods. Beyond the distinct increase in the runtime of HEEDS in conjunction with CFD, the model was considerably more complex to set up. Acquiring access to the software that was hosted on different computational resources to communicate was the source of many issues, with extensive debugging required. In the end this was only solved with a Zoom meeting in which one of the software developers worked through the set up to establish the root of the connectivity issues. Despite the initial difficulties in obtaining results using HEEDS, the methodology showed itself to be extremely powerful. A huge amount of data can be derived in a short period of time and the insight into the design traits that this provides is invaluable.

This performance driven optimisation methodology that relies upon analytical data to drive the search is, in the opinion of the author, the real future of all aspects of engineering design. The potential for enhancing multiple aspects of a design through the efficient search of large numbers of design evaluations it vast, with considerable improvements in performance, whilst also offering savings in cost and time. As numerical methods improve to further reducing the runtime, and as computational resources become more available and cheaper, the uptake of this performance driven optimisation methodology comes with enormous opportunities.

7.3 Recommendations for future research

The work that was undertaken over the course of this thesis has highlighted some related topics that would benefit from further studies. These recommendations are briefly outlined in the present section.

1. Future work studying Numerical Ventilation should investigate the interface capturing scheme settings in more detail. Whilst it is possible to minimise Numerical Ventilation through the mesh refinement, it may not be possible to eradicate it fully using this approach and it is through enhancing the interface capturing scheme that Numerical Ventilation may be fully eradicated.

2. A more detailed investigation into the Linear Wake Assumption would be beneficial. The results of indicated that it became more accurate for higher speeds, so determining under what conditions, if any, it may be considered valid as a topic of interest. In order to rapidly generate data and mitigate the expense and time of running a more extensive experimental test program employing computational means provides a promising solution. The validation data developed by this thesis may be used to validate such a CFD set up.

3. Further study into the flow as it separates aft of the second step would be beneficial in determining when it is appropriate to model the flow using Savitsky's Wake Equations and when the Linear Wake Assumption is more valid. The focus of this study should be on the wetted length that is required for the flow to fully develop so that it may be modelled using Savitsky's Wake Equations. In the present study Chapter 4 investigated the flow aft of the second step, however, this was restricted by the nature of the hull used for the study.

4. An interesting area of future work would be to employ the strategy developed for the calculation of flow intersection and wetted area over the course of Chapter 5 with the higher fidelity 2D+T method. This would remove the reliance upon semi-empirical equations, resulting in a more versatile model as the physical flow is solved for each condition. The potential advantages for employing these rapid evaluation models have been clearly demonstrated in Chapter 8 and robust yet accurate performance prediction methods are desirable.

5. It is an area of future work to employ the method as developed in Chapter 5 for performance prediction of double stepped planing hulls as the performance prediction tool to drive an optimisation search using HEEDS. This will allow a far larger number of design evaluations to be conducted, giving further insight into the design traits of double stepped planing hulls. Additionally, a larger number of speed cases may be rapidly evaluated. The results may be used to derive further information about the design trends and the effects of the input parameters in a manner similar to the single stepped hull optimisation study of Chapter 6.

References

26th ITTC Specialist Committee on CFD in Marine Hydrodynamics (2014) *Practical Guidelines for Ship CFD Applications, ITTC – Recommended Procedures and Guidelines*. doi:10.1016/j.tca.2008.12.030.

AIAA and and, A.I. of A. (1998) *Guide for the Verification and Validation of Computational Fluid Dynamics Simulations, Guide: Guide for the Verification and Validation of Computational Fluid Dynamics Simulations (AIAA G-077-1998(2002))*. Washington, DC: American Institute of Aeronautics and Astronautics, Inc. doi:10.2514/4.472855.

Azcueta, R. (2003) "Steady and Unsteady RANSE Simulations for Planing Crafts," in *FAST 2003 The 7th International Conference on Fast Sea Transportation*. Abano Terme, Italy, pp. 41–48.

Baker, G.S. (1912) "Some Experiments in Connection with the Design of Floats for Hydro-Aeroplanes," *ARC (British) R&M*, no. 70.

Bakhtiari, M. and Ghassemi, H. (2017) "Numerical study of step forward swept angle effects on the hydrodynamic performance of a planing hull," (September). doi:10.17402/228.

Bakhtiari, M., Veysi, S. and Ghassemi, H. (2016) "Numerical Modeling of the Stepped Planing Hull in Calm Water," *International Journal of Engineering*, 29(2). doi:10.5829/idosi.ije.2016.29.02b.13.

Becker, C., Loreto, A. and Shell, J. (2008) "A Systematic study of Stepped Planing Hulls," *Webb Institute* [Preprint].

Bilandi, R.N. *et al.* (2018) "A validation of symmetric 2D + T model based on single-stepped planing hull towing tank tests," *Journal of Marine Science and Engineering*, 6(4). doi:10.3390/jmse6040136.

Bilandi, R.N. *et al.* (2019) "A numerical and analytical way for double-stepped planing hull in regular wave," *VIII International Conference on Computational Methods in Marine Engineering MARINE 2019* [Preprint], (May).

Bilandi, R.N. *et al.* (2020) "Calm-water performance of a boat with two swept steps at high-speeds: Laboratory measurements and mathematical modeling," *Procedia Manufacturing*, 42(April), pp. 467–474. doi:10.1016/j.promfg.2020.02.046.

Bilandi, R.N., Dashtimanesh, A. and Tavakoli, S. (2020) "Hydrodynamic study of heeled double-stepped planing hulls using CFD and 2D+T method," *Ocean Engineering*, 196(December 2019), p. 106813. doi:10.1016/j.oceaneng.2019.106813.

Böhm, C. and Graf, K. (2014) "Advancements in free surface RANSE simulations for sailing yacht applications," *Ocean Engineering*, 90, pp. 11–20. doi:10.1016/J.OCEANENG.2014.06.038.

Brizzolara, S. and Serra, F. (2007) "Accuracy of CFD codes in the prediction of planing surfaces hydrodyamic characteristics," *The 2nd International Conference on Marine Research and Transportation*, (June 2007), pp. 147–158.

Brizzolara, S. and Villa, D. (2010) "CFD SIMULATION OF PLANING HULLS," in *Seventh International Conference On High-Performance Marine Vehicles*. Melbourne, Florida, USA.

Brown, P. and Klosinski, W. (1994a) "Directional Stability Tests of a 30 Degree Deadrise Prismatic Planing Hull," *USGC Report no. CG-27–94* [Preprint].

Brown, P. and Klosinski, W. (1994b) "Directional Stability Tests of Two Prismatic Planing Hulls," *USGC Report no. CG-D- 11-94, U.S. Coast Guard Research and Development Center* [Preprint].

Caponneto, M. (2001) "Practical CFD simulations for planing hulls," in *The 2nd International Euro Conference on High Performance Marine Vehicles (HIPER)*. Hamburg, Germany, pp. 128–138.

Casalone, P. *et al.* (2020) "Unsteady RANS CFD simulations of Sailboat's hull and comparison with full-scale test," *Journal of Marine Science and Engineering*, 8(6). doi:10.3390/JMSE8060394.

Castiglione, T. *et al.* (2011) "Numerical investigation of the seakeeping behavior of a catamaran advancing in regular head waves," *Ocean Engineering*, 38(16), pp. 1806–1822. doi:10.1016/j.oceaneng.2011.09.003.

Di Caterino, F. *et al.* (2018) "A numerical way for a stepped planing hull design and optimization," *Technology and Science for the Ships of the Future - Proceedings of NAV 2018: 19th International Conference on Ship and Maritime Research*, (June), pp. 220–229. doi:10.3233/978-1-61499-870-9-220.

CD Adapco (2018) "Simcenter STAR-CCM+ Documentation."

Celano, T. (1998) "The Prediction of Porpoising Inception for Modern Planing Craft," *SNAME Transaction*, 106, pp. 269–292.

Chase, N. *et al.* (2010) "A Benchmark Study of Optimization Search Algorithms," (February 2015), pp. 1–15.

Chase, N., Rademacher, M. and Goodman, E. (2010) *A Benchmark Study of Optimization Search Algorithms*. MI, USA.

Clement, E.P. (1969) "The Design of Cambered Planing Surfaces for Small Planing Boats," *Naval Ship Research and Development Center, Hydromechanics Laboratory, Report 3011* [Preprint].

Clement, E.P. (1979) "Designing for Optimum Planing Performance," *International Shipbuilding Progress*, 26(295), pp. 61–64.

Clement, E.P. (2005) "Evolution of the Dynaplane Design," *Professional Boat Builder*, October, pp. 164–173.

Clement, E.P. and Blount, D.L. (1963) "Resistance Test of a Systematic Series of Planing Hull Forms," *SNAME Transaction*, pp. 491–579.

Clement, E.P. and Koelbel, J.G. (1991) "Effects of Step Design on the Performance of Planing Motorboats," in *Fourth Biennial Power Boat Symposium*. Miami, pp. B1–B25.

Danielsson, J. and Strømquist, J. (2012) *CONCEPTUAL DESIGN OF A HIGH-SPEED SUPERYACHT TENDER HULL FORM ANALYSIS AND STRUCTURAL OPTIMIZATION*. KTH Royal Institute of Technology.

Dashtimanesh, A., Roshan, F., *et al.* (2020) "Effects of step configuration on hydrodynamic performance of one- and doubled-stepped planing flat plates: A numerical simulation," *Proceedings of the Institution of Mechanical Engineers Part M: Journal of Engineering for the Maritime Environment*, 234(1), pp. 181–195. doi:10.1177/1475090219851917.

Dashtimanesh, A., Tavakoli, S., *et al.* (2020) “Numerical study on a heeled one-stepped boat moving forward in planing regime,” *Applied Ocean Research*, 96(June 2019), p. 102057. doi:10.1016/j.apor.2020.102057.

Dashtimanesh, A., Amirkabir, S.T. and Sahoo, P. (2016) “Development of a simple mathematical model for calculation of trim and resistance of two stepped planing hulls with transverse steps,” in *International Conference on Ships and Offshore Structures ICSOS 2016*. Hamburg, Germany.

Dashtimanesh, A., Esfandiari, A. and Mancini, S. (2017) “Performance Prediction of Two-Stepped Planing Hulls Using Morphing Mesh Approach,” *Journal of Ship Production and Design*, 00(February 2018), pp. 1–13. doi:10.5957/JSPD.160046.

Dashtimanesh, A., Esfandiari, A. and Mancini, S. (2018) “Performance prediction of two-stepped planing hulls using morphing mesh approach,” *Journal of Ship Production and Design*, 34(3), pp. 236–248. doi:10.5957/JSPD.160046.

Dashtimanesh, A., Tavakoli, S. and Sahoo, P. (2017) “A simplified method to calculate trim and resistance of a two-stepped planing hull,” *Ships and Offshore Structures*, 12(1), pp. S317–S329. doi:10.1080/17445302.2016.1262809.

Davidson, K.S.M. and Suarez, A. (1949) “Tests of Twenty Related Models of V-Bottom Motor Boats - E.M.B. Series 50,” *DTMB Report r-47* [Preprint].

Day, J.P. and Haag, R.J. (1952) *Planing Boat Porpoising*. Glen Cove.

Du, L. *et al.* (2019) “Numerical investigation on the scale effect of a stepped planing hull,” *Journal of Marine Science and Engineering*, 7(11). doi:10.3390/jmse7110392.

Esfandiari, A., Tavakoli, S. and Dashtimanesh, A. (2019) “Comparison between the Dynamic Behavior of the Non-stepped and Double-stepped Planing Hulls in Rough Water: A Numerical Study,” *Journal of Ship Production and Design* [Preprint], (May). doi:10.5957/jspd.11170053.

Faison, L.A. (2014) “Design of a High Speed Planing Hull with a Cambered Step and Surface Piercing Hydrofoil,” p. 82.

Ferziger, J.H. and Perić, M. (2002) *Computational Methods for Fluid Dynamics*. Thrid. Berlin: Springer. doi:10.1007/978-3-642-98037-4.

Filing, J. (1993) "Experimental Procedure and Analysis of Stepped Planing Hulls with Applications to Motor Yachts, Patrol Vessels, and Fast Ferries," *Webb Institute* [Preprint].

Fridsma, Gerard (1969) *A systematic study of the rough water performance of planing boats*. Hoboken, New Jersey.

Fridsma, G. (1969) "A Systematic Study of the Rough-Water Performance of Planning Boats," *Report 1275, Davidson Laboratory, Stevens Institue of Technology, Hoboken, New Jersey* [Preprint].

Frisk, D. and Tegehall, L. (2015) *Prediction of High-Speed Planing Hull Resistance and Running Attitude. A Numerical Study Using Computational Fluid Dynamics*. Gothenburg.

Froude, W. (1872) *Experiments to Determine the Resistances at Various Speeds of a Ship of 2,500 Tons, Designed by Reverend C. Meade Ramus*, *Enclosure No. 31*.

Garland, W. (2012) "A Numerical Study of a Two-Dimensional Stepped Planing Surface," *Journal of Ship Production and Design*, 28(2), pp. 60–72. doi:10.5957/JSPD.28.2.120005.

Garland, W.R. (2011) "Stepped Planing Hull Investigation," *SNAME Transaction*, 119(V), pp. 1–11.

Gassman, W. and Kartinen, S. (1994) "An Investigation into the Effects of the Step Location and the Longitudinal Center of Gravity Location on the Performance of Stepped Planing Hulls," *Webb Institute* [Preprint].

Ghadimi, P. *et al.* (2015) "Rooster tail depression by originating a modified transom stern form using a Reynolds averaged Navier Stokes solver," *Scientia Iranica*, 22(3), pp. 765–777. doi:10.1007/0-387-24091-8.

Ghassemi, H., Kamarlouei, M. and Veysi, S.T.G. (2015) "A Hydrodynamic Methodology and CFD Analysis for Performance Prediction of Stepped Planing Hulls," *Polish Maritime Research*, 22(2), pp. 23–31. doi:10.1515/pomr-2015-0014.

Gray-Stephens, A., Tezdogan, T. and Day, S. (2019) "Strategies to Minimise Numerical Ventilation in CFD Simulations of High-Speed Planing Hulls," in *OMAE 2019*. Glasgow, Scotland, pp. 1–10. doi:https://doi.org/10.1115/OMAE2019-95714.

Gray-Stephens, A., Tezdogan, T. and Day, S. (2020a) "Experimental measurement of the nearfield longitudinal wake profiles of a high-speed prismatic planing hull," *Ship Technology Research*, 0(0), pp. 1–27. doi:10.1080/09377255.2020.1836552.

Gray-Stephens, A., Tezdogan, T. and Day, S. (2020b) "Numerical modelling of the nearfield longitudinal wake profiles of a high-speed prismatic planing hull," *Journal of Marine Science and Engineering*, 8(7). doi:10.3390/JMSE8070516.

Gray-Stephens, A., Tezdogan, T. and Day, S. (2021) "Minimizing Numerical Ventilation in Computational Fluid Dynamics Simulations of High-Speed Planning Hulls," *Journal of Offshore Mechanics and Arctic Engineering*, 143(3), pp. 1–10. doi:10.1115/1.4050085.

"HEEDS MDO User Guide Version 2019.2.2" (2019).

Ikeda, Y., Katayama, T. and Okumara, H. (2000) "Characteristics of Hydrodynamic Derivatives in Manoeuvring Equations for Super High-Speed Planing Hulls," in *Proceedings of the 10th international offshore and polar engineering conference*. Seattle: International Society of Offshore and Polar Engineers.

ITTC (2008) "ITTC – Recommended Procedures and Guidelines - Testing and extrapolation methods high speed marine vehicles - Resistance test. 7.5-02-05-01 (Revision 02)," p. 18.

ITTC - Recommended Procedures and Guidelines (2011) *Practical Guidelines for Ship CFD, 26th International Towing Tank Conference*.

ITTC Specialist Committee on CFD in Marine Hydrodynamics (2014) *Specialist Committee on CFD in Marine Hydrodynamics Final report and Recommendations to the 27 th ITTC*. Available at: https://ittc.info/media/6097/sc-cfd.pdf (Accessed: December 11, 2018).

Javaherian, M.J. and Gilbert, C.M. (2021) "Hydrodynamics of High-Speed Planing Craft: Savitsky Method and 2D+t Approach," *SNAME International Conference on Fast Sea Transportation 2021. FAST 2021* [Preprint]. doi:10.5957/FAST-2021-024.

Judge, C. and VanDerwerken, D. (2019) "Comparison of Model-Scale and Full-Scale Planing Craft Accelerations in Waves," *Journal of Ship Production and Design*, 35(02), pp. 182–189. doi:https://doi.org/10.5957/JSPD.12170059.

Kahramanoglu, E., Yildiz, B. and Yilmaz, H. (2018) "Numerical Calculations of Resistance and Running Attitude of a Planing Hull," *Int-Nam 2018* [Preprint], (May).

Kapryan, W.J. and Clement, E.P. (1949) "Effect of Increase in Afterbody Length on the Hydrodynamic Qualities of a Flying-boat Hull of High Length–Beam," *TN-1853 NACA Library* [Preprint].

Von Karman, T. (1929) *The impact on seaplane floats during landing, National Advisory Committee for Aeronautics Technical Notes No.321*. Washington: National Advisory Committee on Aeronautics.

Katayama, T., Iida, T. and Ikeda, Y. (2006) "Effects of Change in Running Attitude on Turning Diameter of Planing Craft," in *Proceedings of the 2nd PAMES and AMEC2006*. South Korea: Pan Asian Association of Maritime Engineering Societies.

Kazemi, H. *et al.* (2019) "Hydrodynamics analysis of stepped planing hull under different physical and geometrical conditions," *Journal of the Brazilian Society of Mechanical Sciences and Engineering*, 41(9), p. 360. doi:10.1007/s40430-019-1866-9.

Kazemi, H. and Salari, M. (2017) "Effects of Loading Conditions on Hydrodynamics of a Hard-Chine Planing Vessel Using CFD and a Dynamic Model," *International Journal of Maritime Technology*, 7(June), pp. 11–18. doi:10.18869/acadpub.ijmt.7.11.

Keuning, J.A. and Terwisga, P.F. (1993) "Resistance Tests of a Series Planing Hull Forms With 30o Deadrise Angle, and a Calculation Model Based on This and Similar Systematic Series," *International Shipbuilding Progress*, 40(424), pp. 333–376.

Keuning, L.J.A. and Gerritsma, J. (1982) "Resistance Tests of a Series of Planing Hull Forms With 25 Degrees Deadrise Angle," *International Shipbuilding Progress* [Preprint].

Khazaee, R., Rahmansetayesh, M.A. and Hajizadeh, S. (2019a) "Hydrodynamic evaluation of a planing hull in calm water using RANS and Savitsky's method," *Ocean Engineering*, 187, p. 106221. doi:10.1016/J.OCEANENG.2019.106221.

Khazaee, R., Rahmansetayesh, M.A. and Hajizadeh, S. (2019b) "Hydrodynamic evaluation of a planing hull in calm water using RANS and Savitsky's method," *Ocean Engineering*, 187(December 2018), p. 106221. doi:10.1016/j.oceaneng.2019.106221.

Korvin-Kroukovsky, B.V., Savitsky, D. and Lehman, W.F. (1949) "Wetted Area and Centre of Pressure of Planing Surfaces," *Davidson Laboratory, Hoboken, NJ, US, Report No. 360* [Preprint].

Lakatoš, M. *et al.* (2020) "Numerical Modelling of a Planing Craft with a V-Shaped Spray Interceptor Arrangement in Calm Water," (October). doi:10.3233/pmst200024.

Larson, L., Stern, F. and Visonneau, M. (2014) *Numerical Ship Hydrodynamics - An Assesment of the Gothenburg 2010 Workshop*. doi:10.1007/978-94-007-7189-5.

Latorre, R. (1982) "Study of the Flow Surrounding a Prismatic Planing Model," *International Shipbuilding Progress*, 29, pp. 289–296.

Latorre, R. (1983) "Study of the Prismatic Planing Model Spray and Resistance Components," *Journal of Ship Research*, 27(3), pp. 187–196.

Latorre, R. and Tamiya, S. (1975) "An Experimental Technique for Studying the Planing Boat Spray and Deriving the Pressure Resistance Components," *14th International Towing Tank Conference*, 4, pp. 562–571.

Lee, E., Pavkov, M. and Mccue-weil, L. (2014) "The Systematic Variation of Step Configuration and Displacement for a Double-step Planing Craft," *Journal of Ship Production and Design*, 30(2), pp. 89–97. doi:10.5957/JSPD.30.2.130040.

Locke, F. (1948) "Tests of a Flat Bottom Planing Surface to Determine the Inception of Planing," *Navy Department, BuAer, Research Division Report No. 1096* [Preprint].

Loni, A. *et al.* (2013) "Developing a Computer Program for Mathematical Investigation of Stepped Planing Hull Characteristics," *International Journal of Physical Research*, 1(2), pp. 34–47. doi:10.14419/ijpr.v1i2.839.

Lotfi, P., Ashrafizaadeh, M. and Esfahan, R.K. (2015) "Numerical investigation of a stepped planing hull in calm water," *Ocean Engineering*, 94, pp. 103–110. doi:10.1016/j.oceaneng.2014.11.022.

De Luca, F. *et al.* (2016) "An Extended Verification and Validation Study of CFD Simulations for Planing Hulls," *Journal of Ship Research*, 60(2), pp. 101–118. doi:10.5957/JOSR.60.2.160010.

De Luca, F. and Pensa, C. (2017) "The Naples warped hard chine hulls systematic series," *Ocean Engineering*, 139, pp. 205–236. doi:10.1016/j.oceaneng.2017.04.038.

De Luca, F. and Pensa, C. (2019) "The Naples Systematic Series – Second part: Irregular waves, seakeeping in head sea," *Ocean Engineering*, 194, p. 106620. doi:10.1016/j.oceaneng.2019.106620.

Mancini, S. (2015) "The problem of verification and validation processes of CFD simulations of planing hulls."

Mancini, S. *et al.* (2018) "A Numerical Way for a Stepped Planing Hull Design and Optimization," in *Proceedings of NAV 2018: 19th International Conference on Ship and Maritime Research*, pp. 220–229. doi:10.3233/978-1-61499-870-9-220.

Mancini, S., de Luca, F. and Ramolini, A. (2017) "Towards CFD guidelines for planing hull simulations based on the Naples Systematic Series," in *7th International Conference on Computational Methods in Marine Engineering, MARINE 2017*. Nantes.

De Marco, A. *et al.* (2017a) "Experimental and numerical hydrodynamic analysis of a stepped planing hull," *Applied Ocean Research*, 64(March), pp. 135–154. doi:10.1016/j.apor.2017.02.004.

De Marco, A. *et al.* (2017b) "Experimental and numerical hydrodynamic analysis of a stepped planing hull," *Applied Ocean Research*, 64(March), pp. 135–154. doi:10.1016/j.apor.2017.02.004.

De Marco, A. *et al.* (2017c) "Experimental and numerical hydrodynamic analysis of a stepped planing hull," *Applied Ocean Research*, 64(March), pp. 135–154. doi:10.1016/j.apor.2017.02.004.

Miranda, S. and Vitiello, L. (2014) "Propulsive Performance Analysis of a Stepped Hull by Model Test Results and Sea Trial Data," (October), pp. 1–8.

Morabito, M. *et al.* (2014) "Experiments on directional stability of stepped planing hulls," in *Transactions - Society of Naval Architects and Marine Engineers*, pp. 456–465.

Morabito, M. (2015) "Prediction of Planing Hull Side Forces in Yaw Using Slender Body Oblique Impact Theory," *Ocean Engineering*, (101), pp. 45–57.

Najafi, A. *et al.* (2019) "Experimental investigation of the wetted surfaces of stepped planing hulls," *Ocean Engineering*, 187, p. 106164. doi:10.1016/J.OCEANENG.2019.106164.

Najafi, A. and Nowruzi, H. (2019) "On hydrodynamic analysis of stepped planing crafts," *Journal of Ocean Engineering and Science*, 4(3), pp. 238–251. doi:10.1016/j.joes.2019.04.007.

Nazemian, A. and Ghadimi, P. (2021) "Automated CFD-based optimization of inverted bow shape of a trimaran ship: An applicable and efficient optimization platform," *Scientia Iranica*, 28(5 B), pp. 2751–2768. doi:10.24200/sci.2020.56644.4833.

Niazmand Bilandi, R., Dashtimanesh, A. and Tavakoli, S. (2019) "Development of a 2D+T theory for performance prediction of double-stepped planing hulls in calm water," *Proceedings of the Institution of Mechanical Engineers Part M: Journal of Engineering for the Maritime Environment*, 233(3), pp. 886–904. doi:10.1177/1475090218797784.

Olin, L. (2015) *Numerical modeling of spray sheet deflection on planing hulls*. KTH Royal Institute of Technology.

Parkinson, J.B., Olson, R.E. and House, R. (1939) "Hydrodynamic and Aerodynamic Tests of a Family of Models of Seaplane Floats with Varying Angles of Deadrise N.A.C.A. Models 57-A, 57-B, and 57-C," *TN-716 NACA Library* [Preprint].

Peters, M. (2010) "Peters On (Fast) Powerboats Part: Part 2," *Professional Boat Builder*, October, pp. 56–71.

Red Cedar Technology (2014) "SHERPA, An Efficient and Robust Optimization (Search) Algorithm," pp. 1–3.

Resistance Committee of 25th ITTC (2008) *Uncertainty Analysis in CFD Verification and Validation Methodology and Procedures*, *ITTC – Recommended Procedures and Guidelines*.

Reyling, C. (1976) "An experimental study of planing surfaces operating in shallow water," *Davidson Laboratory Report SIT-DL-76-1835* [Preprint].

Richardson, L.F. (1911) "The Approximate Arithmetical Solution by Finite Differences of Physical Problems Involving Differential Equations, with an Application to the Stresses in a Masonry Dam," *Philosophical Transactions of the Royal Society A: Mathematical, Physical and Engineering Sciences*, 210(459–470), pp. 307–357. doi:10.1098/rsta.1911.0009.

Sajedi, S.M. and Ghadimi, P. (2020) "Experimental and Numerical Investigation of Stepped Planing Hulls in Finding an Optimized Step Location and Analysis of Its Porpoising Phenomenon," *Mathematical Problems in Engineering*, 2020. doi:10.1155/2020/3580491.

Sambraus, A. (1938) "Planing Surfaces at Large Froude Numbers – Airfoil Comparison," *NACA TM No. 848* [Preprint].

SANCAK, E. and ÇAKICI, F. (2021) "DETERMINATION OF THE OPTIMUM TRIM ANGLE OF PLANING HULLS FOR MINIMUM DRAG USING SAVITSKY METHOD," *Gemi ve Deniz Teknolojisi* [Preprint]. doi:10.54926/GDT.951371.

Savitsky, D. (1964) "Hydrodynamic design of planing hulls," *Marine Technology*, 1(1), pp. 71–95.

Savitsky, D. (2012) "The Effect of Bottom Warp on the Performance of Planing Hulls," in *3rd SNAME Cheaspeake Power Boat Symposium*. Annapolis, MD, USA.

Savitsky, D. and Brown, W. (1976) "Procedures for Hydrodynamic Evaluation of Planing Hulls in Smooth and Rough Water," *Marine Technology*, 13(4), pp. 361–400.

Savitsky, D., DeLorme, M.F. and Datla, R. (2007) "Inclusion of whisker spray drag in performance prediction method for high-speed planing hulls," *Marine Technology And Sname News*, 44(1), pp. 35–56.

Savitsky, D. and Morabito, M. (2010) "Surface Wave Contours Associated with the Forebody Wake of Stepped Planing Hulls," *Marine Technology*, 47(1), pp. 1–16.

Savitsky, D. and Neidinger, J.W. (1954) "Wetted Area and Centre of Pressure of Planing Surfaces at Very Low Speed Coefficients," *Stevens Institute of Technology, Davidson Laboratory Report No. 493* [Preprint].

Savitsky, D., Prowse, R.E. and Lueders, H. (1958) "High-Speed Hydrodynamic Characteristics of a Flat Plate and 20 Degrees Deadrise Surface in Unsymmetrical Planing Conditions," *NACA TN 4187* [Preprint].

Sedov, L.I. (1947) "Scale Effect and Optimum Relation for Sea Surface Planing," *NACA TM No. 1097* [Preprint].

Shoemaker, J.M. (1934) "Tank Tests of Flat and Vee-Bottom Planing Surfaces," *NACA TM No. 509* [Preprint].

Sorensen, E. (2011) *The stepped hull has come of age* , *Soundings Online*. Available at: https://www.soundingsonline.com/boats/the-stepped-hull-has-come-of-age (Accessed: April 20, 2021).

Sottorf, W. (1934) "Experiments with planing surfaces," *National Advisory Committee for Aeronautics Technical Memorandum 661* [Preprint], (March).

Stern, F. *et al.* (2001) "Comprehensive Approach to Verification and Validation of CFD Simulations—Part 1: Methodology and Procedures," *Journal of Fluids Engineering*, 123(4), p. 793. doi:10.1115/1.1412235.

Stern, F., Wilson, R. and Shao, J. (2006) "Quantitative V&V of CFD simulations and certification of CFD codes," *International Journal for Numerical Methods in Fluids*, 50(11), pp. 1335–1355. doi:10.1002/fld.1090.

Su, Y. *et al.* (2012) "Numerical simulation of a planing vessel at high speed," *Journal of Marine Science and Application*, 11(2), pp. 178–183. doi:10.1007/s11804-012-1120-7.

Sukas, O.F. *et al.* (2017) "Hydrodynamic assessment of planing hulls using overset grids," *Applied Ocean Research*, 65, pp. 35–46. doi:10.1016/j.apor.2017.03.015.

Sukas, Ö.F. and Gökçe, M.K. (2016) "Prediction of Hydrodynamic Aspects of a Catamaran Using Overset Grid Design," in *Thirteenth International Conference on Marine Sciences and Technologies Black Sea*. Varna.

Svahn, D. (2009) *Performance Prediction of Hulls with Transverse Steps*. KTH Royal Institute of Technology. Available at: http://www.kth.se/polopoly_fs/1.74882!/Svahn_Thesis.pdf.

Syamsundar, S. and Datla, R. (2008) "Performance Prediction of High-Speed Planing Craft With Interceptors Using a Variation of the Savitsky Method," in *Proceedings of 1st Cheaspeake Power Boat Symposium*. Annapolis, USA.

Taunton, D.J., Hudson, D.A. and Shenoi, R.A. (2010) "Characteristics of a series of high speed hard chine planing hulls – Part 1: Performance in calm water," *International Journal of Small Craft Technology*, 152, pp. 55–75. doi:10.3940/rina.ijsct.2011.b1.97.

Taunton, D.J., Hudson, D.A. and Shenoi, R.A. (2011) "Characteristics of a series of high speed hard chine planing hulls - part II: Performance in waves," *Transactions of* *the Royal Institution of Naval Architects Part B: International Journal of Small Craft Technology*, 153(1). doi:10.3940/rina.ijsct.2011.b1.97.

Tezdogan, T. *et al.* (2015) "Full-scale unsteady RANS CFD simulations of ship behaviour and performance in head seas due to slow steaming," *Ocean Engineering*, 97, pp. 186–206. doi:10.1016/j.oceaneng.2015.01.011.

United Nations (2015) "Adoption of the Paris Agreement," in *21st Conference of the Parties*.

Veysi, S.T.G. *et al.* (2015) "Toward numerical modeling of the stepped and non-stepped planing hull," *Journal of the Brazilian Society of Mechanical Sciences and Engineering*, 37(6), pp. 1635–1645. doi:10.1007/s40430-014-0266-4.

Viola, I.M., Flay, R.G.J. and Ponzini, R. (2012) "CFD analysis of the hydrodynamic performance of two candidate America's cup AC33 hulls," *International Journal of Small Craft Technology*, 154(1), pp. 1–12. doi:10.3940/rina.ijsct.2012.b1.113.

Vitiello, L. *et al.* (2020) "An Overview of Stepped Hull Performance Evaluation: Sea Trial Data vs Full-Scale CFD Simulation," (October). doi:10.3233/pmst200026.

Wagner, H. (1931) "Landing of Seaplanes," *NACA TN No. 622* [Preprint].

Wagner, H. (1932) "The Phenomena of Impact and Planing on Water," *NACA Translation 1366, National Advisory Committee for Aeronautics* [Preprint].

Wang, J. *et al.* (2021) "Inhibition and hydrodynamic analysis of twin side-hulls on the porpoising instability of planing boats," *Journal of Marine Science and Engineering*, 9(1), pp. 1–26. doi:10.3390/jmse9010050.

Wang, S. *et al.* (2012) "RANSE simulation of high-speed planning craft in regular waves," *Journal of Marine Science and Application*, 11(4), pp. 447–452. doi:10.1007/s11804-012-1154-x.

Xing, T. and Stern, F. (2010) "Factors of safety for Richardson extrapolation," *Journal of Fluids Engineering, Transactions of the ASME*, 132(6), pp. 0614031–0640313. doi:10.1115/1.4001771.

Yang, D. *et al.* (2019) "A study on the air cavity under a stepped planing hull," *Journal of Marine Science and Engineering*, 7(12). doi:10.3390/JMSE7120468.

Publications

The following papers have been published in scientific journals and conferences. All of the publications listed below have been drawn from work completed for this thesis.

Journal Papers

1. Gray-Stephens, A., Tezdogan, T. and Day, S. (2020a) 'Experimental measurement of the nearfield longitudinal wake profiles of a high-speed prismatic planing hull', Ship Technology Research. Taylor & Francis, 0(0), pp. 1–27. doi: 10.1080/09377255.2020.1836552.
2. Gray-Stephens, A., Tezdogan, T. and Day, S. (2020b) 'Numerical modelling of the nearfield longitudinal wake profiles of a high-speed prismatic planing hull', Journal of Marine Science and Engineering, 8(7). doi: 10.3390/JMSE8070516.
3. Gray-Stephens, A., Tezdogan, T. and Day, S. (2021) 'Minimizing Numerical Ventilation in Computational Fluid Dynamics Simulations of High-Speed Planning Hulls', Journal of Offshore Mechanics and Arctic Engineering, 143(3), pp. 1–10. doi: 10.1115/1.4050085.

Conference Papers

1. Ventilation in CFD Simulations of High-Speed Planing Hulls', in OMAE 2019. Glasgow, Scotland, pp. 1–10. doi: https://doi.org/10.1115/OMAE2019-95714.

Appendix A – Full Freesurface Elevation Profile Data Set from Chapter 4

The freesurface elevation profile for all methods as calculated for all conditions is presented in this section.

$2ms^{-1}$ Centreline Profiles

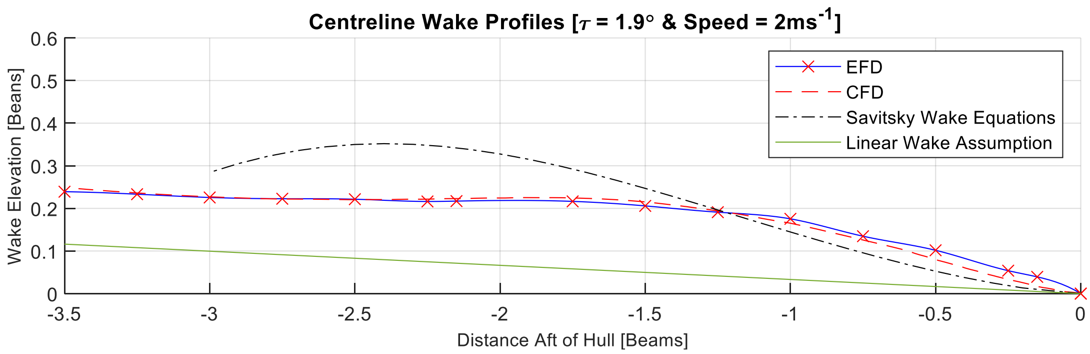

Figure 44 – Centreline freesurface elevation profiles [$\tau = 1.9°$ & speed = $2ms^{-1}$]

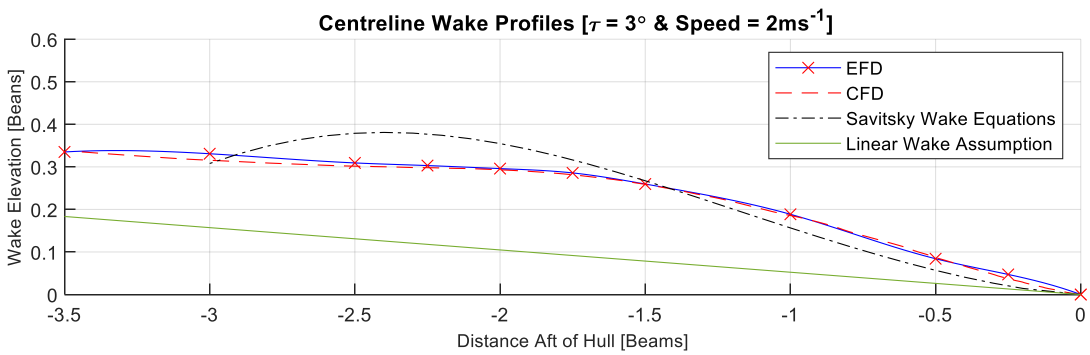

Figure 45 – Centreline freesurface elevation profiles [$\tau = 3°$ & speed = $2ms^{-1}$]

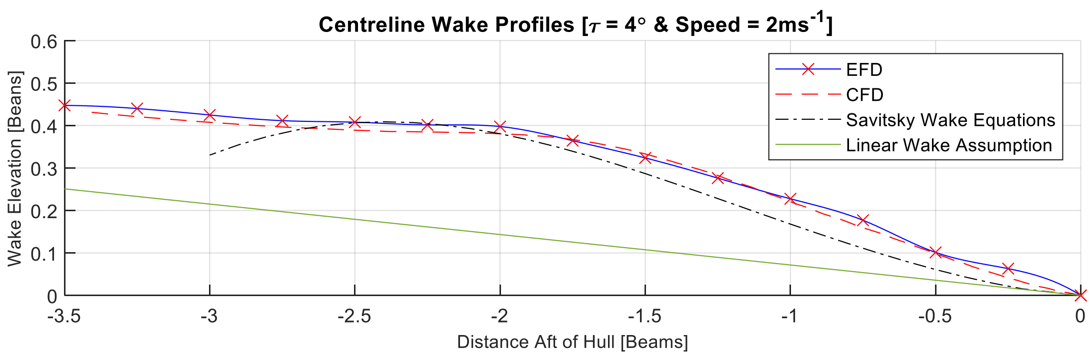

Figure 46 – Centreline freesurface elevation profiles [$\tau = 4°$ & speed = $2ms^{-1}$]

$3ms^{-1}$ Centreline Profiles

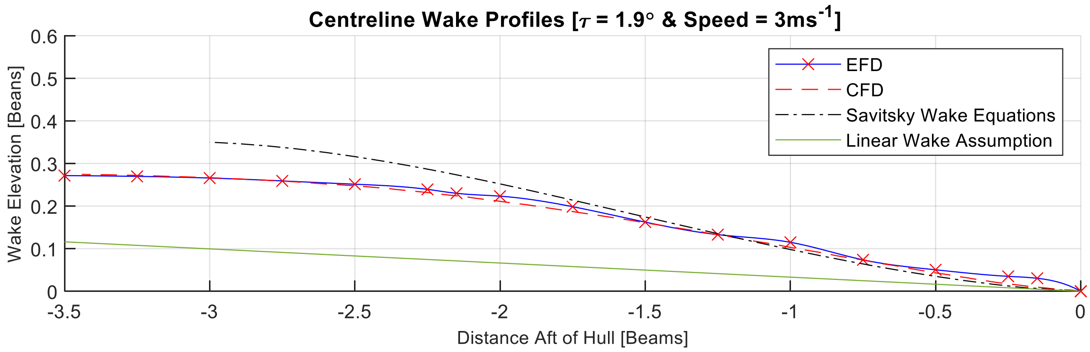

Figure 47 – Centreline freesurface elevation profiles [$\tau = 1.9°$ & speed = 3ms^{-1}]

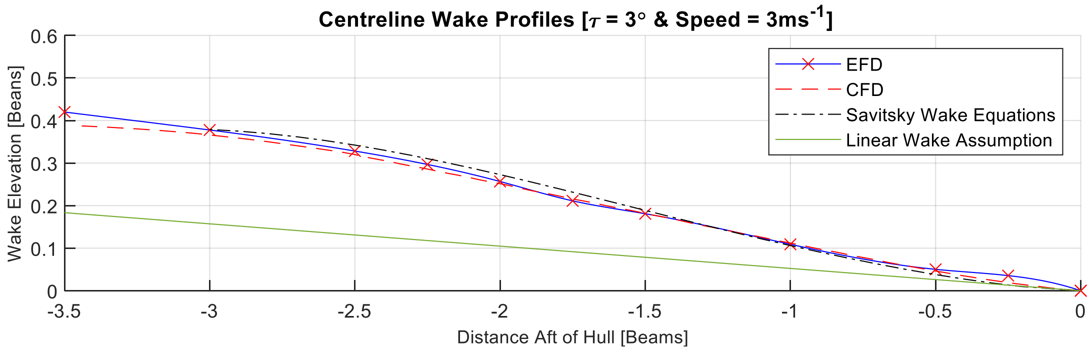

Figure 48 – Centreline freesurface elevation profiles [$\tau = 3°$ & speed = 3ms^{-1}]

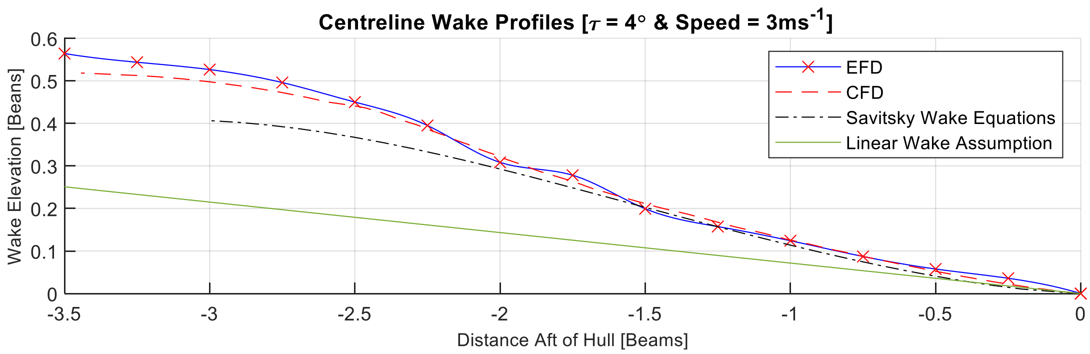

Figure 49 – Centreline freesurface elevation profiles [$\tau = 4°$ & speed = 3ms^{-1}]

$4ms^{-1}$ Centreline Profiles

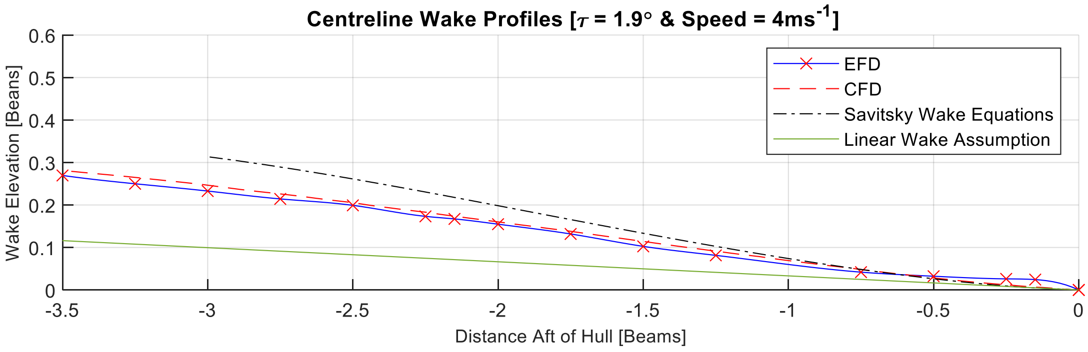

Figure 50 – Centreline freesurface elevation profiles [$\tau = 1.9°$ & speed = $4ms^{-1}$]

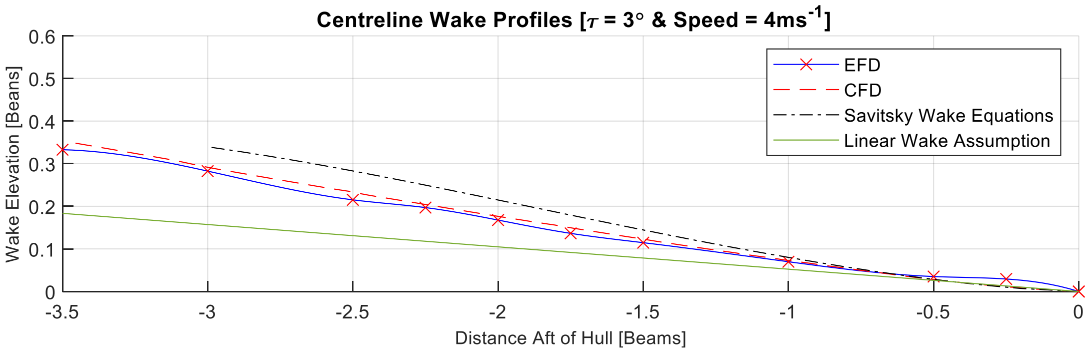

Figure 51 – Centreline freesurface elevation profiles [$\tau = 3°$ & speed = $4ms^{-1}$]

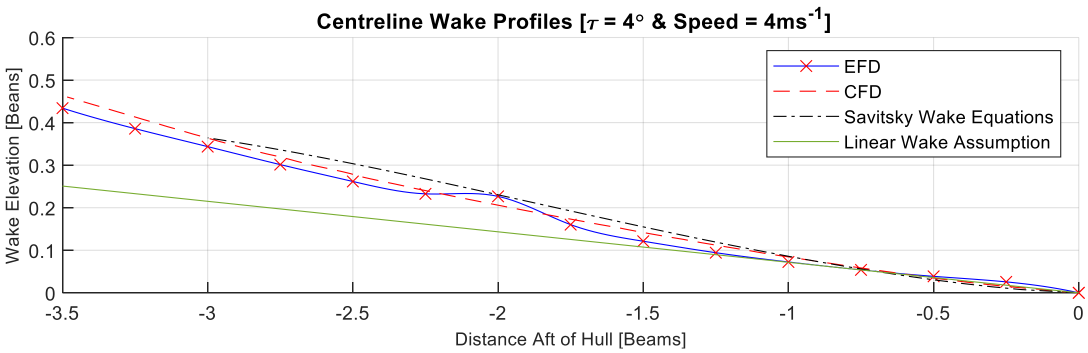

Figure 52 – Centreline freesurface elevation profiles [$\tau = 4°$ & speed = $4ms^{-1}$]

$4.5ms^{-1}$ Centreline Profiles

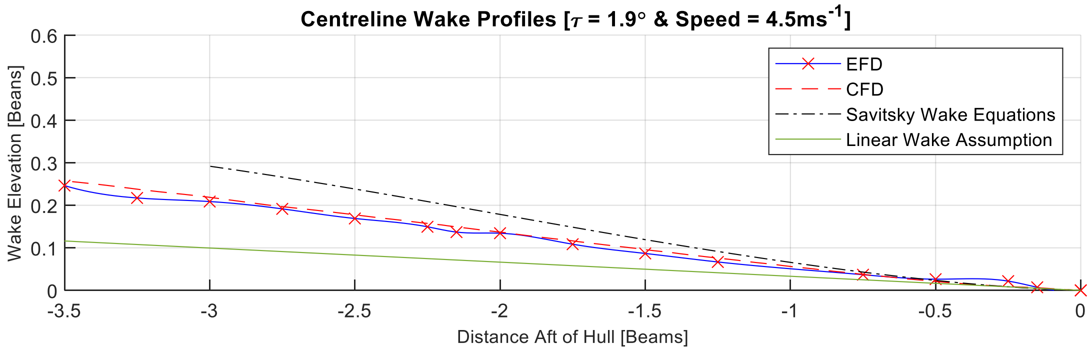

Figure 53 – Centreline freesurface elevation profiles [$\tau = 1.9°$ & speed = $4.5ms^{-1}$]

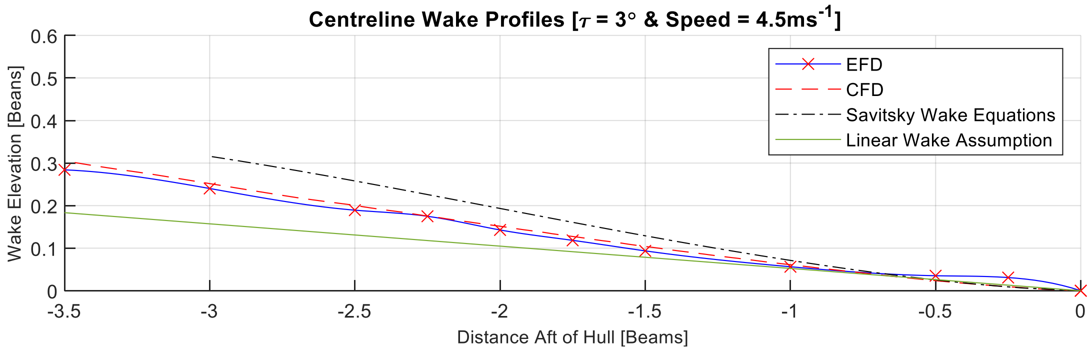

Figure 54 – Centreline freesurface elevation profiles [$\tau = 3°$ & speed = $4.5ms^{-1}$]

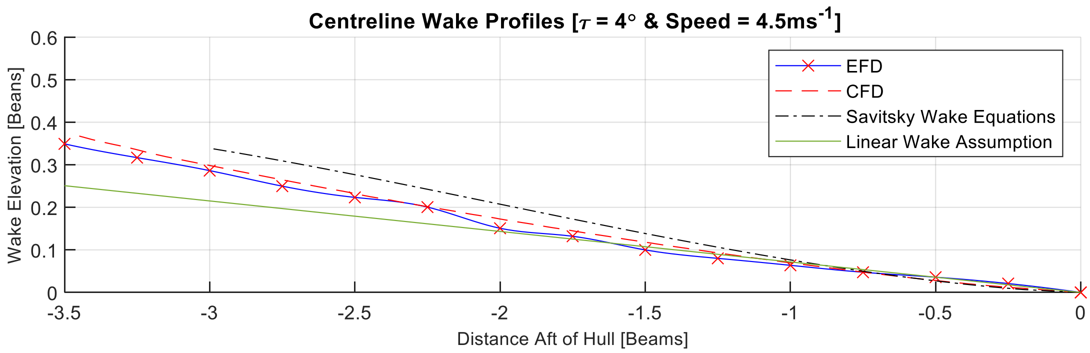

Figure 55 – Centreline freesurface elevation profiles [$\tau = 4°$ & speed = $4.5ms^{-1}$]

$2ms^{-1}$ Quarterbeam Profiles

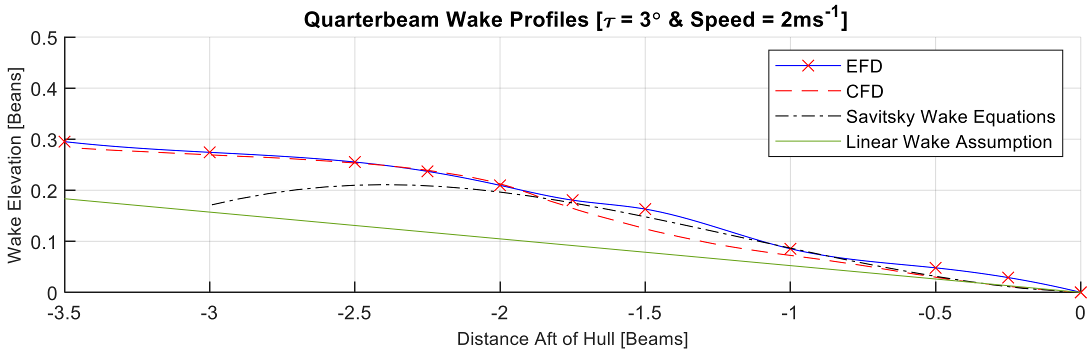

Figure 56 – Quarterbeam freesurface elevation profiles [τ = 3° & speed = 2ms^{-1}]

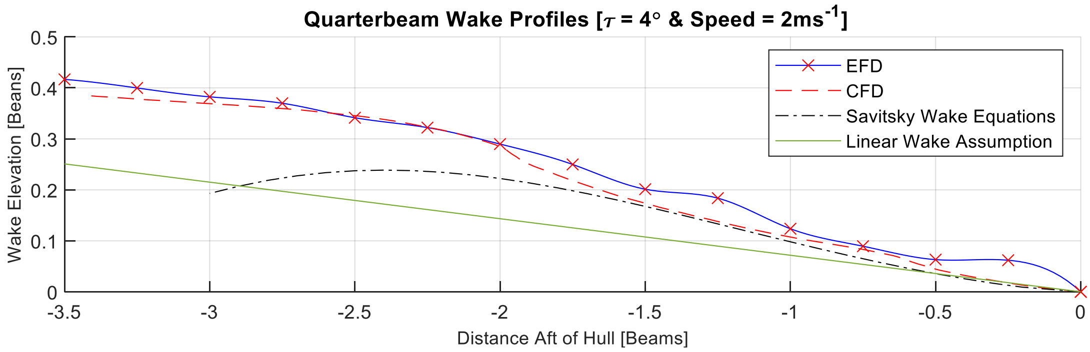

Figure 57 – Quarterbeam freesurface elevation profiles [τ = 4° & speed = 2ms^{-1}]

$3ms^{-1}$ Quarterbeam Profiles

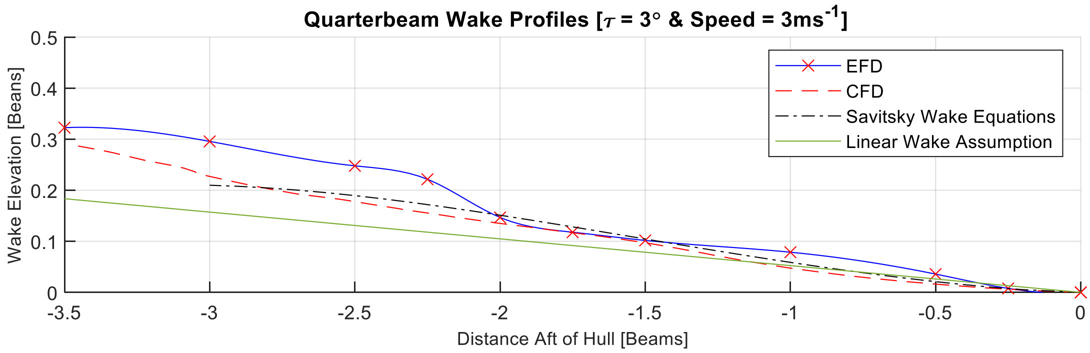

Figure 58 – Quarterbeam freesurface elevation profiles [τ = 3° & speed = 3ms^{-1}]

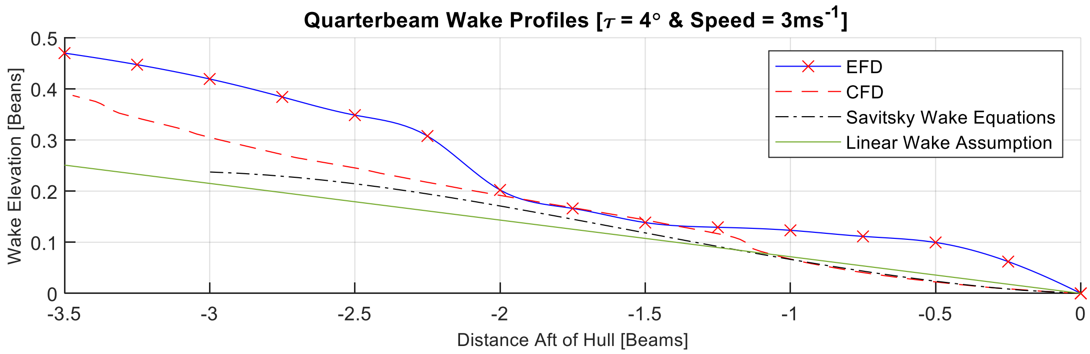

Figure 59 – Quarterbeam freesurface elevation profiles [τ = 4° & speed = 3ms^{-1}]

$4ms^{-1}$ Quarterbeam Profiles

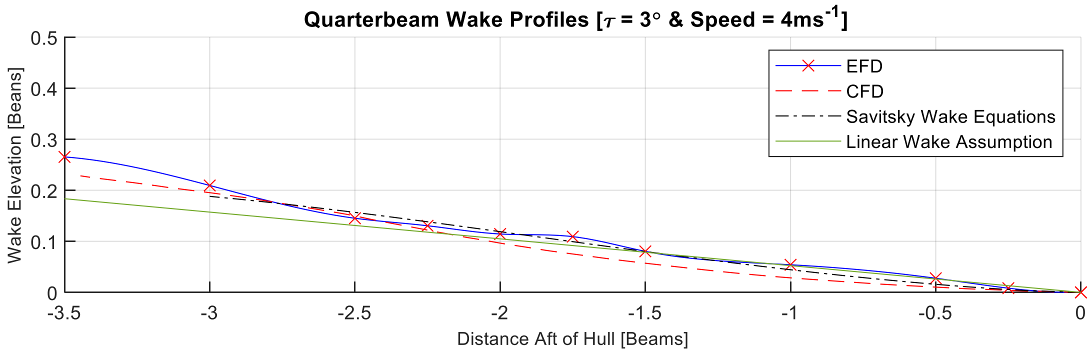

Figure 60 – Quarterbeam freesurface elevation profiles [τ = 3° & speed =4ms^{-1}]

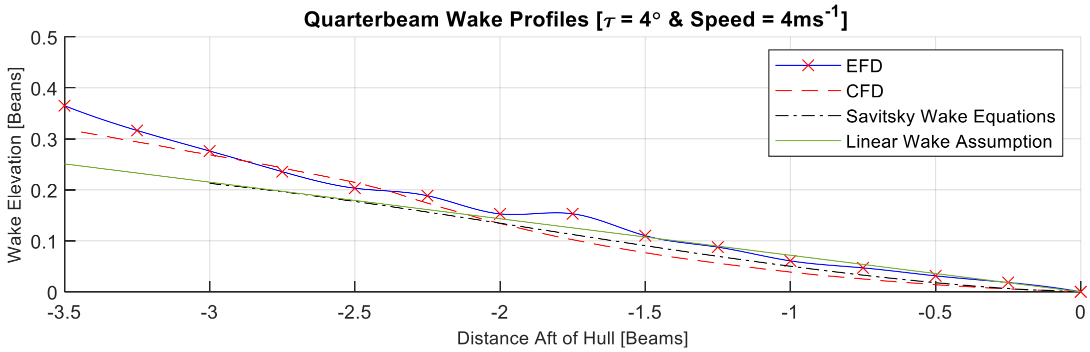

Figure 61 – Quarterbeam freesurface elevation profiles [τ = 4° & speed =4ms^{-1}]

$4.5ms^{-1}$ Quarterbeam Profiles

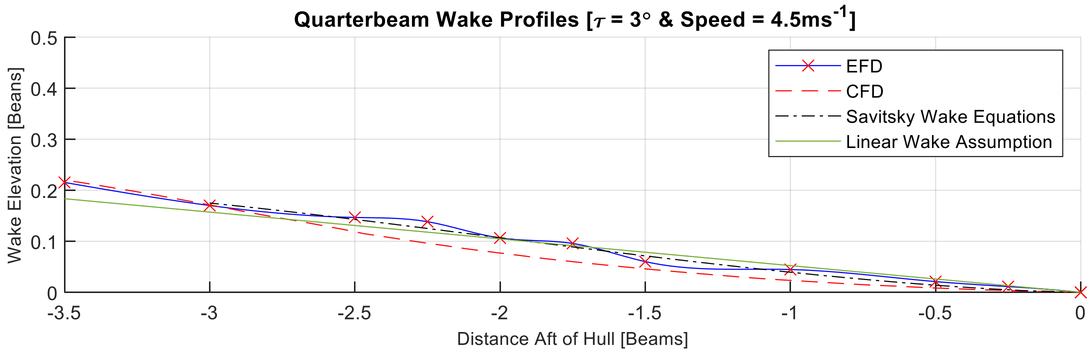

Figure 62 – Quarterbeam freesurface elevation profiles [τ = 3° & speed =4.5ms^{-1}]

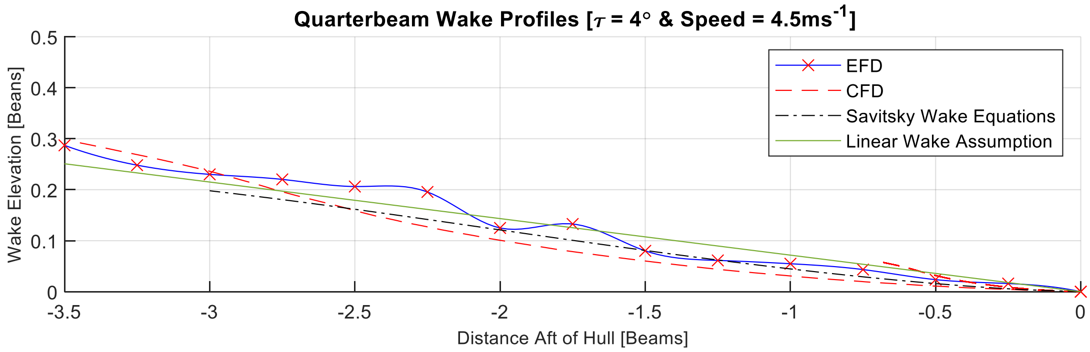

Figure 63 – Quarterbeam freesurface elevation profiles [τ = 4° & speed =4.5ms^{-1}]

Appendix B – Additional Information on HEEDS.MDO Set from Chapter 6

Additional information about the HEEDS MDO set up as employed in Chapter 6 is presented in this section.

Further Info About SHERPA

SHERPA is a very efficient search model, requiring significantly fewer model evaluations than other leading methods do to identify optimized designs. SHERPA has been shown to outperform other algorithms by a factor of two in the number of evaluations required to fully converge to the optimal solution. In cases where the number of evaluations is limited, it has been shown to progress rapidly toward the optimal solutions, with the average solution found by other methods shown less than half as good as those found by SHERPA (Chase *et al.*, 2010).

During optimisation study, HEEDS gives each design evaluation a performance rating so that the levels of success may be judged. This is determined through the returned value of the objective for that design, and the degree to which the constraints are satisfied. A design that is termed high performance is one that satisfies all constraints and has a good rating for its objectives. For designs that satisfy the chosen constraints, the margin by which they meet those constraints is essentially ignored. Once the constraints are satisfied it is only the value of the objective that is used to determine the performance evaluation. The performance value of each design evaluation is calculated by Equation (0.1).

A design that satisfies all constraints is termed a feasible design, regardless of how well the objective is met. The optimisation search looks for the best feasible design, for which the objective is minimised or maximised. As seen in the performance value equation the performance function is the sum of the normalized objective values. If one or more of the constraints are violated, the performance value is reduced by a value that is based upon this violation and determined by the second term in the equation.

$$\sum_{i=1}^{N_{obj}} \left(\frac{LinWt_i * S_i * Obj_i}{Norm_i} \right) - \sum_{j=1}^{N_{con}} \left(\frac{QuadWt_j * ConViol_j^2}{Norm_j^2} \right) \qquad \textbf{(0.1)}$$

Where:

$N_{obj} = Number\ of\ Objectives$

$LinWt_i = The\ linear\ weight\ for\ the\ i^{th}\ objective\ (default\ value\ is\ 1)$

$S_i = sign\ for\ the\ i^{th} objective\ (-1\ for\ minimisation)$

$Obj_i = Response\ for\ the\ i^{th}\ objective$

$Norm_i = \ The\ normalizing\ value\ for\ the\ i^{th}\ objective$

$QuadWt_j$

$= \ The\ quadratic\ weight\ for\ the\ j^{th}\ constraint.\ (default\ value\ is\ 10000.0)$

$ConViol_j$

$= \ The\ amount\ by\ which\ the\ j^{th}\ constraint\ is\ violated.\ (0\ if\ the\ constraint\ is\ met)$

$Norm_j = the\ normlising\ value\ for\ the\ j^{th} constraint$

Further info on Single Stepped Hull Optimisation Set-Up

For the single stepped hull optimisation, the Modified Svahn Model as developed in Chapter 4 and coded in MATLAB was employed as the model that calculated the performance of a candidate hull. Prior to the utilisation of the MATLAB code, it was updated so that it cancelled the search in the case that it failed to converge on a solution, ensuring that the model did not become stuck in an infinite loop.

HEEDS features portals that allow it to integrate several analysis tools in its automated process without having to develop new scripts. When a portal is utilised a new shell script for each evaluation is generated that uses the analysis tool's API to update variable values, run the simulation and the extract results. This shell script is created from a template script file with specific information, such as tags for the input variables and the responses, inserted into predetermined locations. MATLAB is one of the analysis tools for which the portal option was available, so this was employed. This allowed the variables (step location and step height) and the responses (Resistance, Resistance Components and Trim) to be tagged directly in the MATLAB script. Once tagged in the script the shell script developed by HEEDS is populated with the location of the input variables to be changed at the start of an evaluation, and the responses to be extracted and stored upon completion.

Further info on Double Stepped Hull Optimisation Set-Up

For the double stepped hull optimisation, the CFD simulation as developed in Chapter 3 was employed as the model that calculated the performance of a candidate hull. The same process logic was applied as for the single stepped hull however, employing CFD as the design tool led to a far more complex optimisation procedure and was a considerably more computationally intensive process.

Initially a parametric model was to be developed in Rhino Grasshopper. This model was capable of generating a double stepped hull, based on Hull C2, however with a different step configuration. It did this using variables for the first step location, the first step length, and the height of the first and second step. By changing any of the variables the hull was rebuilt to reflect the new step layout. Additionally, in the grasshopper model the interactive Parameters were partitioned from the geometry construction to allow for external Input through ASCII. The Star CCM+ simulation was modified so that it could update the boundaries and generate a new mesh automatically for any geometry that was imported. Finally, HEEDS had to be set up so that it could communicate with, and transfer files to the Linux Cluster HPC. This required a passwordless SSH connection which was not possible with the ARCHIE-WeST HPC so a work around with the Bitvise SSH client was employed. This required extensive debugging to allow ensure that HEEDS was able to submit batch job files to the SLURM resource management software on the HPC.

Once these tools were developed and the HEEDS procedure was set up as outlined in Chapter 6. This process was considerably more complex than the optimisation procedure used for the single stepped hull and required multiple software packages to run and interface with each other on multiple computers. The values of the input variables were determined by HEEDS and passed to Grasshopper through ASCII via a .txt file with tagged values. In order to allow HEEDS to interface with and automate Grasshopper, a batch execution command leveraged Rhino.exe using a Phyton script. Grasshopper then modelled the double stepped hull, which was exported using a custom Visual Basic script. HEEDS then utilised shell scripts and the Bitwise SSH client to transfer the geometry and simulation file to the ARCHIE WeST Linux Cluster, and submit the sbatch job file to the SLURM resource management software. When the job was allocated the relevant computational resources a Java script imported the new geometry into the Star CCM+ file, where it replaced a part that had previously been tagged in HEEDs. Star CCM+ generated a mesh with the new geometry and ran the simulation. Upon completion, the relevant response variables as previously tagged in HEEDS were extracted from the simulation file and passed back to HEEDS on the local PC, where the SHERPA optimisation algorithm determined the next input variables for evaluation based on the previous results and the process repeated.